APPENDIX 2L

GEOLOGIC INVESTIGATION OF SOILS AND THE BEDROCK SURFACE AT UNIT 2 CONTAINMENT SITE. SEABROOK STATION

The information contained in this appendix was not revised, but has been extracted from the original FSAR and is provided for historical information.

GEOLOGIC INVESTIGATIONS

of

SOILS AND THE BEDROCK SURFACE

at

UNIT 2 CONTAINMENT SITE

SEABROOK STATION

PUBLIC SERVICE COMPANY OF NEW HAMPSHIRE
SEABROOK, NEW HAMPSHIRE

October 24, 1974

CONTENTS

Geological Investigations of Soils and the Bedrock Surface Unit 2 Containment Site Seabrook Station Seabrook, New Hampshire

During August and early September, 1974, four trenches 200' in length were excavated to bedrock on an "X" configuration across the area of the Unit 2 containment site at the Seabrook Station, New Hampshire.

The bedrock in the floor of these trenches is gneissoid quartz diorite of the Newburyport pluton, which is commonly fractured at less than 3' intervals in this area by an intersecting pattern of high-angle and low-angle joints. The most prominent and continuous joint se; within the containment area appears to be one which strikes N80-90E, dips steeply to the north, and is characterized by smooth chlorite-coated joint surfaces.

Unconsolidated overburden in the containment area ranges to a maximum of about 16' in thickness, and is characterized by a basal deposit of sand-silt-cobble till locally overlain by a blanket of medium-fine outwash sand. Glacial-marine clay lies between the till and outwash to the east of the containment. Where covered by outwash sand, the upper surface of the till is beveled to a gently undulating, sub-planar erosion surface upon which rest isolated eratic boulders ranging to 3' in diameter.

No evidence of Recent fault displacement was observed on the bedrock surface in the Unit 2 trenches. The sub-planar till/outwash contact horizon, which occurs in three of the four trenches, shows no evidence in these areas of static or dynamic deformation.

1. Purpose of Investigations

Bedrock at the site of the proposed Unit 2 containment is largely obscured by glacial till, glacial-marine clay and outwash sand. Boring E2-1, drilled in December 1972 to a depth of 159.2' on the vertical centerline of Unit 2, encountered thin zones of structural weakness in the diorite bedrock at intervals between elevations -75' and -110'.

These zones are characterized by smooth chlorite-rich surfaces on high-angle joints, and by closely-jointed zones in chlorite-rich portions of the bedrock. High-angle joints in Boring E2-1 dip from 60° to 85°, and most commonly dip 65-70°

Trenching investigations over the Unit 2 site were conducted in August-September 1974 for precautionary purposes, to ascertain the structure of the glacial deposits in the urea and to examine the nature of jointing in the underlying bedrock surface.

2. Borings Investigations Subsequent to Boring E2-1

During April 1974, Eoring E2-5 was drilled to a depth of 97.8' at a iocatior, 33' N13E (True) of the centerline of Unit 2 (see Appendix I for boring log) . This boring encountered jcints with minor chlorite coatings at various elevations, with a zone of smooth chlorite-coated joints between -64 to -79' elevations. These joints dip 55° to 75°, and frequently show pyrite crystal growths over the chlorite surfaces.

During May-June 1974, four inclined borings, E2-15, E2-16, E2-17 and E2- 18, were put down around the periphery of the Unit 2 containment site to develop information relative to engineering of the containment excavation . Logs and orientation data for these borings are presented in a July 31, 1974 report prepared by Geotechnical Engineers, Inc., Winchester, Massachusetts (see Appendix II) .

Borings E2-15 and E2-16, along the west and south edges of the containment, respectively, encountered very few chlorite-coated joints. A polished joint at 88' depth in E2-15 appears likely to represent the projection to depth of a prominent chlorite-coated high-angle joint which is observed on the bedrock surface to trend east-west through the centerline of Unit 2. There are no anomalously polished joints in Boring E2-16.

Boring E2-17, drilled northerly across the east edge of the containment site, encountered polished chlorite-coated joints intermittently at depths of 62-67', 82', 87', 98-103', 137' and 152-156'. Some of these joints appear to correlate with the prominent east-west joint which trends through the centerline of Unit 2. This prominent joint appears to split into a number of high-angle branches as it passes east into the zone of influence of Boring E2-17.

Boring E2-18 encountered numerous individual joints which have minor chlorite coatings. No anomalously polished or chlorite-rich joints were found, however, in the 168' inclined depth drilled.

When examined in conjunction with joint mapping of the bedrock surface (Figure 2), Borings E2-15, E2-16, E2-17 and E2-18 do not indicate the presence of a through-going fault structure in the area of Unit 2. These borings do appear, however, to suggest that the most prominent or continuous high-angle chlorite-coated joint system in the containment area trends approximately east-west (True) through the central part of the containment, and dips 70-80° to the north.

3. Trench Excavations

During August 1974, four trenches were excavated with a backhoe to bedrock across the 'Unit 2 site, to form an "x" whose legs are each approximately 203' long and intersect at right angles at the vertical centerline of the Unit. The legs trend approximately True North, East , South and West (see Figure 1) .

Ground surface elevations in the area of the trenches range from about +10' to +20' . The elevation of the bedrock surface in the floor of the trenches ranges from about -3' at Station 1+80 in the East trench, to +14' at Station 1+85 in the South trench. Profiles of the bedrock surface along the centerlines of the trenches, as surveyed by Public Service Company 'of New Hampshire personnel, are shown on Figures 1 and 3.

4. Bedrock Exposed in the Trenches

Figure 2 shows by half-tone shading the areas of bedrock mapped by J. R. Rand in the several trenches. Although the trenches were excavated to bedrock, throughout, the bedrock in the low elevation areas was too obscured by water and mud to permit the observation of joints or other pertinent structural features. Although much of the bedrock surface is rough and irregular due to glacial plucking or breaking by the backhoe, wide areas of the bedrock are locally smooth and show glacial striations.

Throughout the area exposed by the trenches the bedrock consists predominantly of gneissoid, sometimes quartzitic, quartz diorite which ranges in grain size from fine- to medium-grained. Coarse

hornblende diorite occurs locally in the West and South trenches. Gneissoid banding commonly strikes about N80W and dips very steeply to the north. No diabase dikes were observed in the trenches or in the several borings in the area. The bedrock is commonly fresh and hard in the containment area, with weathering effects limited to surface staining on joints.

A. Faulting

No evidence of offset of the bedrock surface or the overlying glacial sediments was observed in the trenches. Welded breccia fabric, which is seen locally in drill core both in the Unit 2 area and elsewhere throughout the site area, can be seen exposed on a smooth glacially-scoured bedrock surface approximately 5' to the southwest of Boring E2-1 in the trench excavation. This breccia is 1-2" wide, strikes approximately east-west, dips steeply, is annealed and compact, and shows no offset of the glaciated bedrock surface.

B. Jointing

As shown on Figure 2, jointing in the bedrock is closely spaced throughout the Unit 2 containment area, occurring at intervals which rarely exceed 5' and commonly occurring at less than 3' intervals.

High-angle joints (greater than 50° dips) occur in three prominent orientations:

Strike N65-70W	Dip 65-80N
Strike N05-20W	Dip 65-85W
Strike N80-90E	Dip 65-90N

At the centerline of Unit 2, the most continuous joint trend is N80-90E with steep dips to the north. This set is seen commonly to have chlorite-coated surfaces. The N65-70W joints appear to converge and terminate against the N80-90E set, while the N05-20W joints are characteristically short and discontinuous. Slickenside striations which occur on many of the joints exhibit widely divergent directions of movement.

Low-angle joints (less than 50° clips) appear to be somewhat more common than high-angle joints, and occur generally in three prominent orientations:

Strike N25-40E	Dip 35-40° NW and SE
Strike N 15-30W	Dip 35-40° NE and SW
Strike N80-90E	Dip 35-45° North

Low-angle joint surfaces are commonly planar, and occasionally show slickenside striations, with no consistent striation orientation from joint to joint.

From about Station 1+15 to 1+50 in the East trench, the bedrock is subject to closely-spaced jointing, and the upper 1-3' of the bedrock was sufficiently fractured to permit excavation by t'ne backhoe. Joints in this area are chlorite-coated and smooth, and show some polishing on conchoidal surfaces. Thin gray clay fillings occur locally in discontinuous patches between some joints. Slickensides show no preferred orientation, and no strike direction could be determined for this zone.

5. Unconsolidated Glacial Deposits

As shown on trench profiles on Figure 3, brown sand-silt-cobble till directly overlies the bedrock surface throughout the area exposed by the four trenches. Till rises to ground surface throughout the length of the South trench, and rises locally to ground surface in the North trench and in the area of the Unit 2 centerline. Where the till does not rise to ground surface in the trenches, the upper surface of the till is a gently undulating, sub-planar erosion surface on which was deposited a layer of medium-fine outwash sand. At the east end of the East trench, a sequence of interbedded, evenly-layered marine clays and sands lies between the till and the overlying outwash sand layer. At scattered intervals in the West, North and East trenches, isolated boulders ranging to 3' in diameter lie enclosed in outwash sand and rest on the upper surface of the till.

Subsequent to backhoe excavation of the trenches, the contact horizon between the till and overlying outwash sand was exposed and cleaned by hand throughout the length of its exposure in the West, North and East trenches. The contact was inspected and photographed by J. R. Rand throughout its exposed length in these trenches, and its elevation determined by transit leveling along both walls of each of these trenches. The extent of the outwash sand deposits in the trench walls and the elevations of the till/outwash contact from place to place are shown on Figure 2.

No features were observed along this till/outwash contact in any of the trenches to suggest either static or dynamic deformation subsequent to deposition of the sand on the beveled till surface. Throughout the zone of close and slippery bedrock jointing between Stations 1+15 and 1+50 in the East trench, the overlying till/outwash contact horizon is sub-planar and continuous.

Glacial materials overlying the bedrock surface throughout the South trcrich are limited to unsorted, non-layered sand-silt-cobble till. These materials locally show a crude stratification, and nowhere exhibit structures suggestive of post-depositional deformation.

6. Conclusions

Examination of the overburden, bedrock surface and bedrock joints in the Unit 2 trench excavations has revealed several distinctive features which are indicative of the tectonic stability of the bedrock at the site:

A. Intermittent crudely-stratified horizons in the glacial till are not displaced over joints in the underlying bedrock.

B. The undulating, sub-planar erosion surface at the top of the till is through-going and not subject to structural offsets or other deformations suggestive of faulting,

C. Local exposures of glacially-scoured bedrock surfaces are smooth across joints in the bedrock.

D. Slickenside striations on closely-spaced bedrock joints exhibit widely divergent orientations, with no preferred attitude or orientation.

John R. Rand
Consulting Geologist

FIGURES

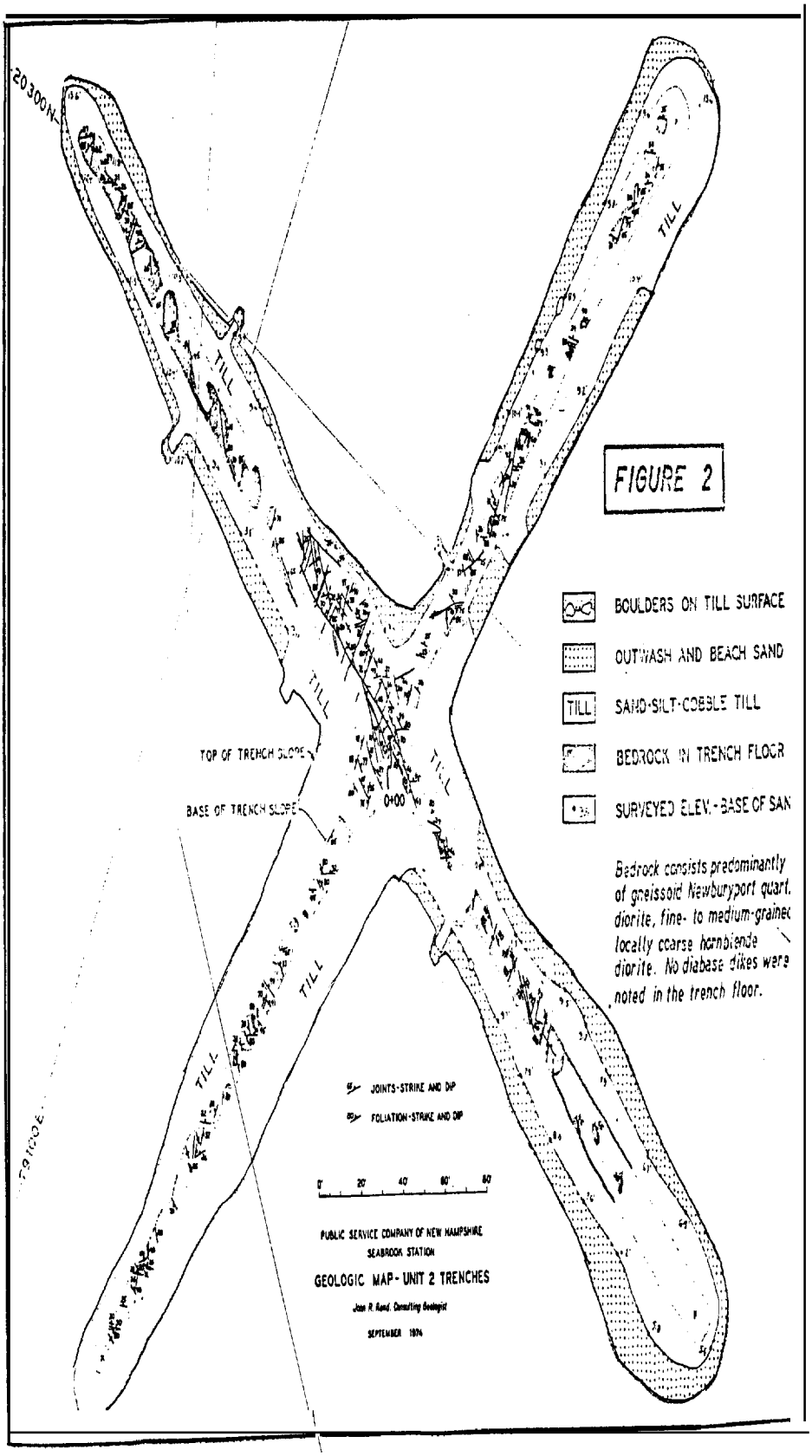
20300N
TILL
TOP OF TRENCH SLOPE
BASE OF TRENCH SLOPE
0+00
FIGURE 2
BOULDERS ON TILL SURFACE
OUTWASH AND BEACH SAND
TILL SAND-SILT-COBBLE TILL
BEDROCK IN TRENCH FLOOR
SURVEYED ELEV.-BASE OF SAN
Bedrock consists predominantly of gneissoid Newburyport quart. diorite, fine- to medium-grained locally coarse hornblende diorite. No diabase dikes were noted in the trench floor.
JOINTS-STRIKE AND DIP
FOLIATION-STRIKE AND DIP
0' 20' 40' 60' 80'
PUBLIC SERVICE COMPANY OF NEW HAMPSHIRE
SEABROOK STATION
GEOLOGIC MAP-UNIT 2 TRENCHES
Joan R. Kuno, Consulting Geologist
SEPTEMBER 1974

APPENDIX 2M

GEOTECHNICAL REPORT - PRELIMINARY REPORT. COMPRESSION TESTS ON STRUCTURAL BACKFILL AND SAND CEMENT, SEABROOK STATION

The information contained in this appendix was not revised, but has been extracted from the original FSAR and is provided for historical information.

PRELIMINARY REPORT
'COMPRESSION TESTS ON
STRUCTURAL BACKFILL AND SAND-CEMENT
SEABROOK STATION

January 24, 1978

Prepared for

PUBLIC SERVICE CO. OF NEW HAMPSHIRE

and

UNITED ENGINEERS AND CONSTRUCTORS, INC.

by

Geotechnical Engineers Inc.
1017 Main Street
Winchester, Massachusetts 01890

Project 77386

TABLE OF CONTENTS

LIST OF TABLES

*To be added when tests are complete.

2. DESCRIPTION OF STRUCTURAL BACKFILL AND RESULTS OF INDEX TESTS

2.1 Description

Beard Pit No. 5 soil is a yellowish-brown gravelly sand containing about two percent fines.

2.2 Grain-Size Distribution Tests

Two sieve analyses were performed. The grain-size distribution of Beard Pit No. 5 soil as received was first determined. The entire sample was subsequently sieved on a No. 4 (4.75 mm) mesh and a grain-size distribution of soil passing the No. 4 mesh was determined. The minus No. 4 material was used for triaxial testing.

2.2.1 Procedure

To determine the grain-size distribution of the original soil, a representative sample was selected, weighed and air-dried. The sample was sieved on a 3/8-in. mesh and aggregates retained were removed, weighed and separately sieved. A representative sample of aggregates passing the 3/8-in. mesh was weighed, oven-dried and washed on a No. 200 (.074 mm) sieve. The soil retained on the No. 200 sieve was oven-dried, weighed and mechanically sieved.

The entire quantity of soil was then sieved on a No. 4 (4.75 mm) mesh and aggregates retained were removed. A representative sample of soil passing the No. 4 mesh was oven-dried and washed on a No. 200 (.074 mm) sieve. Soil retained on the No. 200 sieve was subsequently oven-dried, weighed and mechanically sieved to determine the grain-size distribution of the soil to be used for compaction and triaxial testing.

2.2.2 Results

The grain-size distribution curve of Beard Pit No. 5 soil is presented in Fig. 1.

The grain-size distribution curve of the soil passing the No. 4 (4.75 mm) sieve is presented in Fig. 2.

4. CONSOLIDATED-DRAINED, S, TRIAXIAL TESTS

Six S tests were performed on compacted specimens of Beard Pit No. 5 soil. Only soil passing a No. 4 sieve was used. Specimens were compacted to 90% and 95% of the maximum dry unit weight as determined by ASTM Designation D1557, Method A (Section 3). Tests were performed at effective consolidation pressures of 0.5, 2.0 and 6.0 ksc (7.1, 28.4, 85.3 psi). Test specimens typically had a diameter of 2.9-in. and a height of 6.6-in.

4.1 Procedure

A predetermined quantity of air-dried soil was thoroughly mixed with distilled water to a water content of 14%. The mixture was divided in seven portions of equal weight and placed in covered containers.

The compaction was performed in seven layers within a split mold. The mold was lined with a rubber membrane which was held tightly to the inside of the mold by a small vacuum. The first soil layer was placed in the mold and leveled off. A 1-psi surcharge was lowered onto the soil and vibrated vertically using an Ingersoll-Rand pneumatic hammer. The hammer provided low frequency-high amplitude vibrations. The layer was compacted to a predetermined height to achieve the desired unit weight. The surcharge was removed and the soil surface scarified. Subsequent layers were added and compacted in the same manner to form a test specimen of the desired size and unit weight.

The mold and specimen assembly was then mounted on the bottom platen of a triaxial cell. A vacuum of approximately 15-in. of Hg was applied to the specimen to provide support to the specimen. The mold was removed and the diameter and height of the specimen were measured. A second membrane was placed around the specimen and O-rings attached to seal the membranes to the top and bottom platens.

The triaxial cell was subsequently assembled and flooded with water. A chamber pressure of 0.5 ksc was applied and the vacuum released to distilled water at atmospheric pressure. When the vacuum had dissipated, distilled water was permeated through the specimen to improve saturation by displacing air voids. A back pressure of approximately 10 ksc was utilized to complete saturation. B-values of 0.90 or higher were measured.

The specimen was then consolidated to the desired effective consolidation pressure. Volume changes during consolidation were measured by monitoring the flow of pore water through the drainage system.

The test specimen was subsequently loaded axially at a constant rate of strain of approximately 0.4%/min. During shear the specimen was allowed to drain through both ends. Volume changes were measured by monitoring the flow of pore water. Axial loads were measured with a proving ring and deformations were monitored with an axial dial. The test was terminated at 20% axial strain. The specimen was then removed and oven-dried to determine the weight of solids.

4.2 Stress-Strain Curves For S Tests

Results of the consolidated-drained triaxial, S, tests are plotted in terms of

a. normalized shear stress on the 45° plane, $q/\bar{\sigma}_{3c}$, vs. axial strain, and

b. volumetric strain, $\Delta V/V$, *vs.* axial strain.

The results of individual S tests are presented in Appendix A and Table 2 contains the details of each S test performed.

A summary of S tests performed on specimens initially compacted to a specific 90% compaction are plotted in Fig. 4, and 95% compaction in Fig. 5.

4.3 Moduli and Poisson's Ratios For S Tests

Figs. 6 and 7 are plots of secant modulus and Poisson's ratio, respectively, as a function of axial strain from the triaxial S tests.

Fig. 8 (top) is a plot of the initial tangent modulus and the secant modulus at 50% of the compressive strength versus the effective consolidation pressure, $\bar{\sigma}_{3c}$. At the bottom in Fig. 8 is a similar plot for the values of Poisson's ratios.

6. TESTS ON SAND-CEMENT

We herewith forward results of tests on 2-in. cube specimens of sand-cement, so that the results will be available early in this preliminary form.

In Fig. 13 are plotted the stress-strain curves for unconfined tests on three replicate specimens cured for 7 days, and in Fig. 14 are the stress-strain curves for unconfined tests on three replicate specimens cured for 28 days. Details of these tests are given in Table 4.

The sand-cement specimens were prepared using the same sand and cement that *were* used at the Seabrook site for test batches. The mixtures are shown in Figs. 13'and 14.

It may be seen that the strength increased rapidly with cure time. A strength increase that is logarithmic with time would lead to the predition of an average strength of 180 psi for the specimens cured 90 days. Similarly, the average modulus would increase to 33,800 psi.

7. COEFFICIENT OF SUBGRADE REACTION

7.1 Structural Backfill

To determine reasonable values for the coefficient of subgrade reaction of buried pipes, the following procedure may be used:

1. Determine whether the loading condition is "drained" or "undrained." That is, will volume changes take place during loading (drained), or will volume changes not occur during loading (undrained).

2. Establish the allowable diametral strain of the pipe. That is, select a diameter-strain that the pipe can withstand with an adequate factor of safety. That strain may be as low as 0.1% for stiff, brittle pipes,to 3% or 4% for flexible pipes.

3. Compute the vertical effective stress in the ground at the level of the middle (springline) of the pipe.

4. Choose whether the expected degree of compaction of the structural backfill is 90% Modified or 95% Modified.

5. Given the above data, enter the appropriate table below, and interpolate to obtain a value of $k_s D$, i.e., the coefficient of subgrade reaction times the pipe diameter (in psi).

6. Divide $k_s D$ by the pipe diameter to obtain the value of k_s in pci (pounds/cubic inch).

TABLE 2 - CONSOLIDATED-DRAINED (S) TRIAKIAL TESTS
STRUCTURAL BACKFILL - BEARD PIT 5 SAND
SEABROOK STATION

Test No.	Initial Water Content	Dry Unit Weights			Percent Compaction, P ASTM D1557, A			Effective Consolidation Stress	B Value	At Max. Compressive Stress			Moduli		Poisson's Ratio	
		In Compaction Mold	In Triaxial Cell Initial	In Triaxial Cell After Consolidation	In Compaction Mold	In Triaxial Cell Initial	In Triaxial Cell After Consolidation			Deviator Stress ($\sigma_1 - \sigma_3$)	Axial Strain ε_a	Volume Strain ε_v	Initial E_o	At 50% Max. Stress E_{50}	Initial ν_o	At 50% Max. Stress ν_{50}
	%	pcf	pcf	pcf				ksc		ksc	%	%	psi	psi		
S1	13.8	100.7	100.8	100.8	89.9	90.0	90.0	0.50	0.97	1.64	1.31	0.41	6,260	4,050	0.31	0.43
s2	13.8	100.9	101.0	101.5	90.1	90.2	90.6	2.00	0.95	5.88	2.38	0.08	14,220	11,090	0.17	0.23
s3	13.8	101.0	101.3	102.3	90.2	90.4	91.4	6.00	0.95	15.05	7.28	-0.66	23,750	18,770	0.22	0.23
s4	13.8	106.4	106.4	106.4	95.0	95.0	95.0	0.50	0.95	2.34	1.31	0.92	13,510	9,600	0.33	0.35
S5	13.5	106.3	106.4	106.8	94.9	95.0	95.3	2.00	0.97	7.96	2.62	0.92	21,330	16,140	0.17	0.27
S6	13.7	106.3	106.4	107.3	94.9	95.0	95.8	6.00	0.95	19.35	4.00	0.34	29,150	24,740	0.20	0.27

TABLE 3 - CONSOLIDATED-UNDRAINED ($\bar{R}$) TRIAXIAL TESTS
STRUCTURAL BACKFILL - BEARD PIT 5 SAND
SEABROOK STATION

Test No.	Initial Water Content	Dry Unit Weights			Percent Compaction, P ASTM D1557, A			Effective Consolidation Stress	B Value	At Maximum Compressive Stress			Moduli	
		In Compaction Mold	In Triaxial Cell Initial	In Triaxial Cell After Consolidation	In Compaction Mold	In Triaxial Cell Initial	In Triaxial Cell Consolidation	σ_{3c}		Deviator Stress $(\sigma_1 - \sigma_3)$	Axial Strain ε_a	Effective Minor Principal Stress $\bar{\sigma}_3$	Initial E_o	At 50% Maximum Stress E_{50}
	%	p pcf	c f	pcf				ksc		ksc	%	ksc	psi	psi
$\bar{R}1$	13.7	101.0	101.2	101.2	90.2	90.4	90.4	0.50	0.96	6.86	9.53	2.63	5,830	3,130
$\bar{R}2$	13.5	100.6	100.6	100.9	89.8	89.8	90.1	2.00	0.90	7.94	8.33	3.11	12,730	5,760
ii3	13.8	100.8	101.1	102.2	90.0	90.3	91.2	6.00	0.99	11.32	6.69	. 4.46	38,110	18,630
$\bar{R}7$	13.6	101.0	101.2	102.3	90.2	90.4	91.3	6.00	0.95	12.24	5.73	4.77	24.460	19,050
$\bar{R}4$	13.8	106.3	106.5	106.5	94.9	95.1	95.1	0.50	0.95	19.91	13.83	7.23	11,870	7,180
ii5	13.6	106.3	106.3	106.6	94.9	94.9	95.2	2.00	0.95	21.87	14.53	7.93	19,770	8,390
$\bar{R}6$	13.5	106.3	106.4	107.2	94.9	95.0	95.7	6.00	0.96	27.88	11.58	io.35	44,010	14,220

TABLE 4 - UNCONFINED TESTS ON 2-IN. CUBE SAMPLES OF SAND-CEMENT, 5% CEMENT
SEABROOK STATION

Cure Time days	Test No.	Unit Weight Wet pcf	Unconfined Strength psi	Strain At Peak %	Modulus of Elasticity* psi
7	7-1	124.0	66.7	0.80	10,600
	7-2	123.9	72.5	0.92	10,110
	7-3	126.2	85.3	0.83	13,650
			Avg 74.8		Avg 11,450
28	28-1	127.4	141.6	0.67	33,330
	28-2	126.2	133.8	0.77	19,130
	28-3	126.8	130.0	0.87	22,760
			Avg 135.0		Avg 25,070
90	90-1				
	90-2				
	90-3				

*Modulus computed for the straight line portion of the stress-strain curve, neglecting any curvature at origin, which may be affected by initial seating strains.

FIGURES

Lab. 4-3 rev. 0 28 May 74

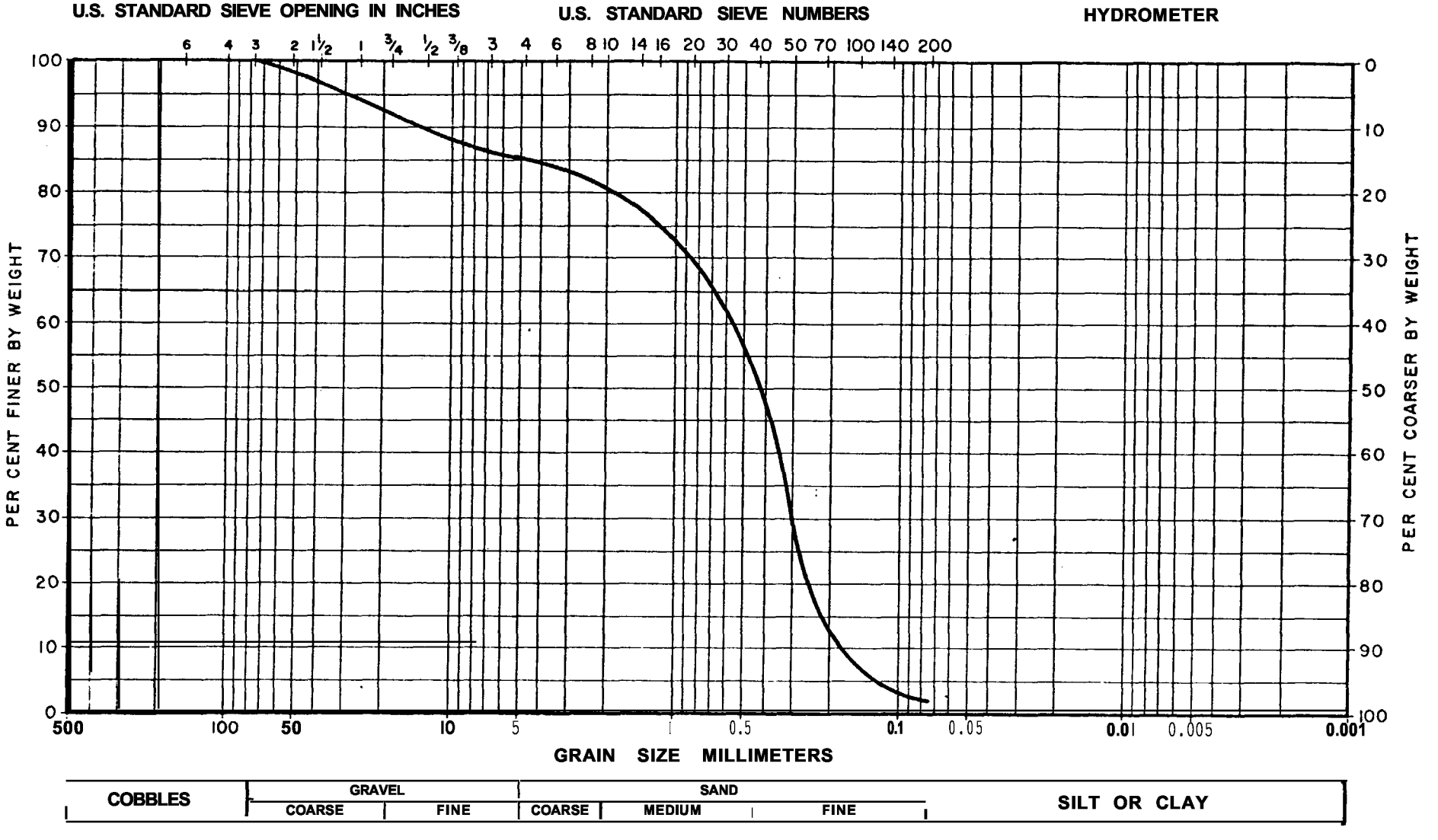

Public Service Company of New Hampshire	Triaxial Tests Structural Backfill	GRAIN-SIZE DISTRIBUTION BEARD PIT NO. 5 SOIL
Geotechnical Engineers Inc. Winchester, Massachusetts	Project 77386	Jan. 23, 1978 Fig. 1

Lab. 4-3 rev. 0 28 May 74

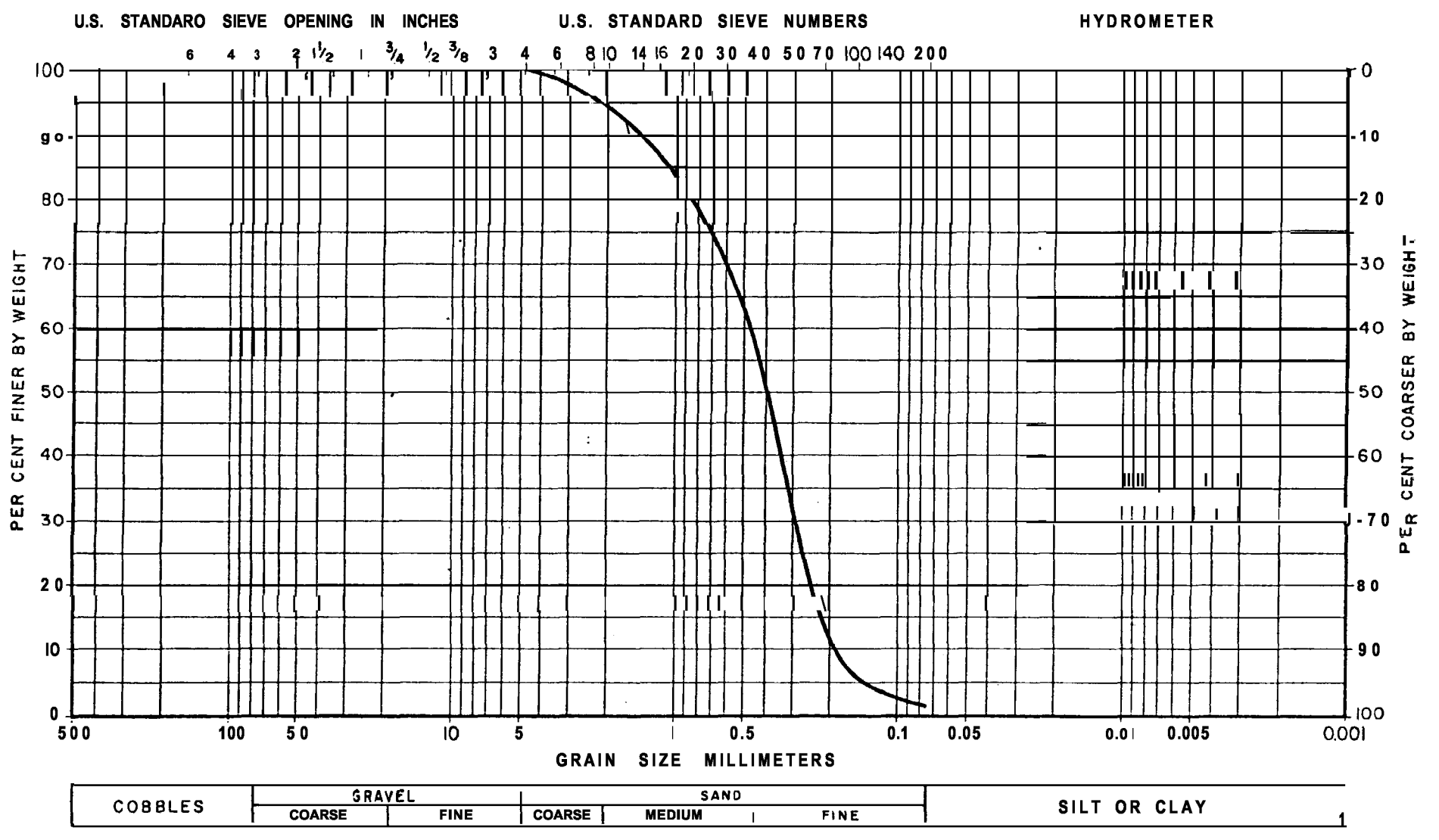

Public Service Company of New Hampshire	Triaxial Tests Structural Backfill	GRAIN-SIZE DISTRIBUTION BEARD PIT NO. 5 SAND - NO. 4 MATERIAL
Geotechnical Engineers Inc. Winchester, Massachusetts	Project 77306	Jan. 23, 1978 Fig. 2

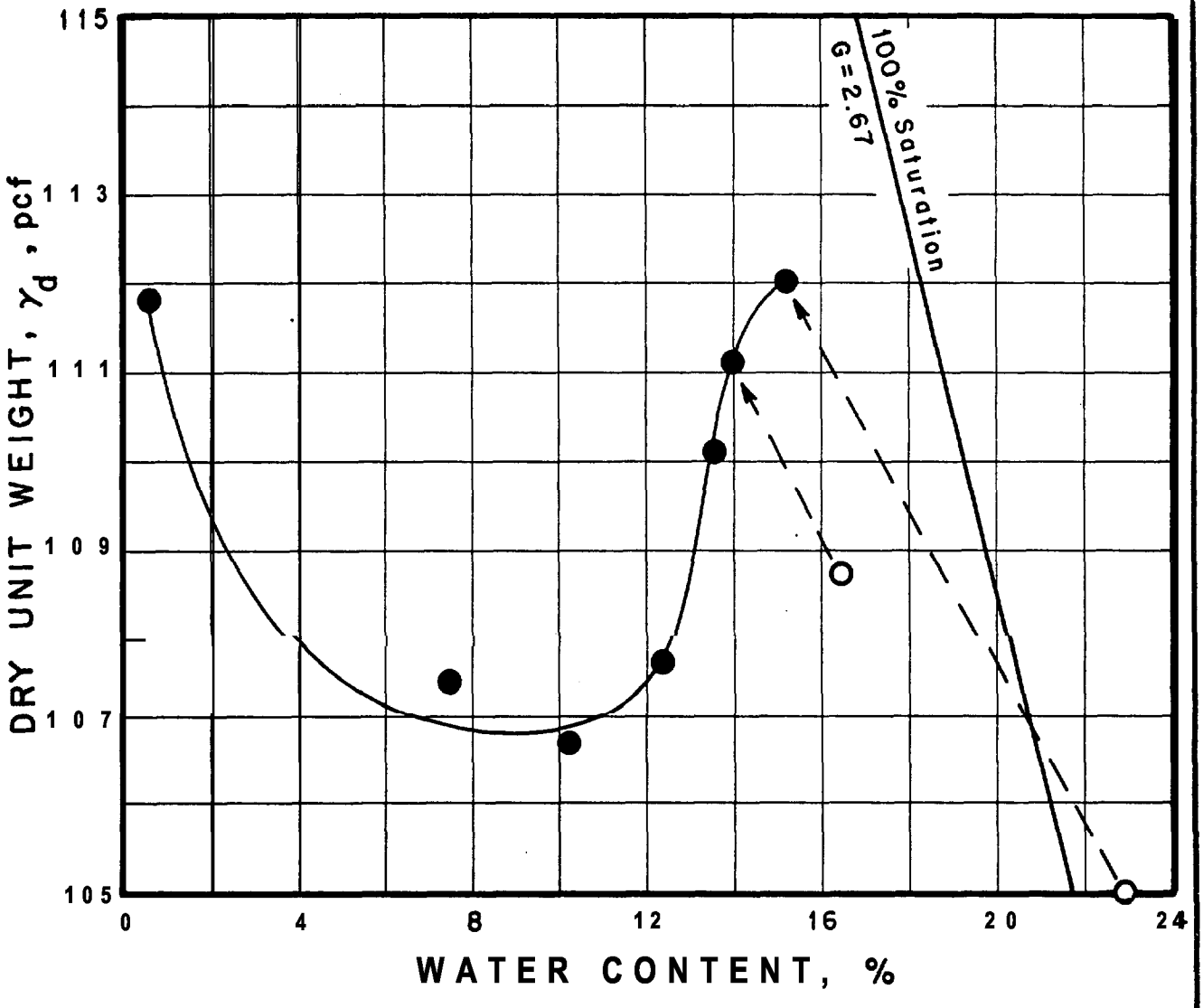

● As mixed before compaction

O After compaction

PUBLIC SERVICE COMPANY OF NEW HAMPSHIRE	TRIAXIAL TESTS STRUCTURAL BACKFILL	MOISTURE - DENSITY RELATION TEST BEARD PIT No.5 SOIL
GEOTECHNICAL ENGINEERS INC. WINCHESTER, MASSACHUSETTS	PROJECT 77386	January 23, 1978 Fig. 3

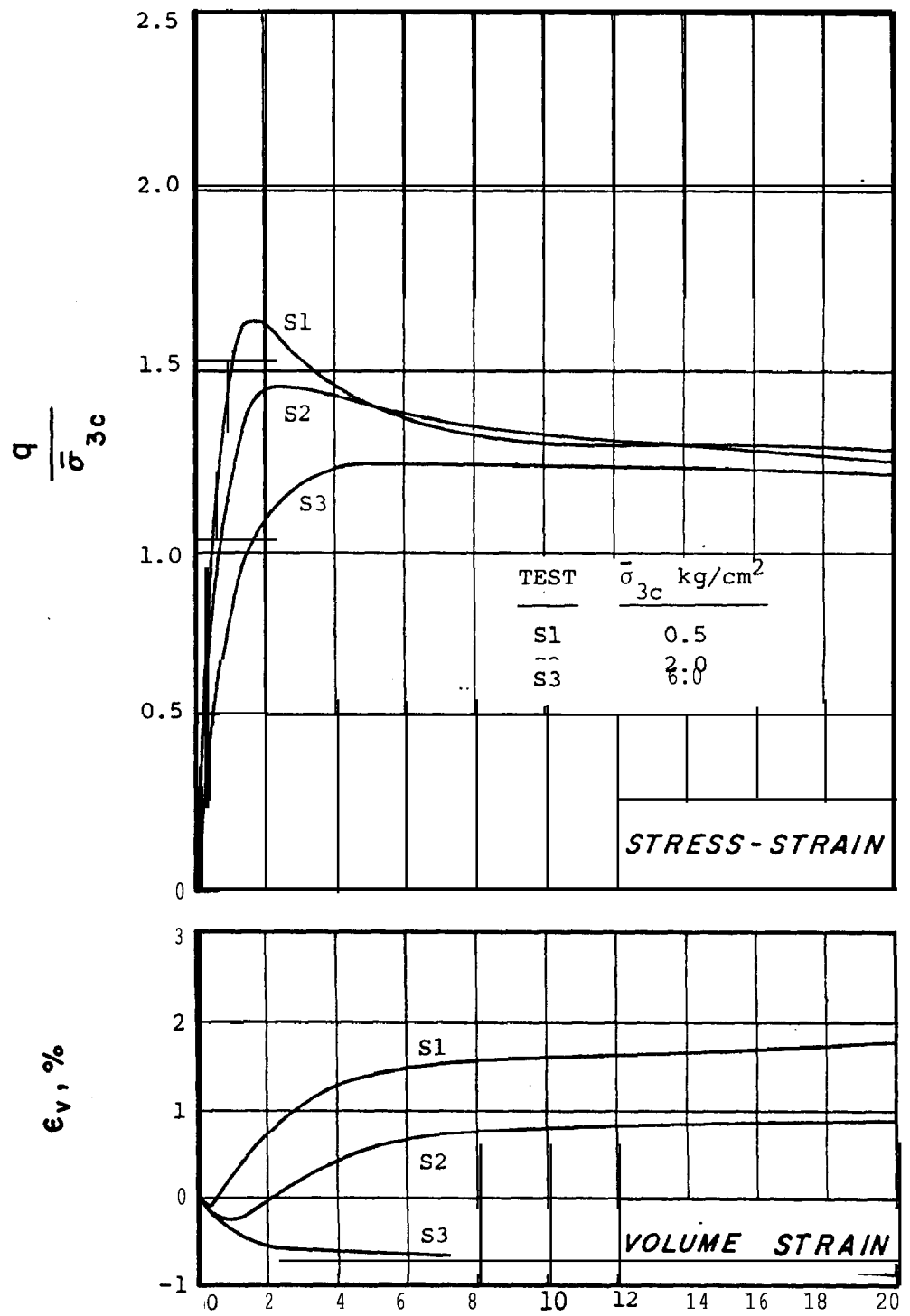

PUBLIC SERVICE COMPANY OF NEW HAMPSHIRE	TRIAXIAL TESTS STRUCTURAL BACKFILL	SUMMARY OF CONSOLIDATED-DRAINED TRIAXIAL TESTS 90% COMPACTION
GEOTECHNICAL ENGINEERS INC. WINCHESTER, MASSACHUSETTS	PROJECT 77366	DECEMBER, 1977 FIG. 4

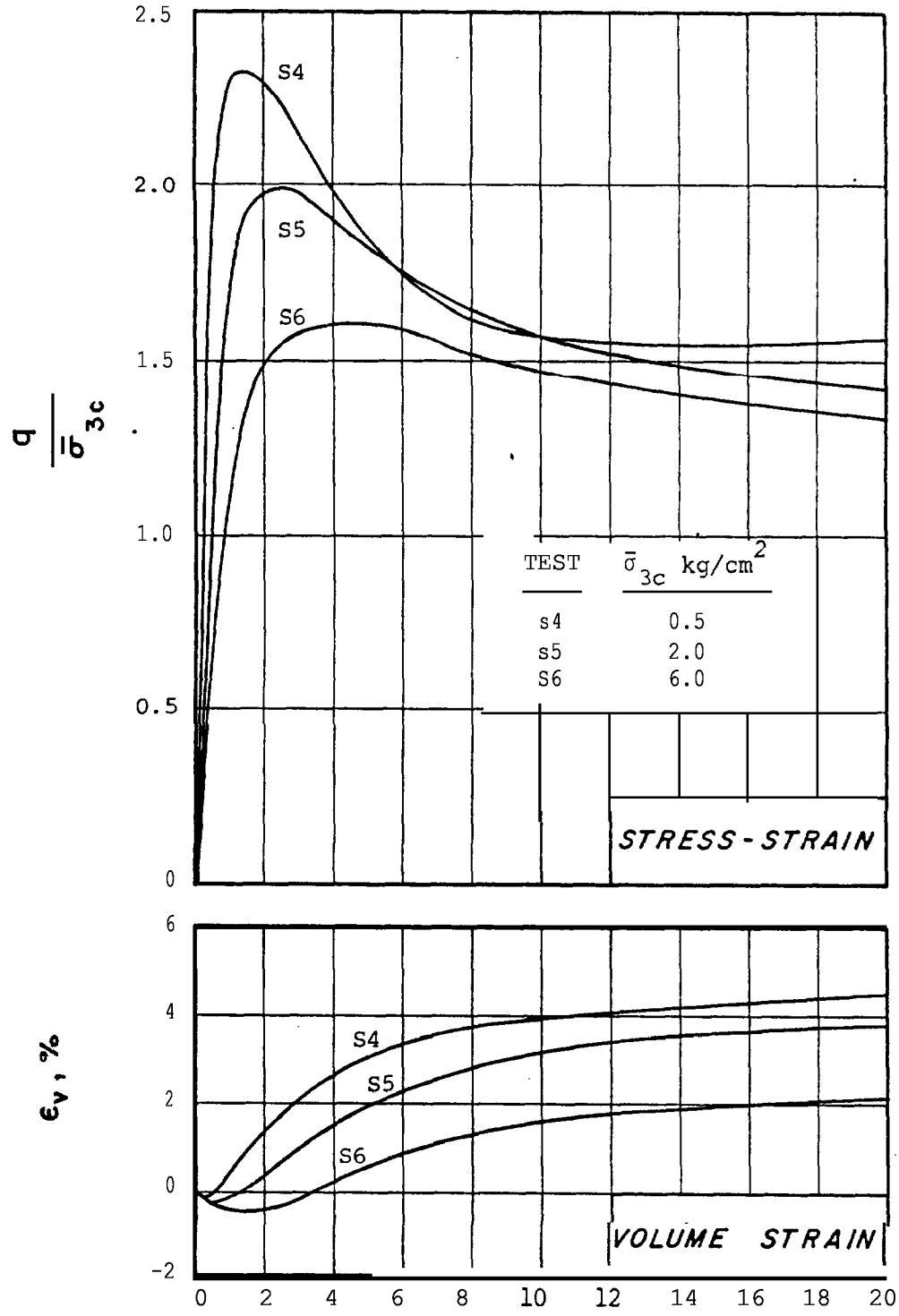

PUBLIC SERVICE COMPANY OF NEW HAMPSHIRE	TRIAXIAL TESTS STRUCTURAL BACKFILL	**SUMMARY OF** CONSOLIDATED-**DRAINED TRIAXIAL TESTS** 95% **COMPACTION**
GEOTECHNICAL ENGINEERS INC. WINCHESTER, MASSACHUSETTS	PROJECT 77386	DECEMBER, 1977 FIG. 5

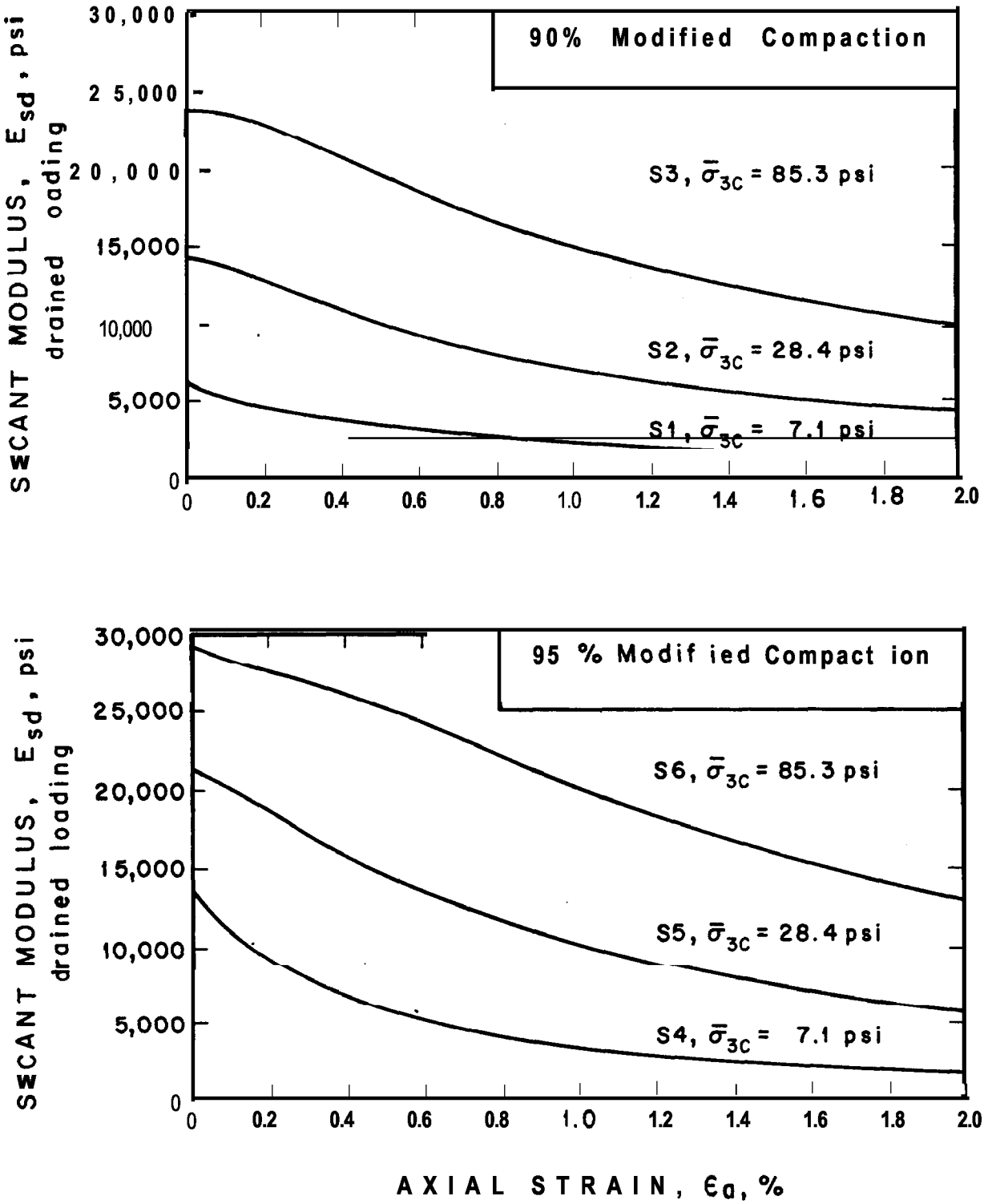

PUBLIC SERVICE COMPANY OF NEW HAMPSHIRE STRUCTURAL BACKFILL	TRIAXIAL TESTS	MODULI FOR DRAINED LOADING
GEOTECHNICAL ENGINEERS INC. WINCHESTER, MASSACHUSETTS	PROJECT 77386	JANUARY 23, 1978 Fig.6

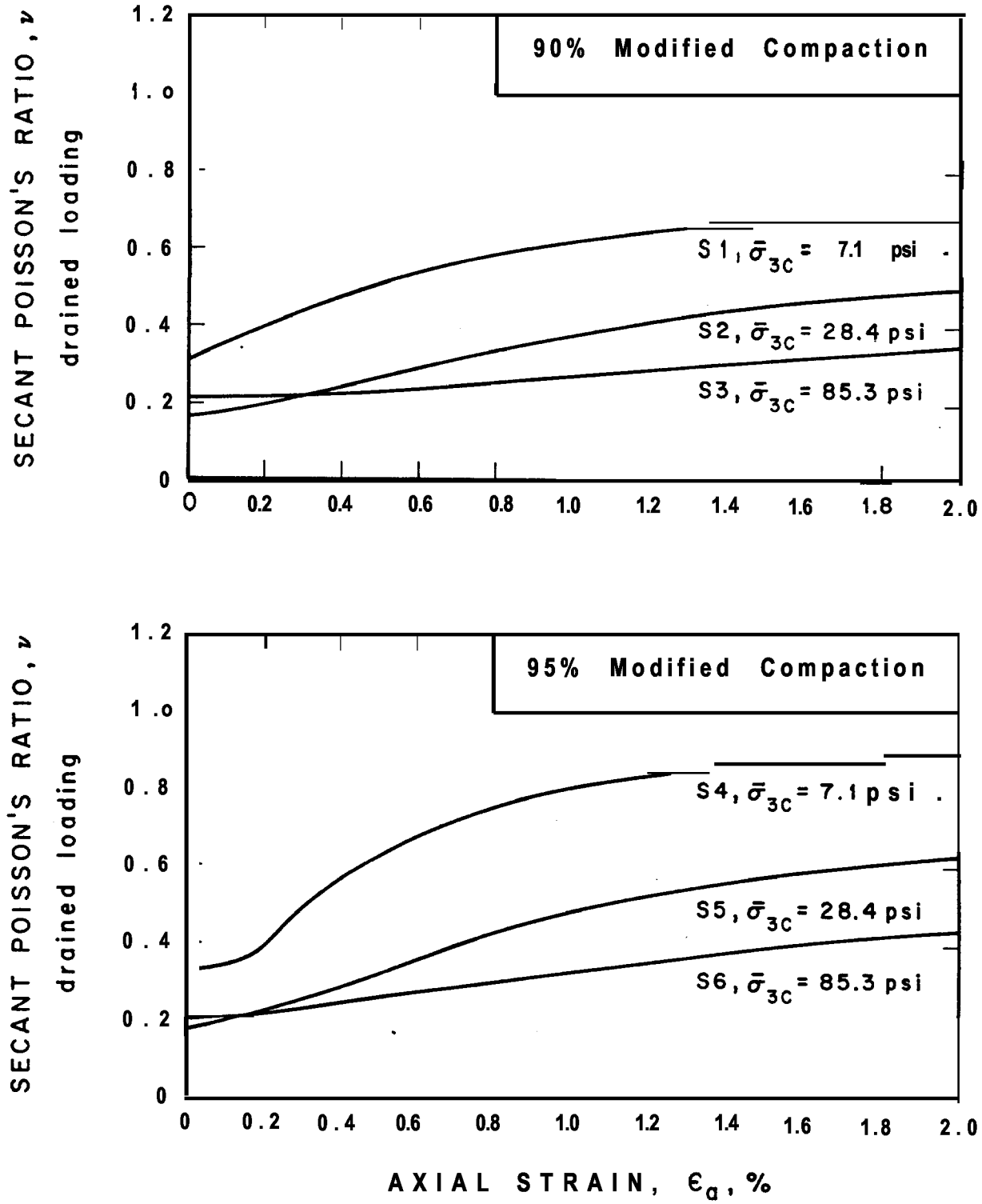

PUBLIC SERVICE COMPANY OF NEW HAMPSHIRE	TRIAXIAL TESTS STRUCTURAL BACKFILL	POISSON'S RATIOS FOR DRAINED LOADING
GEOTECHNICAL ENGINEERS INC. WINCHESTER, MASSACHUSETTS	PROJECT 77386	JANUARY 23,1978 Fig. 7

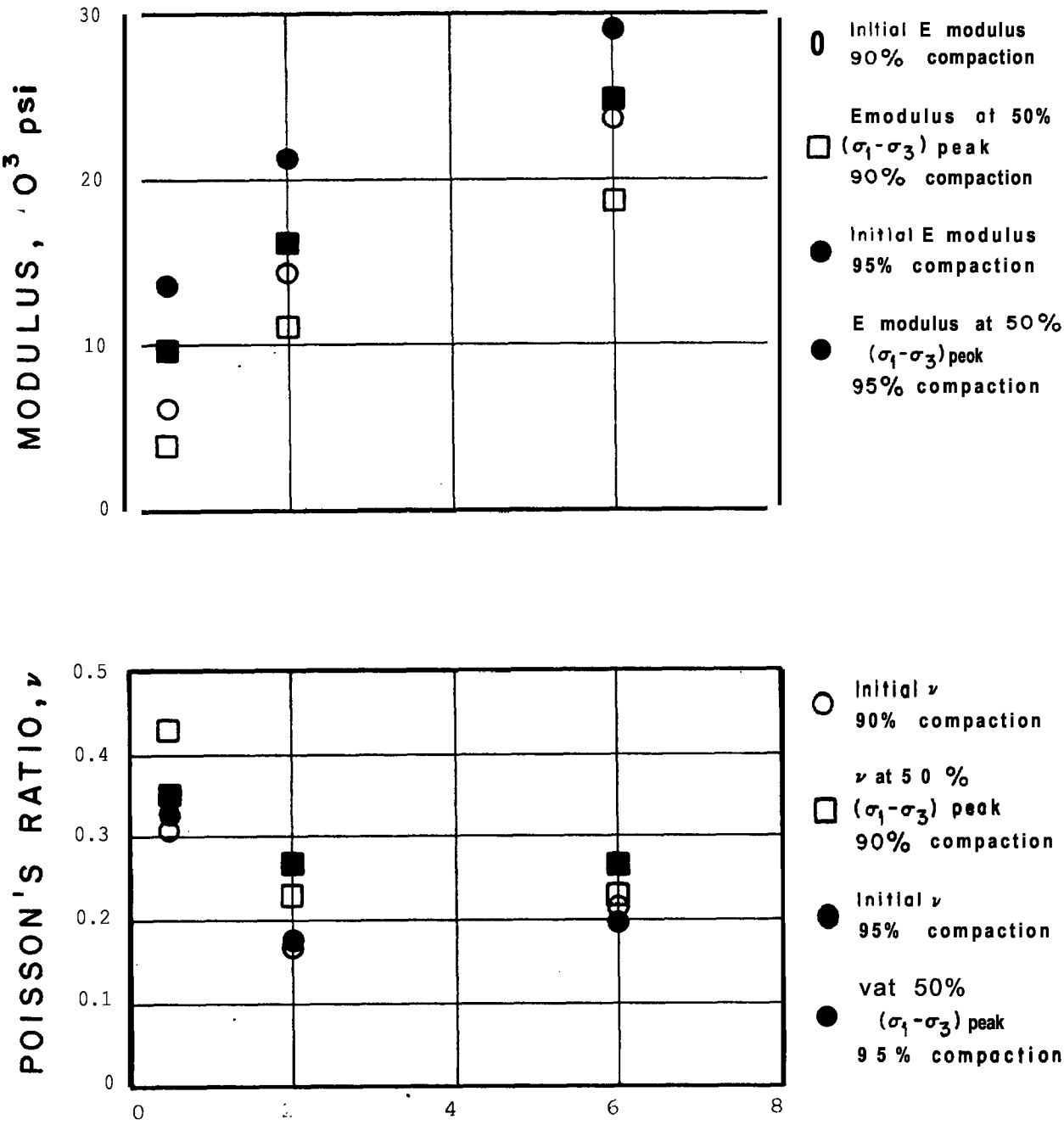

PUBLIC SERVICE COMPANY OF NEW HAMPSHIRE B A C K	TRIAXIAL TESTS STRUCTURAL L L	SUMMARY OF CONSOLIDATED-DRAINED TRIAXIAL TESTS
GEOTECHNICAL ENGINEERS INC. WINCHESTER, MASSACHUSETTS	PROJECT 77386	DECEMBER, 1977 FIG. 8

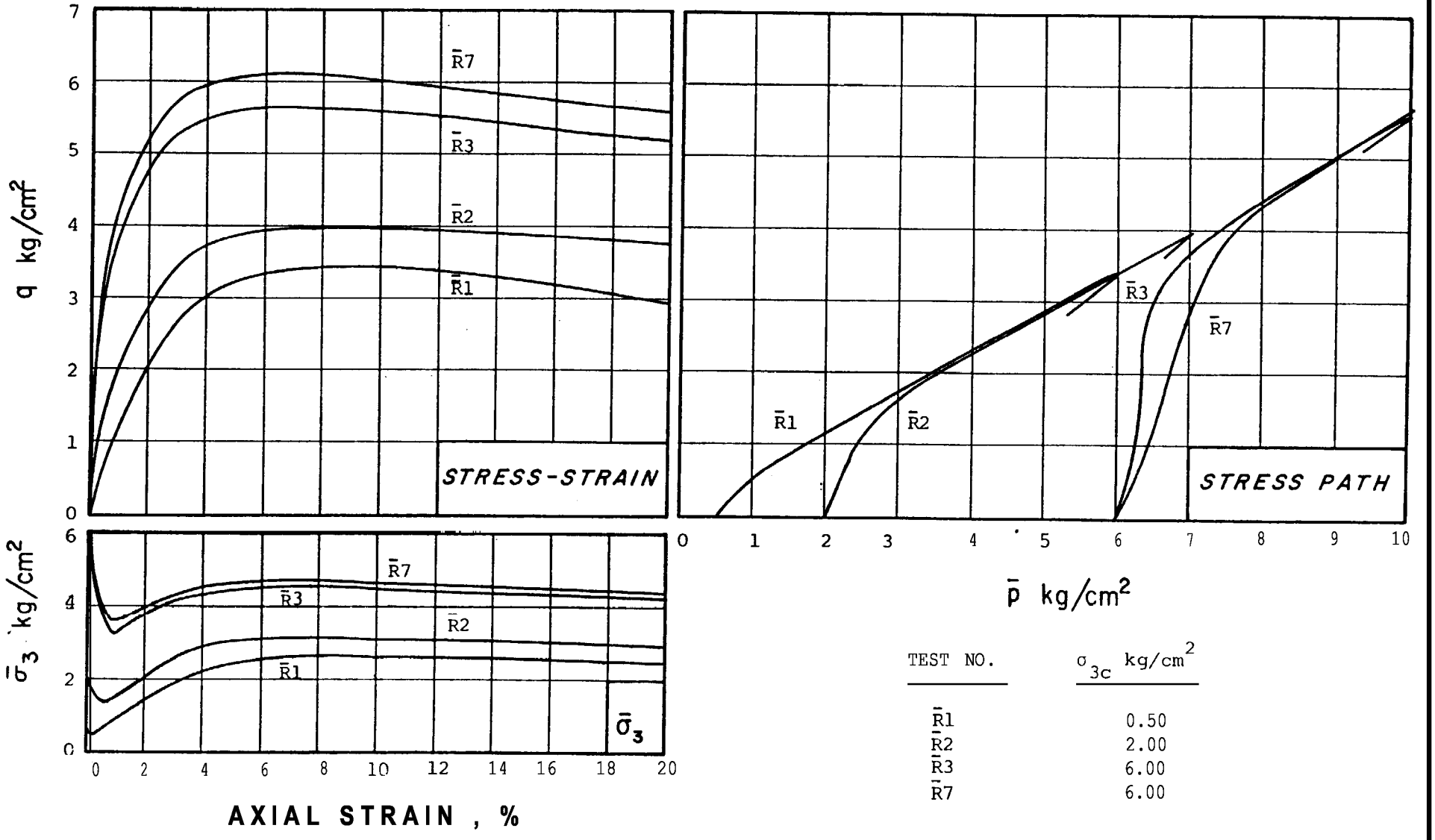

TEST NO.	σ_{3c} kg/cm^2
R̄1	0.50
R̄2	2.00
R̄3	6.00
R̄7	6.00

PUBLIC SERVICE COMPANY OF NEW HAMPSHIRE	TRIAXIAL TESTS STRUCTURAL BACKFILL	SUMMARY OF CONSOLIDATED-UNDRAINED TRIAXIAL TESTS 90% COMPACTION
GEOTECHNICAL ENGINEERS INC. WINCHESTER, MASSACHUSETTS	PROJECT 77386	DECEMBER, 1977 FIG. 9

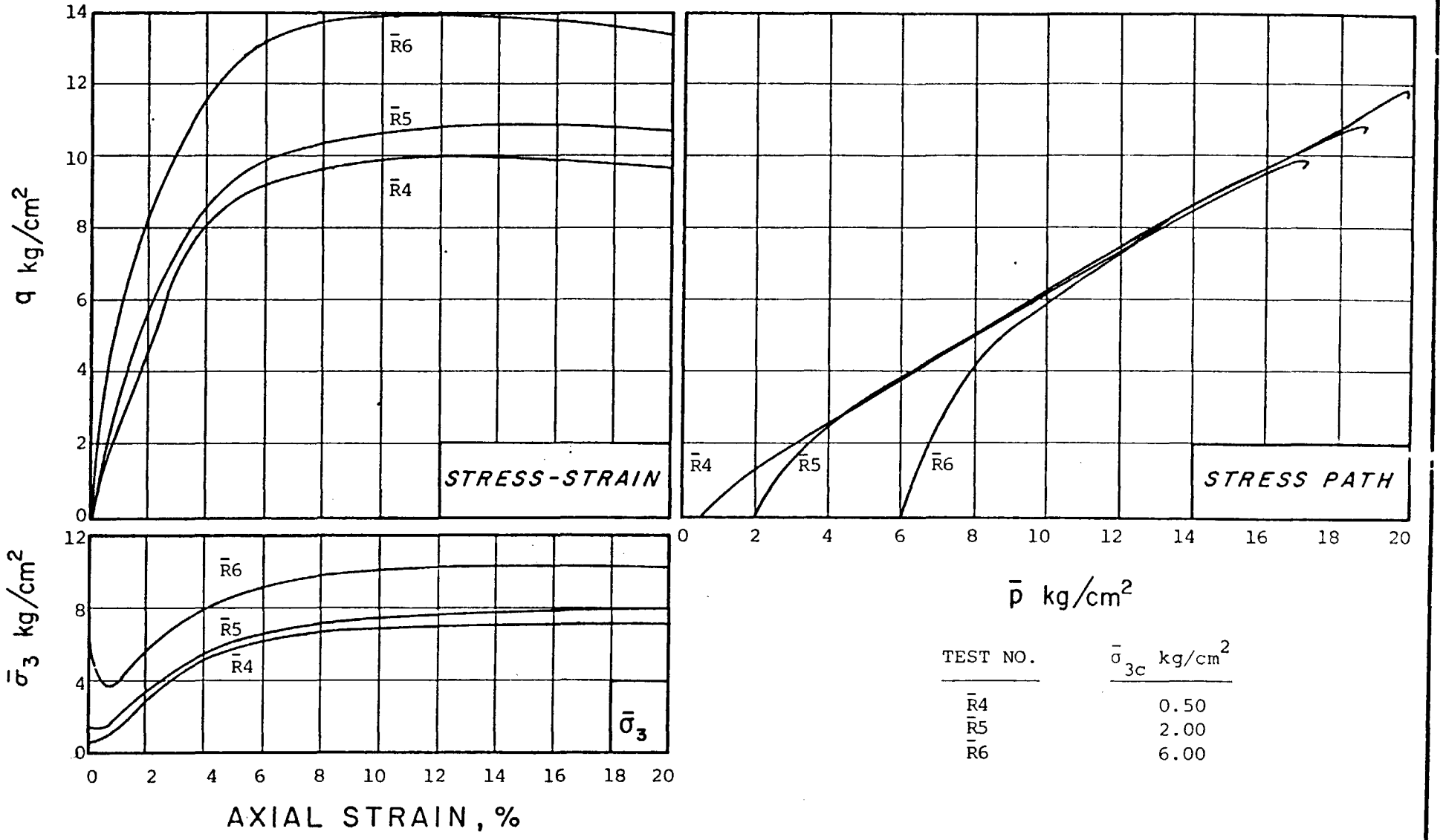

TEST NO.	$\bar{\sigma}_{3c}$ kg/cm²
R̄4	0.50
R̄5	2.00
R̄6	6.00

PUBLIC SERVICE COMPANY OF NEW HAMPSHIRE	TRIAXIAL TESTS STRUCTURAL BACKFILL	SUMMARY OF CONSOLIDATED-UNDRAINED TRIAXIAL TESTS 95% COMPACTION
GEOTECHNICAL ENGINEERS INC. WINCHESTER, MASSACHUSETTS	PROJECT 77386	DECEMBER, 1977 FIG. 10

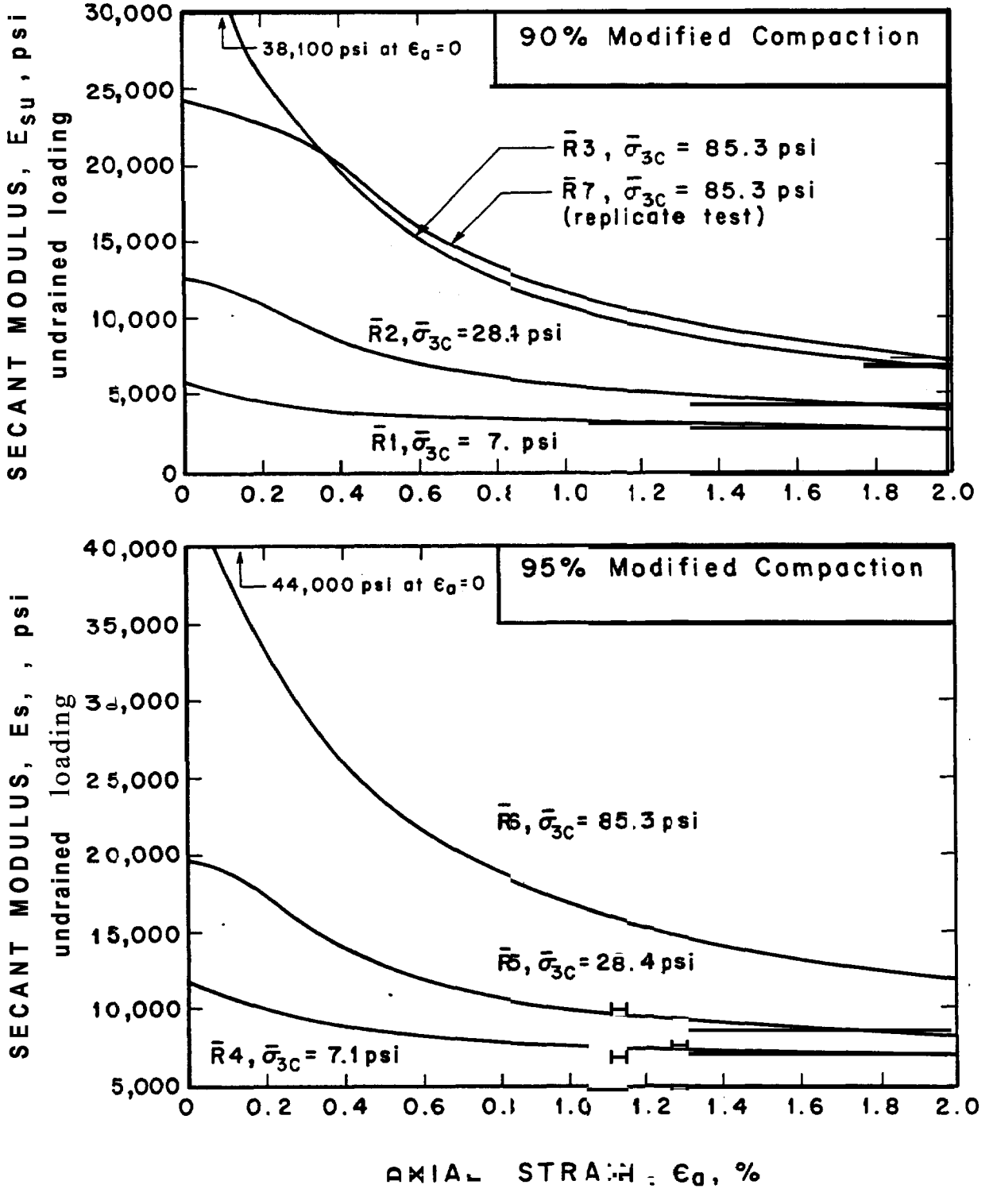

PUBLIC SERVICE COMPANY OF NEW HAMPSHIRE	TRIAXIAL TESTS STRUCTURAL BACKFILL	MODULI FOR UNDRAINED LOADING
GEOTECHNICAL ENGINEERS INC. WINCHESTER, MASSACHUSETTS	PROJECT 77386	JANUARY 23, 1978 Fig. 11

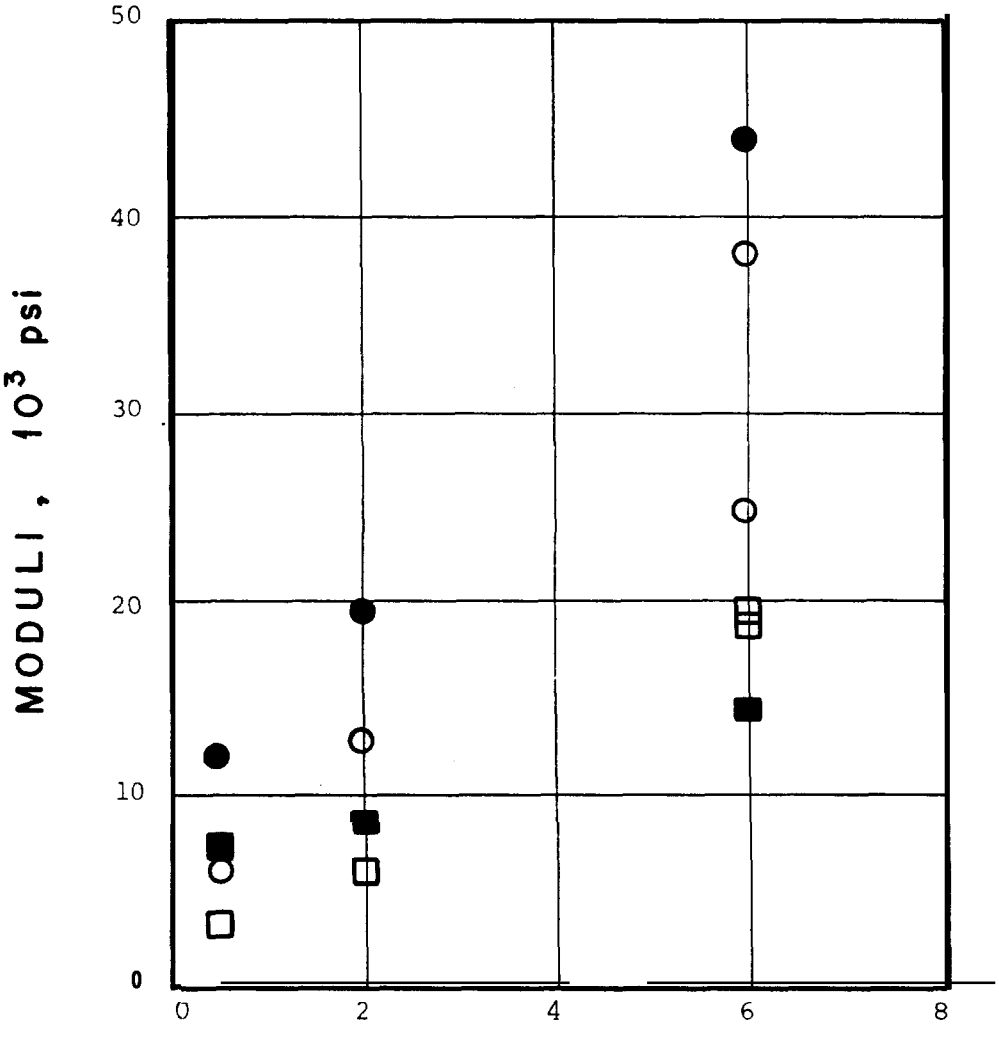

(Multiply by 14.22 for psi)

0'	E_0 90% Compaction
□	E_{50} 90% Compaction
●	E_0 95% Compaction
●	E_{50} 95% Compaction

NOTE POISSON'S RATIO FOR UNDRAINED TESTS MAY BE TAKEN AS 0.49 TO 0.50

PUBLIC SERVICE COMPANY OF NEW HAMPSHIRE	TRIAXIAL TESTS STRUCTURAL BACKFILL	SUMMARY OF MODULI FOR CONSOLIDATED-UNDRAINED TESTS
GEOTECHNICAL ENGINEERS INC. WINCHESTER, MASSACHUSETTS	PROJECT 77386	DECEMBER, 1977 FIG. 12

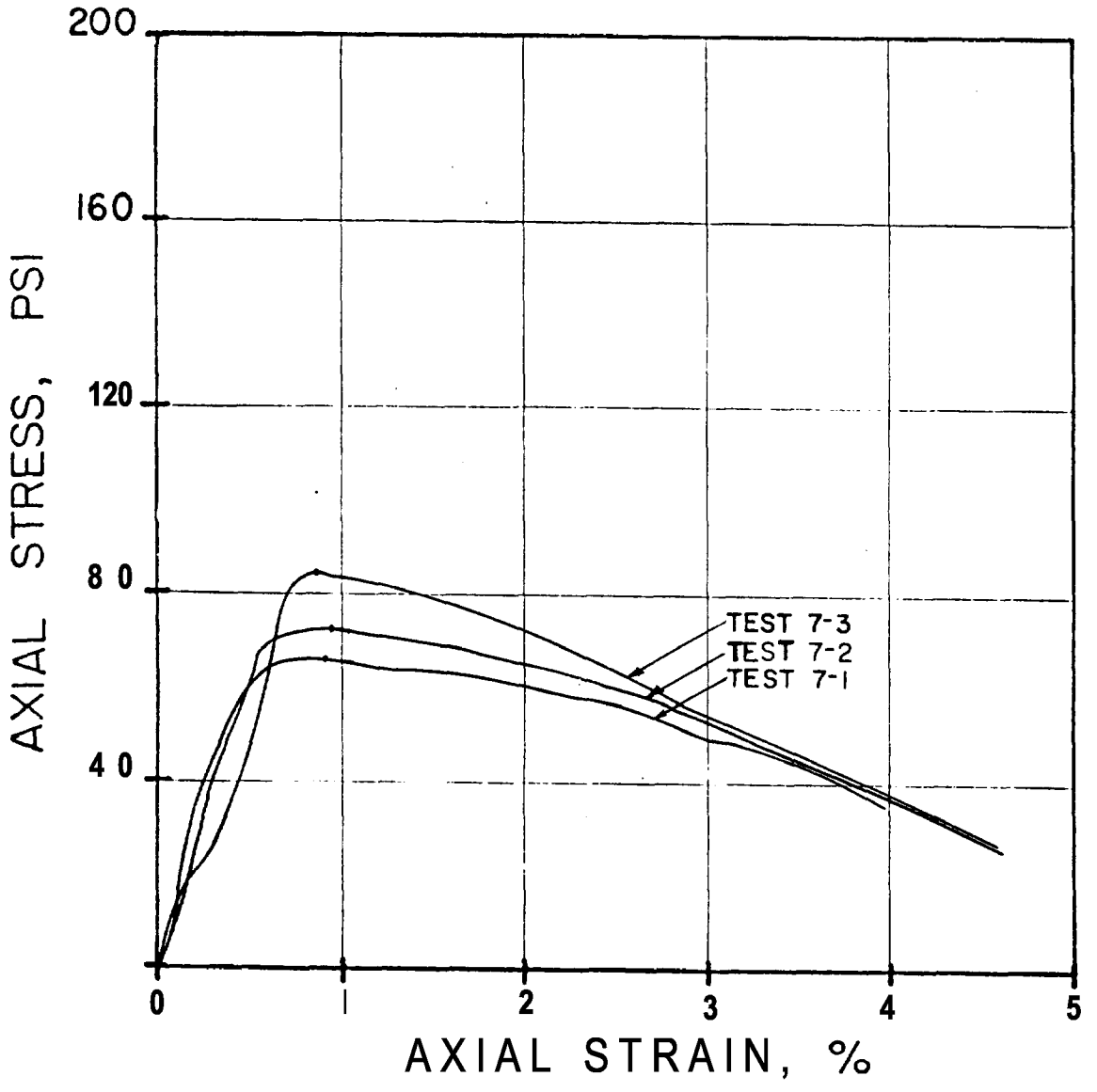

Sand-Cement Mixture (by weight):

1 part cement
16.18 parts sand (oven-dry)
2.79 parts water

Prepared as per ASTM C305

Specimens Tested:

2 in. cube specimens
Cured 7 days
Unit weight after cure (pcf)
7-1 124.0
7-2 123.9
7-3 126.2
Strain control. loading at 1.5 mm/min

Public Service Company of New Hampshire	Triaxial Tests Sand-Cement Backfill Seabrook Station	COMPRESSION TESTS 7-DAY CURE 5% CEMENT
Geotechnical Engineers Inc. Winchester, Massachusetts	Project 77386	January 1978 Fig. 13

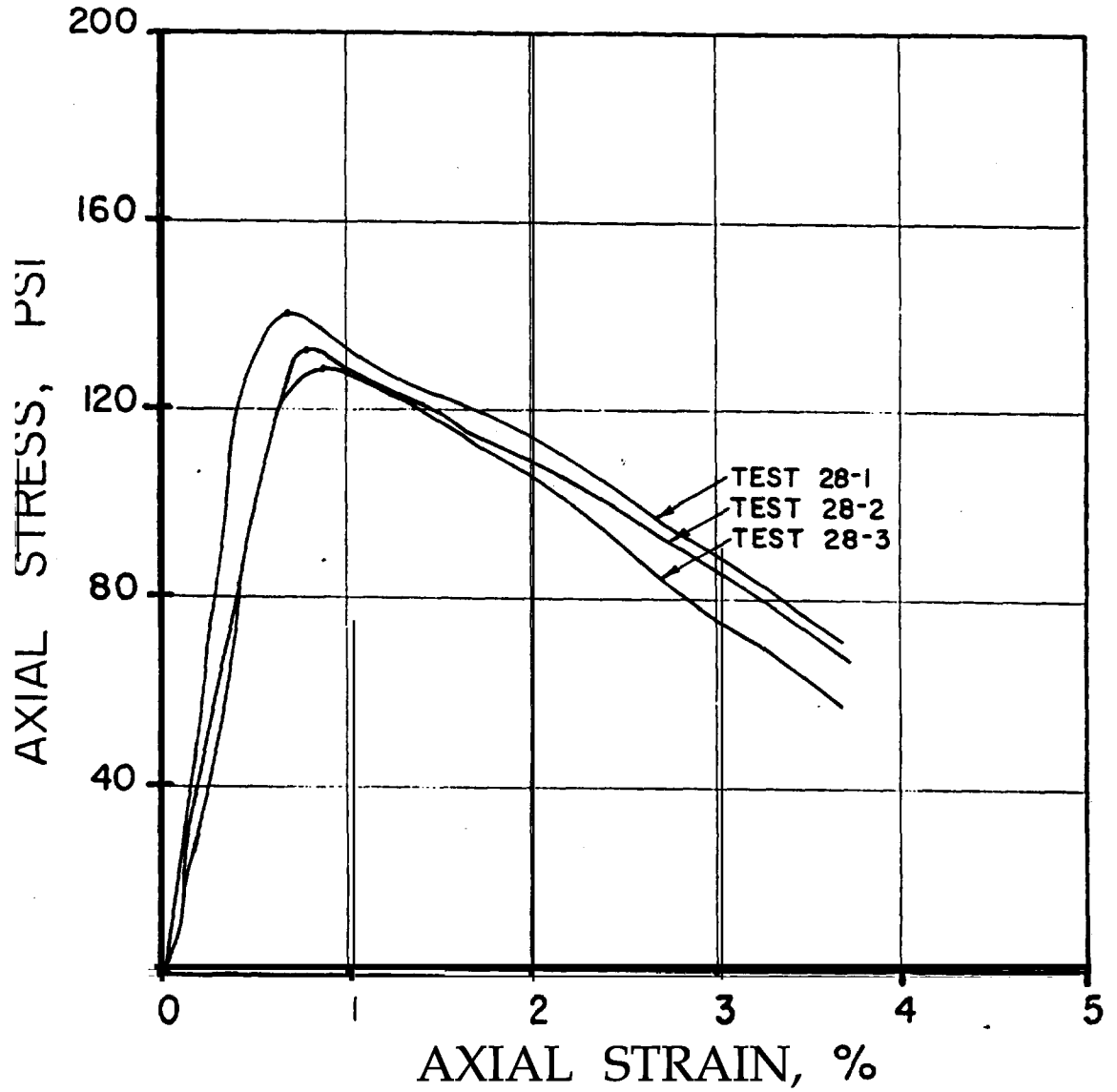

Sand-Cement Mixture (by weight):

1 part cement
16.18 parts sand (oven-dry)
2.79 parts water

Prepared as per ASTM C305

Specimens Tested:

2 in. cube specimens
Cured 28 days
Unit weight after cure (pcf)
28-1 127.4
28-2 126.2
28-3 126.8
Strain control loading at 1.5 mm/min

Public Service Company of New Hampshire	Triaxial Tests Sand-Cement Backfill Seabrook Station	COMPRESSION TESTS 28-DAY CURB 5% CEMENT
Geotechnical Engineers Inc. Winchester, Massachusetts	Project 77386	January 1978 Fig.14

APPENDIX A

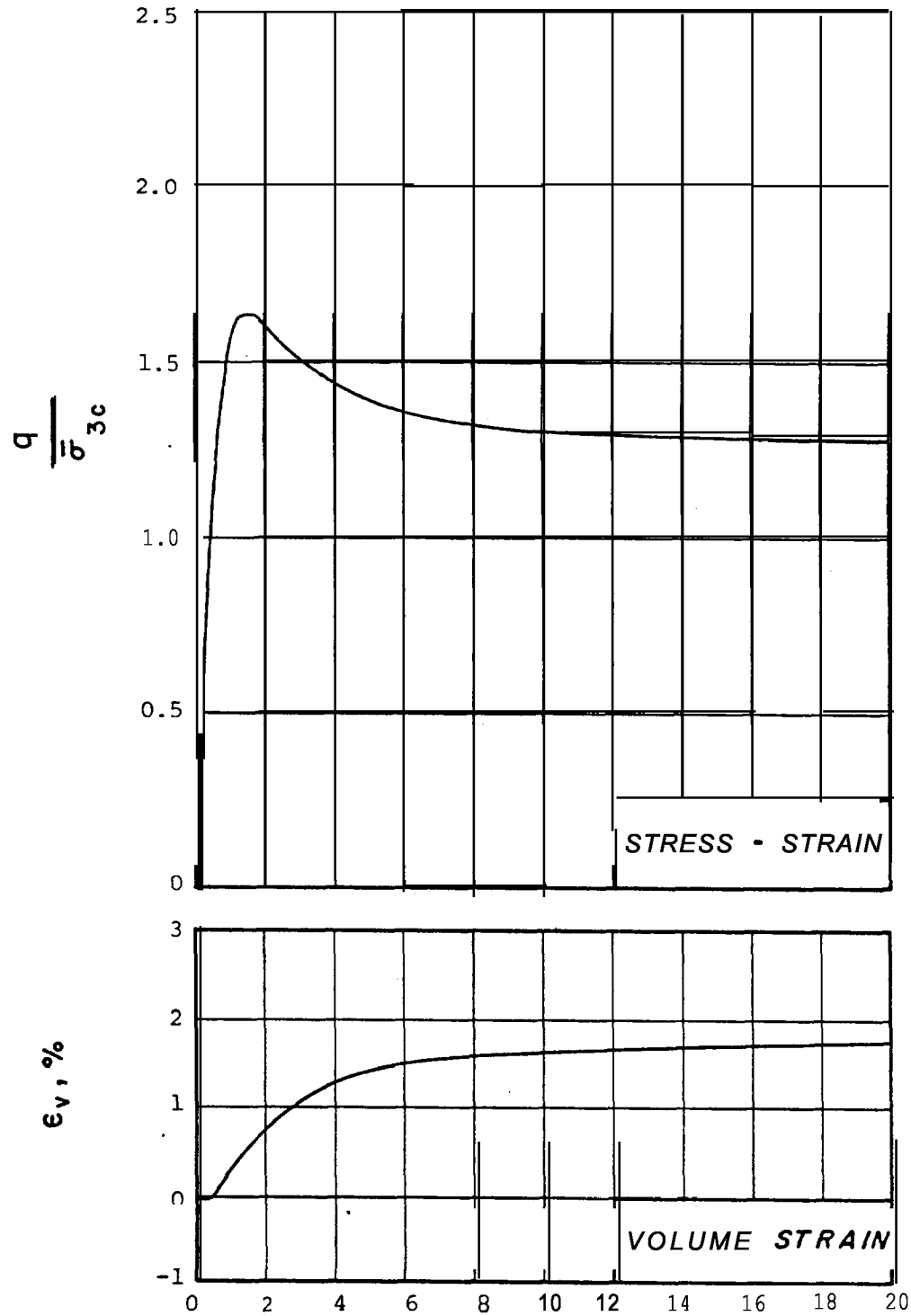

TEST S1 90% Compaction $\bar{\sigma}_{3c}$ = 0.5 kg/cm^2

PUBLIC SERVICE COMPANY OF NEW HAMPSHIRE	TRIAXIAL TESTS STRUCTURAL BACK FILL	CONSOLIDATED-DRAINED TRIAXIAL TEST S1
GEOTECHNICAL ENGINEERS INC. WINCHESTER, MASSACHUSETTS	PROJECT 77386	DECEMBER, 1977 FIG. A.

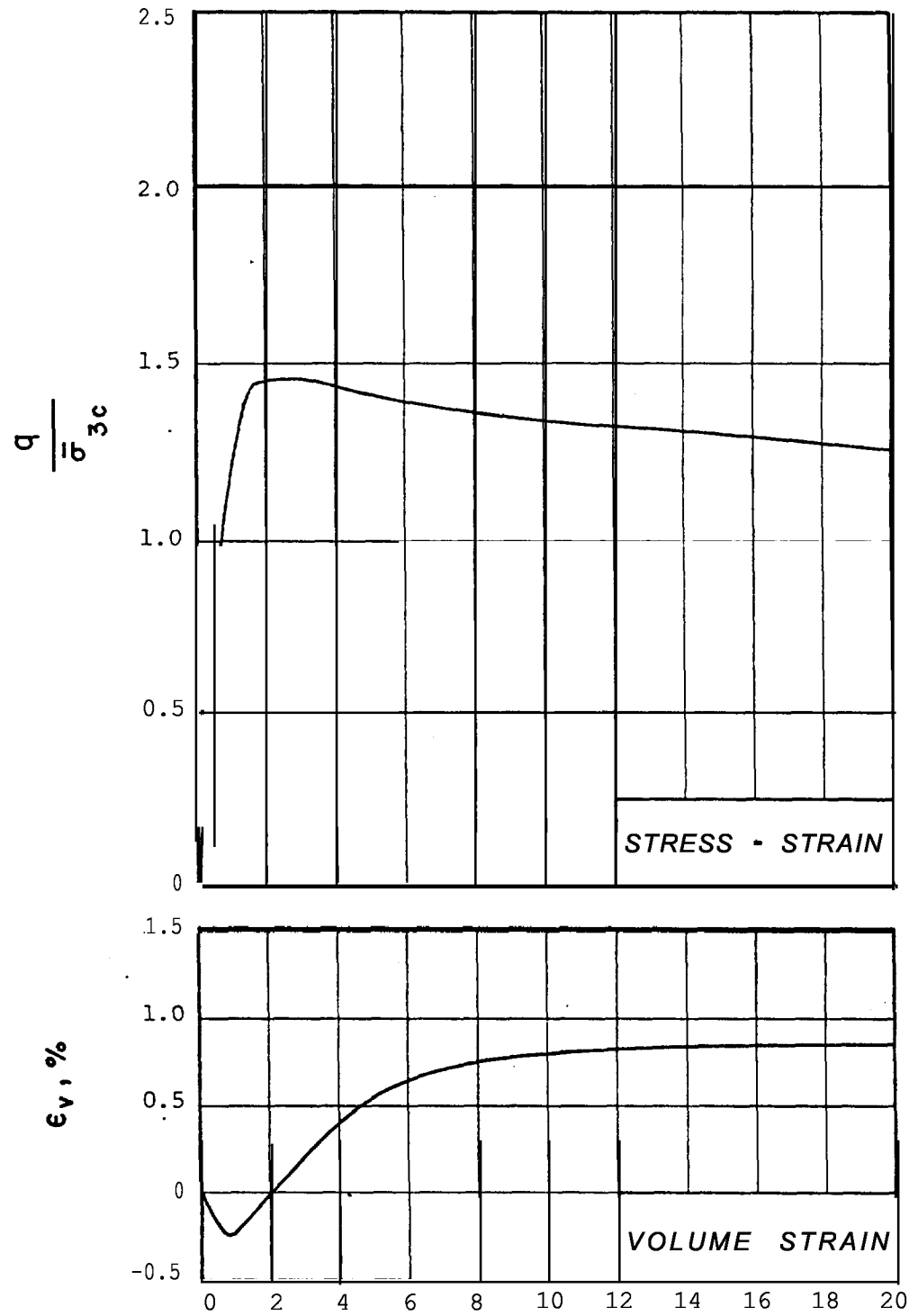

TEST S2 90% Compaction $\bar{\sigma}_{3c}$ = 2.0 kg/cm^2

PUBLIC SERVICE COMPANY OF NEW HAMPSHIRE STRUCTURAL BACKFILL	TRIAXIAL TESTS	**CONSOLIDATED-DRAINED TRIAXIAL TEST S2**
GEOTECHNICAL ENGINEERS INC. WINCHESTER, MASSACHUSETTS	PROJECT 77386	DECEMBER, 1977 FIG. **A2**

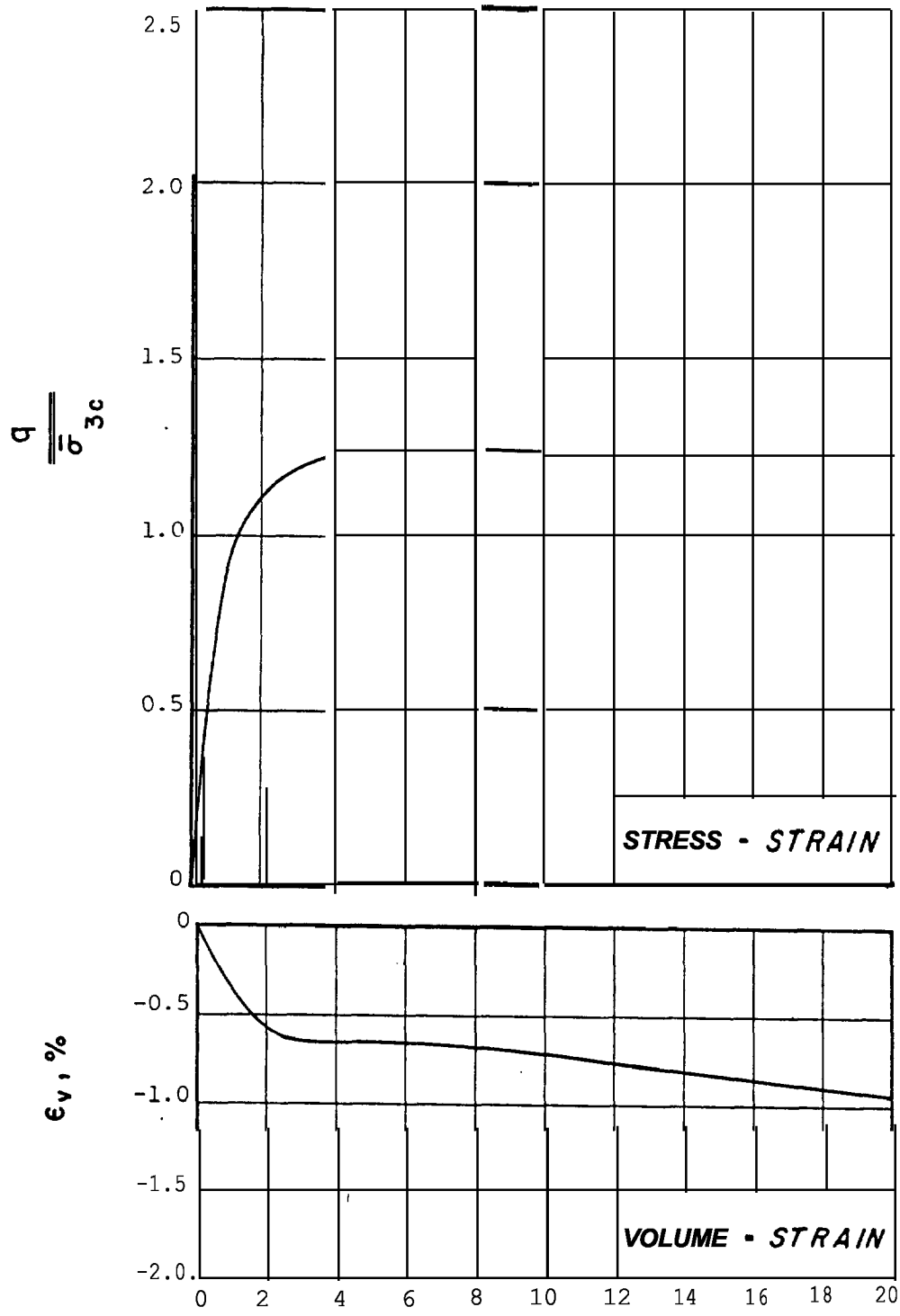

TEST S3 90% Compaction $\bar{\sigma}_{3c}$ = 6.0 kg/cm^2

PUBLIC SERVICE COMPANY OF NEW HAMPSHIRE	TRIAXIAL TESTS STRUCTURAL BACKFILL	CONSOLIDATED-DRAINED TRIAXIAL TEST S3
GEOTECHNICAL ENGINEERS INC. WINCHESTER, MASSACHUSETTS	PROJECT 77386	DECEMBER, 1977 FIG. A3

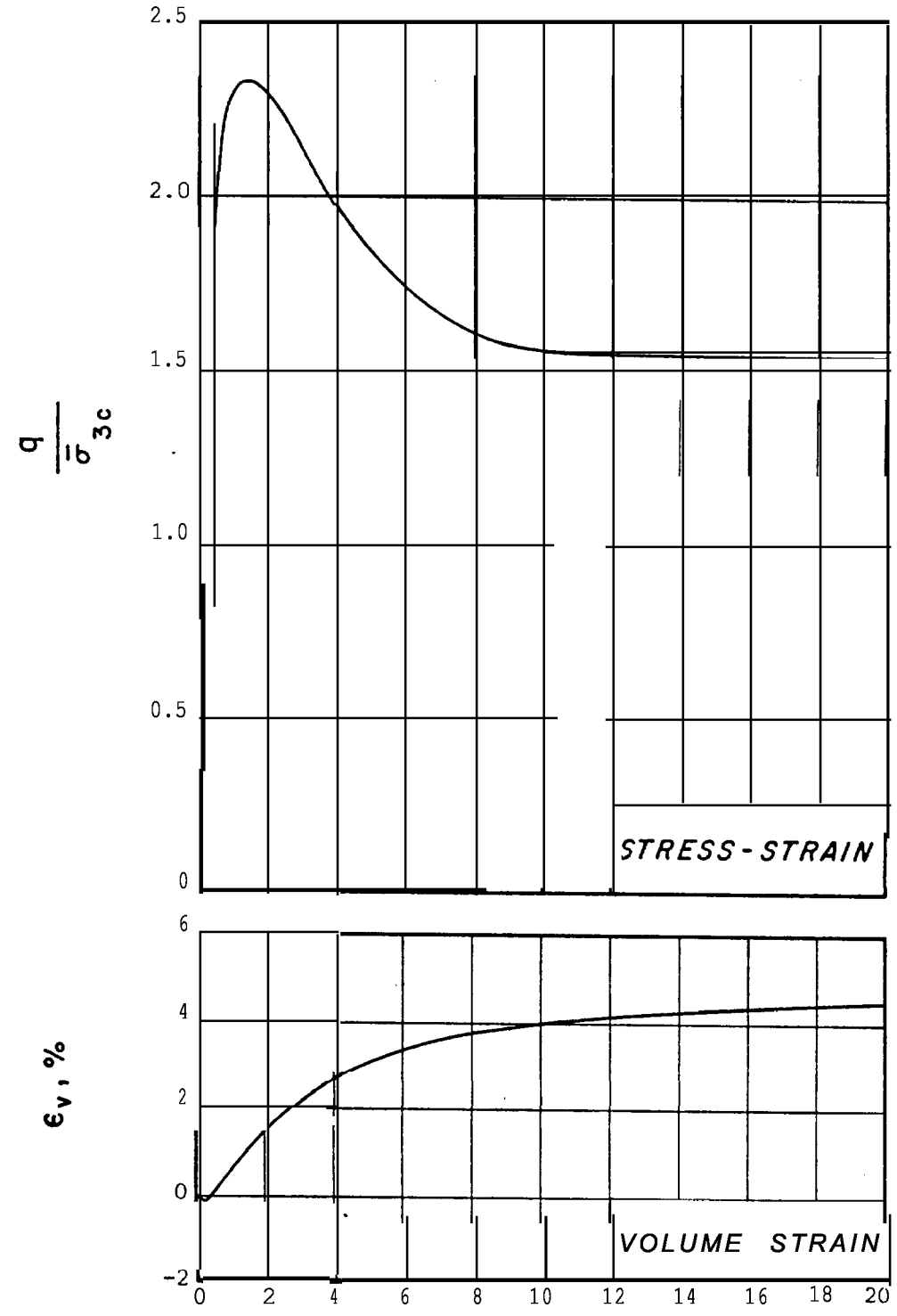

TEST S4 95% Compaction $\bar{\sigma}_{3c}$ = 0.5 kg/cm^2

PUBLIC SERVICE COMPANY OF NEW HAMPSHIRE	TRIAXIAL TESTS STRUCTURAL BACKFILL	CONSOLIDATED-DRAINED TRIAXIAL TEST S4
GEOTECHNICAL ENGINEERS INC WINCHESTER, MASSACHUSETTS	PROJECT 77386	DECEMBER, 1977 FIG. A4

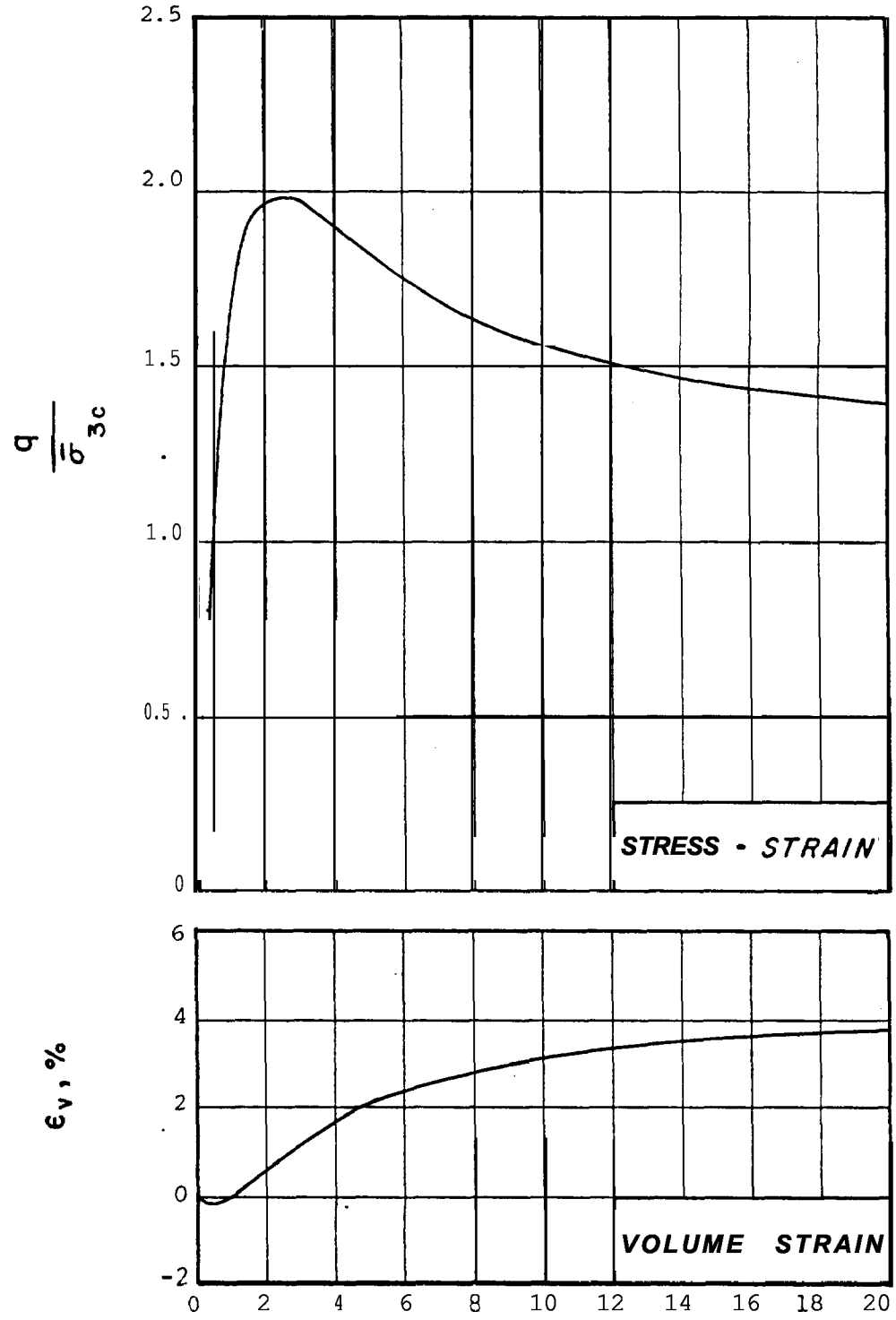

AXIAL STRAIN, %

TEST S5 95% Compaction $\bar{\sigma}_{3c}$ = 2.0 kg/cm^2

PUBLIC SERVICE COMPANY OF NEW HAMPSHIRE	TRIAXIAL TESTS STRUCTURAL BACKFILL	**CONSOLIDATED-DRAINED** TRIAXIAL **TEST** S5
GEOTECHNICAL ENGINEERS INC. WINCHESTER, MASSACHUSETTS	PROJECT 77386 DECEMBER, 1977	FIG. A5

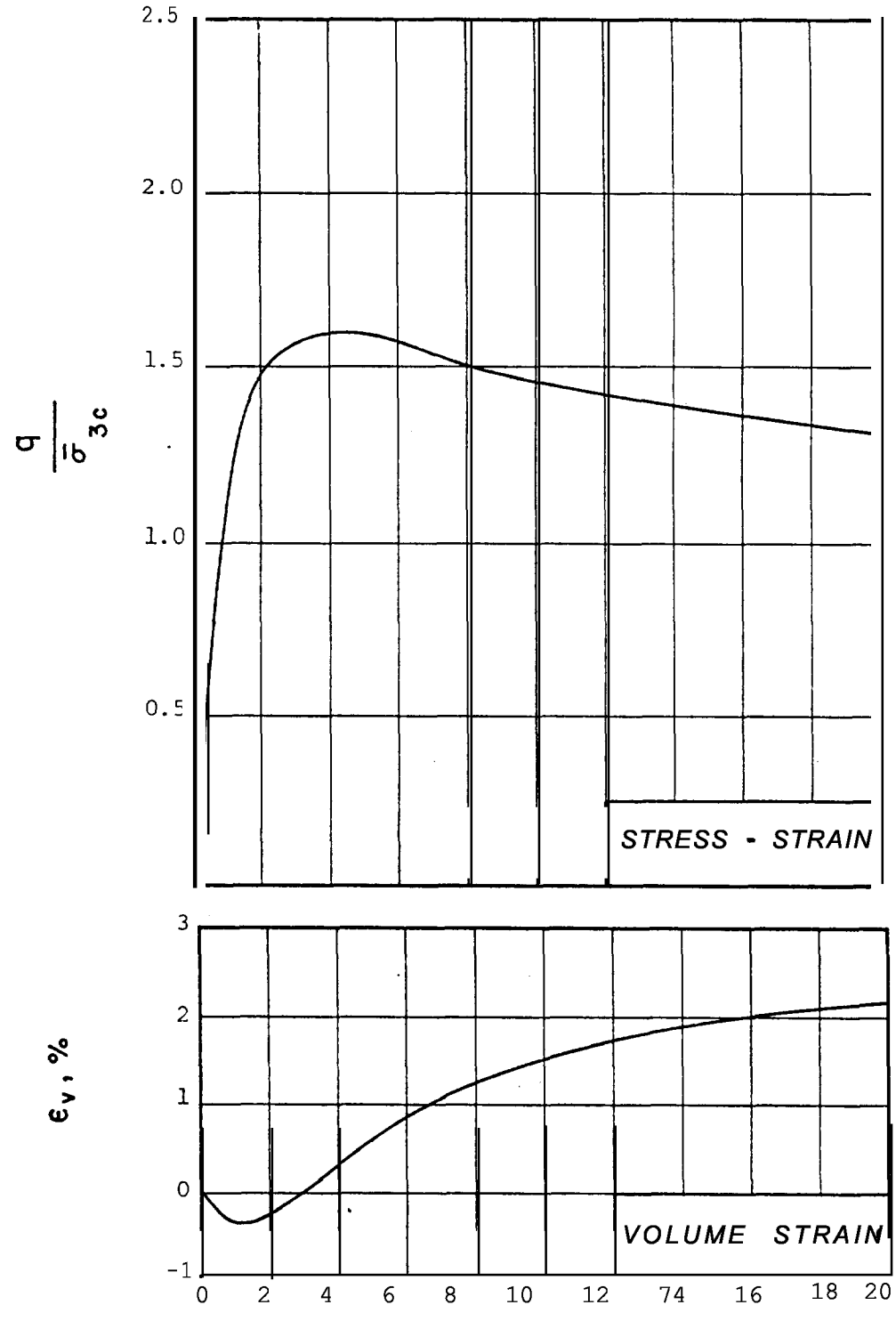

AXIAL STRAIN, %

TEST S6 95% Compaction $\bar{\sigma}_{3c}$ = 6.0 kg/cm^2

PUBLIC SERVICE COMPANY OF NEW HAMPSHIRE	TRIAXIAL TESTS STR UCTURAL BACK FI LL	CONSOLIDATED-DRAINED TRIAXIAL TEST S6
SEOTECHNICAL ENGINEERS INC. VINCHESTER, MASSACHUSETTS	PROJECT 77386	DECEMBER, 1977 FIG. A6

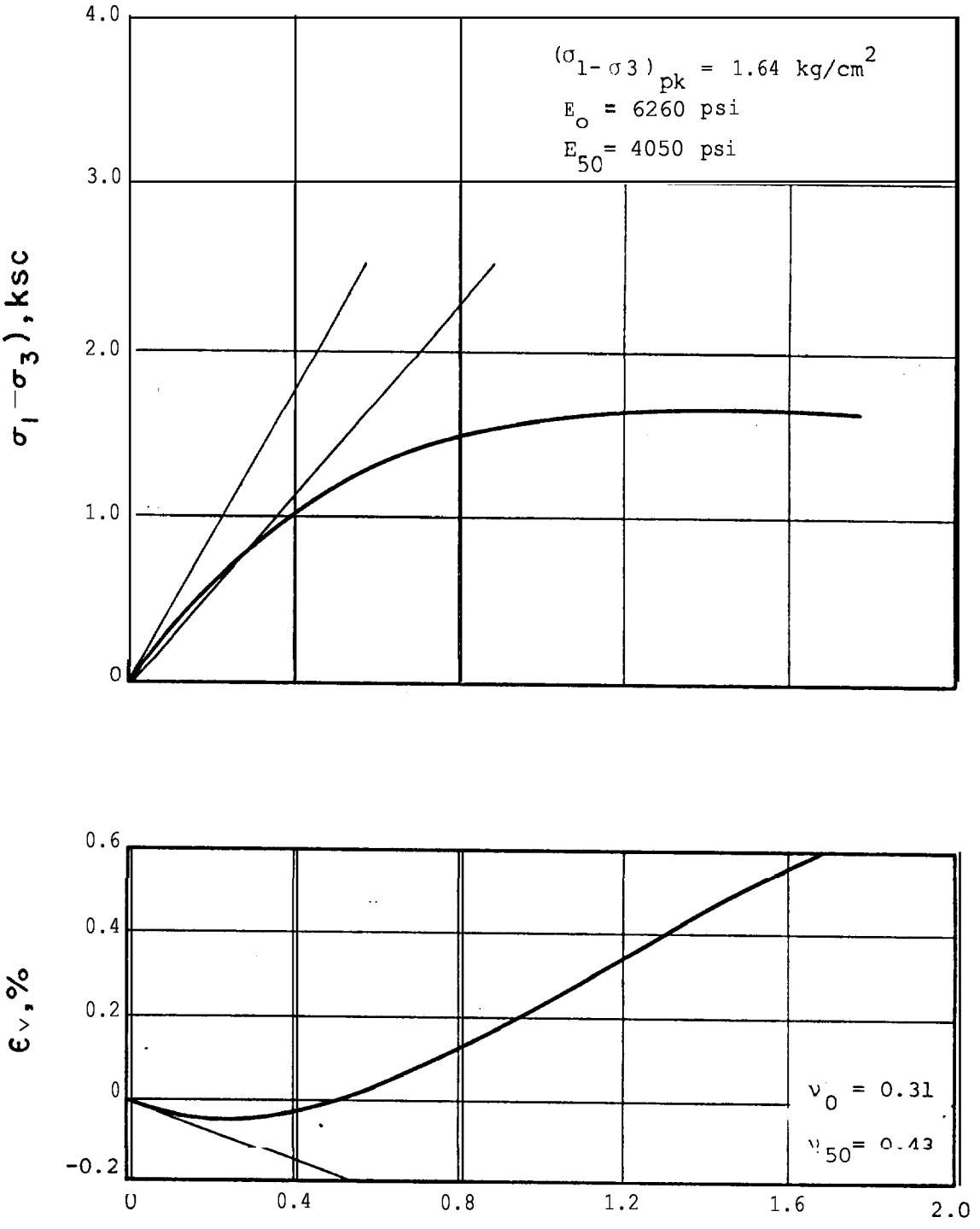

TEST S1 90% Compaction $\bar{\sigma}_{3c}$ = 0.5 kg/cm^2

PUBLIC SERVICE COMPANY OF NEW HAMPSHIRE	TRIAXIAL TESTS STRUCTURAL BACKFILL	CONSOLIDATED-DRAINED TRIAXIAL TEST S1 Expanded Scales
GEOTECHNICAL ENGINEERS INC. WINCHESTER, MASSACHUSETTS	PROJECT 77386	DECEMBER, 1977 FIG. A7

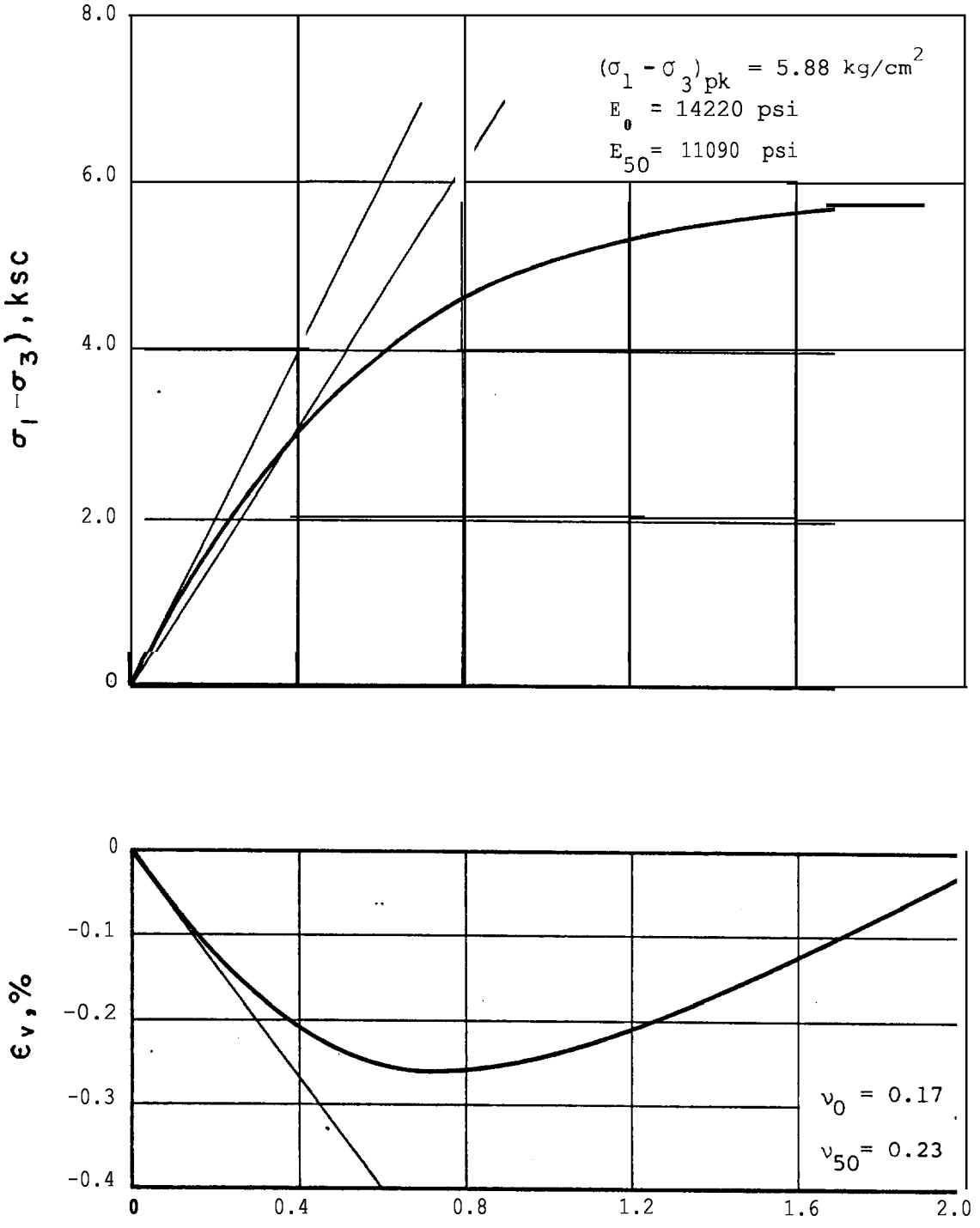

TEST S2 90% Compaction $\bar{\sigma}_{3c}$ = 2.0 kg/cm^2

PUBLIC SERVICE COMPANY OF NEW HAMPSHIRE	TRIAXIAL TESTS STRUCTURAL BACKFILL	CONSOLIDATED-DRAINED TRIAXIAL TEST S2 Expanded Scales
GEOTECHNICAL ENGINEERS INC. WINCHESTER, MASSACHUSETTS	PROJECT 77386	DECEMBER, 1977 FIG. A8

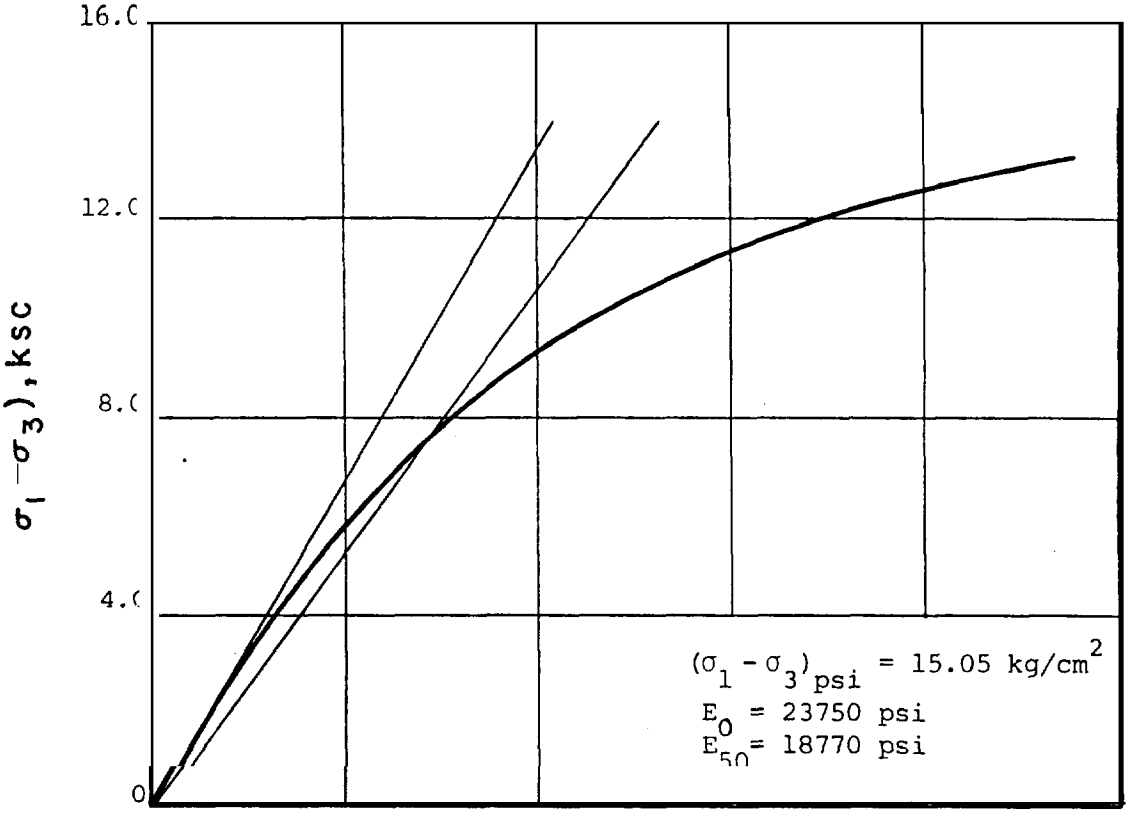

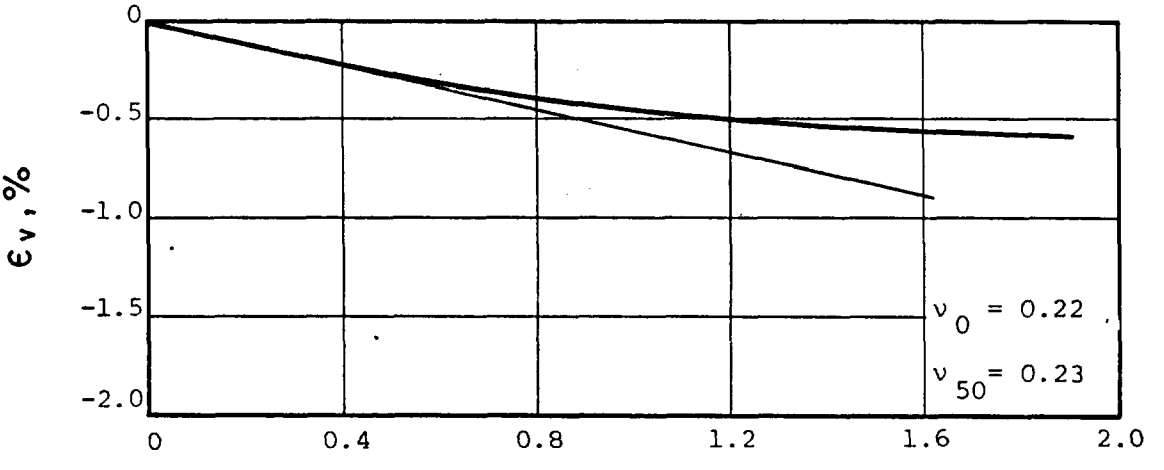

AXIAL STRAIN , %

TEST S3 90% Compaction $\bar{\sigma}_{3c}$ = 6.0 kg/cm^2

PUBLIC SERVICE COMPANY OF NEW HAMPSHIRE	TRIAXIAL TESTS STRUCTURAL BACKFILL	CONSOLIDATED-DRAINED TRIAXIAL **TEST S3** Expanded Scales
GEOTECHNICAL ENGINEERS INC. WINCHESTER, MASSACHUSETTS	PROJECT 77386	DECEMBER, 1977 FIG. A9

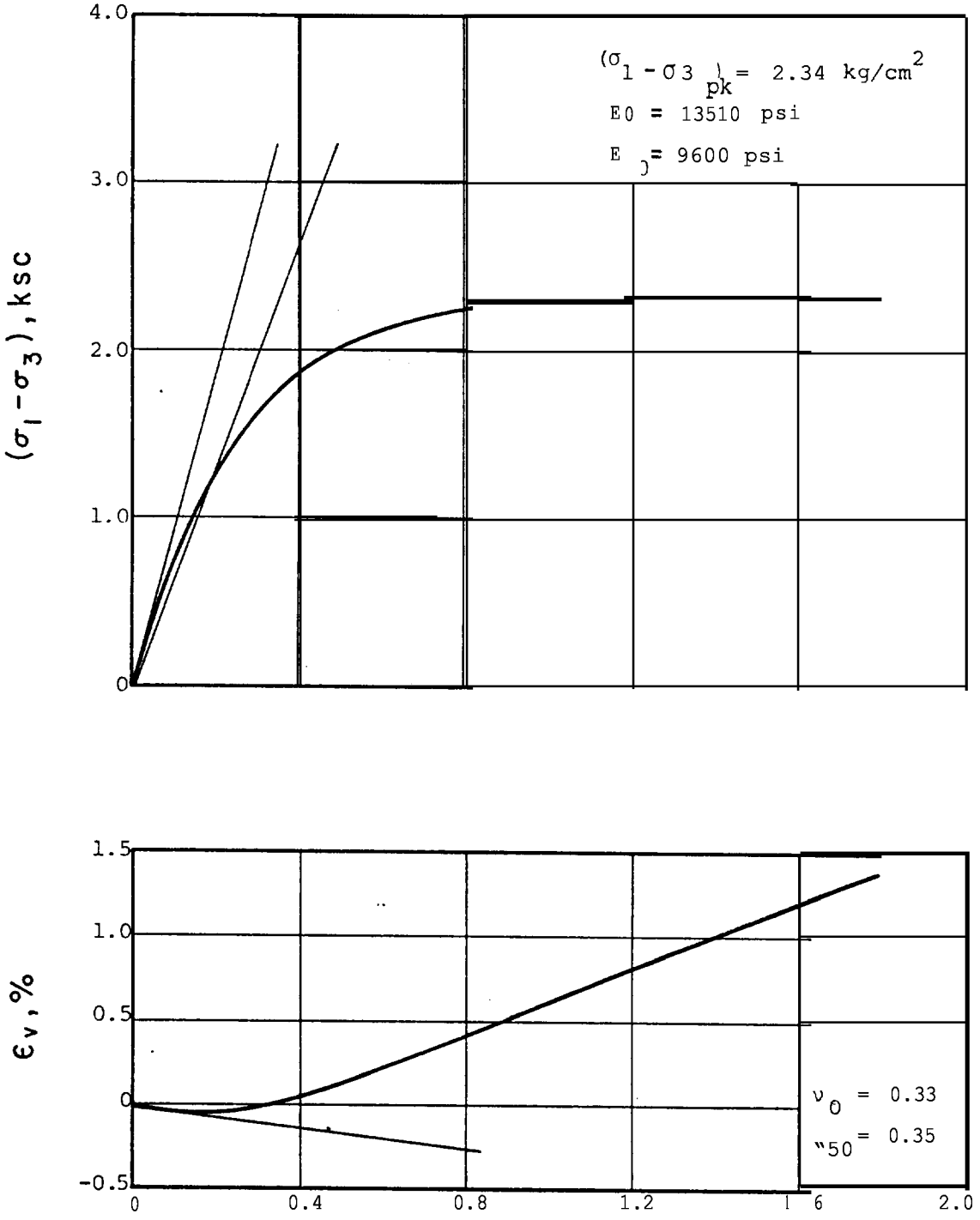

TEST S4 95% Compaction $\bar{\sigma}_{3c}$ = 0.5 kg/cm^2

PUBLIC SERVICE COMPANY OF NEW HAMPSHIRE	TRIAXIAL TESTS STRUCTURAL BACKFILL	CONSOLIDATED-DRAINED TRIAXIAL TEST S4 Expanded Scales
GEOTECHNICAL ENGINEERS INC. WINCHESTER, MASSACHUSETTS	PROJECT 77386	DECEMBER, 1977 FIG. A10

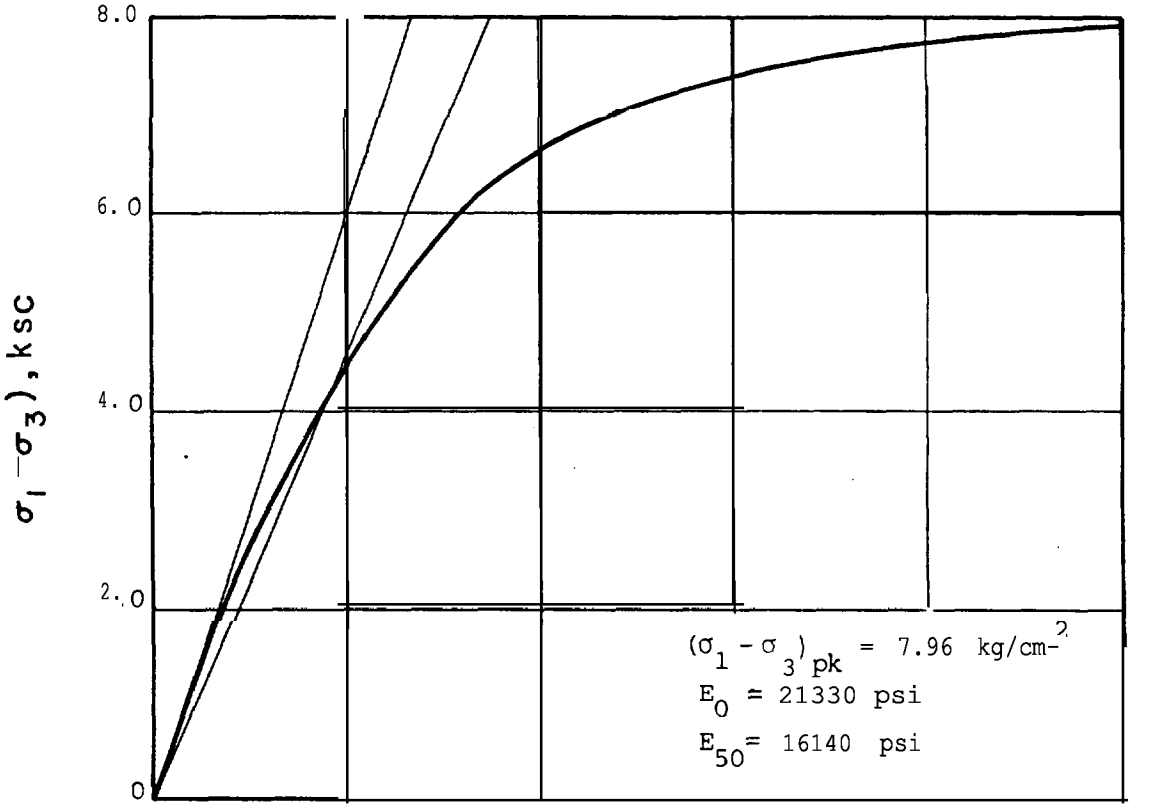

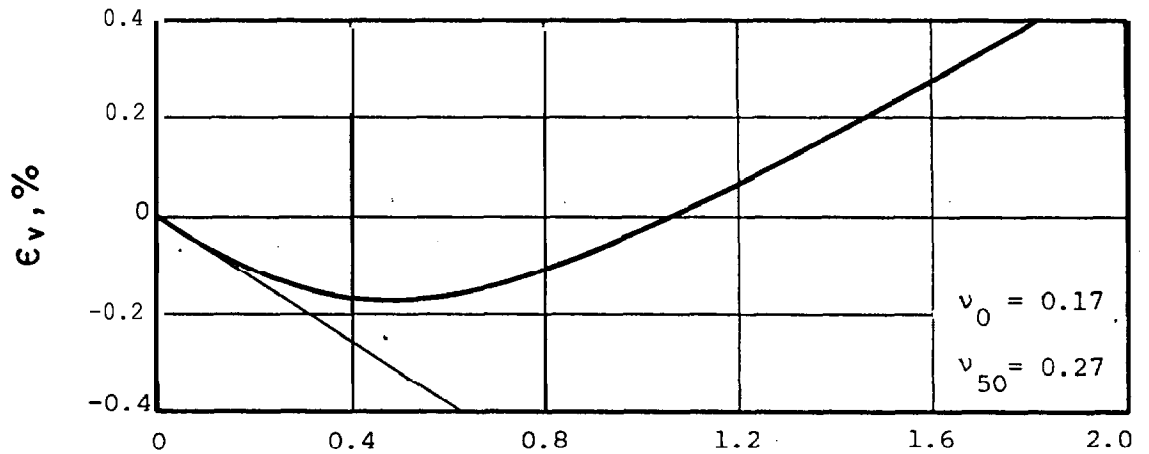

AXIAL STRAIN, %

TEST S5 95% Compaction $\bar{\sigma}_{3c}$ = 2.0 kg/cm^2

PUBLIC SERVICE COMPANY OF NEW HAMPSHIRE	TRIAXIAL TESTS STRUCTURAL	CONSOLIDATED-DRAINED TRIAXIAL TEST S5 Expanded Scales
GEOTECHNICAL ENGINEERS INC. WINCHESTER, MASSACHUSETTS	PROJECT 77386	DECEMBER, 1977 FIG. A1

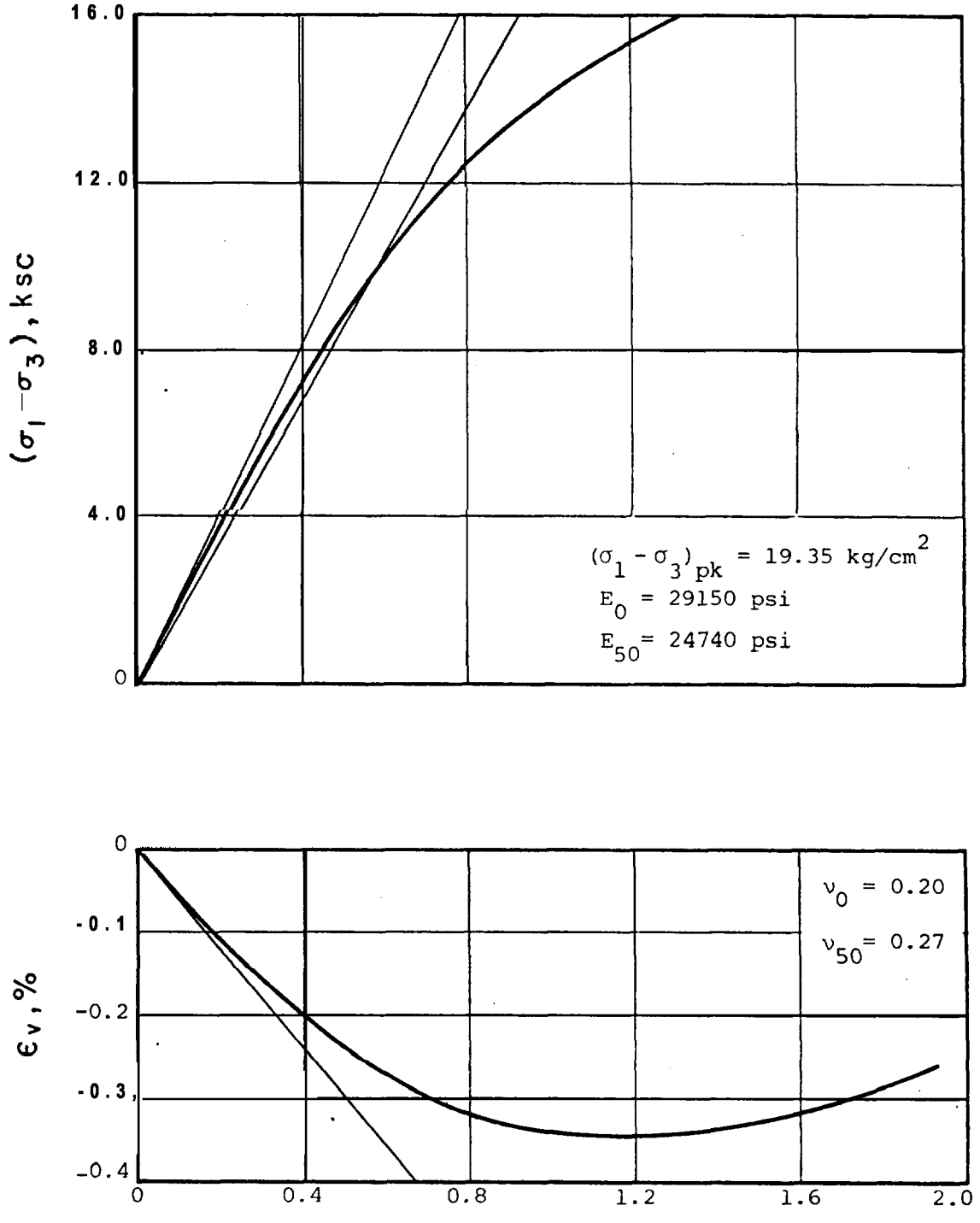

TEST S6 **95% Compaction** $\bar{\sigma}_{3c}$ = **6.0** kg/cm^2

PUBLIC SERVICE COMPANY OF NEW HAMPSHIRE	TRIAXIAL TESTS STRUCTURAL BACKFILL	CONSOLIDATED-DRAINED TRIAXIAL TEST S6 Expanded Scales
GEOTECHNICAL ENGINEERS INC. NINCHESTER, MASSACHUSETTS	PROJECT 77386	DECEMBER, 1977 FIG. A1

APPENDIX B

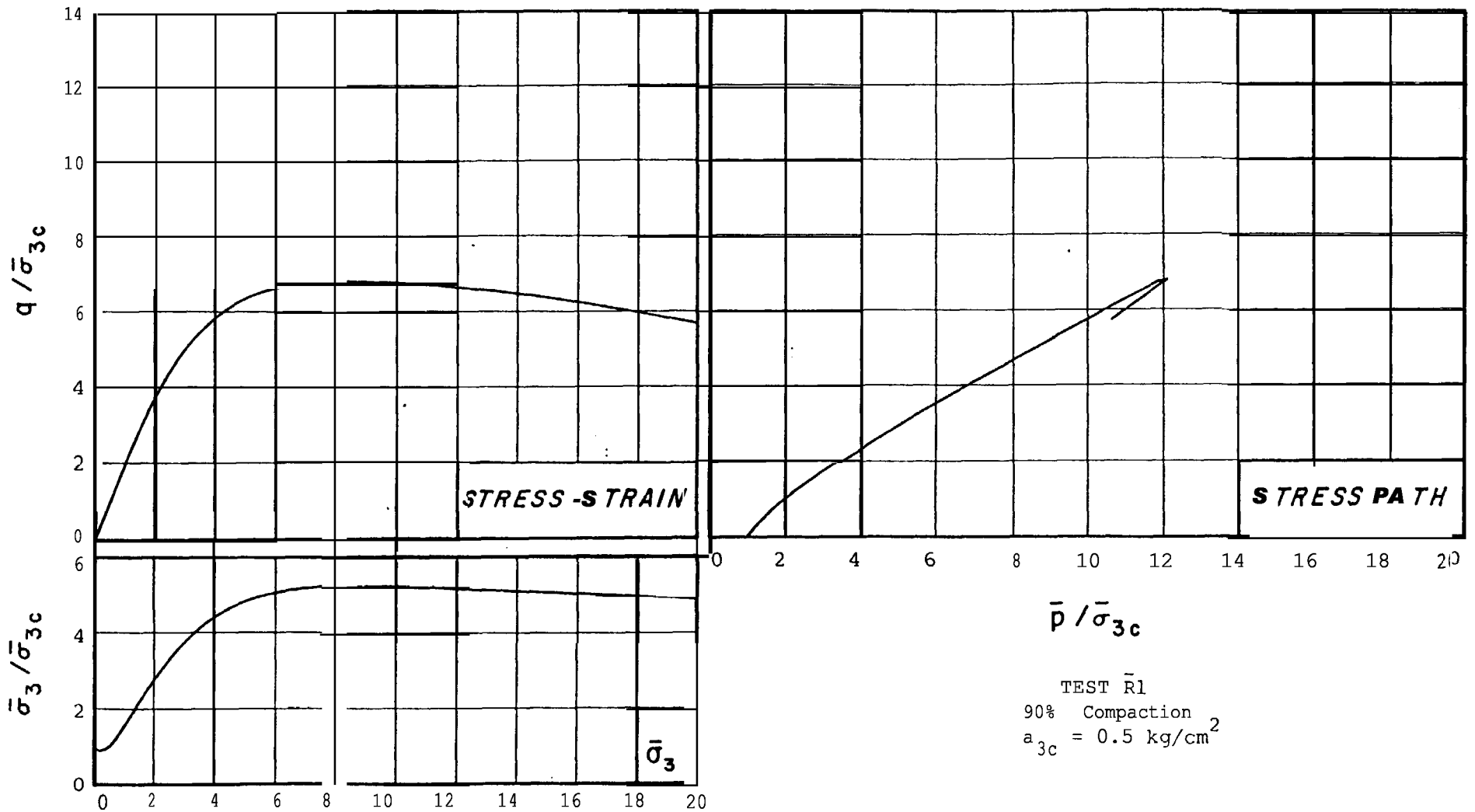

TEST $\bar{R}1$
90% Compaction
a_{3c} = 0.5 kg/cm^2

PUBLIC SERVICE COMPANY OF NEW HAMPSHIRE	TRIAXIAL TESTS STRUCTURAL BACKFILL	CONSOLIDATED-UNDRAINED TRIAXIAL TEST $\bar{R}1$
GEOTECHNICAL ENGINEERS INC. WINCHESTER, MASSACHUSETTS	PROJECT 77386	DECEMBER, 1977 FIG. B.

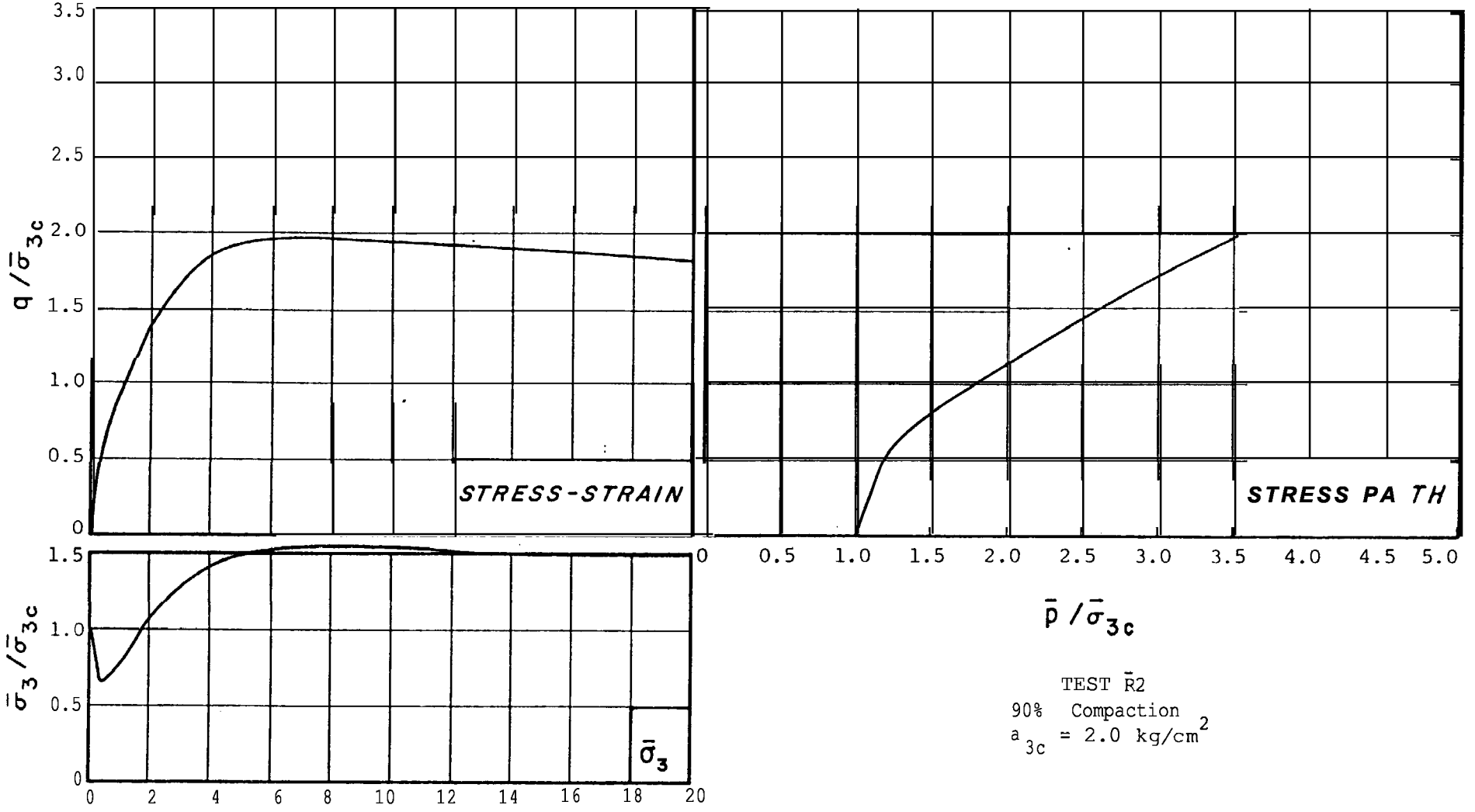

PUBLIC SERVICE COMPANY OF NEW HAMPSHIRE	TRIAXIAL TESTS STRUCTURAL BACKFILL	CONSOLIDATED-UNDRAINED TRIAXIAL TEST $\bar{R}2$
GEOTECHNICAL ENGINEERS INC. WINCHESTER, MASSACHUSETTS	PROJECT 77386	DECEMBER, 1977 FIG. B2

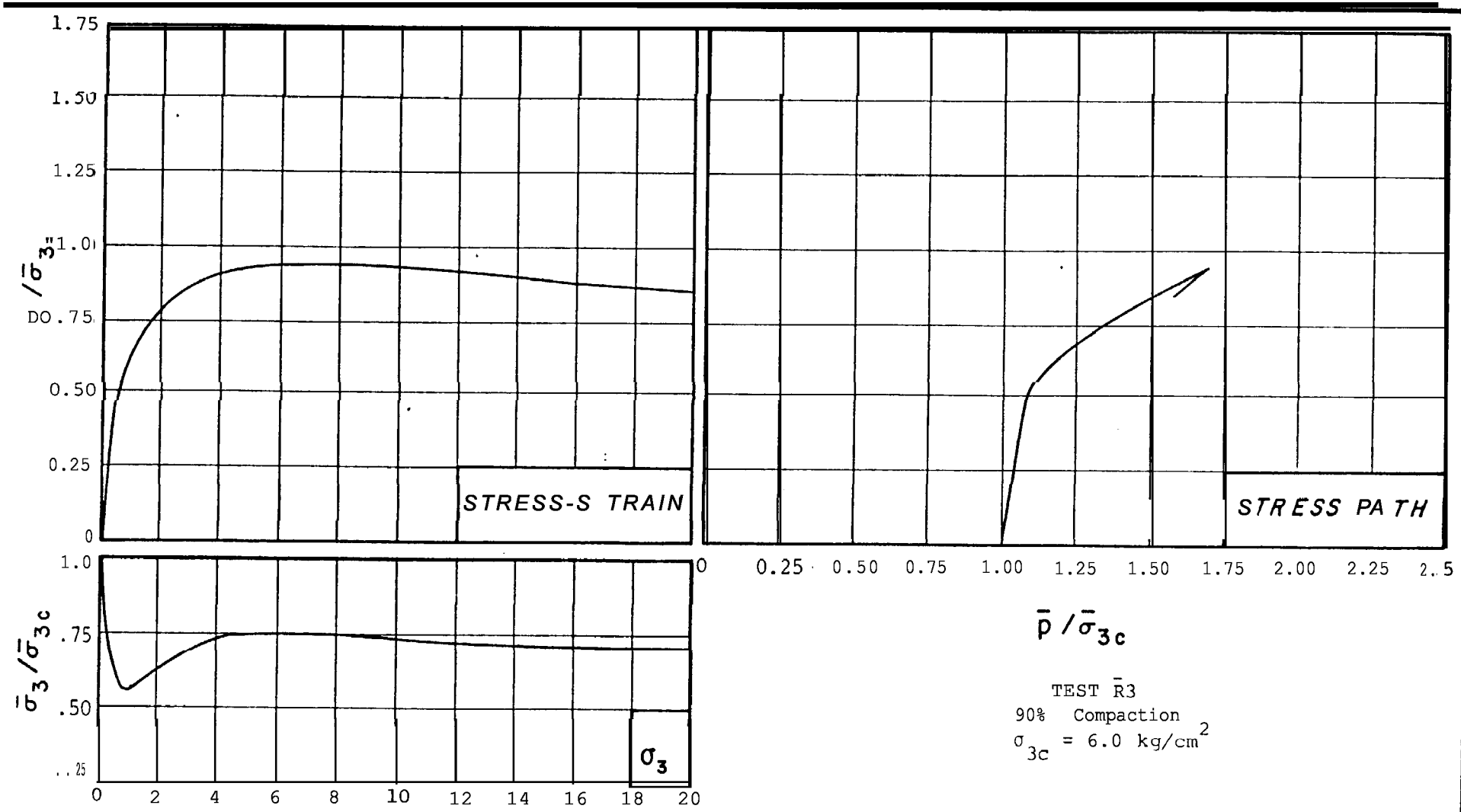

TEST $\bar{R}3$
90% Compaction
σ_{3c} = 6.0 kg/cm^2

PUBLIC SERVICE COMPANY OF NEW HAMPSHIRE	TRIAXIAL TESTS STRUCTURAL	CONSOLIDATED-UIJDRAINED TRIAXIAL TEST $\bar{R}3$
GEOTECHNICAL ENGINEERS INC. WINCHESTER, MASSACHUSETTS	PROJECT 77386	DECEMBER, 1977 FIG. B3

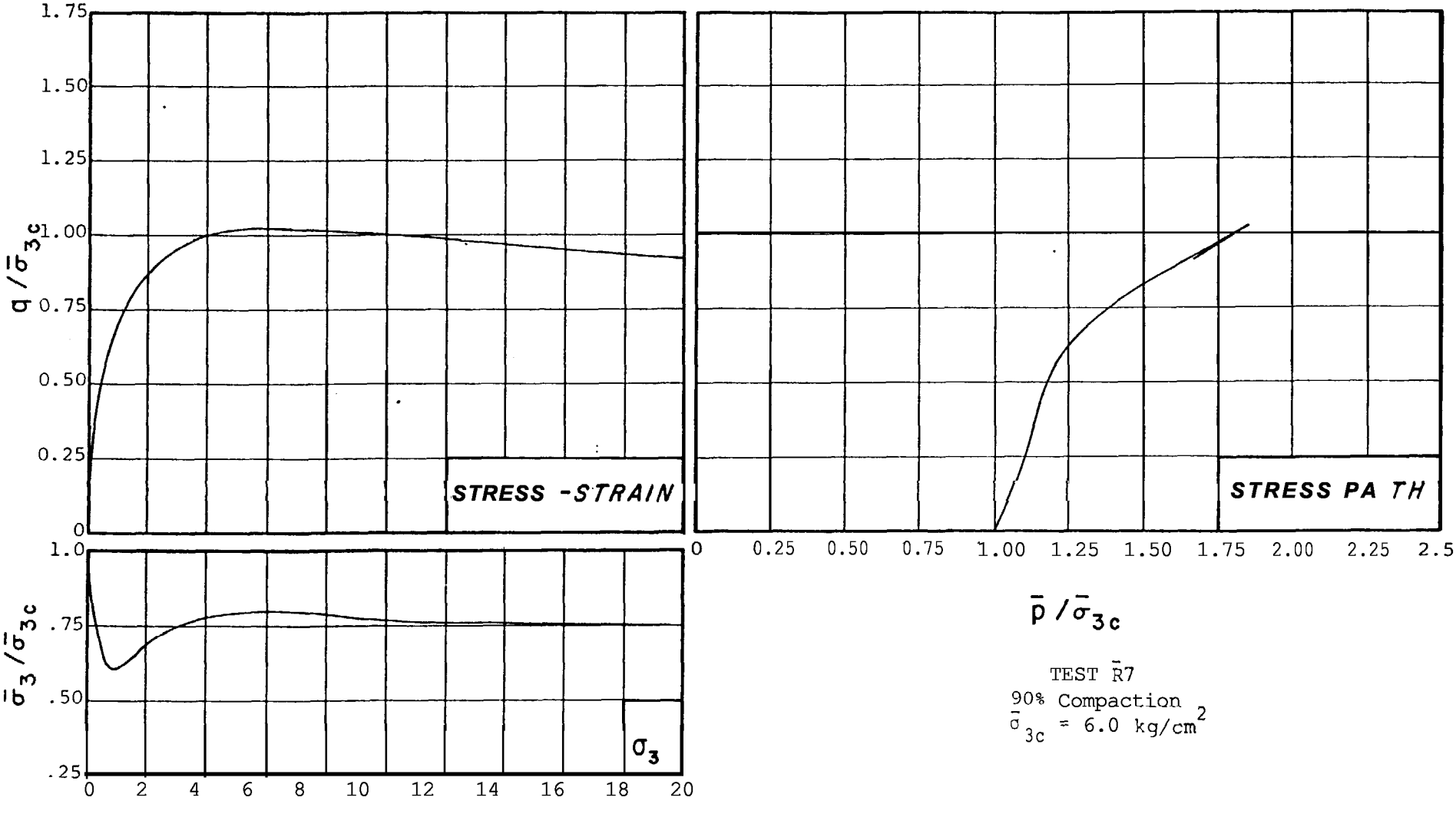

PUBLIC SERVICE COMPANY OF NEW HAMPSHIRE	TRIAXIAL TESTS STRUCTURAL BACKFILL	CONSOLIDATED-UNDRAINED TRIAXIAL TEST R̄7
GEOTECHNICAL ENGINEERS INC. WINCHESTER, MASSACHUSETTS	PROJECT 77386	DECEMBER, 1977 FIG. B 4

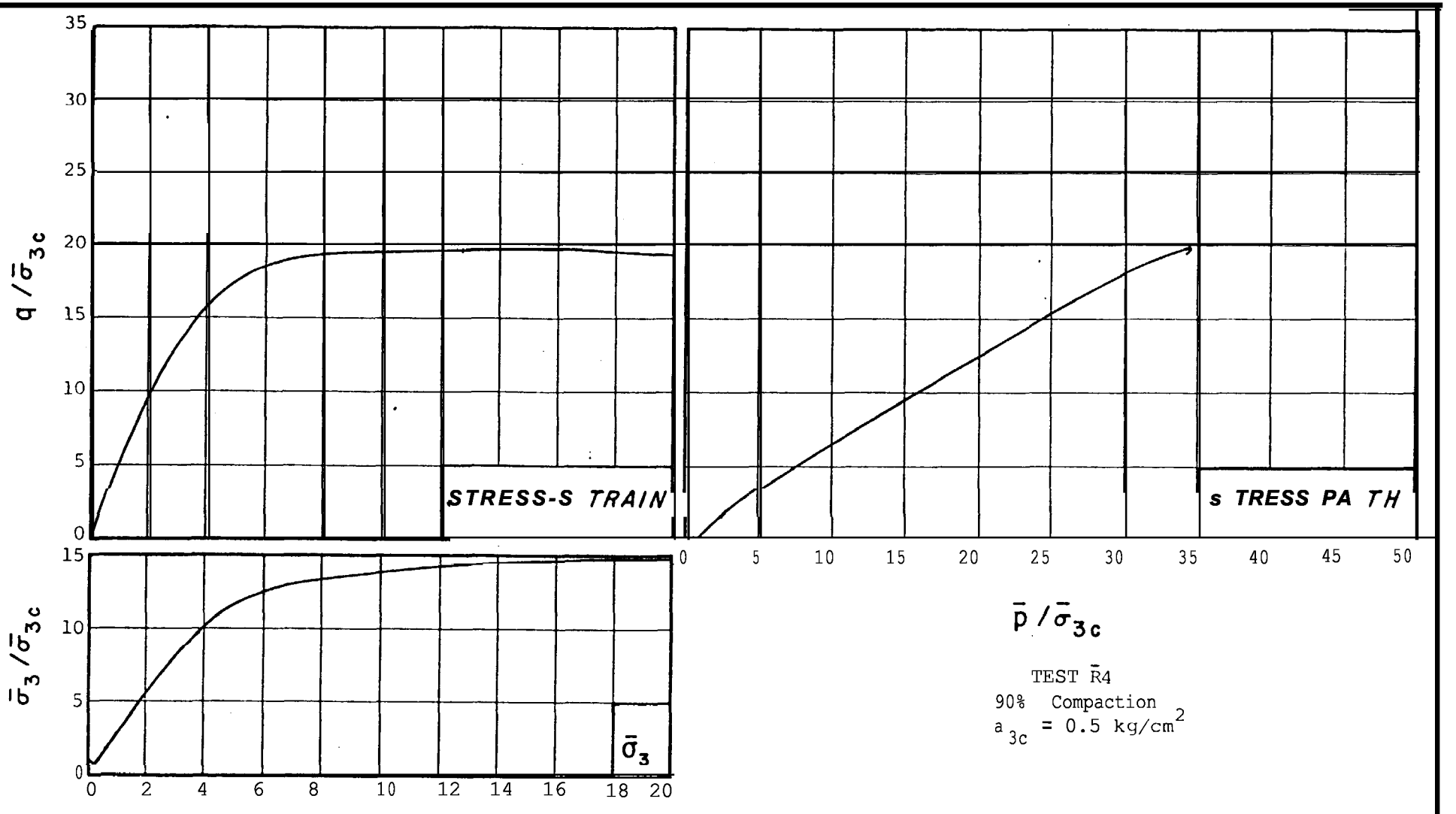

TEST R̄4
90% Compaction
a_{3c} = 0.5 kg/cm^2

PUBLIC SERVICE COMPANY OF NEW HAMPSHIRE STRUCTURAL BACKFILL	TRIAXIAL TESTS	CONSOLIDATED-UNDRAINED TRIAXIAL TEST R̄4
GEOTECHNICAL ENGINEERS INC. WINCHESTER, MASSACHUSETTS	PROJECT 77386	DECEMBER, 1977 FIG. B5

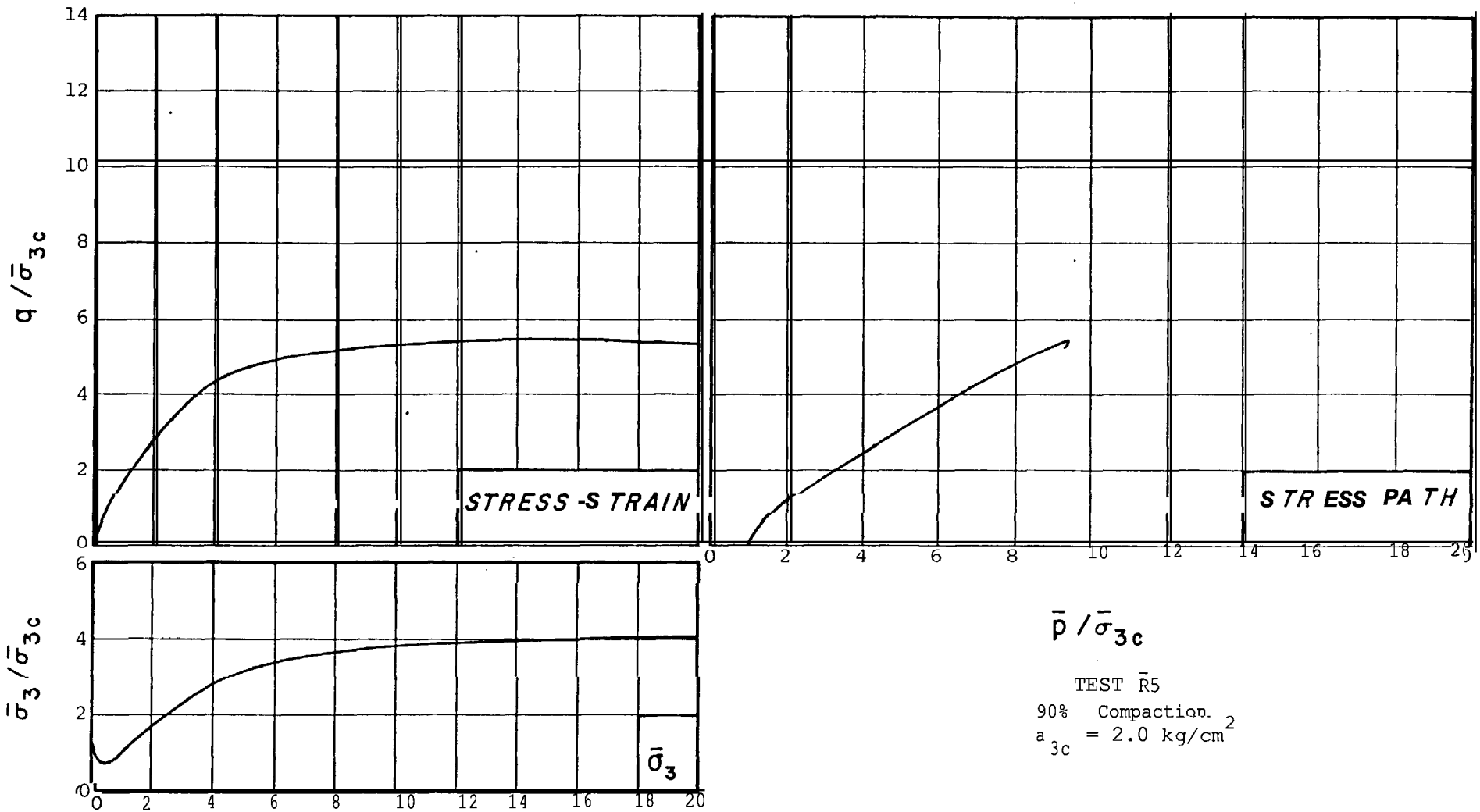

TEST R̄5
90% Compaction.
a_{3c} = 2.0 kg/cm^2

PUBLIC SERVICE COMPANY OF NEW HAMPSHIRE S T R U C T U R A L	TRIAXIAL TESTS B A C K F I L L	CONSOLIDATED-UNDRAINED TRIAXIAL TEST R̄5
GEOTECHNICAL ENGINEERS INC. WINCHESTER, MASSACHUSETTS	PROJECT 77386	DECEMBER, 1977 FIG. B8

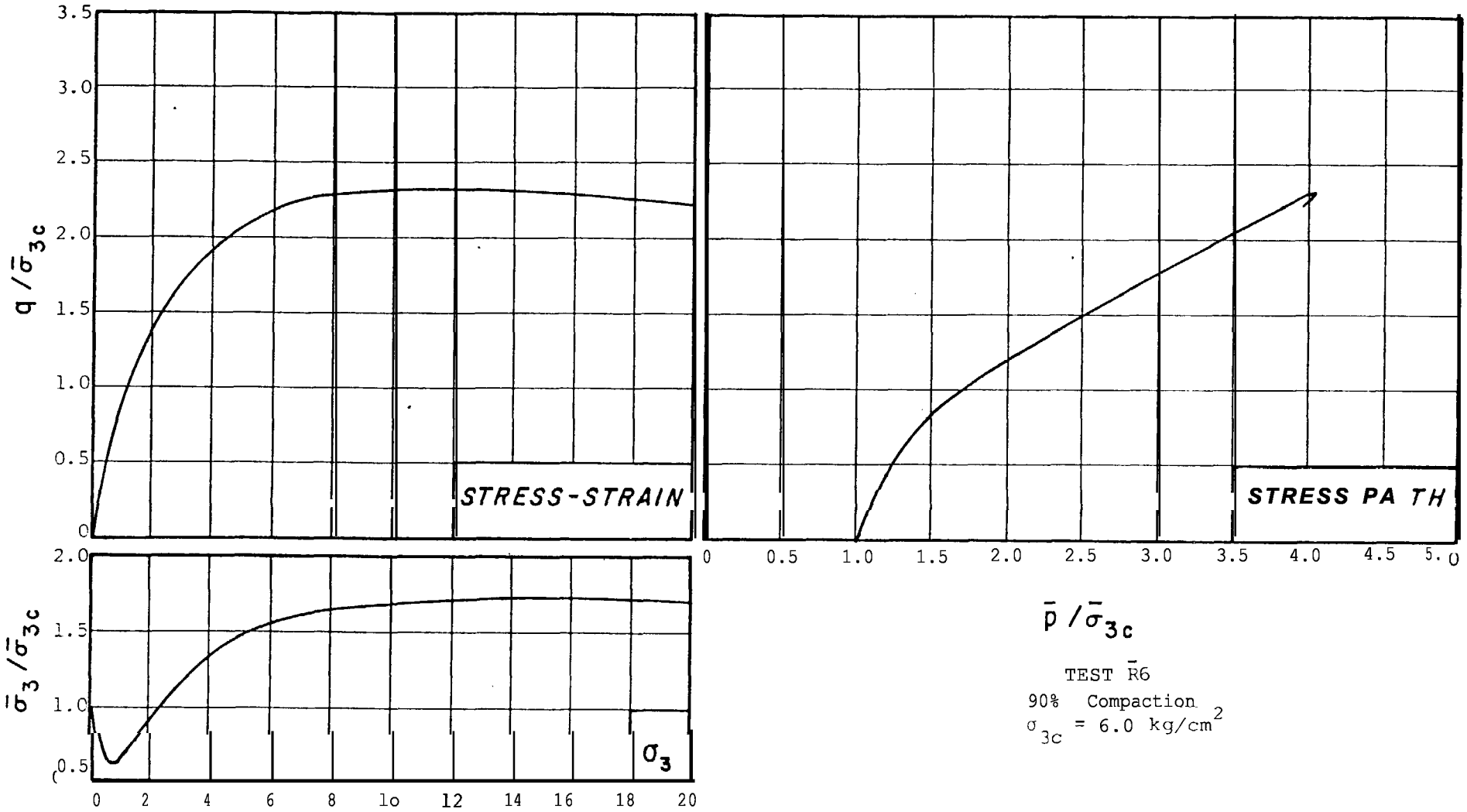

PUBLIC SERVICE COMPANY OF NEW HAMPSHIRE	TRIAXIAL TESTS STRUCTURAL BACKFILL	CONSOLIDATED-UNDRAINED TRIAXIAL TEST R̄6
GEOTECHNICAL ENGINEERS INC. WINCHESTER, MASSACHUSETTS	PROJECT 77386	DECEMBER, 1977 FIG. B7

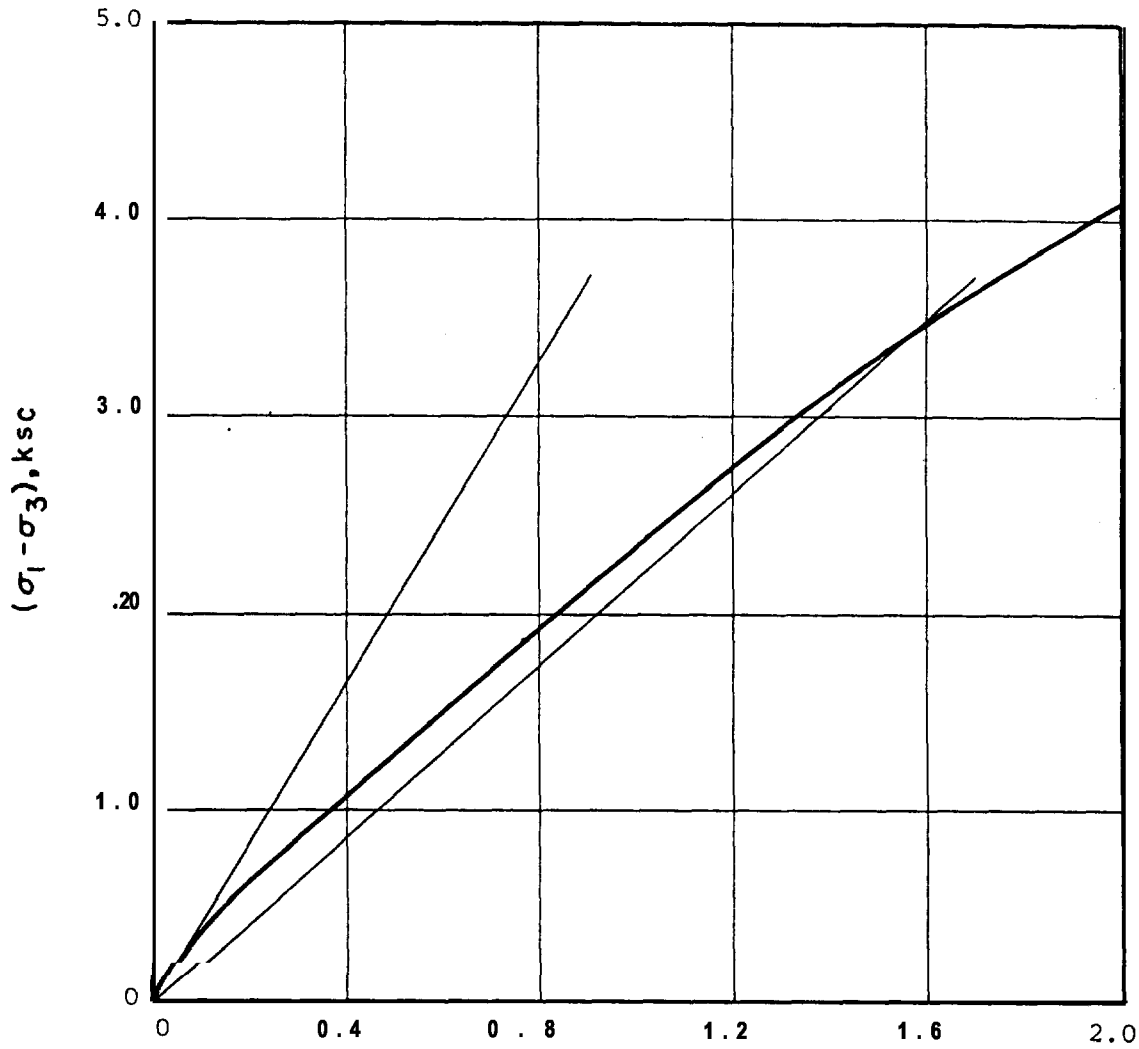

TEST $\bar{R}1$
90% Compaction
$\bar{\sigma}_{3c}$ = 0.5 kg/cm^2

PUBLIC SERVICE COMPANY OF NEW HAMPSHIRE	TRIAXIAL TESTS STRUCTURAL BACKFILL	CONSOLIDATED-UNDRAINED TRIAXIAL TEST $\bar{R}1$ EXPANDED SCALES
GEOTECHNICAL ENGINEERS INC. WINCHESTER, MASSACHUSETTS	PROJECT 77386	DECEMBER, 1977 FIG. B8

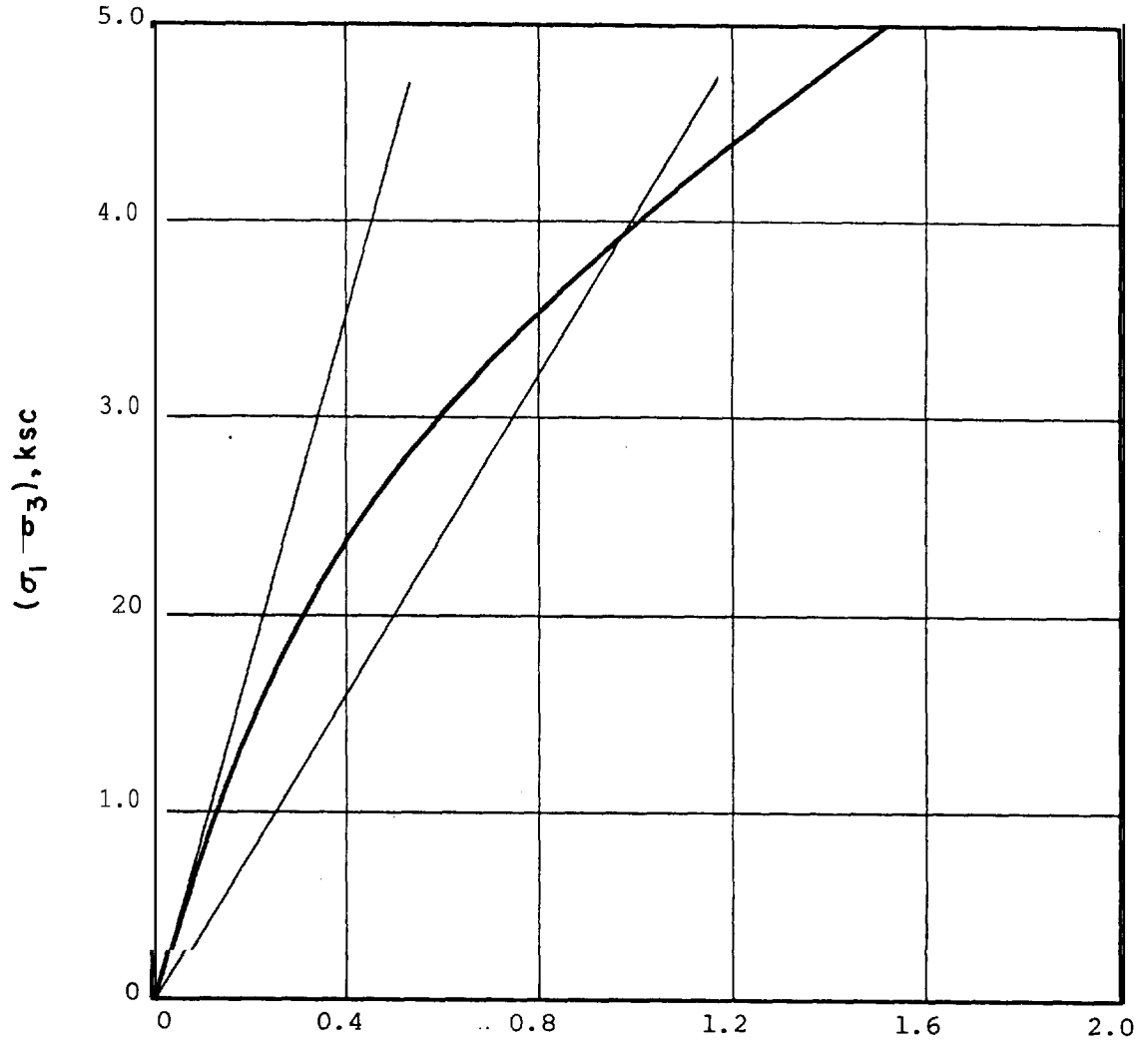

TEST $\bar{R}2$
90% Compaction
a_{3c} = 2.0 kg/cm^2

PUBLIC SERVICE COMPANY OF NEW HAMPSHIRE	TRIAXIAL TESTS STRUCTURAL BACKFILL	CONSOLIDATED-UNDRAINED TRIAXIAL TEST $\bar{R}2$ EXPANDED SCALES
GEOTECHNICAL ENGINEERS INC. WINCHESTER, MASSACHUSETTS	PROJECT 77386	DECEMBER, 1977 FIG. B9

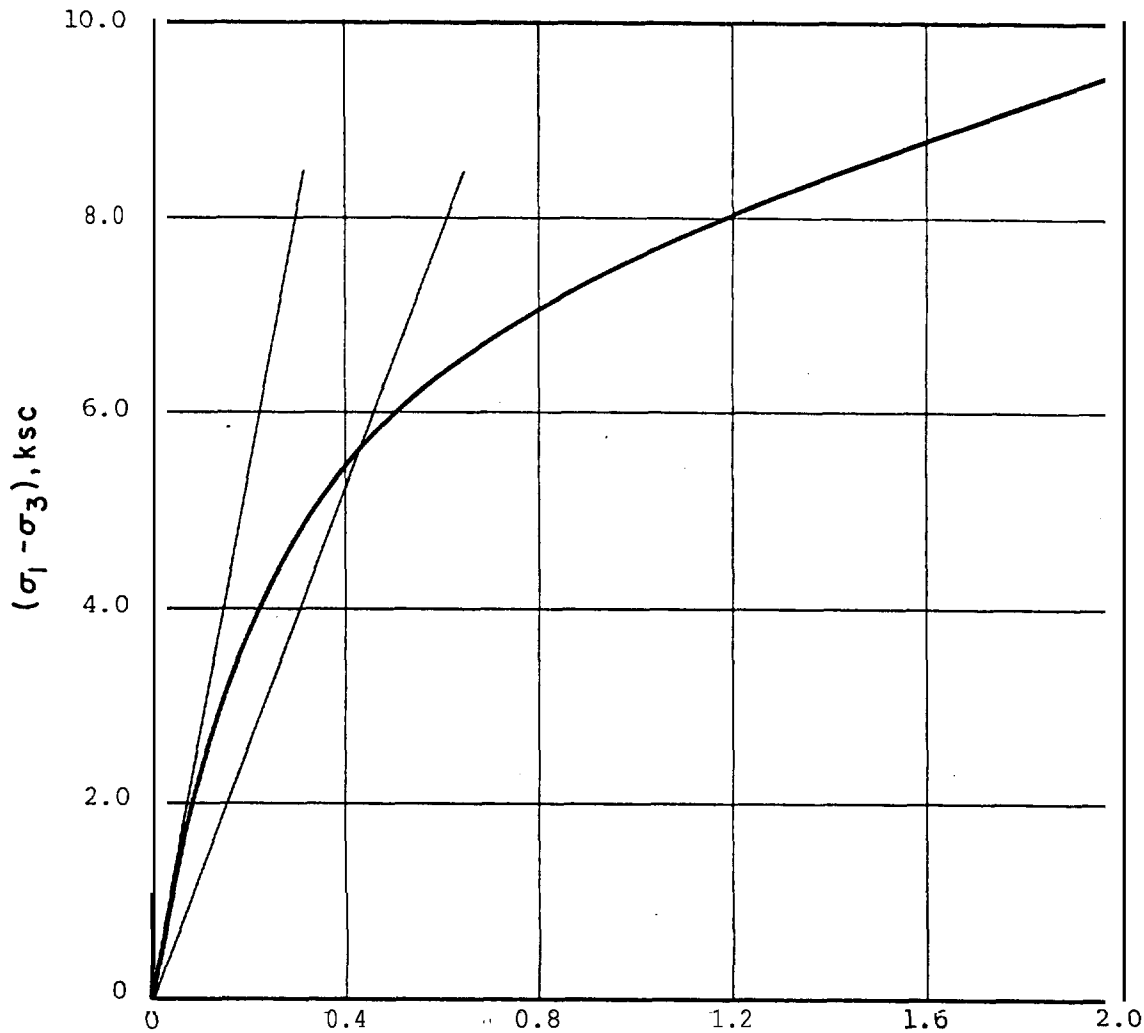

TEST $\bar{R}3$
90% Compaction
σ_{3c} = 6.0 kg/cm^2

PUBLIC SERVICE COMPANY OF NEW HAMPSHIRE	TRIAXIAL TESTS STRUCTURAL BACKFILL	CONSOLIDATED-UNDRAINED TRIAXIAL TEST $\bar{R}3$ EXPANDED SCALES
GEOTECHNICAL E N G I N E E R S I N C . WINCHESTER, MASSACHUSETTS	PROJECT 77386	DECEMBER, 1977 FIG. B1(

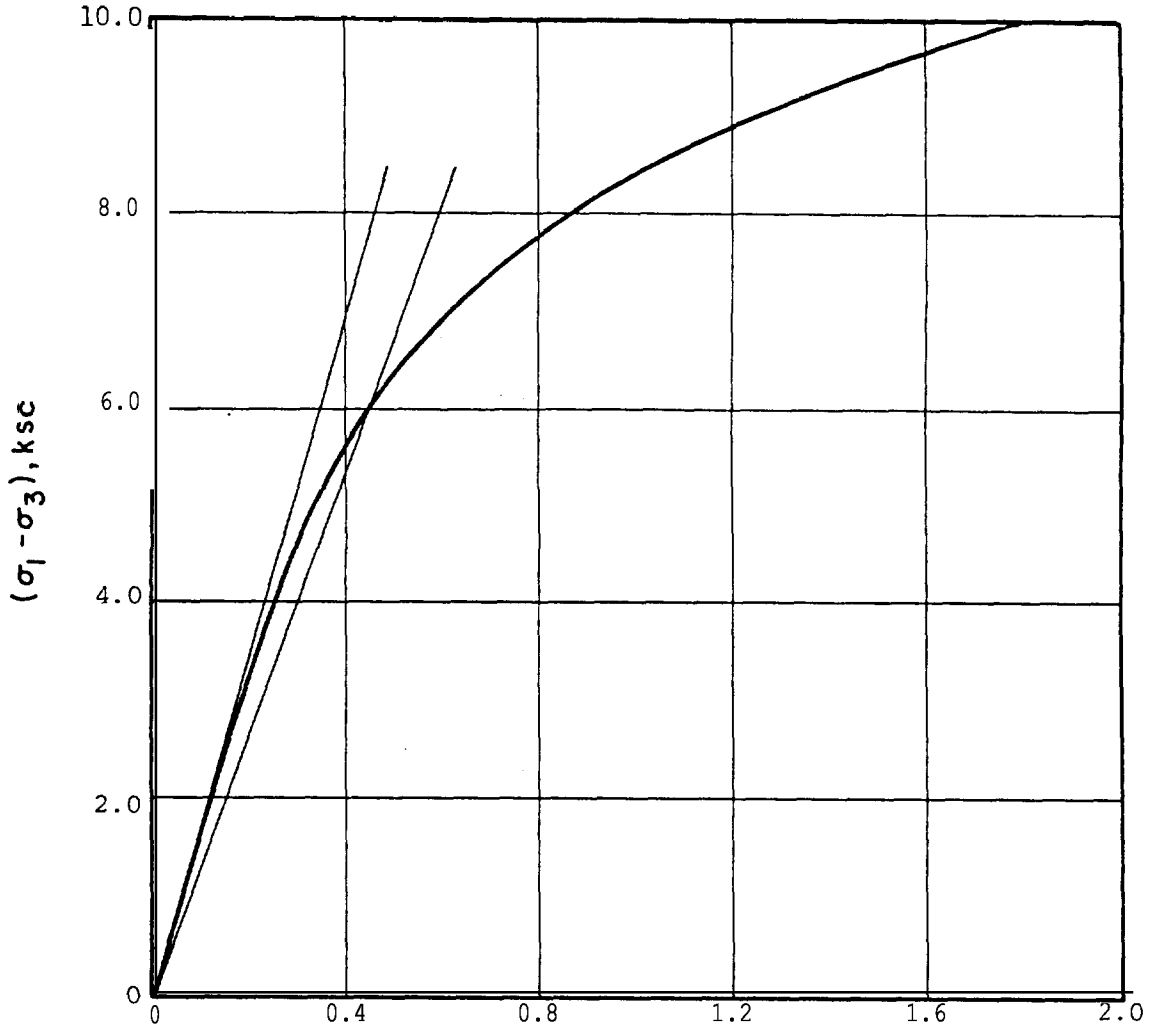

TEST $\bar{R}7$
90% Compaction
$\bar{\sigma}_{3c}$ = 6.0 kg/cm^2

PUBLIC SERVICE COMPANY OF NEW HAMPSHIRE	TRIAXIAL TESTS STRUCTURAL BACKFILL	CONSOLIDATED-UNDRAINED TRIAXIAL TEST $\bar{R}7$ EXPANDED SCALES
GEOTECHNICAL ENGINEERS INC. WINCHESTER, MASSACHUSETTS	PROJECT 77386	DECEMBER, 1977 FIG B1

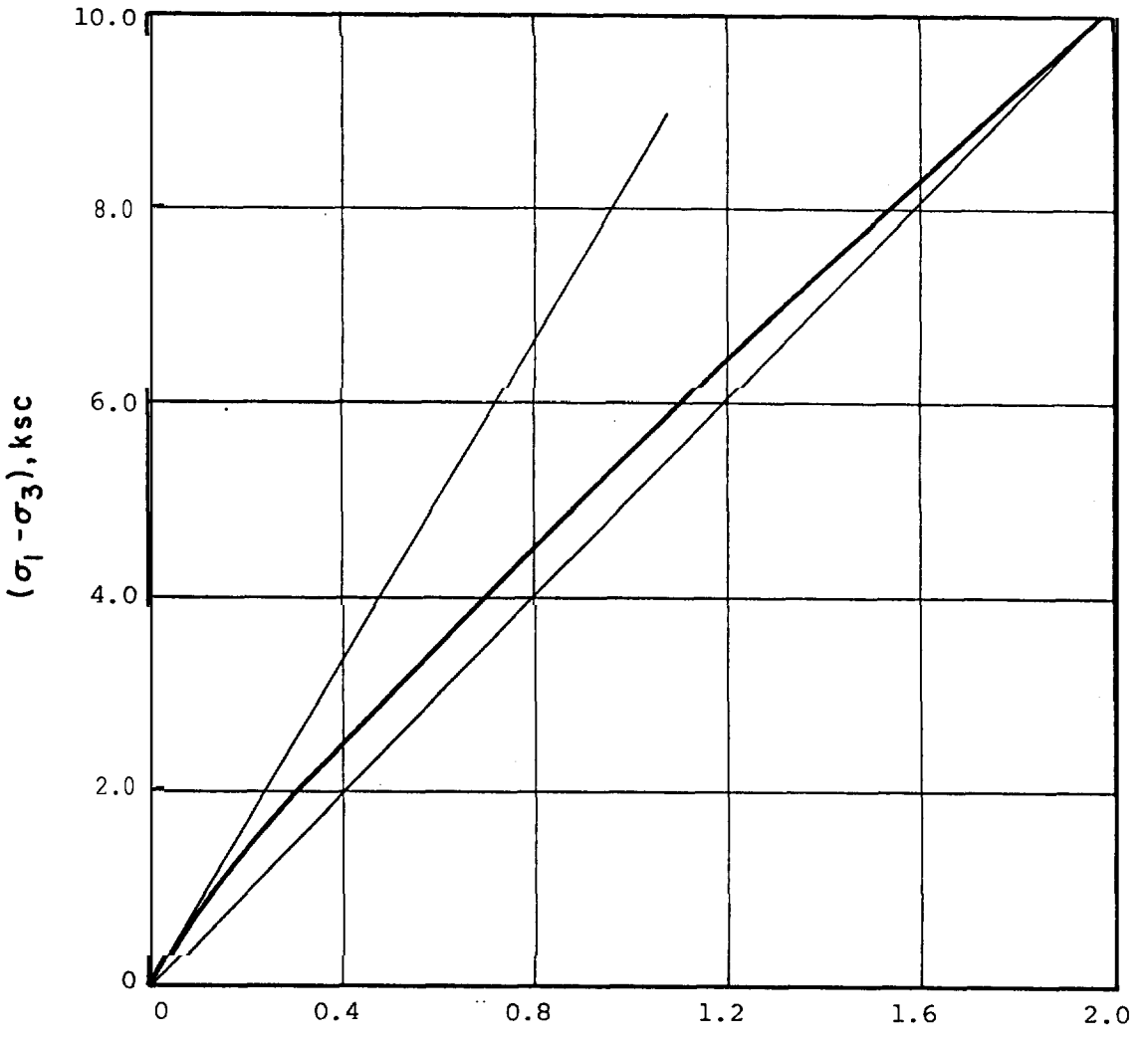

AXIAL STRAIN, %

TEST $\bar{R}4$
90% Compaction
$\bar{\sigma}_{3c}$ = 0.5 kg/cm^2

PUBLIC SERVICE COMPANY OF NEW HAMPSHIRE	TRIAXIAL TESTS STRUCTURAL BACKFILL	CONSOLIDATED-UNDRAINED TRTAXTAL TEST $\bar{R}4$ EXPANDED SCALES
GEOTECHNICAL ENGINEERS, INC. WINCHESTER, MASSACHUSETTS	PROJECT 77386	DECEMBER, 1977 FIGB12

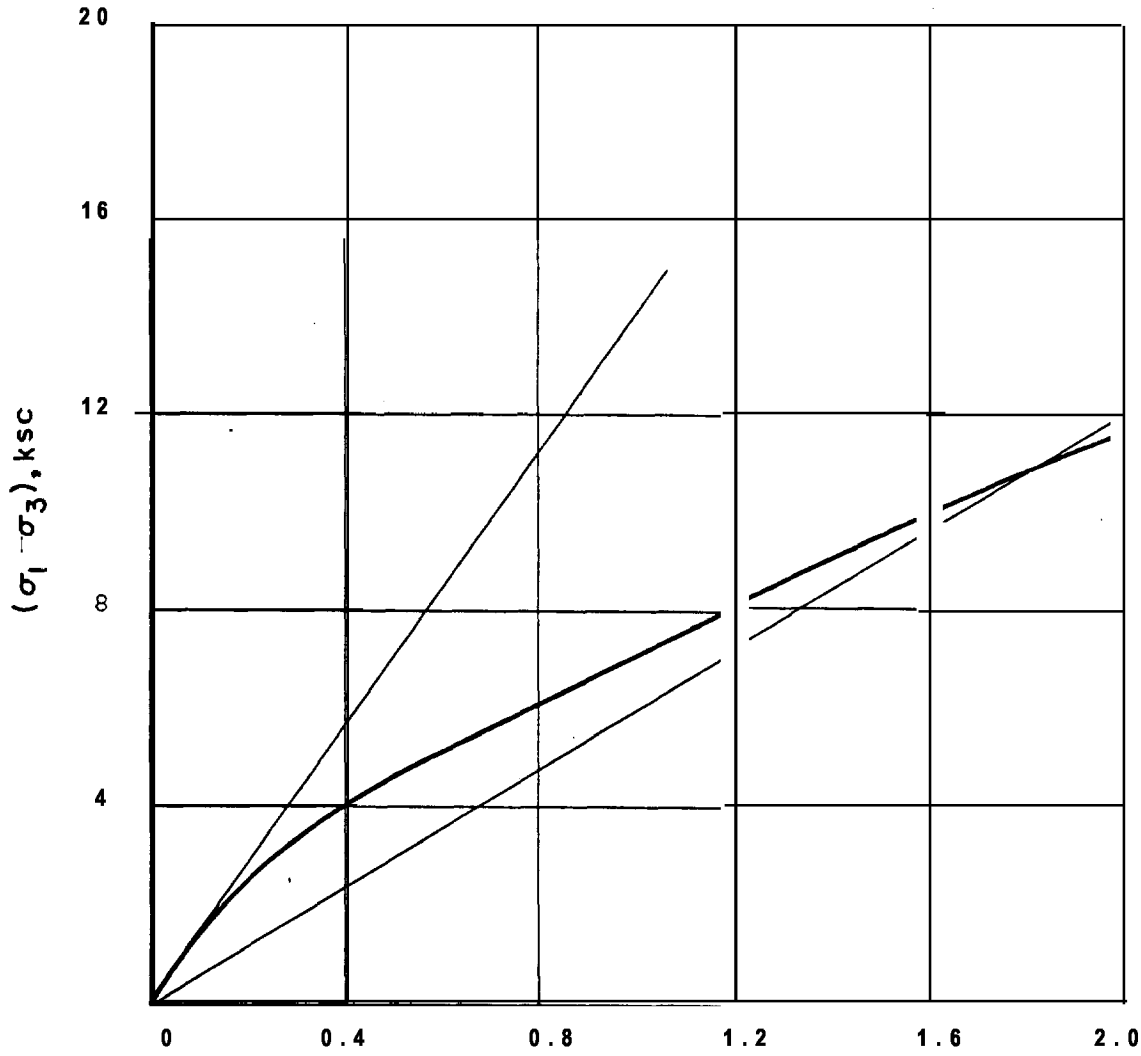

TEST $\bar{R}5$
90% Compaction
$\bar{\sigma}_{3c}$ = 2.0 kg/cm^2

PUBLIC SERVICE COMPANY OF NEW HAMPSHIRE	TRIAXIAL TESTS STRUCTURAL BACKFILL	CONSOLIDATED-UNDRAINED TRIAXIAL TEST $\bar{R}5$ EXPANDED SCALES
GEOTECHNICAL ENGINEERS INC WINCHESTER, MASSACHUSETTS	PROJECT 77386	DECEMBER, 1977 FIG. B1

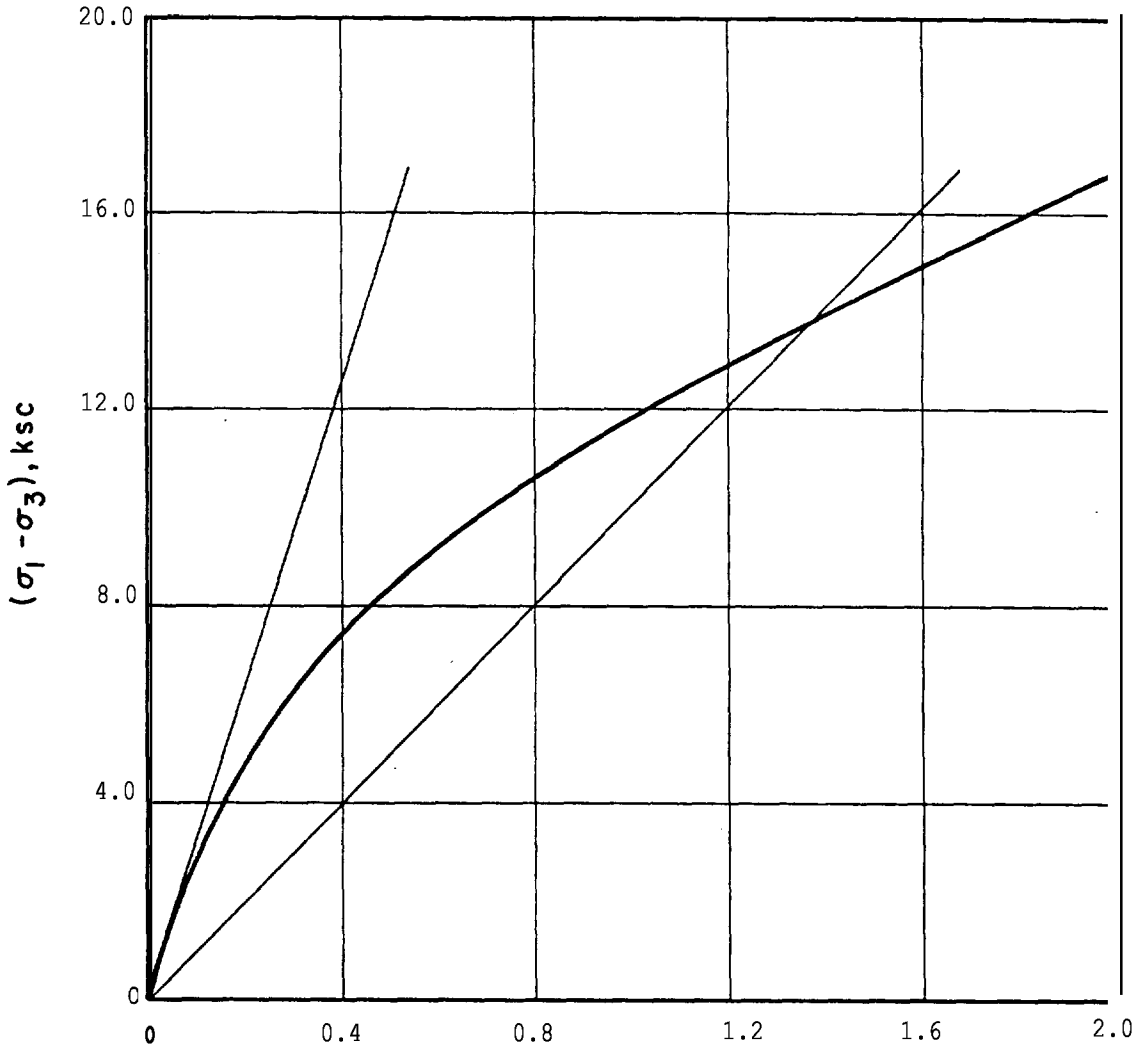

TEST $\bar{R}6$
90% Compaction
$\bar{\sigma}_{3c}$ = 6.0 **kg/cm**^{2}

PUBLIC SERVICE COMPANY OF NEW HAMPSHIRE	TRIAXIAL TESTS STRUCTURAL BACKFILL	**CONSOLIDATED-UNDRAINED TRIAXIAL TEST $\bar{R}6$ EXPANDED SCALES**
GEOTECHNICAL ENGINEERS INC. WINCHESTER, MASSACHUSETTS	PROJECT 77386	DECEMBER, 1977 FIG. B1

GEOTECHNICAL ENGINEERS INC.

1017 MAIN STREET · WINCHESTER · MASSACHUSETTS 01890 (617) 729-1625

PRINCIPALS
RONALD C HIRSCHFELD
STEVE J. POULOS
DANIEL P. LA GATTA
RICHARD F. MURDOCK
GONZALO CASTRO

ASSOCIATES
· CHARLES E. OSGOOD
BARTLETT W. PAULDING, JR

February 14, 1978
Project 77386
File No. 2.0

Mr. John Herrin
Public Service Co. of New Hampshire
1000 Elm Street - 11th Floor
Manchester, NH 03105

Subject: Interim Test Results on Sand-Cement Backfill
Seabrook Station

Reference: Preliminary Report, Compression Tests on Structural Backfill and Sand-Cement
Seabrook Station, GEI, January 24, 1978

Dear Mr. Herrin:

The purpose of this letter is to present data on moduli determined on sand-cement backfill at the request of United Engineers and Constructors Inc. The data herein supplements the data in the reference and will be incorporated in the completed version of that report. The subgrade modulus values were submitted to Mr. Patel of UE&C by telephone on February 13, 1978.

The stress strain curves for three unconfined compression tests on cylindrical specimens are shown in the enclosed Fig. 15 and the test data are summarized in the enclosed Table 5.

The following values of the coefficient of subgrade reaction were computed for the cube and cylindrical specimens cured for 28 days.

k_sD-VALUES FOR SAND-CEMENT BACKFILL
28-DAY CURE

Tabulated values are in psi

Effective Vertical Stress at Springline psi	Allowable Diameter Strain, % 0.02	0.1	0.3	0.5
CUBE SPECIMENS				
0			100,000	
CYLINDRICAL SPECIMENS				
0	200,000	89,000	60,000	36,000

The stress strain curves for the cylindrical specimens show an initial straight line portion with a very high modulus of elasticity. At axial strains of about 0.03% there is a break in the curves and a second straight line is followed up to near the peak strength. The tangent modulus of this second straight line portion of the curves is about one-third of the initial modulus. Fig. 16 shows the variation of the secant modulus with axial strain for the unconfined tests on cylindrical specimens.

Seating problems occurred in the tests on the cube specimens, as seen in Figs. 13 and 14 of the above reference, and thus the high initial modulus observed for the cylindrical samples was not observed for the cubes. However, the second straight line slope for the cylindrical specimens in Fig. 15 is in good agreement with the straight line portion of the curves for the cube specimens. The compressive strength of the cube specimens is somewhat higher than that of the cylindrical specimens, probably as a result of the more significant end restraint of the cube specimens. For these two reasons we feel that the results of tests on cubes and cylinders are consistent with each other, but that the results for tests on cylinders are more reliable and should be used to establish moduli of subgrade reaction.

We have also provided by telephone various friction coefficients and estimates of shear wave velocities in the compacted soil. These data will be confirmed in writing at a later date.

Sincerely yours,

GEOTECHNICAL ENGINEERS INC.

Steve J. Poulos
Principal

SJP:ms
Encl.
cc: R. Pizzuti, YAEC w/1 encl.
D. Rhoads, UE&C w/1 encl.
A. Desai, UE&C w/1 encl.
D. Patel, UE&C, TUO, w/1 encl.

TABLE 5 - COMPRESSION TESTS ON 2.8-IN.-DIAMETER SAND-CEMENT SPECIMENS, 5% CEMENT SEABROOK STATION

Cure Time days	Test No.	Unit Weight Wet pcf	Confining Stress ksc	Compressive Strength psi	Strain At Peak %	Initial Modulus of Elasticity psi
28	28-O-1	126.2	0.00	91.0	0.65	75,000
28	28-O-2	124.8	0.00	88.8	0.58	52,200
28	28-O-3	124.1	0.00	106.1	0.80	34,300
				Avg 95.3		Avg 50,500

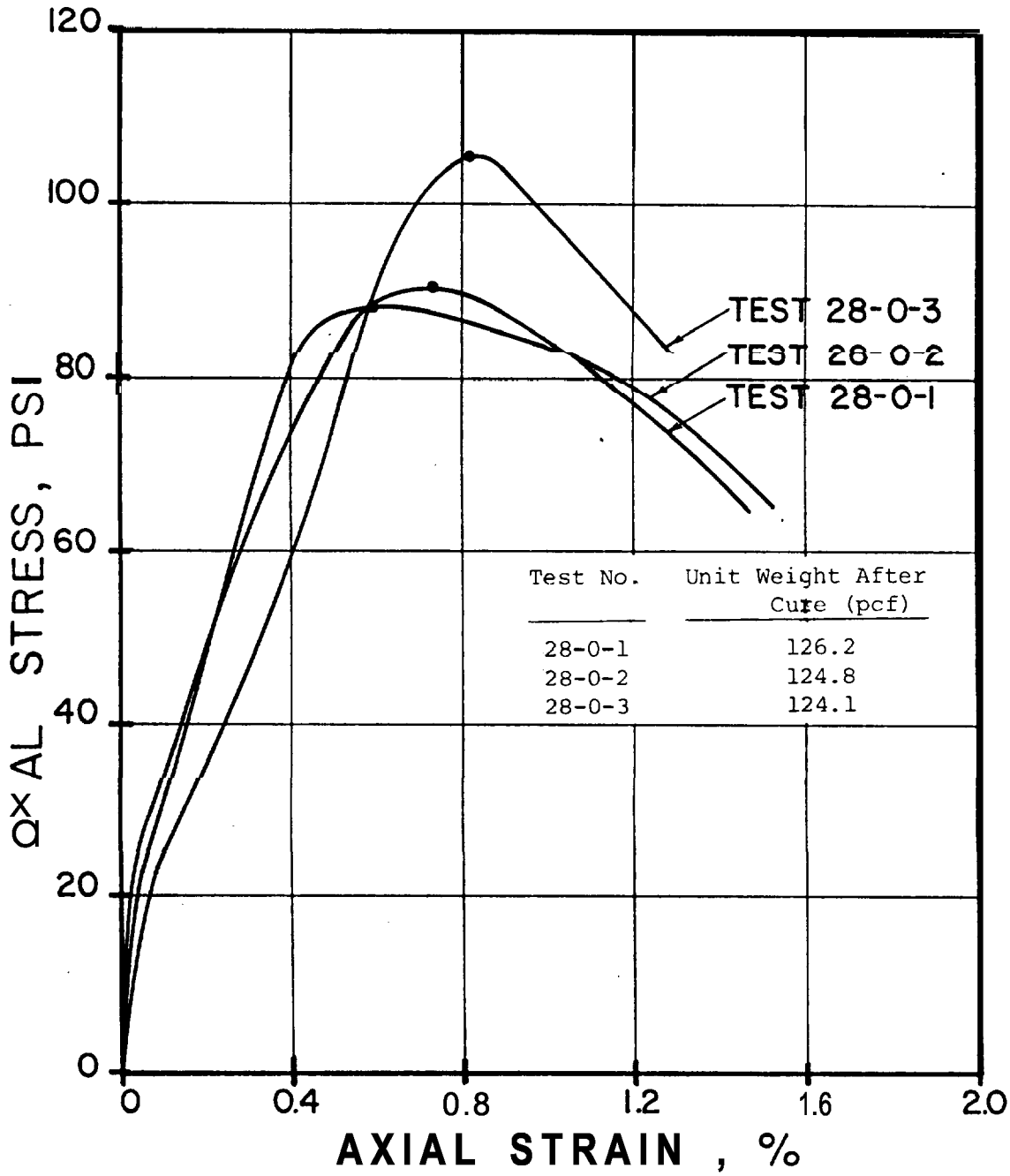

Sand-Cement Mixture:

1 part cement
16.18 parts sand (oven-dry)
2.79 parts water

Specimens Tested:

2.8-in.-diameter specimens
28-day cure
Unconfined tests
Strain control loading at 1.1 mm/min.

Public Service Company of New Hampshire	Triaxial Tests Sand-Cement Backfill Seabrook Station	COMPRESSION TESTS 2.8-IN.-DIAMETER SPECIMEN 5% CEMENT, 28-DAY CURE
Geotechnical Engineers Inc. Winchester, Massachusetts	Project 77386	February 1978 Fig. 15

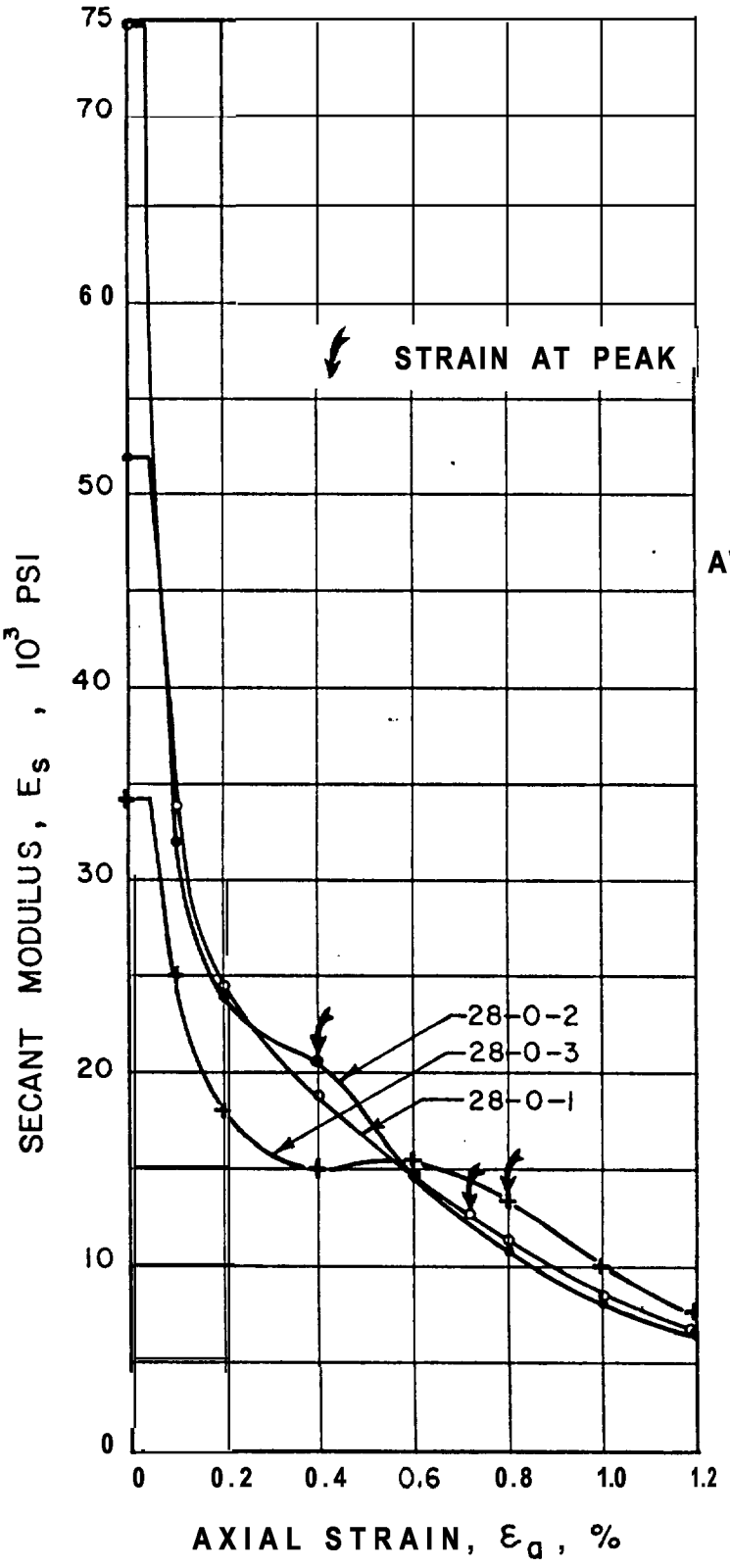

Public Service Company of New Hampshire	Triaxial Tests Sand-Cement Backfill Seabrook Station	SECANT MODULUS VS STRAIN 2.8-IN.-DIA. SPECIMENS 5% CEMENT, 28-DAY CURE
Geotechnical Engineers Inc. Winchester, Massachusetts	Project 77386	February 1978 Fig. 16

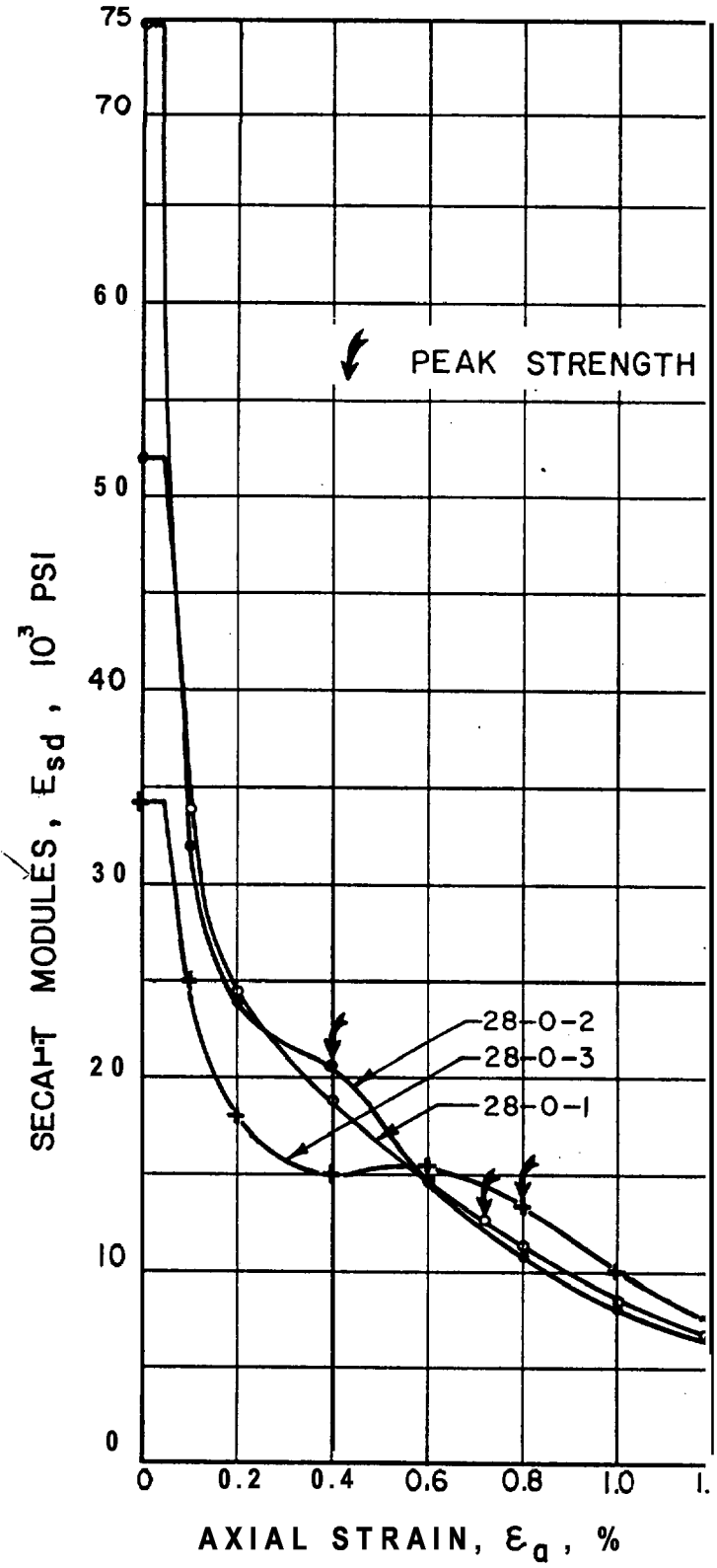

AVERAGE – E_o = 51 ksi

GEOTECHNICAL ENGINEERS INC.

1017 MAIN STREET. WINCHESTER · MASSACHUSETTS 01890 (617) 729-1625

PRINCIPALS
RONALD C HIRSCHFELD
STEVE J. POULOS
DANIEL P. LA GATTA
RICHARD F. MURDOCK
GONZALO CASTRO

ASSOCIATES
CHARLES E. OSGOOD
BARTLETT W. PAULDING, JR

February 27, 1978
Project 77386
File No. 2.0

Mr. John Herrin
Public Service Co. of New Hampshire
1000 Elm Street-11th floor
Manchester, NH 03105

Subject: Interim Test Results on Sand-Cement Backfill Seabrook Station

Reference: Preliminary Report, Compression Tests On Structural Backfill and Sand-Cement Seabrook Station, GEI, January 24, 1978

Bear Mr. Herrin:

The purpose of this letter is to present additional data on moduli determined on sand-cement backfill. These data supplement the data in the reference and in our letter of February 14.

These triaxial tests were performed on cylindrical specimens of sand-cement. The specimens were cured for 33 days instead of the intended 28 days because of the February 6, 1978 blizzard here in Boston. The test data are summarized in a revised Table 5 and the stress strain curves are presented in Fig. 17.

The modulus and strength data were estimated for 28-day curing on the basis of the rate of change of modulus and strength with time as measured using the cube specimens (see referenced report). The estimated values of strength and modulus for 28-day cure also are shown in Table 5.

The values of the coefficient of subgrade reaction were computed for several strain levels in the same manner as those shown in the preliminary report of January 24 and the letter of February 14. The following table lists all values obtained to date for the sand-cement specimens.

k_sD-VALUES FOR SAND-CEMENT BACKFILL
28-DAY CURE, 5% CEMENT

Tabulated values are in psi

Effective Vertical Stress at Springline psi	Allowable Diameter Strain, %			
	0.02	0.1	0.3	0.5
CUBE SPECIMENS				
0			100,000	
CYLINDRICAL SPECIMENS				
0	200,000	89,000	60,000	36,000
42.7		138,000	163,000	129,600

Sincerely yours,

GEOTECHNICAL ENGINEERS INC.

Steve J. Poulos
Principal

GC:ms
Encl.

cc: R. Pizzuti, YAEC w/1 encl.
D. Rhoads, UE&C w/1 encl.
A. Desai, UE&C w/1 encl.
D.. Patel, UE&C, 7UO, w/1 encl.

TABLE 5 - COMPRESSION TESTS ON 2.8-IN.-DIAMETER SAND-CEMENT SPECIMENS, 5% CEMENT[1)]
SEABROOK STATION

Cure Time days	Test No.	Unit Weight Wet pcf	Confining Stress ksc	Compressive Strength psi	Strain at Peak %	Initial Modulus of Elasticity psi
28	28-O-1	126.2	0.00	91	0.65	75,000
28	28-O-2	124.8	0.00	89	0.58	52,200
28	28-O-3	124.1	0.00	106	0.80	34,300
33	33-3-1	124.4	42.7	372	2.10	35,000
28	Estimated[2)]			365		33,600
33	33-3-2	124.1	42.7	376	2.40	33,300
28	Estimated[2)]			369		31,700
33	33-3-3	124.8	42.7	364	1.40	40,000
28	Estimated[2)]			357		38,400

NOTE: 1) The percentage of cement is computed as the ratio of the weight of cement to the total weight of sand, cement, and water, and then multiplying that ratio by 100.

2) The strengths and moduli for 28-day cure was estimated based on the rates of change measured for the cube specimens.

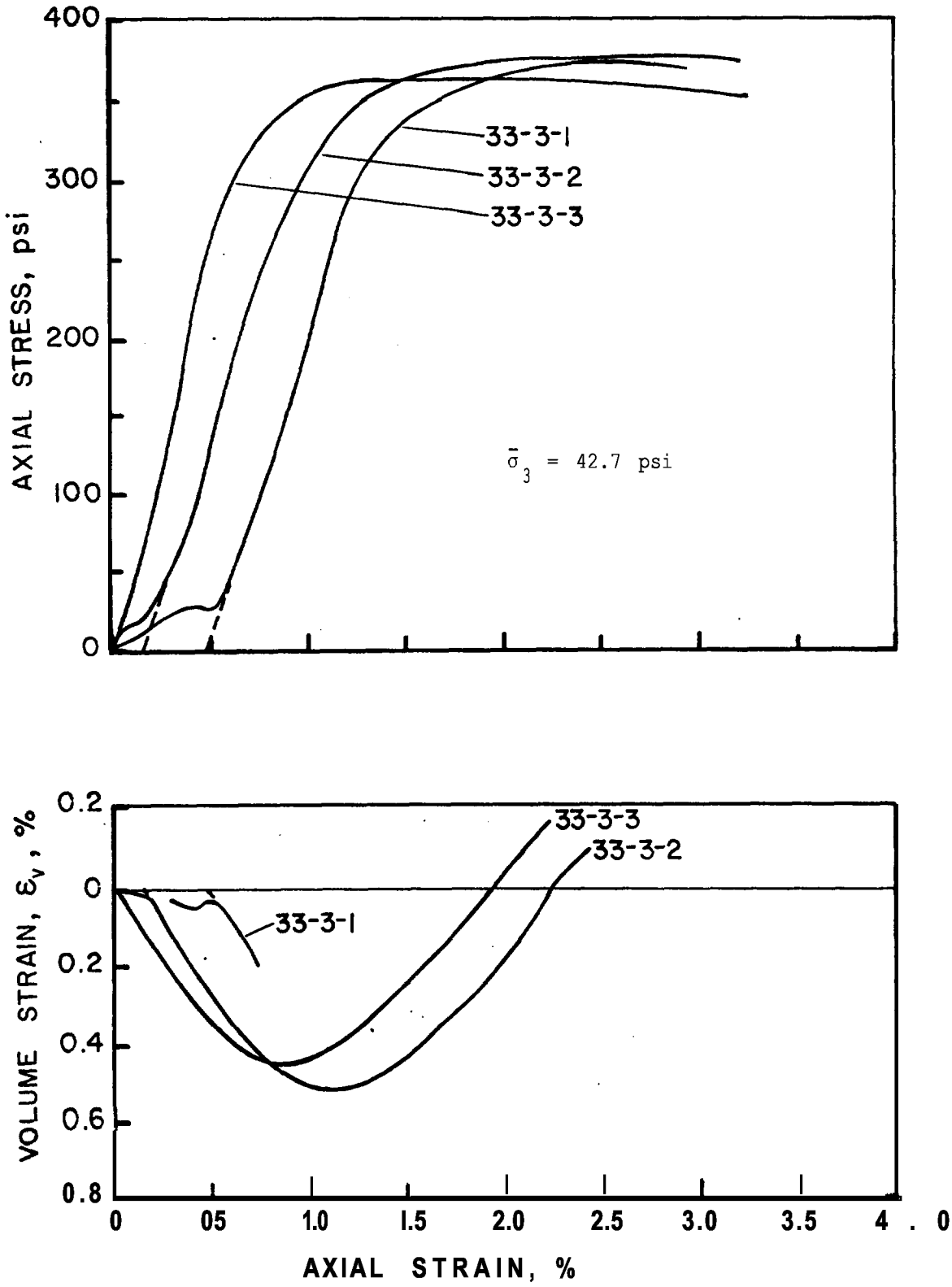

Public Service Company of New Hampshire	Triaxial Tests Structural Backfill	SAND-CEMENT SPECIMENS 2.8-IN.-DIA., 5% CEMENT 33-DAY CURE, $\bar{\sigma}_3$ = 42.7p
Geotechnical Engineers Inc. Winchester, Massachusetts	Project 77386	Feb. 23, 1978 Fig. 17

GEOTECHNICAL ENGINEERS INC.

1017 MAIN STREET. WINCHESTER. MASSACHUSETTS 01890 (617) 729-1625

PRINCIPALS
RONALD C. HIRSCHFELD
STEVE J. POULOS
DANIEL P. LA GATTA
RICHARD F. MURDOCK
GONZALO CASTRO

ASSOCIATES
CHARLES E. OSGOOD
BARTLETT W. PAULDING, JR.

March 10, 1978
Project 77386
File No. 2.0

Mr. John Herrin
Public Service Co. of New Hampshire
1000 Elm Street - 11th Floor
Manchester, NH 03105

Subject: Interim Test Results on Sand-Cement Backfill
Seabrook Station

Reference: Preliminary Report, Compression Tests On Structural Backfill and Sand-Cement
Seabrook Station, GEI, January 24, 1978

Dear Mr. Herrin:

The purpose of this letter is to present additional data on moduli determined on sand-cement backfill. These data supplement the data in the reference and in our letters of February 14 and 27.

Three triaxial tests were performed on cylindrical specimens of sand-cement. The specimens were cured for 28 days and were tested under a confining stress of 7.1 psi. The test data are summarized in a revised Table 5.

The values of the coefficient of subgrade reaction were computed for several strain levels in the same manner as those shown in the preliminary report of January 24 and the letters of February 14 and 27. The following table lists all values obtained to date for the sand-cement specimens:

k_sD-VALUES FOR SAND-CEMENT BACKFILL
28-DAY CURE, 5% CEMENT

Tabulated values are in psi

Effective Vertical Stress at Springline psi	Allowable Diameter Strain, %			
	0.02	0.1	0.3	0.5
CUBE SPECIMENS				
0			100,000	
CYLINDRICAL SPECIMENS				
0	200,000	89,000	60,000	36,000*
7.1	115,000	106,000	79,600	50,600*
42.7		138,000	163,000	129,600

*Modulus value determined at strains greater than the strain at peak compressive strength.

Geotechnical Engineers Inc.

Project 77386
Revised March 6, 1978

Three unconfined tests were performed on cube specimens of sand-cement cured for 90 days. The test data are summarized in a revised Table 4.

The stress-strain curves for the additional tests will be transmitted as soon as they have been drafted.

Sincerely yours,

GEOTECHNICAL ENGINEERS INC.

Steve J. Poulos
Principal

GC/SJP:ms
Encl.
cc: R. Pizzuti, YAEC
D. Rhoads, UE&C
A. Desai, UE&C
D. Patel, UE&C 7UO

TABLE 4 - UNCONFINED TESTS ON 2-IN. CUBE SAMPLES OF SAND-CEMENT, 5% CEMENT SEABROOK STATION

Cure Time days	Test No.	Unit Weight Wet pcf	Unconfined Strength psi	Strain At Peak %	Modulus of Elasticity* psi
7	7-1	124.0	66.7	0.80	10,600
	7-2	123.9	72.5	0.92	10,110
	7-3	126.2	85.3	0.83	13,650
			Avg 74.8		Avg 11,450
28	28-1	127.4	141.6	0.67	33,330
	28-2	126.2	133.8	0.77	19,130
	28-3	126.8	130.0	0.87	22,760
			Avg 135.0		Avg 25,070
90	90-1	124.4	117.9	0.95	26,320
	90-2	124.5	139.4	1.08	27,030
	90-3	125.0	133.7	0.84	31,250
			Avg 130.3		Avg 28,200

*Modulus computed for the straight line portion of the stress-strain curve, neglecting any curvature at origin, which may be affected by initial seating strains.

Geotechnical Engineers Inc.

Project 77386
January 23, 1978
Revised March 6, 1978

TABLE 5 - COMPRESSION TESTS ON 2.8-IN.-DIAMETER SAND-CEMENT SPECIMENS, 5% CEMENT[1]
SEABROOK STATION

Cure Time days	Test No.	Unit Weight Wet pcf	Confining Stress ksc	Compressive Strength psi	Strain at Peak %	Initial Modulus of Elasticity psi
28	28-0-1	126.2	0.0	91	0.65	75,000
28	28-0-2	124.8	0.0	89	0.58	52,200
28	28-0-3	124.1	0.0	106	0.80	34,300
33	33-3-1	124.4	42.7	372	2.10	35,000
28	Estimated[2]			372		34,600
33	33-3-2	124.1	42.7	376	2.40	33,300
28	Estimated[2]			376		32,900
33	33-3-3	124.8	42.7	364	1.40	40,000
28	Estimated[2]			364		39,600
28	28-.5-1	124.6	7.1	119	0.60	32,600
28	28-.5-2	123.9	7.1	134	0.90	22,900
28	28-.5-3	124.3	7.1	122	0.97	17,400

NOTE: 1) The percentage of cement is computed as the ratio of the weight of cement to the total weight of sand, cement, and water, and then multiplying that ratio by 100.

2) The strengths and moduli for 28-day cure was estimated based on the rates of change measured for the cube specimens.

Geotechnical Engineers Inc.

Project 77386
February 7, 1978
Revised-February 24, 1978
Revised March 6, 1978

APPENDIX 2N

GEOTECHNICAL REPORT TEST FILL STUDY OF QUARTZITE MOLE CUTTINGS

The information contained in this appendix was not revised, but has been extracted from the original FSAR and is provided for historical information.

TEST FILL STUDY
OF
QUARTZITE MOLECUTTINGS

Submitted to

Public Service Company of New Hampshire

Submitted by

Geotechnical Engineers Inc.
1017 Main Street
Winchester, Massachusetts 01890

July 13, 1979
Project 76301

William R. Fisher
Senior Engineer

Steve J. Poulos
Principal

TABLE OF CONTENTS

LIST OF TABLES

LIST OF FIGURES

1. INTRODUCTION

1.1 Purpose

The intake and discharge tunnels at Seabrook Station are being excavated using a tunnel boring machine, more commonly termed a mole. The excavated material from the mole is a widely-graded crushed stone commonly termed tunnel muck, which, for this report, shall be termed "molecuttings."

The purpose of the test fill study was to determine if the quartzite molecuttings obtained from-the tunnel excavations could be used for Safety and Nonsafety-Related Structural Fill. Construction of the test fills provided the opportunity to observe the behavior of the molecuttings during placement and obtain data necessary to develop procedures to control the compaction of the molecuttings during placement.

1.2 Background

The molecuttings from the quartzite bedrock in the tunnels are widely-graded crushed stone containing up to 13% passing the No. 200 sieve. The grain size curve of the molecuttings plots below the lower limit of the Safety and Nonsafety-Related Structural Backfill specification. The resistivity of the molecuttings is generally below the specified minimum value of 10,000 ohms-cm^3. Thus, although the molecuttings appeared superior to the gravelly sand structural fill as a backfill material, it was rejected because the gradation and resistivity requirements did not comply with the specifications. Use of the molecuttings for Safety and Nonsafety-Related Structural Fill required that selected tests be performed which would demonstrate that the molecuttings were as good or better than the presently used gravelly sand when both materials were placed at the same percent compaction. Investigation of the resistivity problem was addressed by UE&C.

The Safety and Nonsafety-Related Structural Fill is used for backfill around pipes and conduits, under floor slabs, roads, etc. For these applications the deformation characteristics of the backfill will control the soil support of the pipes and settlements of structures. One method of determining the deformation properties of a soil is by determining the soil modulus by the use of a plate load test. Plate load tests were performed on carefully constructed test fills consisting of (a) gravelly sand, (b) molecuttings, and (c) a test fill of essentially alternating layers of gravelly sand and molecuttings which herein will be referred to as the stratified gravelly sand and molecuttings test fill

The modulus from each test fill was used as a means of comparing the desirability of the molecuttings versus the gravelly sand for use as Safety and Nonsafety-Related Backfill.

The molecuttings are widely graded and contain high percentages of stone retained on the 3/4-in. sieve. In many cases the percent retained on the 3/4-in. sieve exceeds the allowable limits for the Modified AASHO compaction test (D1557). Thus, it was necessary to determine by means of field and laboratory tests performed during construction of the test fill how construction control of the placement of the molecuttings should be handled.

1.3 Summary

The results of the plate load tests indicate that the molecuttings will provide superior support for pipes and structures than the gravelly sand currently accepted for Safety and Nonsafety-Related Structural Fill when both materials are placed at the same percent compaction. The molecuttings and gravelly sand will provide about equivalent deformation properties when the percent compaction of the molecuttings is as much as 2 to 3% lower than the gravelly sand. Therefore, the use of molecuttings for Safety and Nonsafety-Related Structural Fill is recommended. Further, it is recommended that the percent compaction of the molecuttings for Safety and Nonsafety-Related Structural Fill be 95% and 93%, respectively.

The molecuttings used in constructing these test fills were widely graded crushed stone with up to 7% passing the No. 200 sieve. The water content of the material varied from 3 to 4% up to 10% during placement. Because of the grain-size distribution compaction of the molecuttings was sensitive to fluctuations in the water content of the material. Based on data obtained from tests performed during construction of the test fills, limitations on the grain-size distribution and water content of the molecuttings during placement have been recommended in Section 5.

Construction of the test fills indicated that placement of the molecuttings can be controlled by modifying standard testing procedures. The in-place dry density can be measured using the nuclear density meter and the laboratory reference dry density determined by modifying the currently specified compaction tests.

Details of the construction of the test fills, performance and results of the plate load tests, and procedures for control of placement and compaction of molecuttings are presented in the following sections.

2. CONSTRUCTION OF TEST FILLS

Four test fills were constructed for this study. The orientation of the test fills is shown in Fig. 1. The soils and details of placement for each test fill is presented below.

2.1 Gravelly Sand

Gravelly sand satisfying the requirements for Safety and Nonsafety-Related Structural Fill Specifications 9763-8-5 and 9763-8-4 was placed in 8-in. -thick loose lifts and compacted to a minimum of 95% of the maximum dry density as determined by ASTM D1557, Method D. Satisfactory compaction was generally achieved by applying water to the surface of the loose lift and compacting with six coverages with the Mikasa double drum roller. Eight lifts of gravelly sand were placed and compacted, resulting in a total height of about 4 ft.

2.2 Molecuttings (Controlled Placement)

The construction of this test fill was controlled to achieve the compaction requirements of Safety and Nonsafety-Related Structural Fill (i.e., 95% of the maximum dry density as determined by ASTM D1557).

Molecuttings were placed in 8-in. loose lifts and compacted to 95% compaction. To achieve 95% compaction, control of the water content to within a few percent of the optimum water content, and numerous coverages with the Mikasa double drum roller was required. Attempts at controlling the water content included mixing of wet and dry molecuttings and adding water to molecuttings with water contents 2 to 3% below optimum. Molecuttings placed at water contents several percent higher than optimum could not achieve 95% compaction until sufficient drainage had reduced the water content to near the optimum value. Eight lifts of molecuttings were placed and compacted resulting in a total height of about 4 ft.

2.3 Molecuttings (No Special Controls)

Construction of this test fill involved the placement of the molecuttings with limited control of water content and a specified compactive effort. The molecuttings were generally placed in G-in. loose lifts and compacted by six coverages with the Mikasa double drum roller. In some instances, water content control was limited to permitting drainage of a compacted layer overnight before placement of the succeeding layer. Eight lifts of molecuttings were placed and compacted.

2.4 Stratified Molecuttings and Gravelly Sand

The first three lifts of this test fill were constructed the same way as the test fill of Molecuttings (No Special Controls). The water content of the molecuttings placed for the third lift was about 3% higher than optimum. The surface of the third lift was saturated and became severely rutted during compaction. Sandwiching layers of gravelly sand between layers of molecuttings was done to determine (1) if the gravelly sand provided drainage of sandwiched layers of molecuttings and (2) the feasibility of constructing a backfill of stratified gravelly sand and molecuttings (which may be required in the zone of frost penetration). Therefore, lifts 4 and 6 were constructed using gravelly sand. Lift 4 was compacted with six coverages of the Mikasa double drum roller and lift 6 was compacted to at least 95% compaction. Molecuttings for lifts 5, 7 and 8 were generally placed in 8-in. loose lifts with limited water content control and compacted with six coverages of the Mikasa double drum roller.

3. PERCENT COMPACTION OF TEST FILLS

3.1 Gravelly Sand

The percent compaction of each lift was determined by performing in-place density tests and laboratory compaction tests. The average percent compaction of the gravelly sand test fill was 97.4%.

The in-place density for each lift, after compaction, was determined by performing two 6-in. -diameter Sand Cone (SC) tests and three Nuclear Density Meter (NDM) tests. The in-place density determined by the NDM was generally performed at probe depths of 4 in. and 8 in. The two SC tests were performed adjacent to two of the NDM tests to provide a comparison of the water content and dry density measured by each 'method. The SC and NDM tests were generally performed within a 5-ft radius of the plate load test location. .

One-point compaction samples were obtained adjacent to the SC and NDM test locations. The one-point samples were compacted in accordance with ASTM D1557, Method D. The maximum dry density for the one-point sample was determined by plotting the one-point dry density on a family of curves for the gravelly sand and interpolating the maximum dry density. The percent compaction was computed by dividing the in-place dry density by the corresponding one-point compaction determined maximum dry density. Table 1 presents the summary of the percent compaction achieved in the test fill. A profile of the test fill and the average percent compaction for each lift is shown on Fig. 2.

Three compaction tests were performed in accordance with ASTM D1557, Method D, on bag samples of gravelly sand obtained from material placed in lifts 2, 4 and 7. The compaction curves and related grain-size curves performed by Pittsburgh Testing Labs are shown on Figs. 4 and 5, respectively.

3.2 Molecuttings (Controlled Placement)

The average percent compaction achieved for this test fill was 96.7%. The in-place density of each lift after compaction was determined by performing several NDM tests and, when the soil conditions were acceptable, one 12-in.-diameter SC test. The SC test was performed adjacent to a NDM test to provide a comparison of the water content and dry density measured by each method. Observations in the field and data from tests indicated that the hole excavated for the SC test tended to squeeze in or reduce in volume when the molecuttings were placed and compacted

at water contents above or near optimum. Results from the SC tests when these conditions existed gave unreasonably high dry densities, and, as a result, SC tests were considered valid only when they were performed in areas where the water content of the molecuttings was less than 5%. A more complete discussion of this problem is presented in Section 5. The SC and NDM tests were generally performed within about a 5-ft radius of the plate load test.

Generally, several NDM tests were required before a lift of the molecuttings was compacted to a dry density that was estimated to provide 95% compaction. One-point compaction samples were obtained adjacent to the series of NDM and SC tests that indicated about 95% compaction had been achieved. The one-point samples were compacted in accordance with ASTM D1557, Method C, except the minus 1½-in. material was included for compaction. The maximum dry density for the one-point sample was determined by plotting the one-point dry density on a family of compaction curves for molecuttings and interpolating the maximum dry density.

Correction of the in-place dry density to account for the plus 1½-in. material, which was removed for the laboratory test, was necessary in order to determine the percent compaction. Details of the correction procedure are presented in Appendix A. The percent compaction was computed by dividing the corrected in-place dry density by the corresponding maximum dry density determined by the one-point compaction technique. Table 2 presents the summary of the percent compaction achieved in the test fill. A profile of the test fill and the average percent compaction for each lift is presented in Fig. 2.

Two compaction tests were performed in accordance with ASTM D1557, Method C, except the minus 1½-in. material was included and there was no limit on the percent retained on 1&-in. sieve on bag samples of molecuttings from lifts 4 and 6. The compaction curves and related grain-size curves are shown on Figs. 6 and 7, respectively.

3.3 Molecuttings (No Special Controls)

The average percent compaction of this test fill was 93.0%. The water content of the molecuttings during placement was generally above optimum and was not controlled during compaction. Sand Cone tests to determine the in-place dry density were not performed because of the inaccuracy in performing the test in molecuttings compacted at water contents near or above optimum. The in-place dry density was determined by performing at least

two and most usually three to five NDM tests at probe depths of 4 and 8 in. The NDM tests were generally performed within a 5-ft radius of the plate load test location.

One-point compaction samples were obtained adjacent'to the series of NDM tests that indicated the next lift of molecuttings could be placed. In some cases after a lift had been compacted, NDM tests performed, and one-point samples obtained, the lift was permitted to drain overnight and additional NDM tests taken in the morning. One-point compaction samples generally were not obtained for the NDM tests performed after drainage. The procedure to compute the percent compaction for each in-place density test was the same as described in the previous section.

Table 3 presents the summary of the percent compaction achieved in the test fill. A profile of the test fill and the average percent compaction for each lift is presented in Fig. 3.

Two compaction tests were performed in accordance with ASTM D1557, Method C, except the minus 1½-in. material was included and there was no limit on the percent retained on the 1½-in. sieve on bag samples obtained from lifts 2A and 7A. The compaction curves and the grain-size curve for lift 2A are shown on Figs. 6 and 7, respectively.

3.4 Stratified Molecuttings and Gravelly Sand

The average percent compaction of the gravelly sand and molecuttings test fill was 92.8%. Molecuttings were used for lifts 1, 2, 3, 5, 7, and 8 for this test fill. The in-place dry density and percent compaction of the molecuttings was determined in accordance with the procedure described in the previous section. Lifts 4 and 6 of the test fill were constructed using gravelly sand. The in-place density for lift 4 was determined by four NDM tests. One SC test and 3 NDM tests were performed in lift 6. The maximum dry density and computation of the percent compaction at each in-place density test location was as described in the section for gravelly sand. Table 4 presents the summary of the percent compaction in the test fill. A profile of the test fill and the average percent compaction of each lift is presented in Fig. 3.

4. PLATE LOAD TESTS

Five plate load tests were performed on the four test fills. The plate load test number, test fill and date of the test is presented below.

Plate Load Test No.	Test Fill	Date of Test
1	Gravelly Sand	June 7, 1979
2	Molecuttings (No Special Control) .	June 14, 1979
3	Stratified Molecuttings and Gravelly Sand	June 15, 1979
4	Molecuttings (Controlled Placement)	June 18, 1979
5	Molecuttings (No Special Control)	June 27, 1979

The locations of the tests are indicated on Fig. 1 and details of the procedure are presented in Appendix B. In brief the procedure was as follows: an 18-in.-diameter steel plate was generally placed 12 in. below the surface of the test fill and loaded to produce contact stresses to 4 tsf and then to 12 tsf. Deflections of the plate were measured and recorded.

The results of the plate load tests are presented in Figs. B2 through B6. Values of Young's Modulus, E, were calculated from the results of the plate load tests using elastic theory. A description of the analysis is presented in Appendix B. A summary of the modulus calculated for each test is presented in Table 5. The percent compaction indicated in Table 5 represents the average percent compaction of lifts within the zone of significant stress increase due to the load on the plate. For an 18-in.-diameter plate this zone is about 18- to 36-in.-thick.

The soil modulus determined by the plate load test vs percent compaction is plotted on Fig. 8. The results indicate that the molecuttingshave a much higher modulus than the gravelly sand when both materials are compacted to the same percent compaction. In fact, the modulus of the molecuttings compacted to 93% compaction is approximately equivalent to the modulus of the gravelly sand placed at 97% compaction. Plate Load Test No. 5 (PLT-5) was performed 13 days after and about 4 ft away from Plate Load Test No. 2 (PLT-2). The soil modulus for PLT-5 was about two times

the modulus for PLT-2. The increase in modulus may have been caused by densification of the molecuttings as a result of drainage over the 13 day period between the performance of the two tests. Assuming that the molecuttings were saturated after PLT-2 and the water content reduced by 1% during a period of 13 days, the in-place dry density would have increased by 2 to 3 pcf or about a 1 to 2% increase in the percent compaction. The modulus for PLT-5, as a result of the densification, nearly plots on the line from PLT-2 to PLT-4.

Test PLT-3 was performed on the stratified molecuttings and gravelly sand test fill. The average percent compaction of the molecuttings and gravelly sand was 92.5 and 96.1%, respectively. Plate load tests, PLT-2 and PLT-1, were performed on separate test fills of molecuttings and gravelly sands compacted to about the same percent compaction and the moduli were 7,300 psi and 10,100 psi, respectively. The moduli determined for the stratified test fill, however, was 17,000 psi. Based on the results of PLT-1 and PLT-2 the anticipated modulus determined by FLT-3 was between 8 and 10,000 psi. The high modulus measured by PLT-3 may have been caused by one or more of the following factors:

1. Distribution of the load may have been more rapid for the layered fill than in a homogeneous fill, and

2. Drainage of the molecuttings and related increases in dry density and modulus may have accelerated faster in the stratified test fill than in the homogeneous molecuttings (No Special Controls) test fill due to drainage through the gravelly sand layers.

5. PLACEMENT AND FIELD CONTROL OF MOLECUTTINGS

The purpose of this section is to present recommendations for the placement and field control of molecuttings based on field and laboratory data obtained during construction of the test fills.

Review of the data obtained provided the information necessary to make recommendations on the limits for grain size, lift thickness, determination of in-place density and percent compaction, and control of water contents of the molecuttings. A discussion of each of the items is presented below.

5.1 Grain-Size Limits

Grain-size analyses were performed on thre'e samples of the molecuttings used for the test fills. The grain-size curves are presented on Fig. 7. The molecuttings were generally widely graded with uniformity coefficients of 45 to 100. The maximum particle size was generally less than 3-in.-diameter and the percent by weight passing the No. 200 sieve was from 5 to 7%. Based on these and other grain-size analyses recommendations for gradation requirements were developed and are presented in Appendix A.

5.2 Lift Thickness

The molecuttings were placed in 8-in.-thick loose lifts during construction of the test fills. Observations made during placement of the molecuttings indicated that the ability to achieve a specific percent compaction was mostly affected by the water content of the material rather than the thickness of the lift. When the molecuttings were placed at water contents above optimum, a specific degree of compaction generally **was** not achieved until the water content was reduced to'or below the optimum water content as a result of drainage. The time required for drainage is a function of the lift thickness and, therefore, where 95% and 93% compaction is required, lift thicknesses of 8-in. and 12-in. are recommended. The 12-in.-thick loose lift in areas where 93% compaction is required was recommended based on the fact that the average percent compaction of 93.0% was achieved for the molecuttings (No Special Controls) test fill without the benefit of extensive compactive efforts.

5.3 Determination of In-Place Dry Density

The nuclear density meter (NDM) provides a much faster determination of the field in-place dry density and water content than the sand cone (SC). The accuracy of the NDM tests performed in the gravelly sand and molecuttings was verified by comparing the results of adjacent NDM and SC tests.

5.3.1 Gravelly Sand

Generally, two SC tests were performed adjacent to two NDM tests on each lift of the test fill to compare the in-place dry density and water content measured by each method.. The in-place water content determined by the sand cone versus nuclear density meter is plotted on Fig. 9. The data indicate that both methods measure essentially the same water content at values less than 8% and, as the water content increases, the NDM measures a lower value than the SC. As a result, a correction was applied to the water content measured by the NDM to compute the in-place dry density... A plot of sand cone versus nuclear density meter determined in-place dry density is shown on Fig. 10. The correlation of the densities determined by each method was considered to be poor. The correlation may have been improved if more frequent moisture checks had been performed during construction of the test fill.

5.3.2 Molecuttings

Twelve-inch-diameter sand cone tests were performed in the molecuttings to reduce the effects that the maximum particle size and percentage of material larger than the 1½-in. sieve would have on in-place dry density determination. The in-place dry density and water content determined by the SC test was compared to the results from adjacent 8-in.-deep NDM tests. Comparison of the results indicated the water content determined by the NDM averaged 1.7% higher than that determined by the sand cone. The 1.7% difference in water contents was confirmed by performing water content checks at random NDM test locations. A 1.7% bias correction was applied to the water contents determined by the NDM. A plot of sand cone determined water content versus nuclear density meter water content (with a 1.7% bias correction) is presented on Fig. 11.

The plot shows there is a good correlation between the sand cone and nuclear density meter (after bias correction) water content determinations. A second water content check was made on molecuttings.after the test fill was completed which indicated that the bias had increased to 2.5%. Because the water content bias changed significantly within a period of two weeks periodic checks of the bias are recommended.

The in-place dry density determined by the sand cone test and the 8-in. NDM test after correction for the water content bias is plotted on Fig. 12. The solid dots and dashed circles represent in-place dry density measurements at water contents less than 5% and greater than 5%, respectively. The data indicate that there is good correlation of dry densities determined by both methods at water contents less than 5% and that the SC measured higher dry densities than the NDM at water contents above 5%. For this test fill the SC tests performed in molecuttings compacted at water contents above 5% are not considered valid for the reasons presented in the following discussion.

When the molecuttings were placed at water contents above about 5%, the compacted surface would exhibit a spongy behavior when one walked across the surface. The degree of sponginess increased as the moisture increased above the optimum water content. The sponginess is believed to be caused by water and air pore pressures. The net effect was that as the sand cone hole was excavated the pore pressures at the walls of the hole were relieved by the walls moving laterally into the hole until an equilibrium of the pore pressure at the walls of the hole was reached. Thus, by the time the volume of the hole was measured a significant decrease in the volume of the hole had occurred but the quantity of soil excavated was from the original volume. The result was that the dry soil excavated was divided by a reduced volume which resulted in an inaccurately high computed dry density.

The SC and NDM test results indicate that the NDM can be used to determine the in-place dry density and water content of molecuttings. The water content bias should be checked periodically to account for changes that occur in the molecuttings. Details of a recommended placement procedure arepresented in Appendix A.

5.4 Determination of Percent Compaction

The field and laboratory data indicated the nuclear density meter could be used to determine the in-place dry density after the appropriate water content bias had been determined for the molecuttings being tested.

The preferred field procedure for determing the percent compaction of compacted soil is as follows:

1. Gbtain a one-point sample of the soil before compaction.

2. Perform the' one-point compaction test in the lab and determine the maximum dry density from a family of curves.

3. Perform the in-place dry density of the compacted lift using the nuclear density meter at or near the location of where the one-point sample was taken.

This procedure can be used for the molecuttings if at least three nuclear density meter determinations of the in-place dry density are made. The average of the three tests should be used to represent the in-place density for computation of the percent compaction. The above procedure will reduce the effect that minor variations in the character of the molecuttings will have on the in-place dry density determination.

The use of a standard laboratory compaction test or one which was slightly modified was considered the best method of determining the maximum dry density of the molecuttings. The Modified AASHG Compaction Test, ASTM D1557, permits the use of minus 3/4-in. material to be compacted in 6-in. molds. Grain-size analyses performed on molecuttings indicate that nearly 50% of the sample is retained on the 3/4-in. sieve, and, as a result, the material passing the 3/4-in. sieve would behave much differently than the total sample during compaction. A sample of the molecuttings that would represent the compaction behavior of the material was considered possible if the amount of coarse material removed was limited to about 20% by weight of the total sample. This could generally be achieved by removing material retained on the 1½-in. sieve. For the test fill the laboratory compaction used was ASTM D1557, Method C, except the plus 1½-in. material was removed. Because this compaction test, as modified above, was used for the test fill and gave reasonable results its use is recommended for performing laboratory compaction tests on the molecuttings.

5.5 Water Content Control

The laboratory compaction curves for compaction tests performed on samples of molecuttings show a sharp peak in dry density at the optimum water content, Fig. 6. The dry density drops as the water increases or decreases from the optimum value. The laboratory data show that small variations in water content significantly affect the degree of compaction that can be achieved in the molecuttings. This behavior was also observed during placement and compaction of the molecuttings in the test fills. In the test fill where placement of the molecuttings was controlled, the required percent compaction generally could only be achieved by controlling the water content, by either wetting or drying, of the molecuttings. The most efficient compaction of the molecuttings was when the water content was from about 4 to 6%. Therefore, the water content of the molecuttings should not differ from optimum by more than $\pm$ 1%, for most efficient compaction.

TABLES

TABLE 1 - SUMMARY OF FIELD DENSITY TESTS
GRAVELLY SAND TEST FILL
QUARTZITE MOLECUTTINGS STUDY
SEABROOK STATION

Lift No.	Sample No.	One-Point Compaction			Laboratory Maximum Dry Density	In-Place Dry Density, pcf		Percent Compaction
		Percent +3/4-in. Material	Water Content	Dry Density		Total Sample	Corrected For +3/4-in. Material	
		%	%	γ_d, pcf	γ_d, pcf			%
1	ND-1	One-point samples not obtained			122.1 (1)	120.9	This column does not apply for compaction test performed using ASTM D1557, Method D	99.0 (3)
	ND-2					123.7		101.3 (3)
	ND-3					121.1		99.2 (3)
	SC-1					118.1		96.7 (3)
2	SC-1	11.1	9.7	120.9	123.0	115.0		93.5
	ND-2	4.8	10.0	116.8	120.5	117.1		97.2
	SC-3	9.4	9.0	120.1	123.0	120.3		97.8
	ND-4 (1)	8.1	9.2	117.9	122.0	119.5		97.2
	ND-5 (1)	N.A.	13.0	122.3	122.3	119.2		97.4 (3)
3	ND-1	One-point samples not obtained				123.0		100.6 (3)
	SC-2					126.0		103.2 (3)
	ND-3					121.4		99.4 (3)
	SC-4					122.5		100.3 (3)
	ND-5 (1)	N.A.	5.2	115.5	122.1	121.5		99.4 (3)
4	ND-1 (2)	8.5	4.9	117.8	125.5	119.1		94.9
	SC-2 (2)	8.5	4.9	117.8	125.5	120.5		96.0
	ND-3 (2)	5.0	7.4	119.1	124.0	124.1		100.0
	SC-4 (2)	5.0.	7.4	119.1	124.0	118.8		95.8
	ND-5	5.8	7.0	121.5	126.0	119.0		94.4

NOTES: (1) One-point compaction sample performed by Pittsburgh Testing Labs.
(2) One one-point compaction sample obtained for sand cone and nuclear density test performed adjacent to each other.
(3) Percent compaction computed using maximum dry density determined by Pittsburgh Testing Lab.

TABLE 1 - SUMMARY OF FIELD DENSITY TESTS
GRAVELLY SAND TEST FILL
QUARTZITE MOLECUTTINGS STUDY
SEABROOK STATION

Lift No.	Sample No.	One-Point Compaction: Percent +3/4-in. Material, %	One-Point Compaction: Water Content, %	One-Point Compaction: Dry Density γ_d, pcf	Laboratory Maximum Dry Density γ_d, pcf	In-Place Dry Density, pcf: Total Sample	In-Place Dry Density, pcf: Corrected For +3/4-in. Material	Percent Compaction, %
5	ND-1 (2)	4.8	9.7	124.5	125.0	125.5		100.4
	SC-2 (2)	4.8	9.7	124.5	125.0	123.8		99.0
	ND-3	5.8	10.3	123.1	124.0	120.9		97.5
	SC-4 (2)	13.0	9.3	126.4	127.0	124.9		98.0
	ND-5 (2)	13.0	9.3	126.4	127.0	121.3		95.5
6	ND-1 (2)	3.9	10.0	122.3	123.2	117.8		95.6
	ND-2 (2)	13.2	8.4	126.0	127.0	118.7		93.5
	SC-3 (2)	13.2	8.4	126.0	127.0	125.7		99.0
	SC-4 (2)	9.1	7.6	123.3	126.5	123.0		97.2
	ND-5 (2)	9.1	7.6	123.3	126.5	126.6		99.7
7	ND-1 (2)	5.9	6.8	120.5	126.5	122.5		96.8
	SC-2 (2)	5.9	6.8	120.5	126.5	123.8		97.9
	ND-3 (2)	10.7	7.8	121.0	124.8	121.6		97.4
	SC-4 (2)	10.7	7.8	121.0	124.8	123.2		98.7
	ND-5	11.3	7.6	121.5	125.8	121.9		96.9
8	ND-1	One-point samples not obtained				119.6		98.9 (3)
	SC-2					118.9		98.3 (3)
	ND-3					120.2		99.4 (3)
	SC-4					118.8		98.3 (3)
	ND-5 (1)	N.A.	13.8	117.9	120.9	116.2		96.1 (3)

NOTES: (1) One-point compaction sample performed by Fittsburgh Testing Lab.
(2) One one-point compaction sample obtained for sand cone and nuclear density test performed adjacent to each other.
(3) Percent compaction computed using maximum dry density determined by Pittsburgh Testing Lab.

TABLE 2 - SUMMARY OF FIELD DENSITY TESTS

MOLECUTTINGS (CONTROLLED PLACEMENT) TEST FILL

QUARTZITE MOLECUTTINGS STUDY

SEABROOK **STATION**

Lift No.	Sample No.	One-Point Compaction			Laboratory Maximum Dry Density	In-Place Dry Density, pcf		Percent Compaction
		Percent +1½-in. Material, %	Water Content, %	Dry Density γ_d, pcf	γ_d, pcf	Total Sample	Corrected For +1½-in. Material	%
1	ND-12	One-point			N.A.	145.5	N.A.	N.A.
	ND-13	samples not			N.A.	144.0	N.A.	N.A.
	ND-14	obtained			N.A.	142.6	N.A.	N.A.
	ND-15				**N.A.**	**146.9**	144.5	N.A.
2	ND-8	10.8	5.1	145.4	151.0	150.0	146.9	97.3
	ND-9	24.9	5.1	146.0	151.5	149.5	140.9	93.0
	ND-10 (1)			143.3	(2)			
	SC-11 (1)	(1) 7 (2)	3.7	143.3 (2)	153.0 (2) 153.0	161.5 152.4	150.5 158.4	98 (3)
3	ND-10	11.4	4.6	145.9	152.0	143.1	139.0	91.4
	ND-12 (1)			144.9	(2)			
	SC-12 (1)	10 4.4 (2)	4.1 4.4	144 144.9 (2)	152.0 (2) 152.5	151.8 146.5 152.4	150.7 142.8 149.8	98.2 93.9 98.2
4	ND-1	7.3	5.0	151.2	154.0	149.4	147.4	95.7
	ND-2	8.2	4.6	148.3	154.0	148.3	145.9	94.7
	ND-3 (1)	6.8	4.3	147.5	154.0	144.9	142.7	92.6
	SC-4 (1)	(2)		147.5 (2)	154.0 (2)	149.7	149.7	97.2

NOTES: (1) One one-point compaction sample obtained for sand cone and nuclear density test performed adjacent to each other.

(2) Laboratory one-point compaction test results and interpolated maximum dry density are from adjacent nuclear density meter one-point compaction samples and test results.

(3) In-place dry density measured is in error for reasons discussed in the text.

TABLE 2 - SUMMARY OF FIELD DENSITY TESTS
MOLECUTTINGS (CONTROLLED PLACEMENT) TEST FILL
QUARTZITE MOLECUTTINGS STUDY
SEABROOK STATION

Lift No.	Sample No.	One-Point Compaction			Laboratory Maximum Dry Density	In-Place Dry Density, pcf		Percent Compaction
		Percent +1½-in. Material %	Water Content %	Dry Density γ_d, pcf	γ_d, pcf	Total Sample	Corrected For +1½-in. Material	%
5	ND-8	5.6	4.9	148.7	155.0	150.6	149.1	96.2
	ND-9	7.7	4.1	146.5	155.0	148.0	145.7	94.0
	ND-10 (1)	14.5	4.7	146.0 (2)	153.0 (2)	149.4	145.0	94.8
	SC-11 (1)	(2)		146.0	153.0	162.3	160.6	(3)
6	ND-4	16.9	4.0	146.0	155.0	152.6	146.0	95.5
	ND-5 (1)	7.8	4.5	147.9	153.0	150.2	148.1	96.8
	ND-6 (1)	7.5	4.2	148.3	154.0	152.3	150.4	97.7
	SC-7 (1)	(2)		148.3	154.0			
7	ND-4	12.5	4.9	145.2	151.0	147.1	143.1	94.8
	ND-5	12.2	5.0	147.5	152.0	149.5	145.9	96.0
	ND-6	10.4	4.6	146.3	152.0	147.6	144.4	95.0
8	ND-1	One-point samples not obtained				146.0	N.A.	N.A.
	ND-2					146.5	N.A.	N.A.
	ND-3					146.1	N.A.	N.A.

NOTES: (1) One one-point compaction sample obtained for sand cone and nuclear density test performed adjacent to each other.

(2) Laboratory one-point compaction test results and interpolated maximum dry density are from adjacent nuclear density meter one-point compaction samples and test results.

(3) In-place dry density measured is in error for reasons discussed in the text.

TABLE 3 - SUMMARY OF FIELD DENSITY TESTS
MOLECUTTINGS (NO SPECIAL CONTROLS) TEST FILL
QUARTZITE MOLECUTTINGS STUDY
SEABROOK STATION

Lift No.	Sample No.	One-Point Compaction			Laboratory Maximum Dry Density	In-Place Dry Density, pcf		Percent Compaction
		Percent +1½-in. Material %	Water Content %	Dry Density γ_d, pcf	γ_d, pcf	Total Sample	Corrected For + 1½-in. Material	%
1	ND-4	One-point				146.3		N.A.
	ND-5	samples not				142.4		N.A.
	ND-6	obtained				145.5		N.A.
	ND-7					149.1	149.1	N.A.
2	ND-4	12.3	4.6	147.7	155.0	149.4	145.7	94.0
	ND-5	10.6	5.8	149.0	152.0	145.8	144.5	95.1
	ND-6	14.5	5.5	149.6	152.0	145.8	142.3	93.6
	SC-7	12.3	4.6	147.7	155.0	157.8	154.5	91.0
3	ND-5	6.0	6.7	147.0	151.0	143.7	141.7	93.8
	ND-6	9.2	6.2	147.8	151.0	141.9	138.5	91.7
4	ND-1	10.6	6.5	148.8	151.1	144.7	141.1	93.3
	ND-2	15.5	6.6	146.0	151.0	143.0	137.1	90.8
5	ND-1	12.3	4.9	148.9	153.0	150.9	147.5	96.4
	ND-2	12.3	5.0	148.1	152.0	152.2	149.0	98.0
	ND-3	24.8	4.7	147.7	153.0	140.5	129.0	84.3
6	ND-5	23.5	4.3	153.3	156.0	154.2	147.7	94.7
	ND-6	8.5	3.6	145.1	153.0	145.1	142.3	93.0
	ND-7	9.4	5.6	153.6	155.0	143.3	140.0	90.3

TABLE 3 - SUMMARY OF FIELD DENSITY TESTS
MOLECUTTINGS (NO SPECIAL CONTROLS) TEST FILL
QUARTZITE MOLECUTTINGS STUDY
SEABROOK STATION

Lift No.	Sample No.	One-Point Compaction			Laboratory Maximum Dry Density	In-Place Dry Density, pcf		Percent Compaction
		Percent +1½-in. Material	Water Content %	Dry Density γ_d, pcf	γ_d, pcf	Total Sample	Corrected For +1½-in. Material	%
7	ND-7	5.1	3.1	141.2	149.0	140.0	138.1	92.7
	ND-8	4.0	3.4	140.1	148.0	139.2	137.7	93.0
	ND-9	7.5	3.9	143.6	151.0	148.8	146.6	97.1
8	ND-1	One-point samples not obtained				144.4	N.A.	N.A.
	ND-2					125.0	N.A.	N.A.
	ND-3					144.3	N.A.	N.A.

TABLE 4 - SUMMARY OF FIELD DENSITY TESTS
STRATIFIED MOLECUTTINGS AND GRAVELLY SAND TEST FILL
QUARTZITE MOLECUTTINGS STUDY
SEABROOK STATION

Lift No.	Sample No.	One-Point Compaction: Percent + 1½-in. Material, %	One-Point Compaction: Water Content, %	One-Point Compaction: Dry Density γ_d, pcf	Laboratory Maximum Dry Density γ_d, pcf	In-Place Density, pcf: TOY-11 Sample	In-Place Density, pcf: Corrected For +1½-in. Material	Percent Compaction, %
3	ND-7	15.0	5.7	149.3	153.0	148.8	144.1	94.2
	ND-8	12.2	6.0	148.8	152.0	145.9	141.8	93.3
4(1)	ND-3	11.3(2)	5.6	118.3	125.0	114.3	N.A.	91.4
	ND-4	11.5(2)	2.7	122.2	124.0	108.1	N.A.	87.2
	ND-5	3.3(2)	3.0	115.1	123.0	108.2	N.A.	88.0
	ND-6	7.4(2)	4.9	116.9	124.5	110.6	N.A.	88.8
5	ND-4	10.4	4.3	145.7	151.0	151.3	148.5	98.4(3)
	ND-5	16.3	3.8	144.8	153.0	138.1	130.8	85.5(3)
6(1)	SC-1(4)	N.A.	N.A.	123.3	127.5	123.8	N.A.	97.1
	ND-2(4)	14.1(2)	7.2	123.3	127.5	121.1	N.A.	95.0
	ND-3	2.7(2)	6.8	118.8	124.5	119.3	N.A.	95.8
	ND-4	12.4(2)	8.3	120.3	124.0	119.6	N.A.	96.5
7	ND-10	4.8	2.7	137.5	148.0	140.2	138.4	93.5
8	ND-4	One point samples not obtained				147.3	N.A.	N.A.
	ND-5					140.8	N.A.	N.A.

NOTES: (1) Gravelly sand used for the construction of Lift.
(2) Values represent percent +3/4-in. material.
(3) Nuclear density probe may have penetrated gravelly sand layer below.
(4) One one-point compaction sample obtained for SC-1 and ND-2.

TABLE 5 - SUMMARY OF PLATE LOAD TESTS RESULTS
QUARTZITE MOLECUTTINGS STUDY
SEABROOK STATION

Plate Load Test No.	Soil At Test Location	Soil Modulus, psi		Average Percent Compaction	Remarks
		Virgin	Reload		
1	Gravelly Sand	10,100-10,500	20,000-29,700	97.1	
2	Mole Cuttings (No Special Control)	7,300-7,700	25,200-40,300	92.6	
3	Stratified Mole Cuttings and Gravelly Sand	17,000-26,100	41,200-45,300	M.C.=92.5 G.S.=96.1	Ave. Percent Compaction 93.7
4	Mole Cuttings (Controlled Placement)	28,300-35,900	54,300-66,600	95.3	
5	Mole Cuttings (No Special Control)	13,200-21,200	43,100-49,200		Performed 13 days after PLT-2

FIGURES

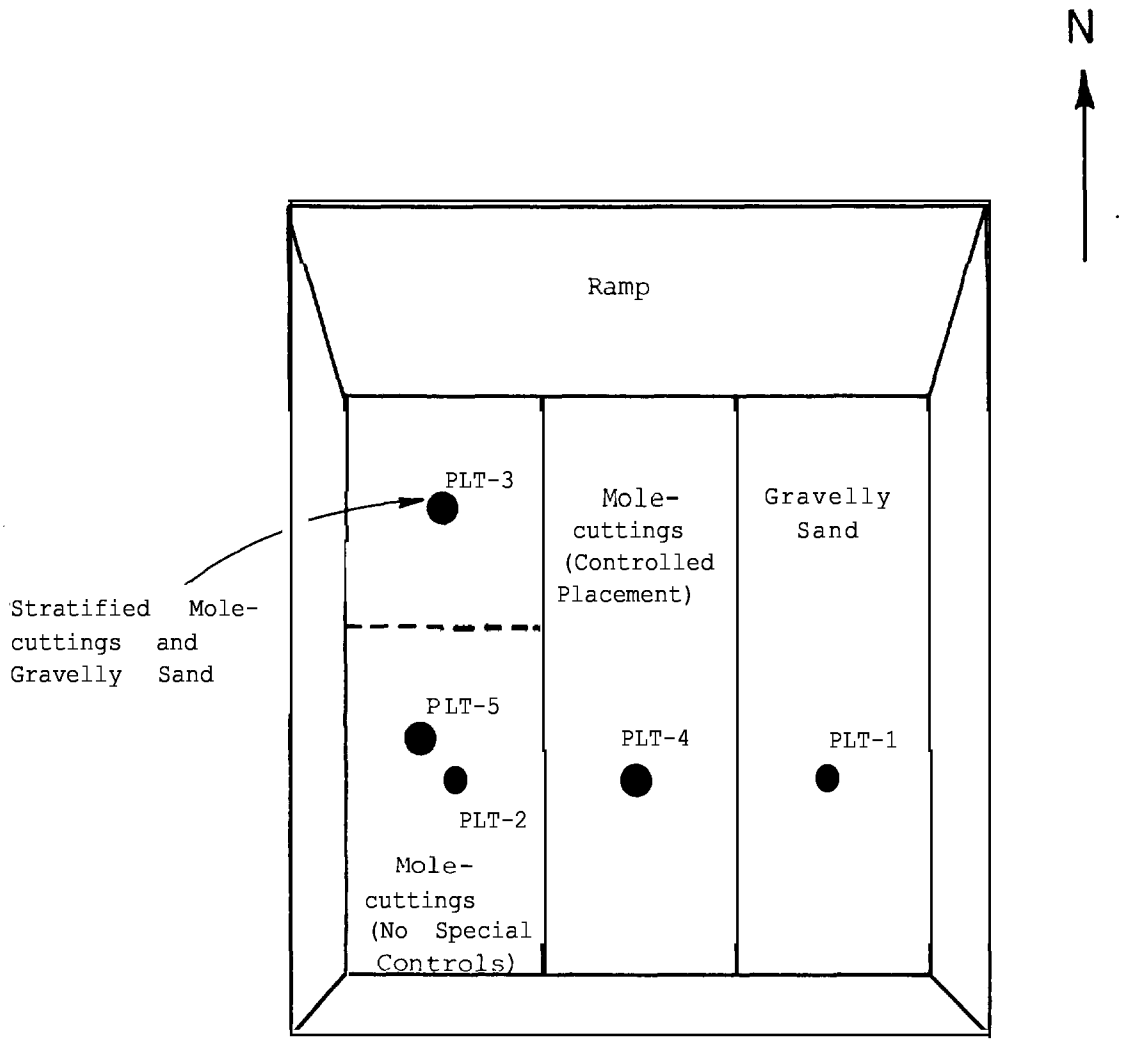

Not To Scale

Public Service Company of New Hampshire	Quartzite Molecuttings Study	PLAN VIEW OF TEST FILLS
GEOTECHNICAL ENGINEERS INC. WINCHESTER, MASSACHUSETTS	Project 76301	July 11, 1979 Fig. 1

PROFILE OF GRAVELLY SAND
TEST FILL

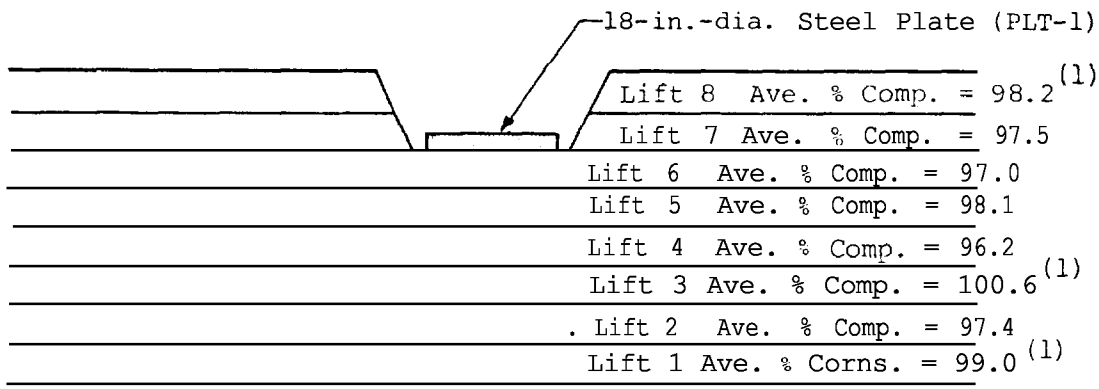

Scale: 1" = 2.5'

1. One-point compaction samples not obtained. Average percent compaction is based on maximum dry density provided by PTL.

PROFILE OF MOLECUTTINGS
(CONTROLLED PLACEMENT) TEST FILL

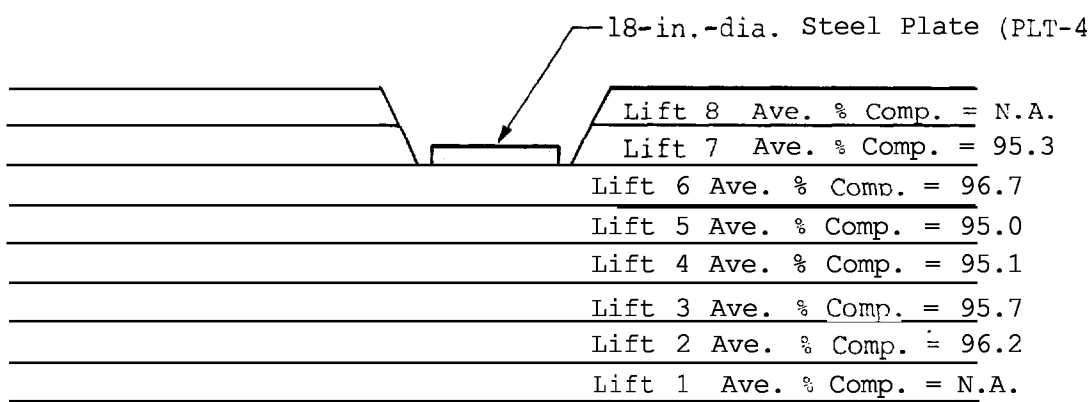

Scale: 1" = 2.5'

PROFILE OF MOLECUTTINGS
(NO SPECIAL CONTROLS) TEST FILL

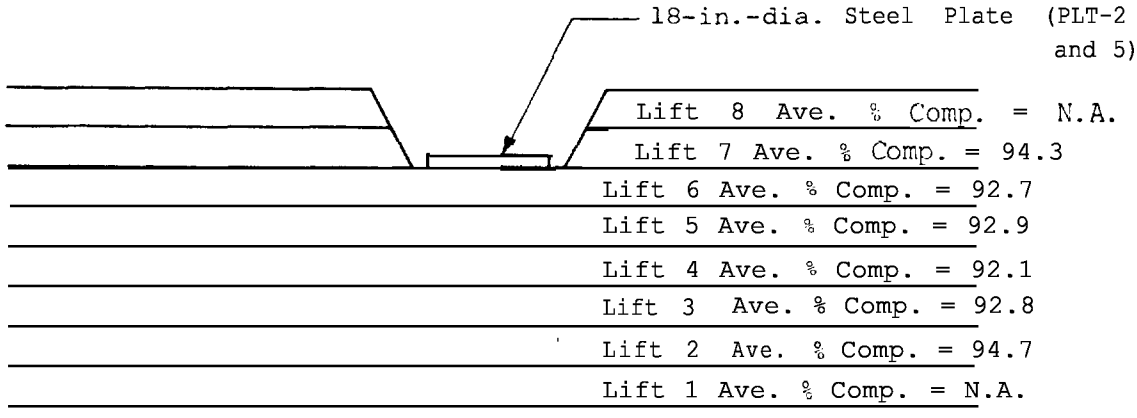

Scale: 1" = 2.5'

PROFILE OF STRATIFIED MOLECUTTINGS
AND GRAVELLY SAND TEST FILL

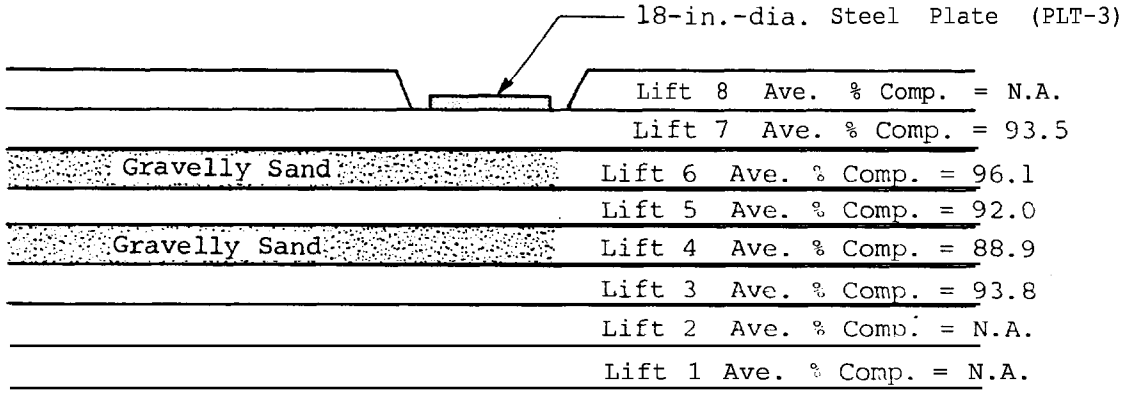

Scale: 1" = 2.5'

Public Service Company of New Hampshire	Quartzite Molecuttings Study	PROFILE OF TEST FILLS
GEOTECHNICAL ENGINEERS INC WINCHESTER • MASSACHUSETTS	Project 76301	July 11, 19 79 Fig. 3

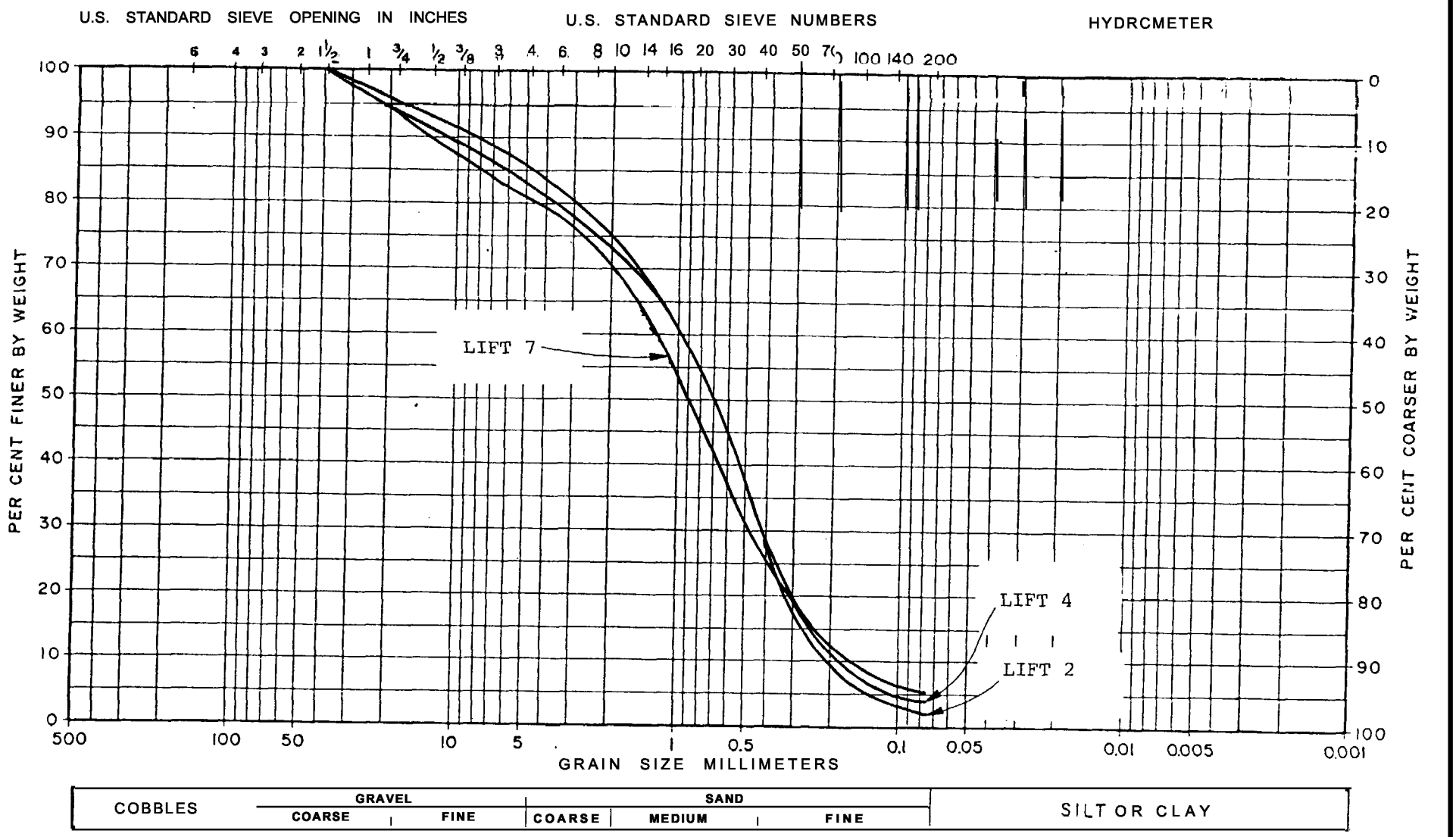

Grain-size analyses per'formed by Pittsburgh Testing Labs.

Public Service Company of New Hampshire	Quartzite Molecuttings Study	GRAIN SIZE CURVES GRAVELLY SAND TEST FILL
GEOTECHNICAL ENGINEERS INC WINCHESTER • MASSACHUSETTS	Project 76301	July 11, 1979 Fig. 5

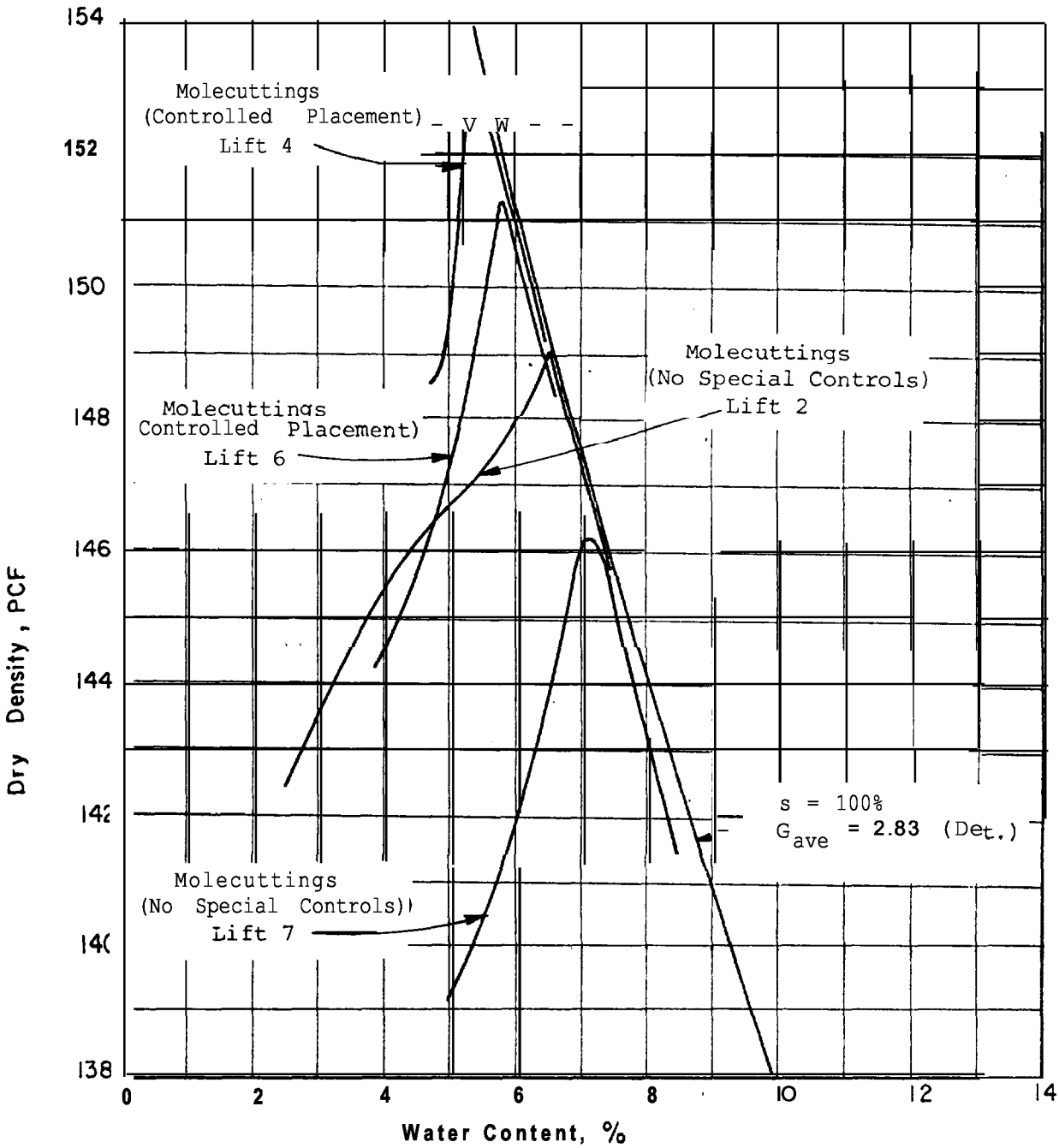

NOTE: 1. Compaction test performed in accordance with ASTM D1557, Method C, except the plus 1½-in. material was discarded and no limitation placed on the percent retained on the 1½-in. sieve.

Public Service Company of New Hampshire	Quartzite Molecuttings Study	. COMPACTION CURVES Molccuttings
GEOTECHNICAL ENGINEERS INC WINCHESTER, MASSACHUSETTS	Project 76301	July 12, 1979 Fig. 6

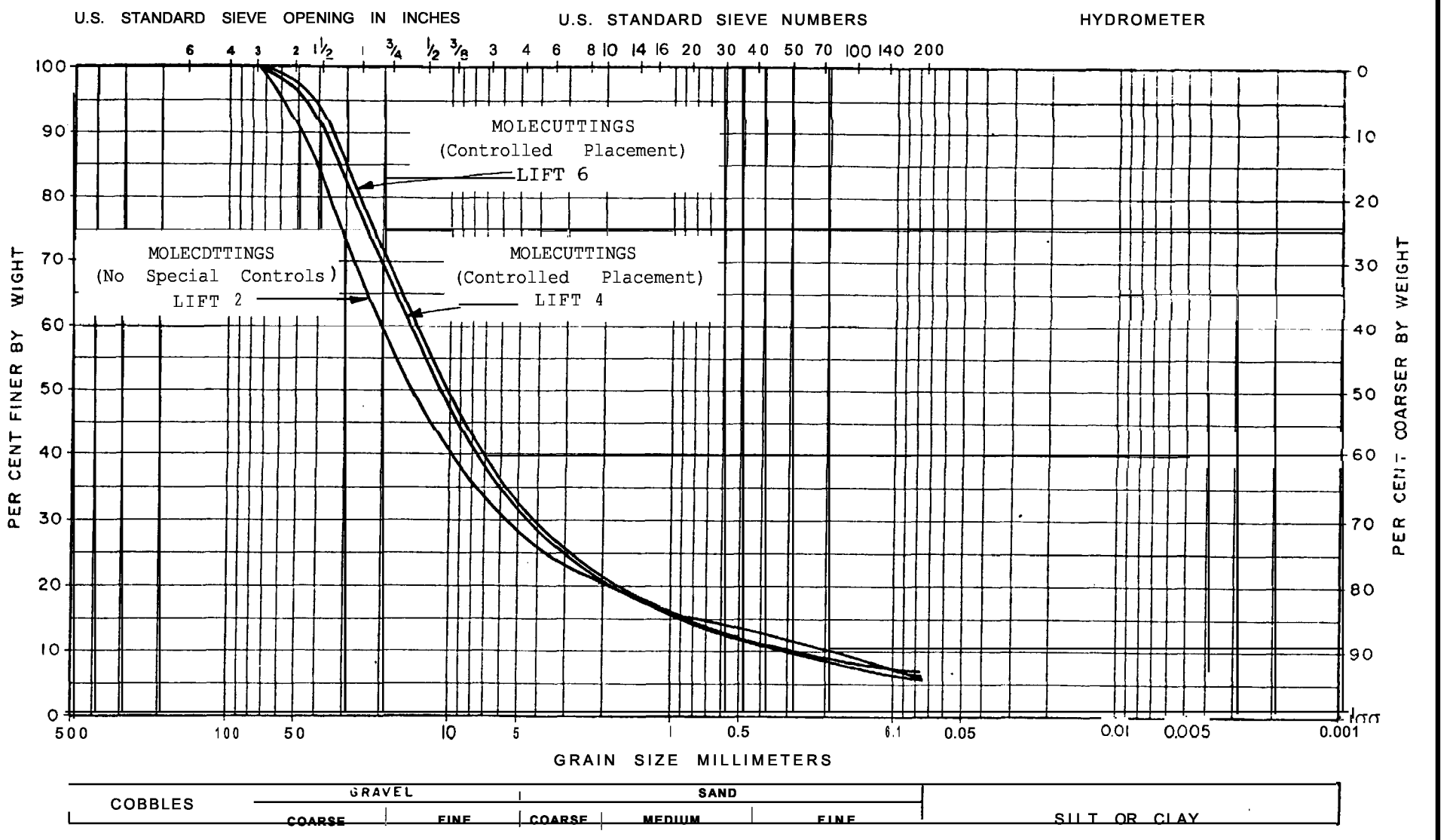

Grain-size analyses performed using successive elutriation.

Public Service Company of New Hampshire	Quartzite Molecuttings study	GRAIN SIZE CURVES SAMPLES OF MOLECUTTINGS
GEOTECHNICAL ENGINEERS INC WINCHESTER . MASSACHUSETTS	Project 76301	July 11, 1979 Fig. 7

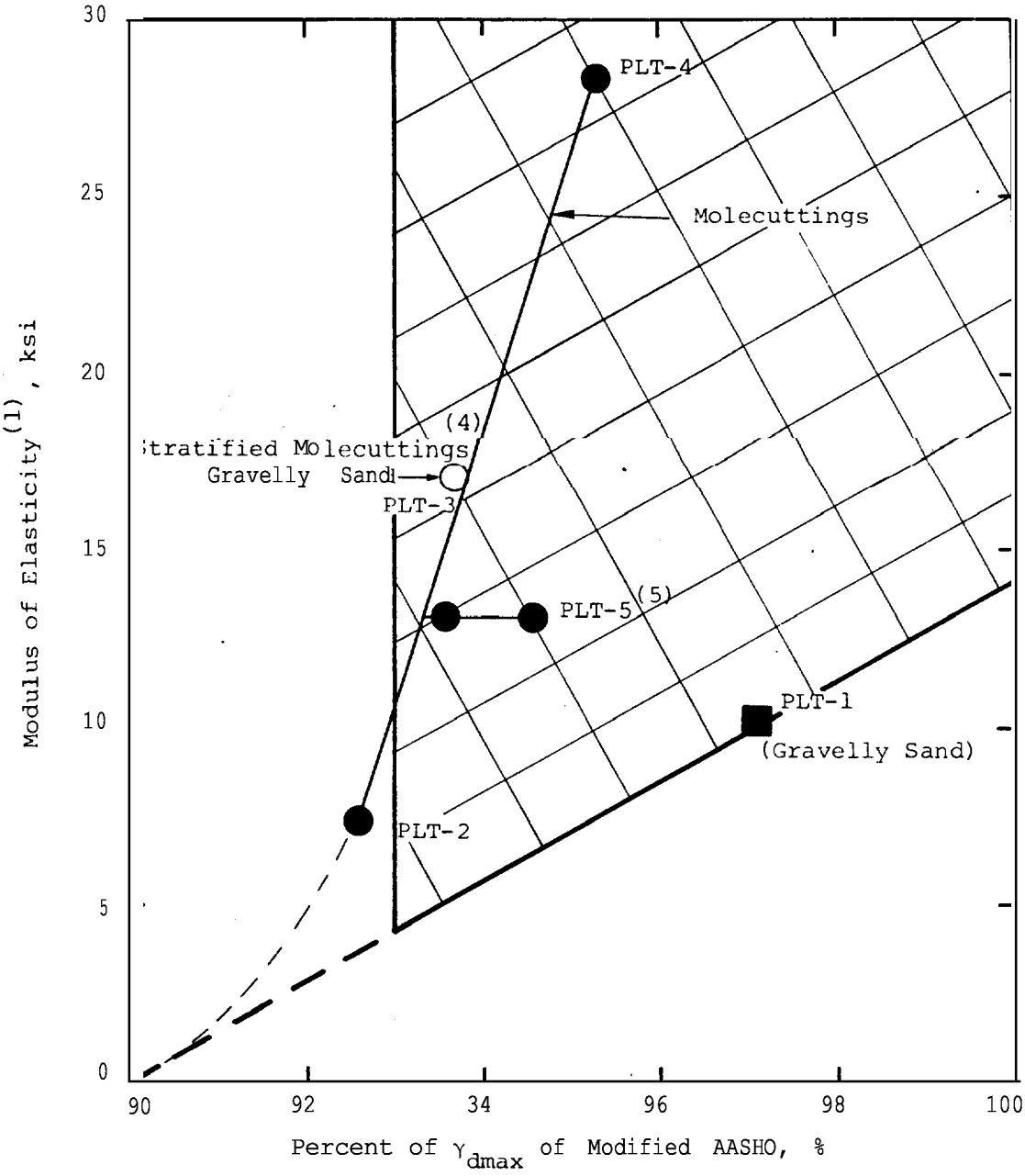

NOTES:
1. Modulus of elasticity computed using theory of elasticity for semi-infinite, isotropic soil.
2. Modulus of elasticity value plotted is minimum value from virgin loading curve.
3. Percent compaction is the average percent compaction of the first three layers of soil under the plate.
4. Percent compaction the average percent compaction of two layers of molecuttings and one layer of gravelly sand.
5. Range in percent compaction is estimated. See discussion in text.

Public Service Company of New Hampshire	Quartzite Molecuttings Study	MODULUS OF ELASTICITY VERSUS PERCENT COMPACTION MOLECUTTINGS-GRAVELLY SAND
GEOTECHNICAL ENGINEERS INC WINCHESTER • MASSACHUSETTS	Project 76301	July 11, 1979 Fig. 8

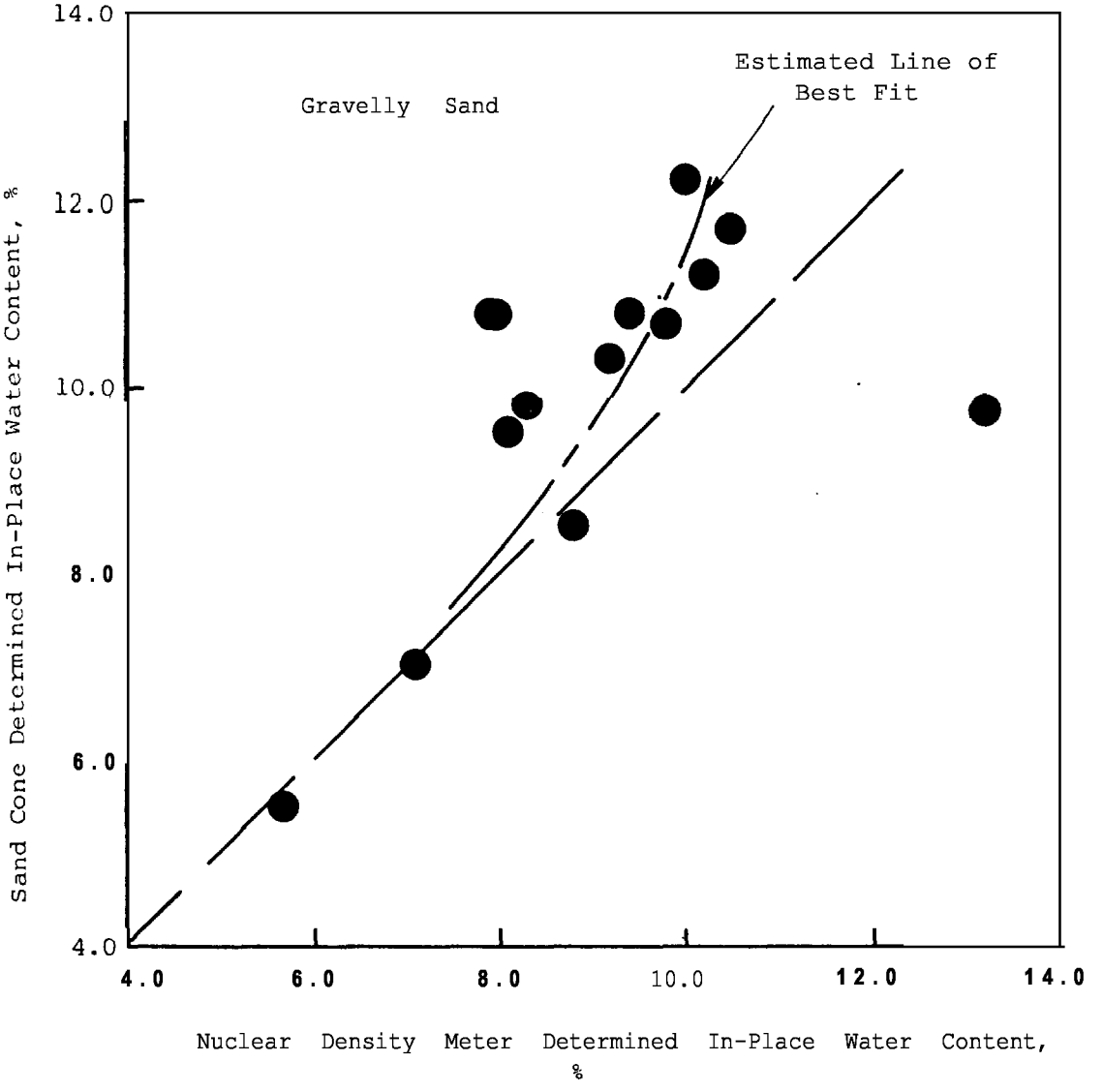

Public Service Company of New Hampshire	Quartzite Molecuttings Study	WATER CONTENT SAND CONE VS NUCLEAR DENSITY METER GRAVELLY SAND
GEOTECHNICAL ENGINEERS INC WINCHESTER • MASSACHUSETTS	Project 76301	July 11, 1979 Fig. 9

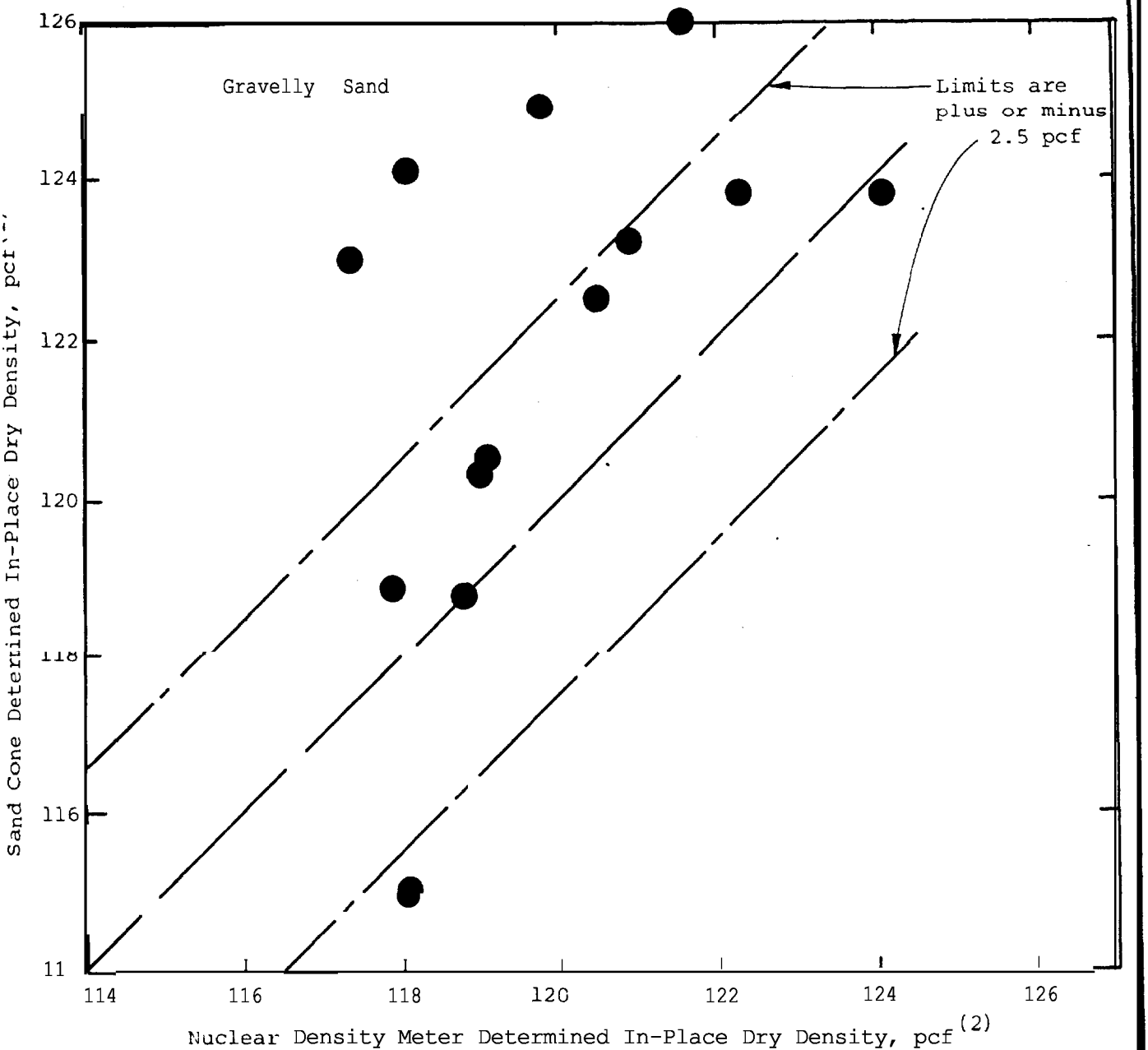

NOTES: 1. In-place dry density includes plus 3/4-in. material. .

2. In-place dry density based on 8-in. deep nuclear test. Densities have been corrected for water content bias according to plot of "W" sand versus "W" nuclear for gravelly sand:
   cone device

3. Sand Cone and Nuclear Density Meter determinations were performed adjacent to each other (about 6-12 in. apart).

Public Service Company of New Hampshire	Quartzite Molecuttings study	SAND CONE VS NUCLEAR DENSITY METER DET. IN-PLACE DRY DENSITY --- GRAVELLY SAND
GEOTECHNICAL ENGINEERS INC WINCHESTER, MASSACHUSETTS	Project 76301	July 11, 1979 Fig. 10

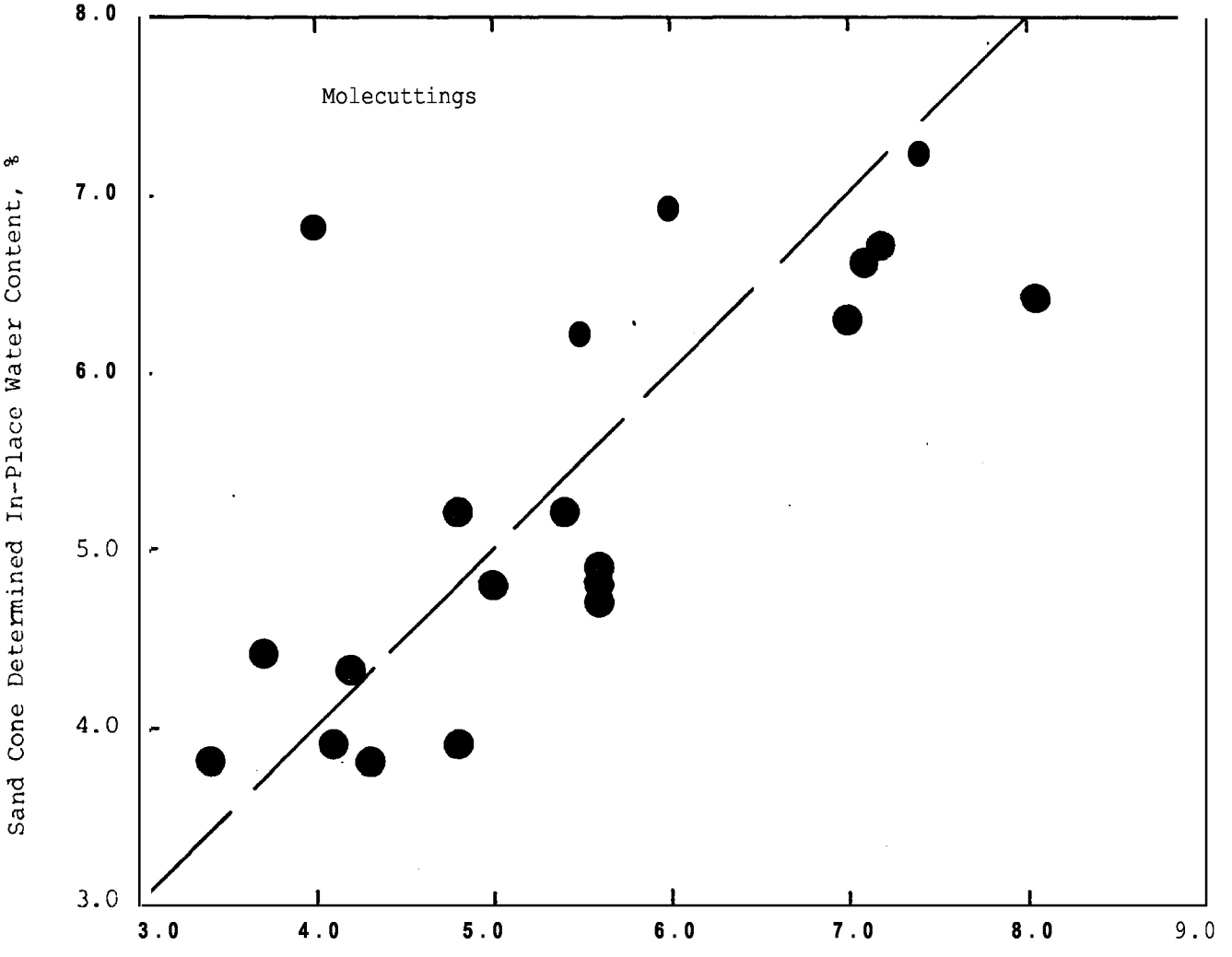

NOTES: 1. In-place water content is based on 8-in. deep nuclear test.

Public Service Company of New Hampshire	Quartzite Molecuttings Study	WATER CONTENT SAND CONE VS NUCLEAR DENSITY METER MOLECUTTINGS
GEOTECHNICAL ENGINEERS INC WINCHESTER • MASSACHUSETTS	Project 76301	July 11, 1979 Fig. 11

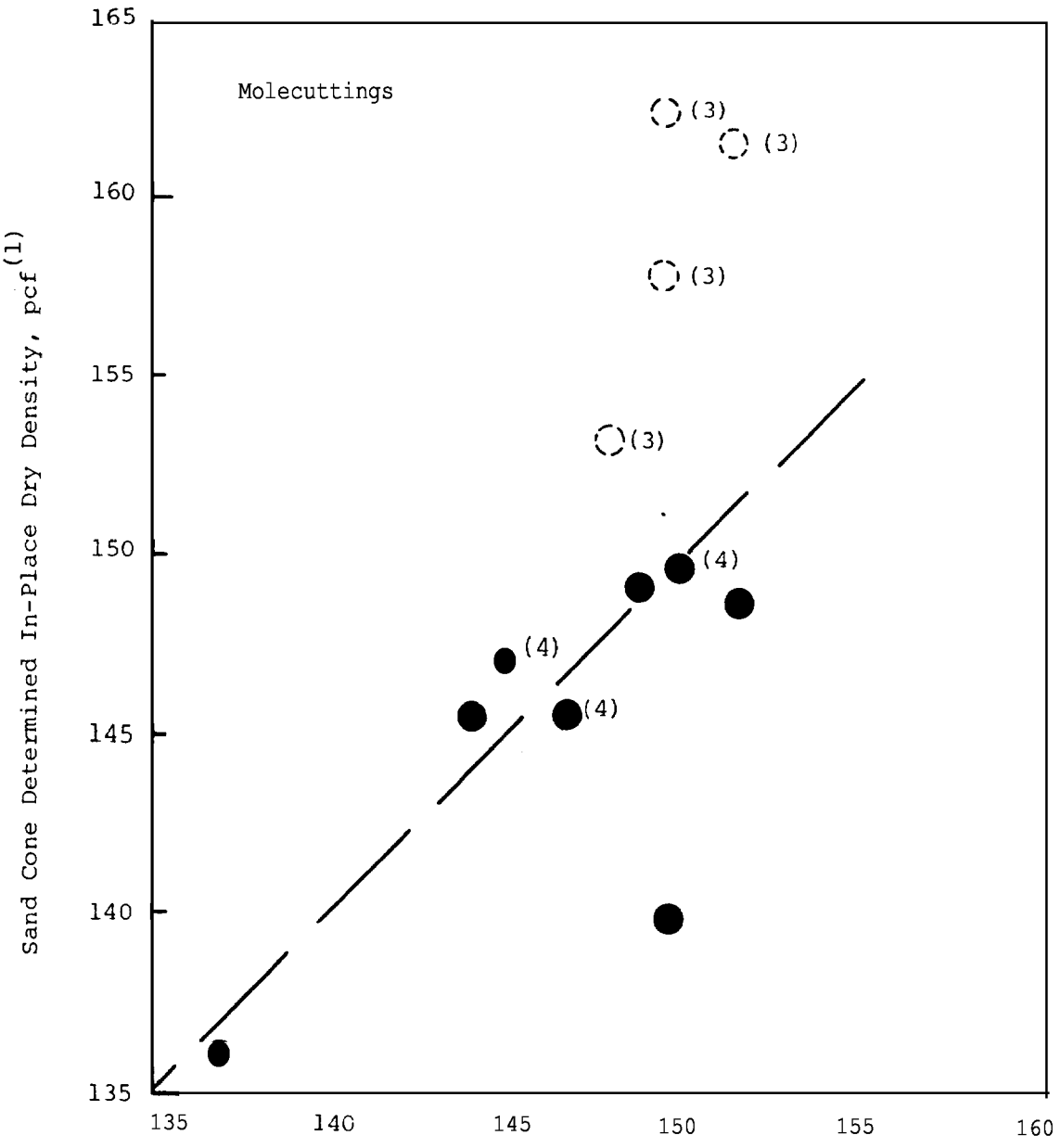

NOTES:
1. In-place dry density is uncorrected for the plus 1½-in. material.
2. In-place dry density is based on the 8-in. deep nuclear test, except where noted.
3. Water content of Sand Cone was greater than 5.0%.
4. In-place density is based on 4-in. deep nuclear test.

Public Service Company of New Hampshire	Quartzite Molecuttings Study	SAND CONE VS NUCLEAR DENSITY METER DET. IN-PLACE DRY DENSITY MOLECUTTINGS
GEOTECHNICAL ENGINEERS INC WINCHESTER · MASSACHUSETTS	Project 76301	July 11, 1979 Fig. 12

APPENDIX A

SAFETY-RELATED STRUCTURAL FILL

A. MATERIAL

1. Gradation for molecuttings should meet the following criteria:

3 in.	100
1½ in.	100-70
3/4 in.	100-35
3/8 in.	100-17
No. 4	75-10
No. 20	32-0
No. 40	22-o
No. 200	10-0

2. The uniformity coefficient, D_{60}/D_{10}, should be not less than 5.

B. PLACEMENT

1. Molecuttings should be placed in 8-in.-thick loose lifts and compacted to 95% of maximum dry density as determined by ASTM D1557 with exceptions for testing noted in Section C.2.

2. The water content of the molecuttings should be at optimum $\pm$ 1% during placement. The water content during placement of quartzite molecuttings should be stockpiled or otherwise treated to reduce the water content to less than 6%. If the water content is less than 4%, the addition of water during compaction will be necessary if satisfactory compaction is to be achieved.

3. Molecuttings should not be placed in direct contact with pipes, culverts, or other structures sensitive to abrasion and/or high point loads.

4. The pore fluid of the molecuttings is brackish and, as a result, the resistivity of the muck is likely to be below the minimum limit of 10,000 ohms-cm^3. United Engineers is to develop recommendations for placement of the molecuttings in areas when high resistivity of backfill material is required.

C. TESTING AND FIELD CONTROL

1. Due to anticipated variations in rock type the molecuttings should be monitored daily by determining the grain-size distribution, water content, and rock type for at least one typical sample. The grain-size analysis should be performed by using a wet sieving technique and every tenth test should be performed by using the elutriation method, without pre-drying of the sample. The frequency of testing may be reduced in time after those testing become familiar with the material and thus capable of judging when the material is or is not acceptable.

   a. If the percent passing the #200 sieve material is greater than 10%, the material should not be used.

   b. If the water content is greater than 1% above optimum, the molecuttings should be stockpiled or treated to reduce the water content to optimum.

2. A family of at least three compaction curves should bc developed using ASTM D1557, Method C, except that the minus 1½-inch material shall be used. Each compaction curve should be accompanied by a grain-size analysis. Additional compaction curves should be performed once every 7,500 yards or earlier if visual changes in the molecuttings grain size is observed.

3. A bag sample of the molecuttings should be obtained after the loose lift has been placed and before compaction begins. The sample should be large enough to perform a laboratory one-point compaction test and to measure the percent material retained on the l&inch sieve.

4. Separate the plus 1½-in. material and calculate its percentage by weight of the entire sample.

5. A one-point compaction test should be'performed on the bag sample of molecuttings in accordance with ASTM D1557, Method C, except that the minus 1½-in. sieve material shall be used. The maximum dry density for

this sample, γ_{dx}, is determined by plotting the one-point dry density on the family of curves and interpolating the maximum dry density for the minus 1½-in. material.

6. The in-place dry density should be determined by performing at least three nuclear density meter tests. The average dry density should be used to compute the percent compaction. This method should reduce the effects of sharp variations in the molecuttings on the in-place dry density determinations.

   a. The water content bias for the nuclear density meter should be corrected for use in molecuttings. The water content bias should be checked weekly.

7. The percent compaction is determined by dividing the corrected in-place dry density by the laboratory maximum dry density as determined in 6. above. A formula to compute the corrected in-place dry density, to correct for the quantity of plus 1½-in. material, is presented below.

$$\gamma_{dc} = \frac{\gamma_{ND} - RG\gamma_w}{1-R}$$

where γ_{dc} = corrected in-place dry density for the minus 1½-in. sieve material
γ_{ND} = average in-place dry density determined by using nuclear density meter
γ_w = unit weight of water
G = specific gravity of molecuttings
R = percent, by weight of the total sample retained on the 1½-in. sieve

The percent compaction is computed as follows:

$$\text{Percent Compaction } P(\%) = \frac{\gamma_{dc}}{\gamma_{dx}} \times 100 .$$

γ_{dx} = Maximum dry density of minus 1½-in. material determined in Step 5. from the family of curves and the one-point compaction.

NONSAFETY-RELATED STRUCTURAL FILL

A. MATERIAL

1. Gradation for molecuttings should meet the following criteria:

3 in.	100
1½ in.	100-70
3/4 in.	100-35
3/8 in.	100-17
No. 4	75-10
No. 20	32-0
No. 40	22-o
No. 200	10-0

2. The uniformity coefficient (D_{60}/D_{10}) should not be less than 5.

B. PLACEMENT

1. Molecuttings should be placed in 12-in.-thick loose lifts and compacted to 93% of maximum dry density as determined by ASTM D1557 with exceptions noted in Section C.2 for Safety-Related Structural Fill.

2. Molecuttings can be sandwiched between presently accepted gravelly sand structural fill. When molecuttings and gravelly sand are alternated in the backfill, the following limits are recommended.

   a. Molecuttings should be placed in 8-in.-thick loose lifts and compacted to 93% of maximum dry density as determined by ASTM D1557.

   b. Gravelly sand should be placed in accordance with the present specification for structural fill (i.e., 8-in. loose lifts compacted to 95% of ASTM D1557).

3. The water content of the molecuttings should be at optimum + 1% during placement if no gravelly sand layers are present. When the molecuttings and gravelly sand are placed in alternating layers, the water content of the molecuttings may be permitted to be as high as 2% above optimum. If the water content of the molecuttings exceeds the suggested limits of water content, the molecuttings should be stockpiled or otherwise treated to alter the water content. If the water content is low, say 2 to 4%, the addition of water during compaction may be necessary to achieve satisfactory compaction.

4. Molecuttings should not be placed in direct contact with pipes, culverts, or other structures sensitive to abrasion and high point loads.

5. The pore fluid of the molecuttings is brackish and, as a result, the resistivity is likely to be below the minimum limit of 10,000 ohms-cm^3. United Engineers is to develop recommendations for placement of the molecuttings in areas when high resistivity of backfill material is required.

C. TESTING AND FIELD CONTROL

Testing and field control for use of molecuttings in non-safety-related areas is the same as for safety-related areas except for Section C.1.b, which should read as follows:

b. When the water content of the molecuttings is outside of the range of optimum $\pm$ 1%, the material should be stockpiled or treated to reduce the water content to within the suggested limit before placement.

RANDOM FILL

A. MATERIAL

The molecuttings to be used as Randon Fill should comply with the present specification as described in Specification No. 9763-8-4, Section 3.2.2 dated September 27, 1974.

B. PLACEMENT

1. Molecuttings should be placed in 12-in.-thick loose lifts and compacted to 90 % of maximum dry density as determined by ASTM D1557 with exceptions noted in Section C.2 for Safety-Related Structural Fill.

2. Although limits on the water content of the molecuttings are not necessary, the most efficient compaction will occur at optimum water content ± 1%.

C. TESTING AND FIELD CONTROL

Testing and field control for use of molecuttings as Random Fill should be the same as outlined for Safety-Related areas with the following exceptions:

C.1.a The gradation of the molecuttings should comply with present specifications for Random Fill.

C.1.b No limit on the water content of the molecuttings is recommended. The maximum permissible water content in the field will be dictated by the ability to achieve the required percent compaction.

APPENDIX B

APPENDIX B

PLATE LOAD TEST

B-1 Purpose

The plate load tests were performed to determine the deformation characteristics of gravelly sand and molecuttings. The results of the plate load tests provided the basis for comparison of the two materials and to determine the effect that percent compaction has on their deformation characteristics.

B-2 Procedure

For each test a 24-in.-diameter hole was excavated to a depth of 12 in., except for test PLT-3 which was 6 in. deep. An 18-in.-diameter, 1-in.-thick steel plate was placed on a thin layer of liquid hydrous stone which was placed directly on the bottom surface of the test hole. Additional 1-in.-thick steel plates 14-in. and 10-in. in diameter were placed in a pyramid arrangement on top of the 18-in. plate.

After the hydrous stone and plates were in place, the plate was loaded by a hydraulic jack reacting against the underside of a loaded, flat-bed trailer, as illustrated in Fig. B-1.

The loads were measured using a calibrate pressure gage.

Deformations of the plate were measured using three dial indicators attached to a reference beam as illustrated in Fig. B-1. The dial indicators were graduated to .001 mm. The reference beam supports were separated from the center of the plate by about 72 in., which was a sufficient distance for deflections under the supports to be negligible during loading of the plate.

The loading sequence for each test was as follows:

1. Applied load to develop contact stress of 4 tons per square foot (tsf) in four equal increments.
2. Unload to zero load in two equal increments.
3. Repeat load-unload cycle to 4 tsf.
4. Load to develop contact stress of 12 tsf in six equal increments.

5. Unload to zero load in three equal increments.

6. Repeat load-unload cycle to 12 tsf two more times.

Each loading or unloading increment was held constant until the rate of deformation of the plate was less than .001 mm/min.

The air temperature when the plate load tests were performed was about 80° F.

B-3 Results

The load versus displacement curves for the five plate load tests are illustrated in Figs. B-2 through B-6. The slope of the virgin load curve was generally straight except for test PLT-2 and PLT-3 where slight curvature was observed. The slope of the reload curves were much flatter than the virgin curve and the slopes of the repeated reload-unload cycles were parallel as would be expected.

Values of Young's Modulus, E, were calculated from the results of the plate load tests using elastic theory. The solution for the settlement of a loaded, rigid circular plate on an elastic half space is as follows:

$$s = \frac{qD(1-\nu^2)I}{E}$$ (From Poulos and Davis, p. 166)

where s = settlement
q = average stress on the plate = $\frac{4P}{\pi D^2}$
P = load on the plate
D = diameter of the plate
ν = Poisson's ratio
I = influence factor = $\pi/4$
E = Young's Modulus

Assuming a value $\nu = 0.3$ and rearranging to compute E, yields:

$$E = \frac{0.91P}{DS}$$

The modulus calculated is the average modulus within the zone of significant stress which for an 18-in. plate would extend between 18 to 36 inches beneath the plate.

The moduli calculated using this method are presented in Table B1. For each test tangent moduli were calculated using the straight segments of the load and reload curves.

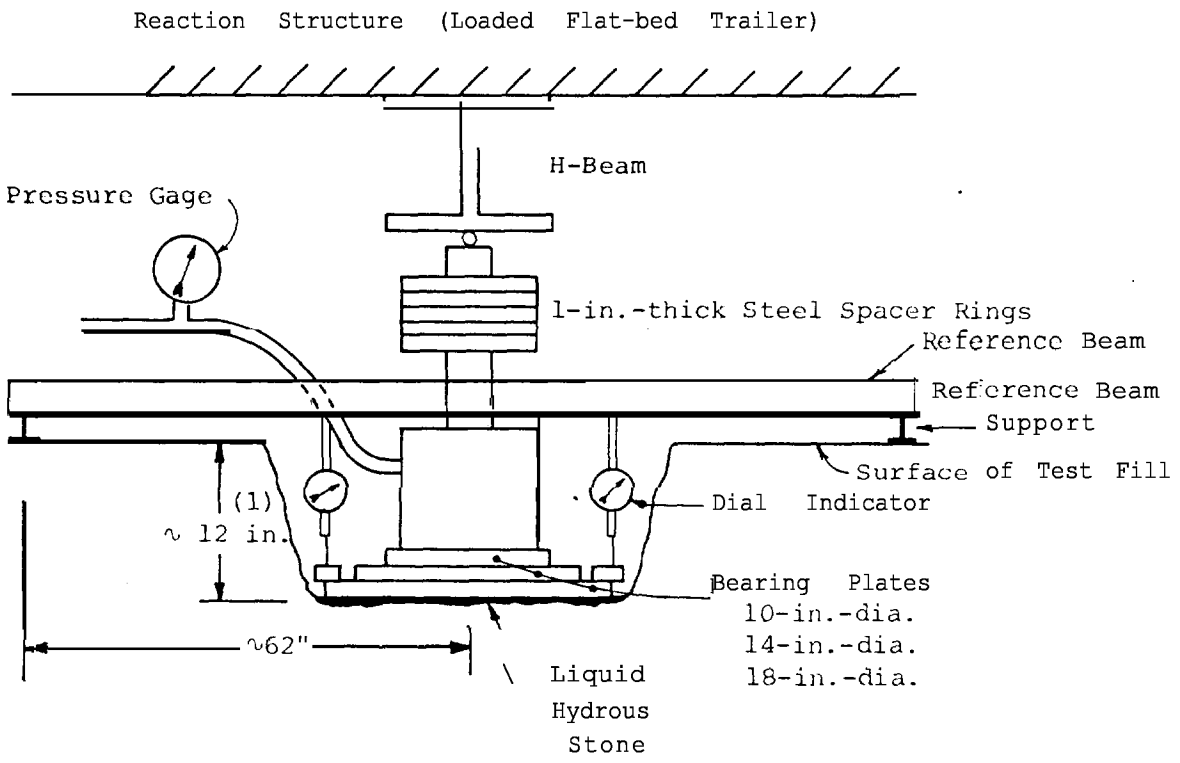

NOTE: 1. Depth for PLT-3 was about 6-in.

Schematic Illustration of Plate Load Test Equipment
(Not To Scale)

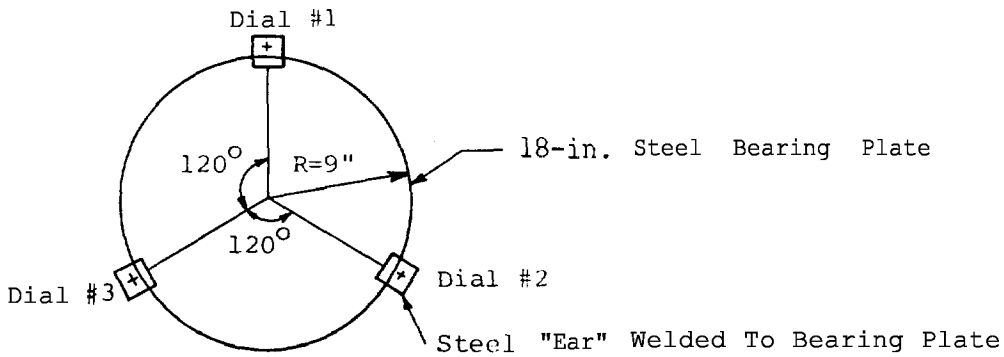

Dial indicators #1, #2, and #3 monitored displacement of "ears" attached to circumference of bearing plate.

Plan Showing Locations of Dial Indicators
(Not To Scale)

Public Service Company of **New** Hampshire	Quartzite Molecuttings Study	PLATE BEARING TEST EQUIPMENT
GEOTECHNICAL ENGINEERS INC WINCHESTER • MASSACHUSETTS	Project 76301	July 12, 1979 Fig.B1

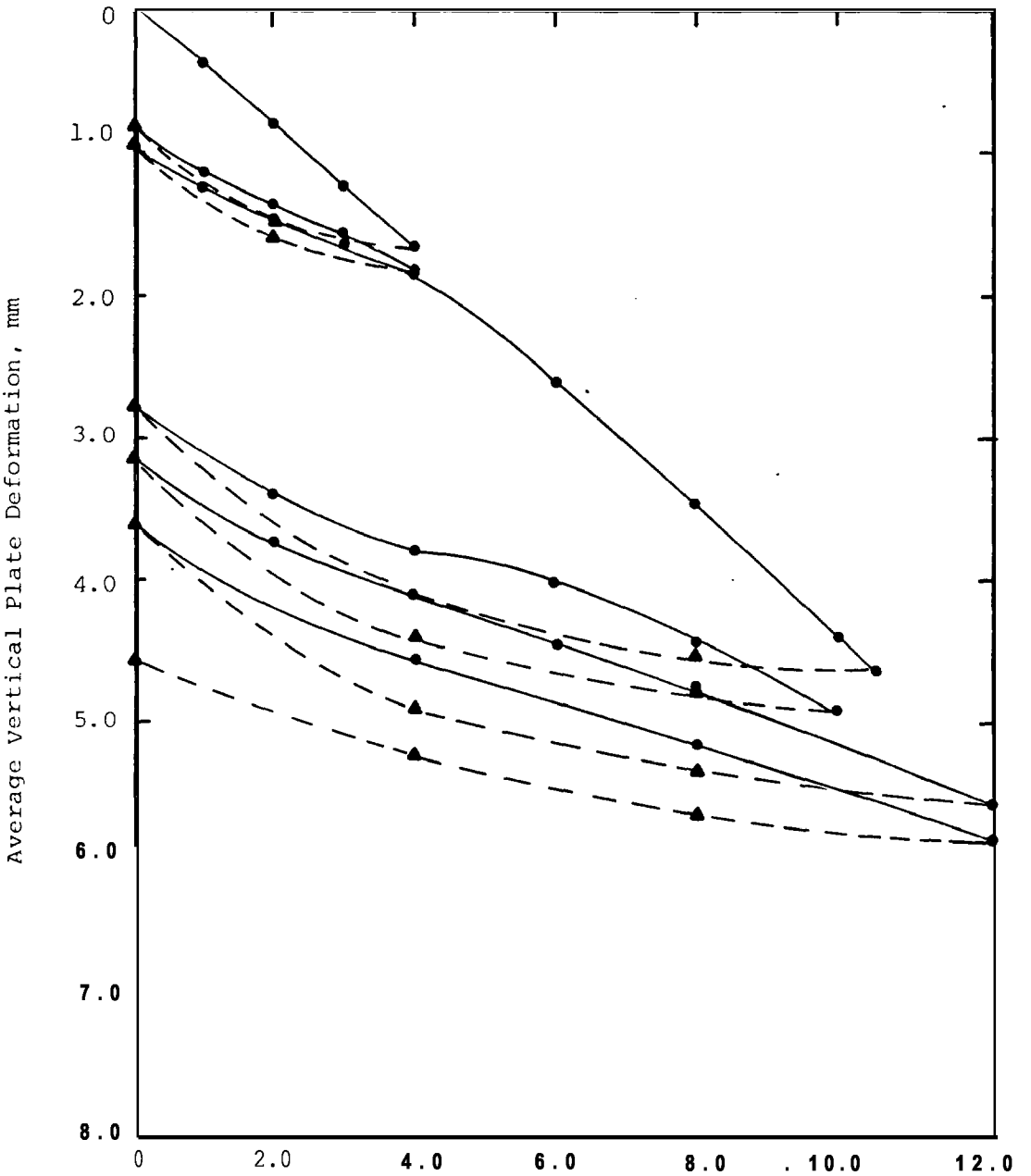

Date Performed: June 7, 1979
By: W. Fisher/R. Gardner
Plate Diameter: 18-in.

Public Service Company of New Hampshire	Quartzite Molecuttings Study	VERTICAL STRESS VS DEFORMATION PLATE LOAD TEST - PLT-1 GRAVELLY SAND
GEOTECHNICAL ENGINEERS INC WINCHESTER • MASSACHUSETTS	Project 76301	July 11 1979 Fig. B2

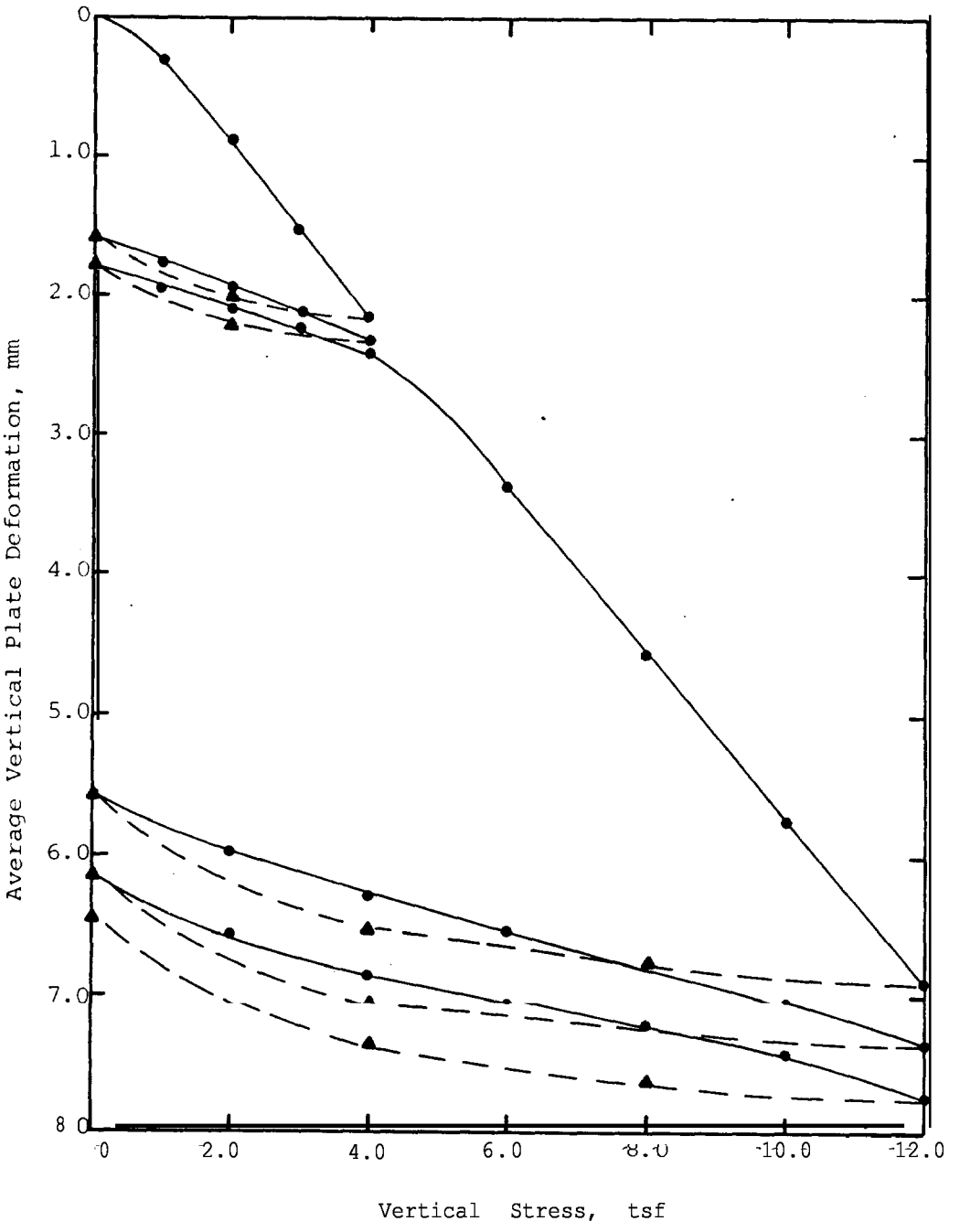

Date Performed: June 14, 1979
By: W. Fisher/R. Gardner
Plate Diameter: 18-in.

Public Service Company of New Hampshire	Quartzite Molecuttings Study	VERTICAL STRESS VS DEFORMATION PLATE LOAD TEST - PLT-2 MOLECUTTINGS (NO SP. CON.)
GEOTECHNICAL ENGINEERS INC WINCHESTER, MASSACHUSETTS	Project 76301	July 11, 1979 Fig. B3

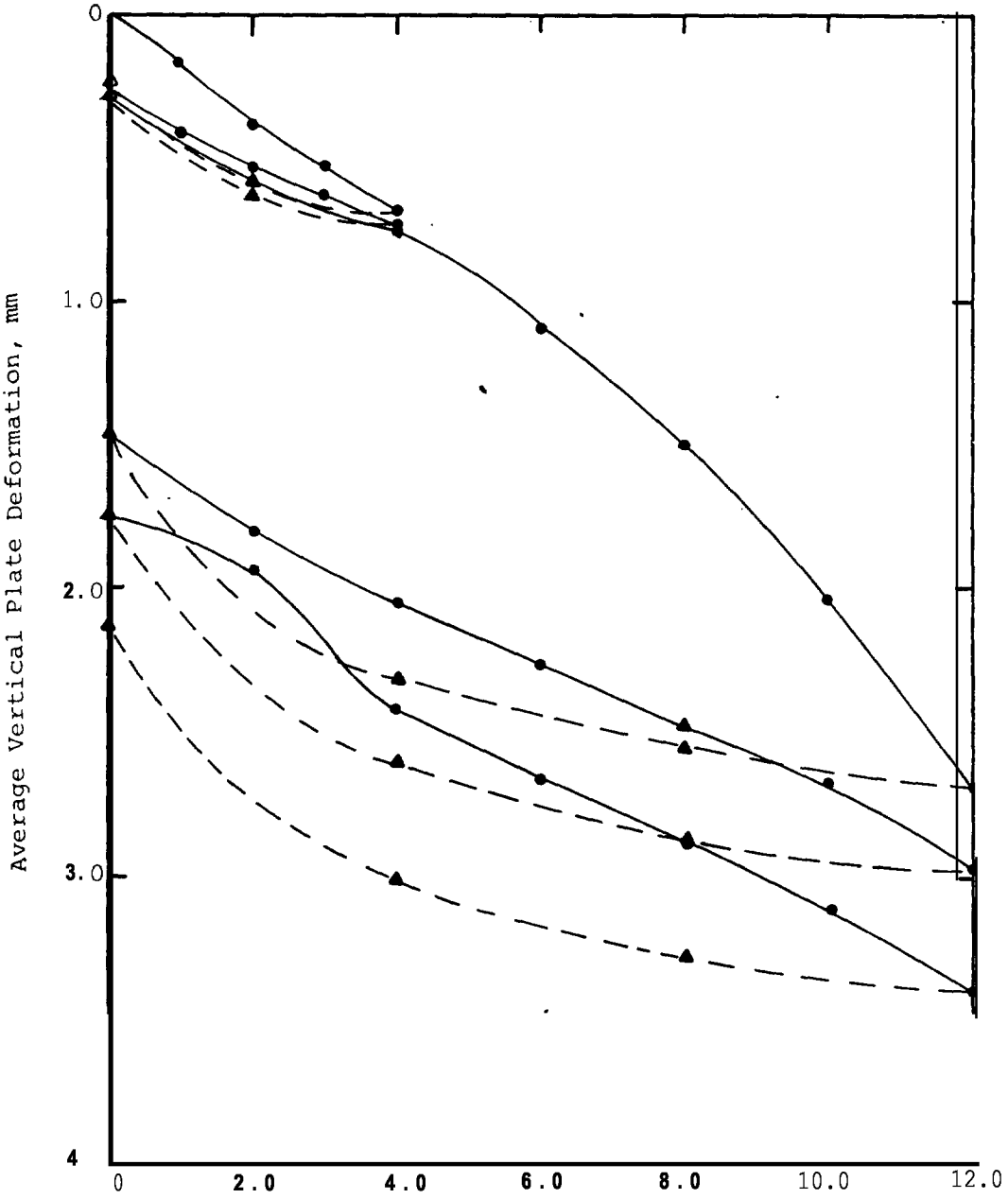

Date Performed: June 15, 1979
By: W. Fisher/R. Gardner
Plate Diameter: 18-in.

Public Service Company of Newhampshire	Quartzite Molecuttings Study	VERTICAL STRESS VS DEFORMATION PLATE LOAD TEST - PLT-3 ST. MOLECUTTINGS & GR. SI
GEOTECHNICAL ENGINEERS INC WINCHESTER • MASSACHUSETTS	Project 76301	July 11, 1979 Fig. B4

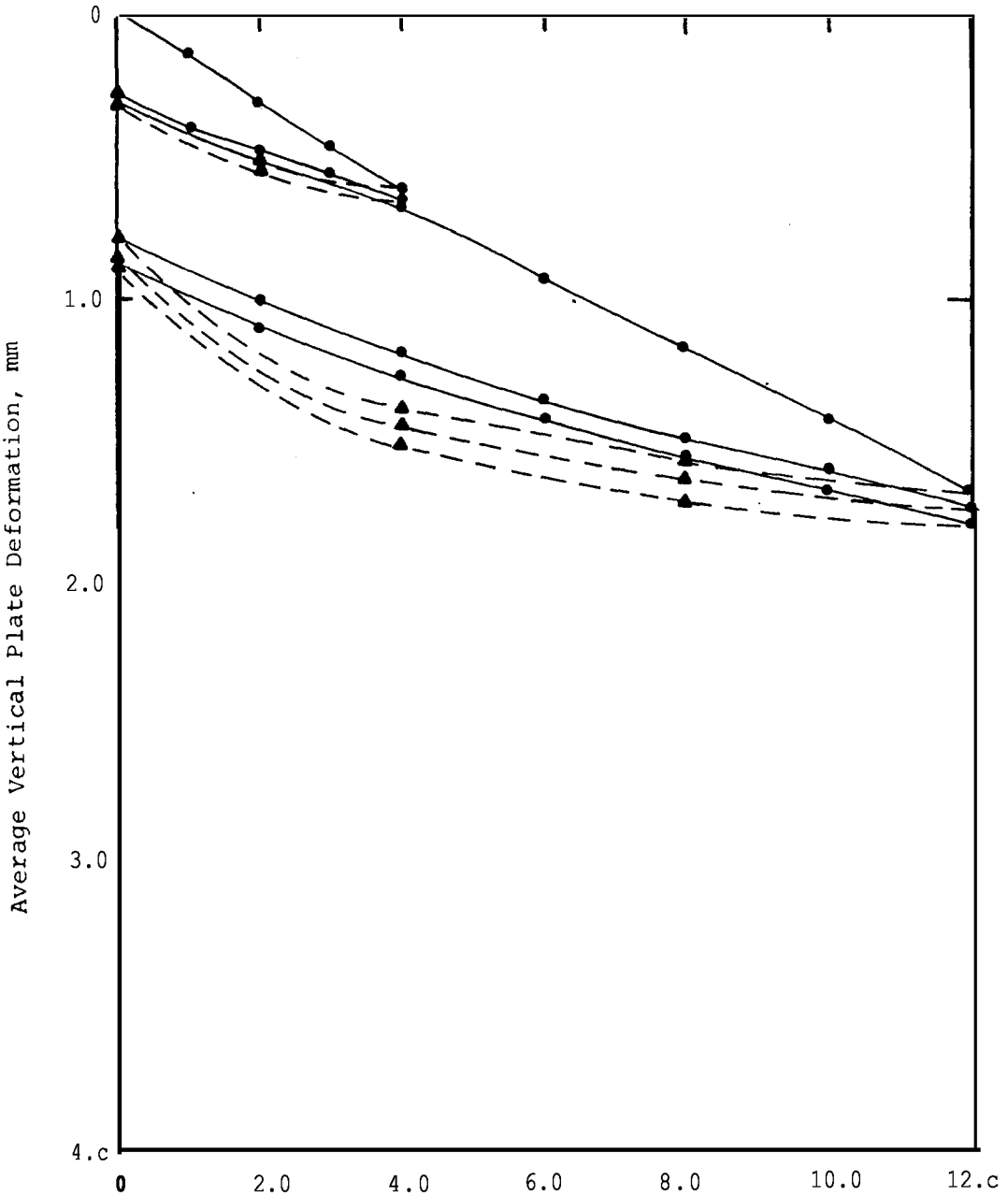

Date Performed: June 18, 1979
By: W. Fisher/R. Gardner
Plate Diameter: 18-in.

Public Service Company of New Hampshire	Quartzite Molecuttings Study	VERTICAL STRESS VS DEFORMATION PLATE LOAD TEST - PLT-4 MOLECUTTINGS (CON. PLACE a.
GEOTECHNICAL ENGINEERS INC WINCHESTER • MASSACHUSETTS	Project 76301	July 11, 1979 Fig. B5

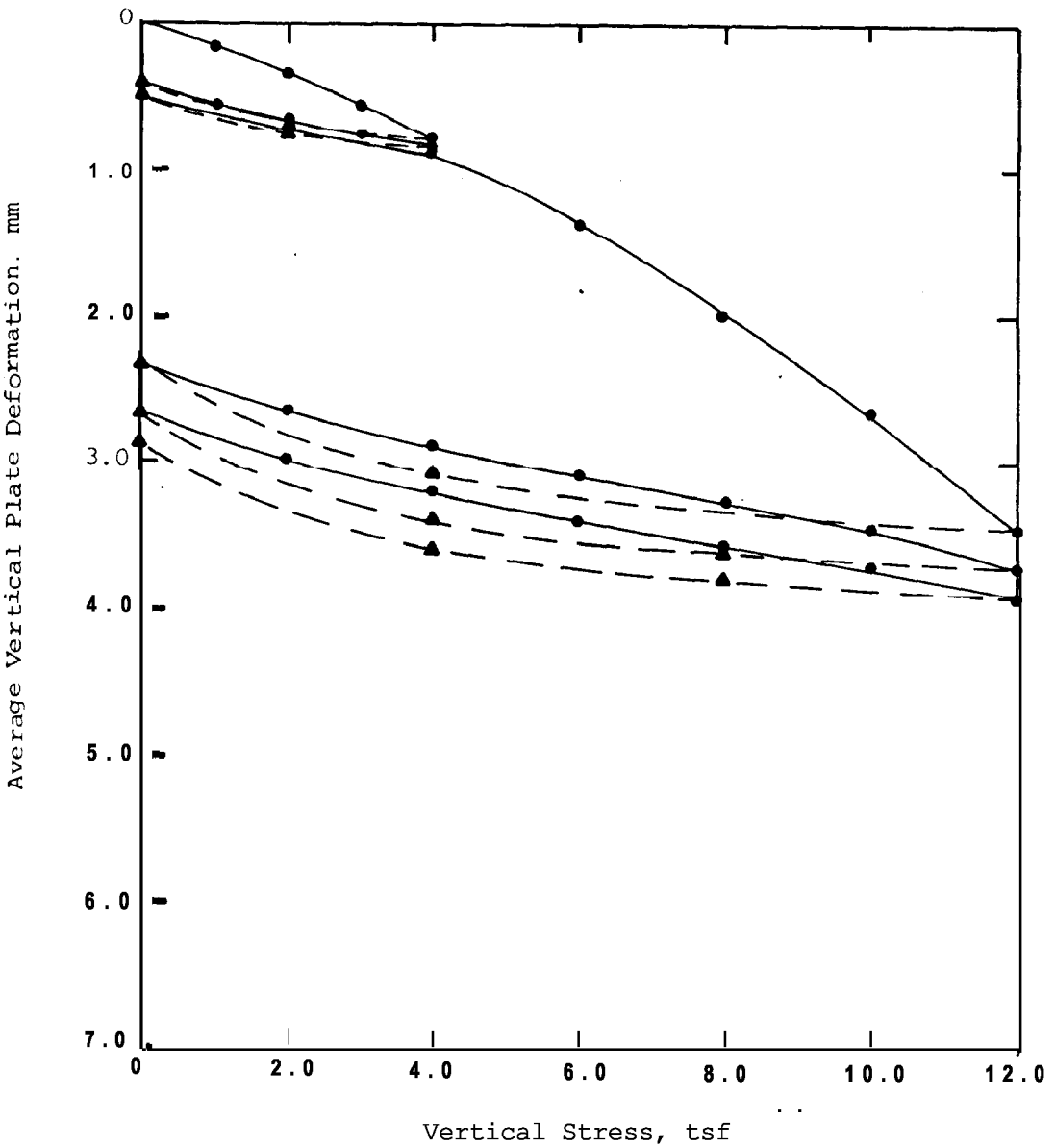

Date Performed: June 27, 1979
By: W. Fisher
Plate Diameter: 18-in.

Public Service Company of New Hampshire	Quartzite Molecuttings Study	VERTICAL STRESS VS DEFORMATION PLATE LOAD TEST - PLT-5 MOLECUTTINGS (NO SP. CON.
GEOTECHNICAL ENGINEERS INC WINCHESTER - MASSACHUSETTS	Project 76301	July 11, 1979 Fig. B6

TABLE - SUMMARY OF FIELD DENSITY TESTS

Lift No.	Sample No.	One-Point Compaction: Percent +3/4-in. Material, %	One-Point Compaction: Water Content, %	One-Point Compaction: Dry Density, γ_d, pcf	Laboratory Maximum Dry Density, γ_d, pcf	In-Place Dry Density, pcf: Total Sample	In-Place Dry Density, pcf: Corrected For +3/4-in. Material	Percent Compaction, %

APPENDIX 20

GEOTECHNICAL REPORT • DISCUSSION OF DERIVATION OF COEFFICIENTS OF SUBGRADE REACTION

The information contained in this appendix was not revised, but has been extracted from the original FSAR and is provided for historical information.

GEOTECHNICAL ENGINEERS INC.
1017 MAIN STREET. WINCHESTER. MASSACHUSETTS 01890 (617) 729-1625

PRINCIPALS
RONALD C. HIRSCHFELD
STEVE J. POULOS
DANIEL P. LA GATTA
RICHARD F. MURDOCK
GONZALO CASTRO

ASSOCIATES
CHARLES E. OSGOOD
BARTLETT W. PAULDING, JR

March 22, 1978
Project 77386
File No. 2.0

Mr. John Herrin
Public Service Co. of New Hampshire
1000 Elm Street - 11th Floor
Manchester, NH 03105

Subject: Discussion of Derivation of Coefficients of Subgrade Reaction

Dear Mr. Herrin:

In the following we describe some techniques that we have developed to convert the moduli obtained from triaxial tests to moduli of subgrade reaction for various loading conditions. We present this information to complement various telephone conversations with D. Patel of UE&C.

Computation of Coefficients of Subgrade Reaction

The coefficient of subgrade reaction, k_s, represents soil deformation, due to pressure acting along a boundary surface, as if the soil were composed of independent springs, each representing a unit of area with a spring constant k_s. The spring constant is defined as a pressure divided by a displacement. Such a representation is convenient for analytical purposes but neglects the influence of adjacent loaded surface areas on the displacement of any given point on the boundary surface. Thus, the coefficient of subgrade reaction is not a unique number for an elastic material but is a function of the size of the loaded area, the pressure distribution, and the geometry of the material. For a soil, the modulus of subgrade reaction is also dependent on the method or sequence of loading, i.e., the stress path.

On the basis of the theory of elasticity, we have computed coefficients of subgrade reaction for the structural backfill and the sand cement for three geometries of loading using the modulus of elasticity and Poisson's ratio data obtained in the triaxial test results. The geometries of loading studied are illustrated in Figs. 1 through 9 and are as follows:

1. Circular or square footing subjected to vertical load.

2. Pressure inside a cylindrical cavity in the soil mass assuming a plane strain condition. This is representative, for example, for the loading produced by thermal expansion of the cross section of a buried pipe.

3. Pressure inside a cylindrical cavity with simultaneous application of a vertical surcharge, p, and a horizontal pressure, $k_o p$. This loading is an approximate representation of the placement of fill over a buried pipe, which deforms to produce an increased lateral stress around the pipe. A plane strain condition was assumed.

The modulus of elasticity and Poisson's ratio used in the computations are strain dependent and were selected for the average strain in the region of the soil mass that contributes most to the displacements, namely, within a distance of one diameter from the pipe and one footing width below the footing base. These strains were correlated with the displacements which, in turn, were expressed in terms of footing settlement divided by footing width, 6/B, or in terms of the diameter strain of the pipe, ε_d. In Figs. 1 through 9, the values of the coefficient of subgrade reaction are plotted as a function of (T/B or ε_d and confining pressure. Confining pressure is to be taken as the effective overburden pressure computed at the elevations shown in the figures. An exception to the above procedure is that for the surcharge type loading, a constant Poisson's ratio of 0.3 was used.

The elastic modulus E and Poisson's ratio v used as a basis for the coefficient of subgrade reaction computations were obtained from triaxial compression tests in which the minor principal stresses were kept constant and the major principal stress was increased monotonically until the specimen failed. Such a stress path would be sufficient to determine E and v for an elastic material. However, soil is not elastic and E and v are dependent on the stress path or stress history. In particular, higher values of E would be obtained for repeated or cyclic loading. For the static load conditions, we feel that the values of subgrade reaction presented are reasonable estimates for the in-situ loading conditions. As shown in the next section, the values compare well with values given in published literature. We recommend, however, that when these values are used, sensitivity analyses should be made to assure that the designs are safe for a range 25% above and below the given values.

Comparison With Published Coefficients of Subgrade Reaction

The coefficients of subgrade reaction obtained from the GEI tests were compared with data presented by K. Terzaghi in the paper entitled

"Evaluation of Coefficients of Subgrade Reaction ," *Geotechnique*, vol. 5, 1955, pp. 297-326.

For shallow footings the vertical coefficient of subgrade reaction for a one square foot plate, k_{s1}, is estimated by Terzaghi to range between 300 and 1,000 ton/cu ft for dense sands, i.e., a range for k_{s1} x B of 4,000 to 14,000 psi. These values are intended for shallow footings, e.g., a typical depth of embedment, D_f, of 4 ft, and for a width, B, of one foot. Thus, they are representative of confining pressures equivalent to a depth of 4.5 ft or about 4 psi.

The coefficient of horizontal subgrade reaction is given by Terzaghi for a 1 sq ft vertical area at a given depth, and it is assumed to be proportional to the effective stress at that depth. For example, for dense sands at a confining pressure of 10 psi, a range of $k_s D$ of 7,000 to 14,000 psi is indicated.

The GEI data for structural backfill, for strains of about 1%, Figs. 1, 2, 4 and 5, agree with Terzaghi's data. No specific information on strain level is given by Terzaghi for his data, but he indicates that the data are applicable to a factor of safety against bearing capacity failure that is larger than two. It is also implicit that the factor of safety would not be much more than 2. Perhaps it lies in the range of 2 to 4. For such factors of safety, the results of plate load tests on sands (1 sq ft plate) would indicate typical settlements of 0.1 in. to 0.3 in., which would be equivalent to a vertical strain on the order of 1% in the soil adjacent to the plate. Thus, the data for the structural backfill obtained from the triaxial tests correspond to coefficients of subgrade reaction within the range given by Terzaghi.

Sincerely yours,

GEOTECHNICAL ENGINEERS INC.

Gonzalo Castro
Principal

Steve J. Poulos
Principal

GC/SJP:ms
Encl.
cc w/encl.: R. Pizzuti, YAEC
D. Rhoads, UE&C
A. Desai, UE&C
D. Patel, UE&C

FIGURES

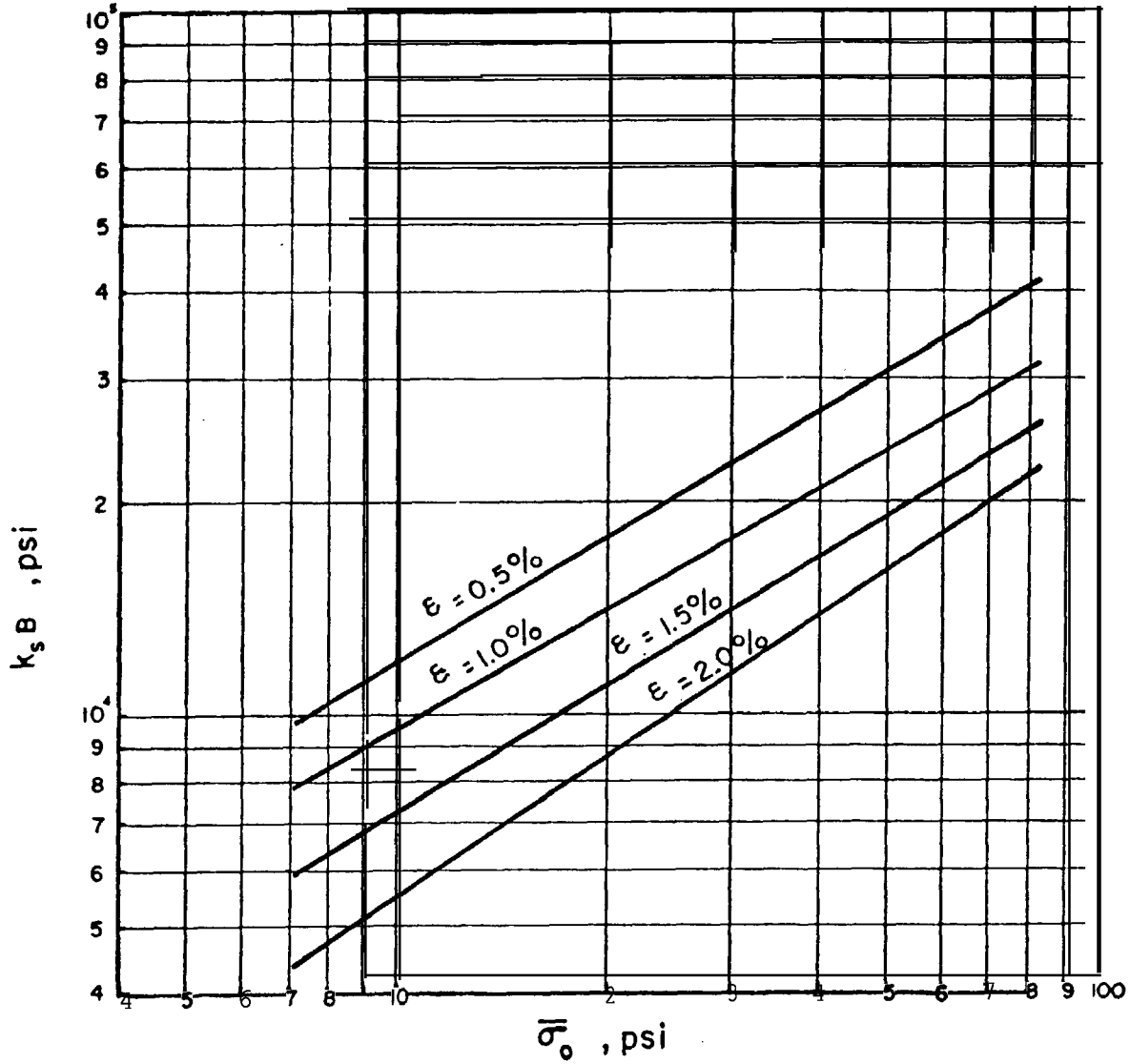

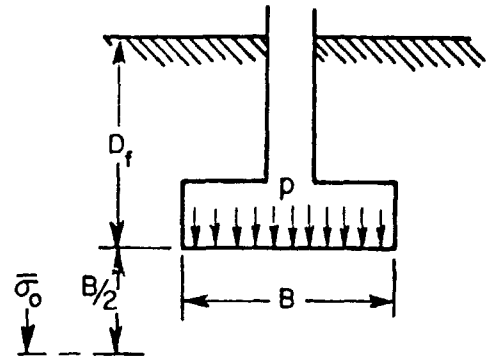

δ = SETTLEMENT

$k = \frac{p}{\delta}$

$\varepsilon = \frac{\delta}{B}$

$\bar{\sigma}_o$ = EFFECTIVE VERTICAL STRESS AT DEPTH (D_f t B/2)

Public Service Company of New Hampshire	Subgrade Reaction Sand and Sand-Cement Backfill	FOOTING PRESSURE ON STRUCTURAL BACKFILL 90% COMPACTION
Geotechnical Engineers Inc. Winchester, Massachusetts	Project 77386	March 13, 3.978 Fig. 1

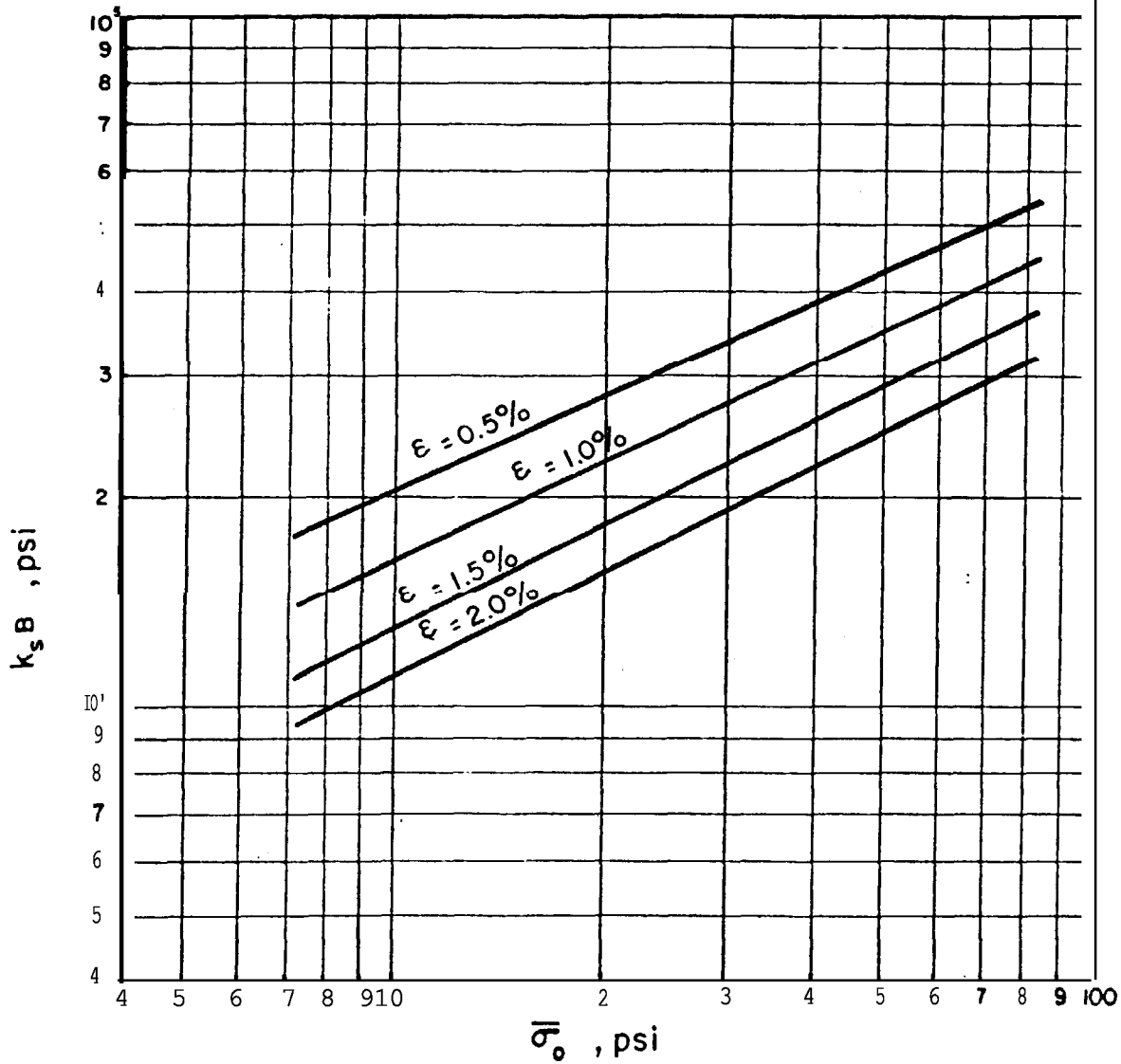

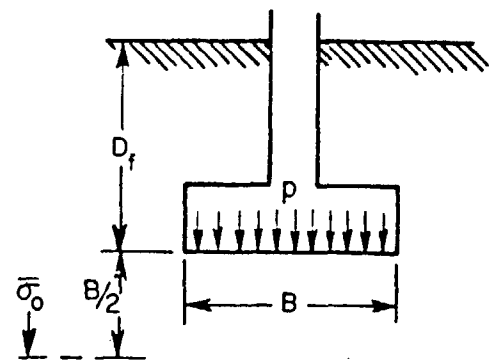

δ = SETTLEMENT

$k = \frac{p}{\delta}$

$\varepsilon = \frac{\delta}{B}$

$\bar{\sigma}_o$ = EFFECTIVE VERTICAL STRESS AT DEPTH (D_f t B/2)

Public Service Company of New Hampshire	Subgrade Reaction Sand and Sand-Cement Backfill	FOOTING PRESSURE ON STRUCTURAL BACKFILL 95% COMPACTION
Geotechnical Engineers Inc. Winchester, Massachusetts	Project,.77386	March 13, 1978 Fig. 2

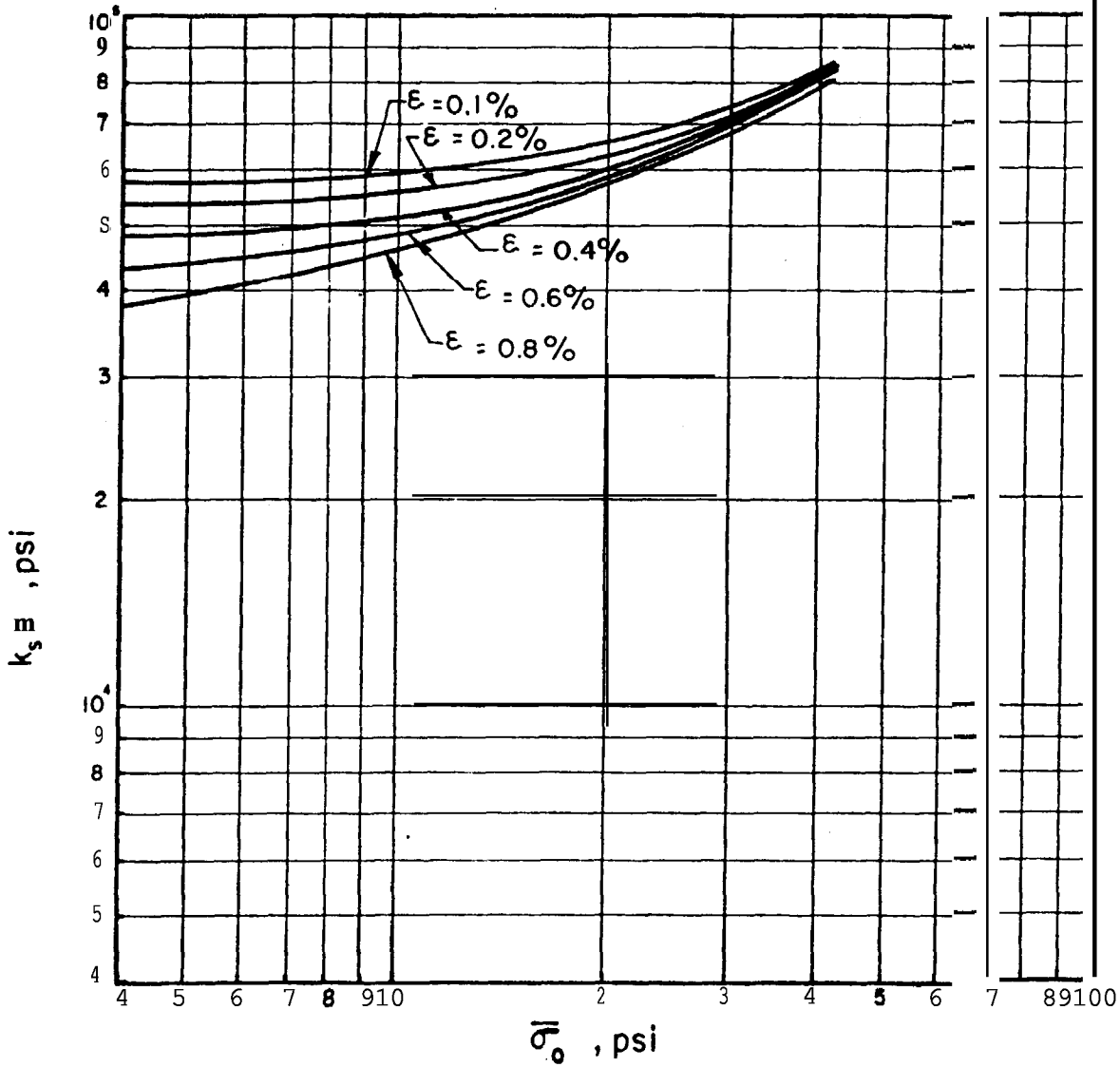

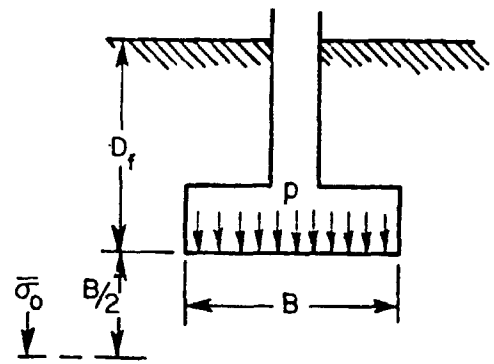

δ = SETTLEMENT

$k = \frac{p}{\delta}$

$\varepsilon = \frac{\delta}{B}$

$\bar{\sigma}_o$ = EFFECTIVE VERTICAL STRESS AT DEPTH (D_f + B/2)

Public Service Company of New Hampshire	Subgrade Reaction Sand and Sand-Cement Backfill	FOOTING PRESSURE ON SAND-CEMENT BACKFILL
Geotechnical Engineers Inc. Winchester, Massachusetts	Project 77386	March 13, 1978 Fig.3

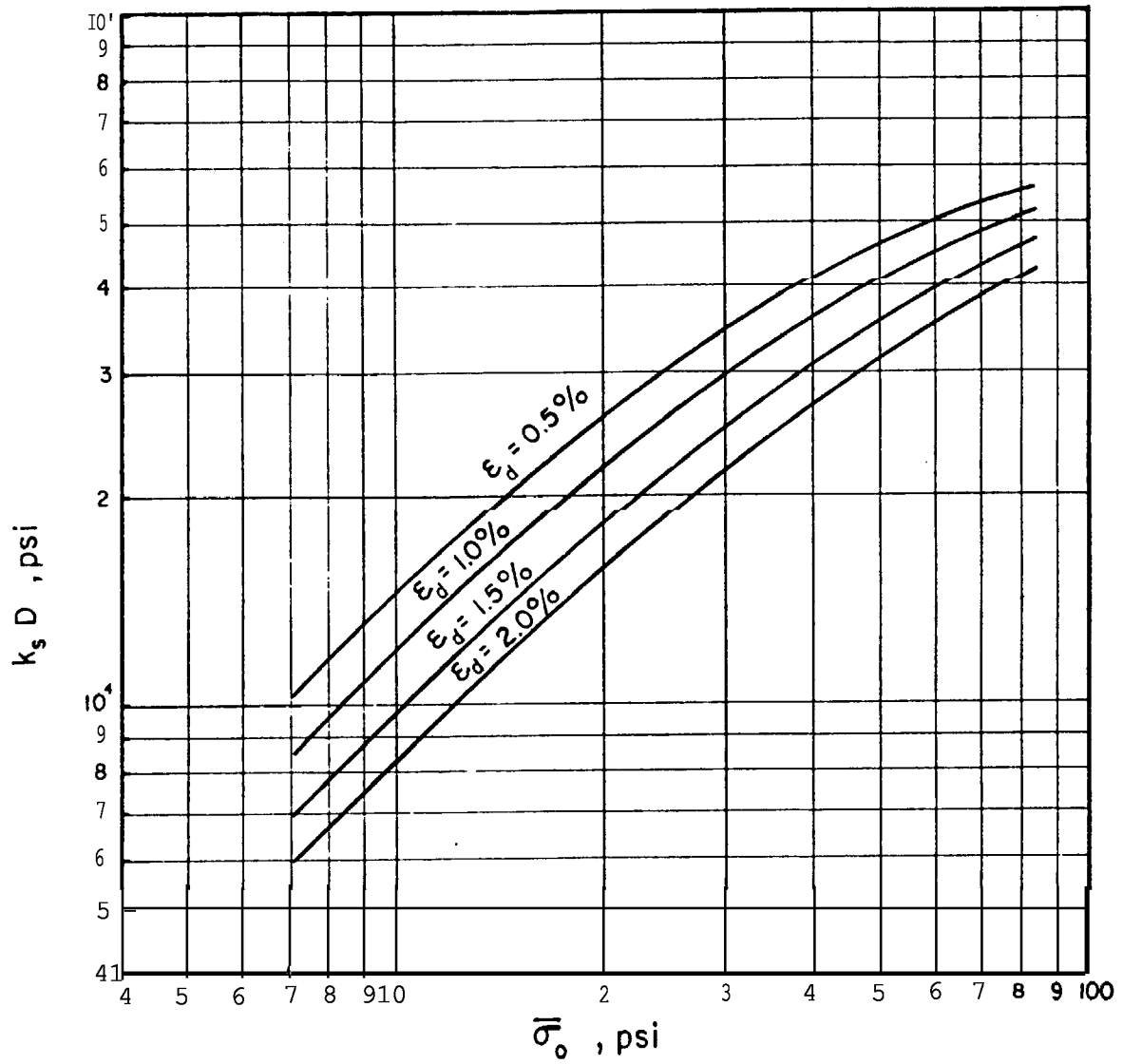

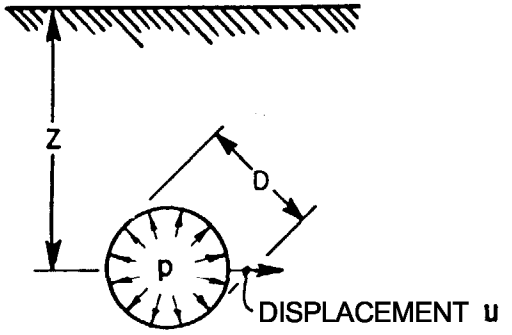

$k_s = \frac{p}{u}$

$\bar{\sigma}_o$ = EFFECTIVE VERTICAL STRESS AT DEPTH Z

$\varepsilon_d = \frac{2u}{D}$

Public Service Company of New Hampshire	Subgrade Reaction Sand and Sand-Cement Backfill	INTERNAL PRESSURE PIPE BURIED IN STRUCTURAL BACKFILL 90% COMPACTION
Geotechnical Engineers Inc. Winchester, Massachusetts	Project 77386	March 13, 1978 Fig. 4

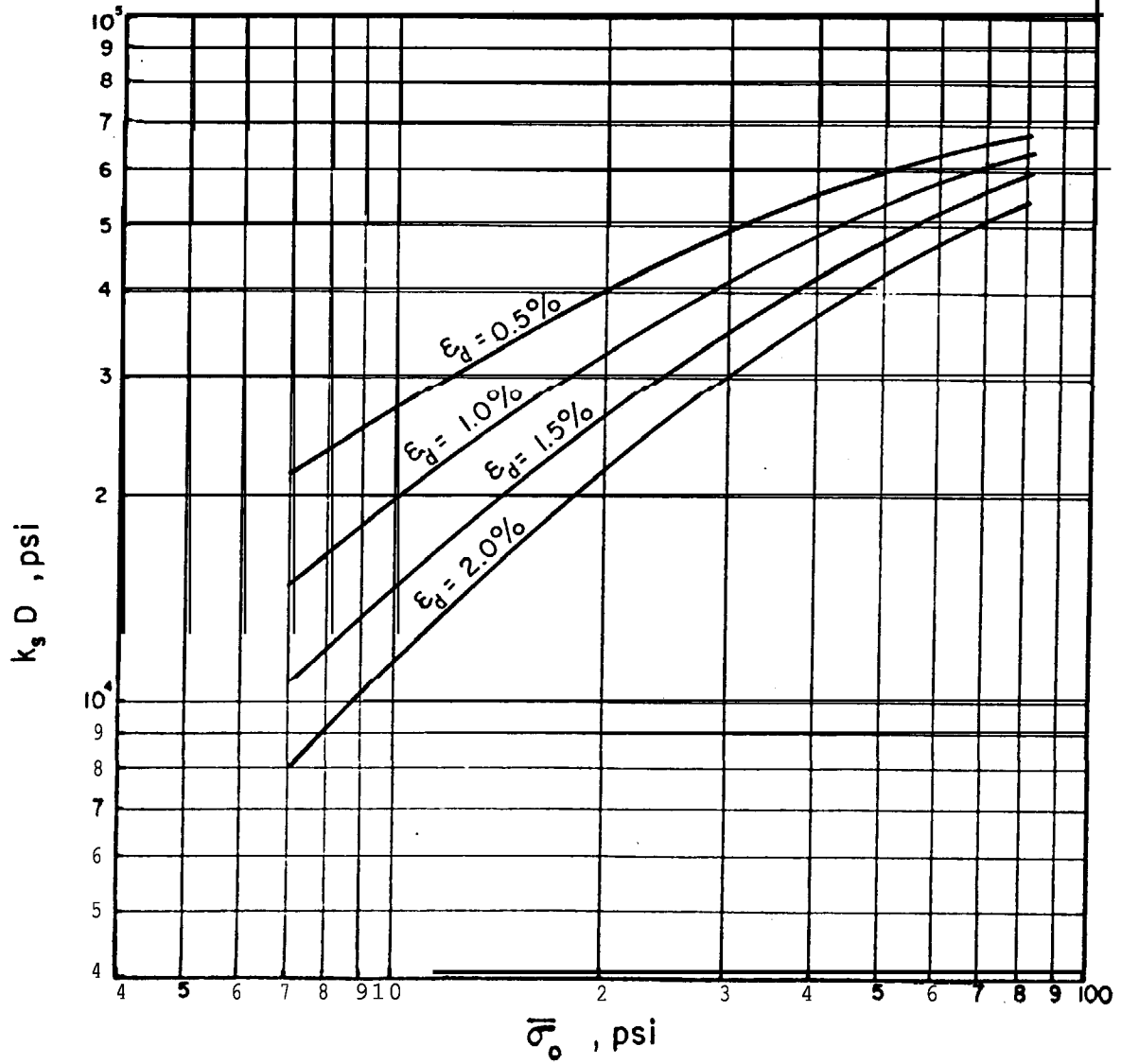

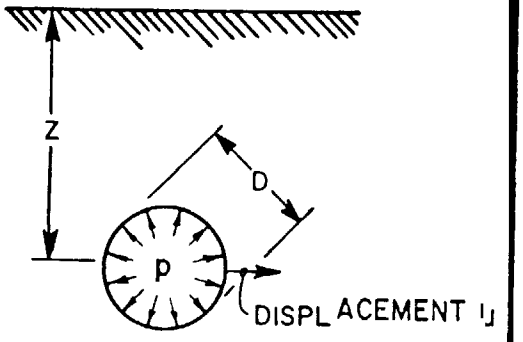

$k_s = \frac{p}{u}$

$\overline{\sigma_o}$ = EFFECTIVE VERTICAL STRESS AT DEPTH Z

$\varepsilon_d = \frac{2u}{D}$

Public Servide Company of New Hampshire	Subgrade Reaction Sand and Sand-Cement Backfill	INTERNAL PRESSURE PIPE BURIED IN STRUCTURAL BACKFILL 95% COMPACTION
Geotechnical Engineers Inc. Winchester, Massachusetts	Project 77386	March 13, 1978 Fia. 5

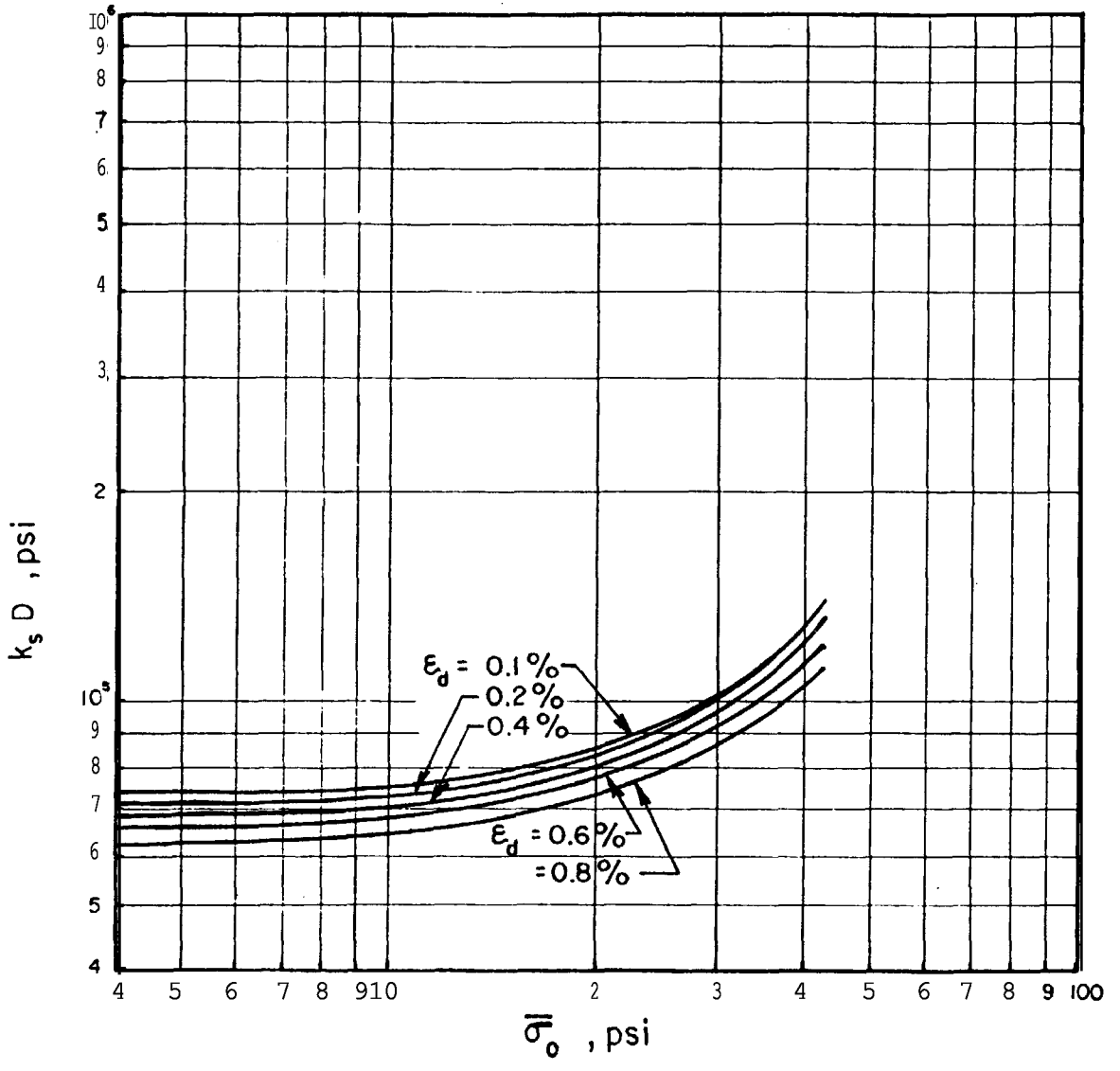

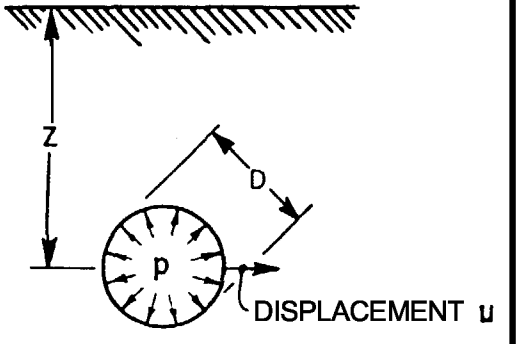

$k_s = \frac{p}{u}$

$\bar{\sigma}_o$ = EFFECTIVE VERTICAL STRESS AT DEPTH Z

$\varepsilon_d = \frac{2u}{D}$

Public Service Company of New Hampshire	Subgrade Reaction Sand and Sand-Cement Backfill	INTERNAL PRESSURE PIPE BURIED IN SAND-CEMENT BACKFILL
Geotechnical Engineers Inc. Winchester, Massachusetts	Project 77386	March 13, 1978 Fig. 6

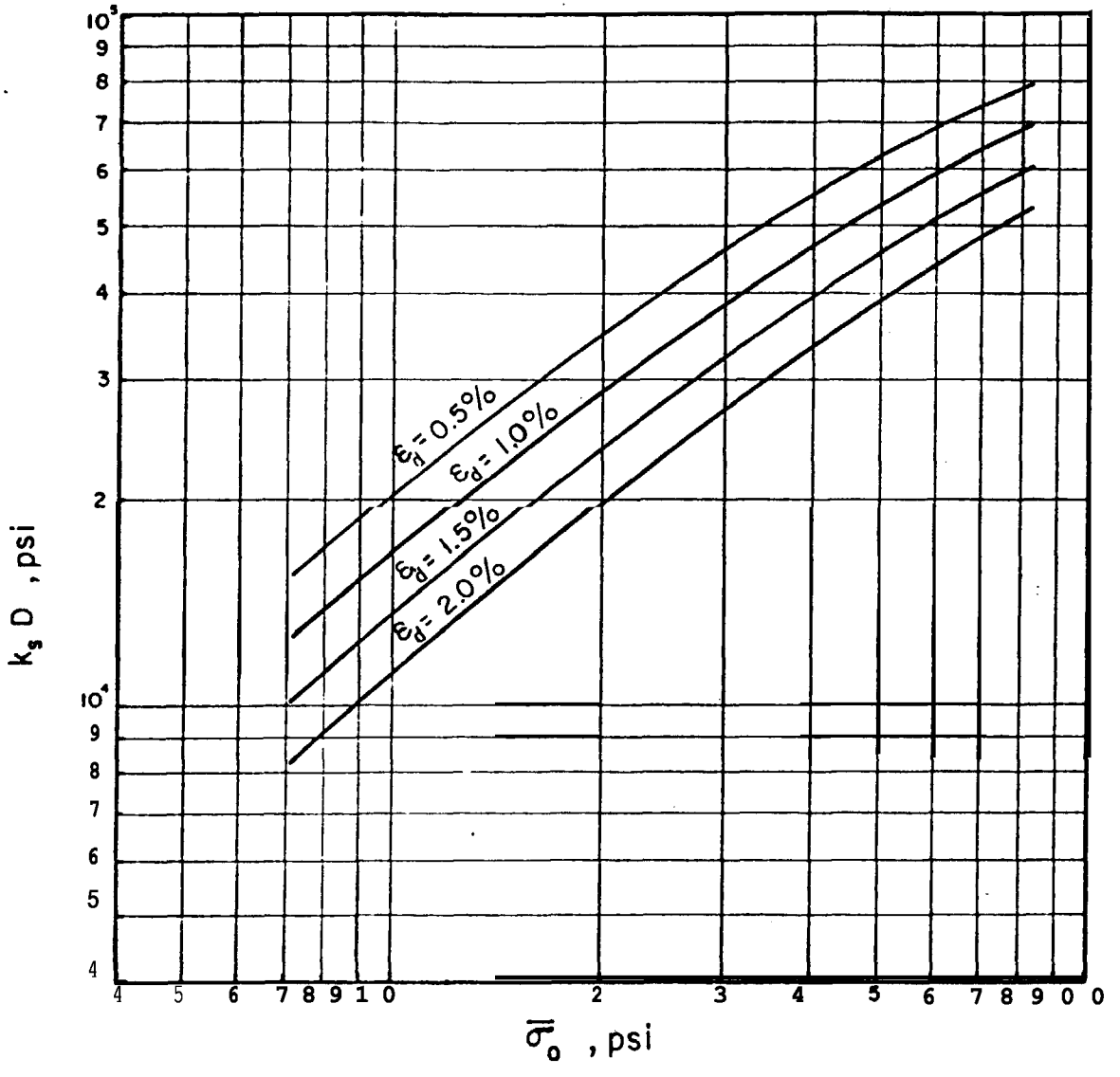

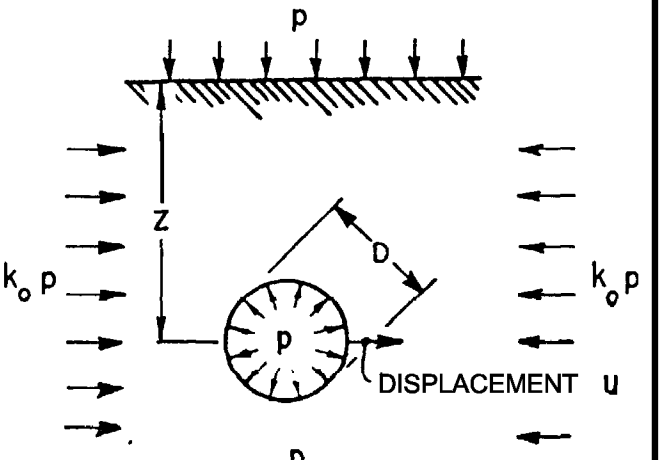

$$k_s = \frac{p}{u}$$

$$\varepsilon_d = \frac{2u}{D}$$

$\bar{\sigma}_o$ = EFFECTIVE VERTICAL STRESS AT DEPTH Z

Public Service Company of New Hampshire	Subgrade Reaction Sand and Sand-Cement Backfill	SURCHARGE PRESSURE ON PIPE IN STRUCTURAL BACKFILL 90% COMPACTION
Geotechnical Engineers Inc. Winchester, Massachusetts	Project 77386	March 13, 1978 Fig. 7

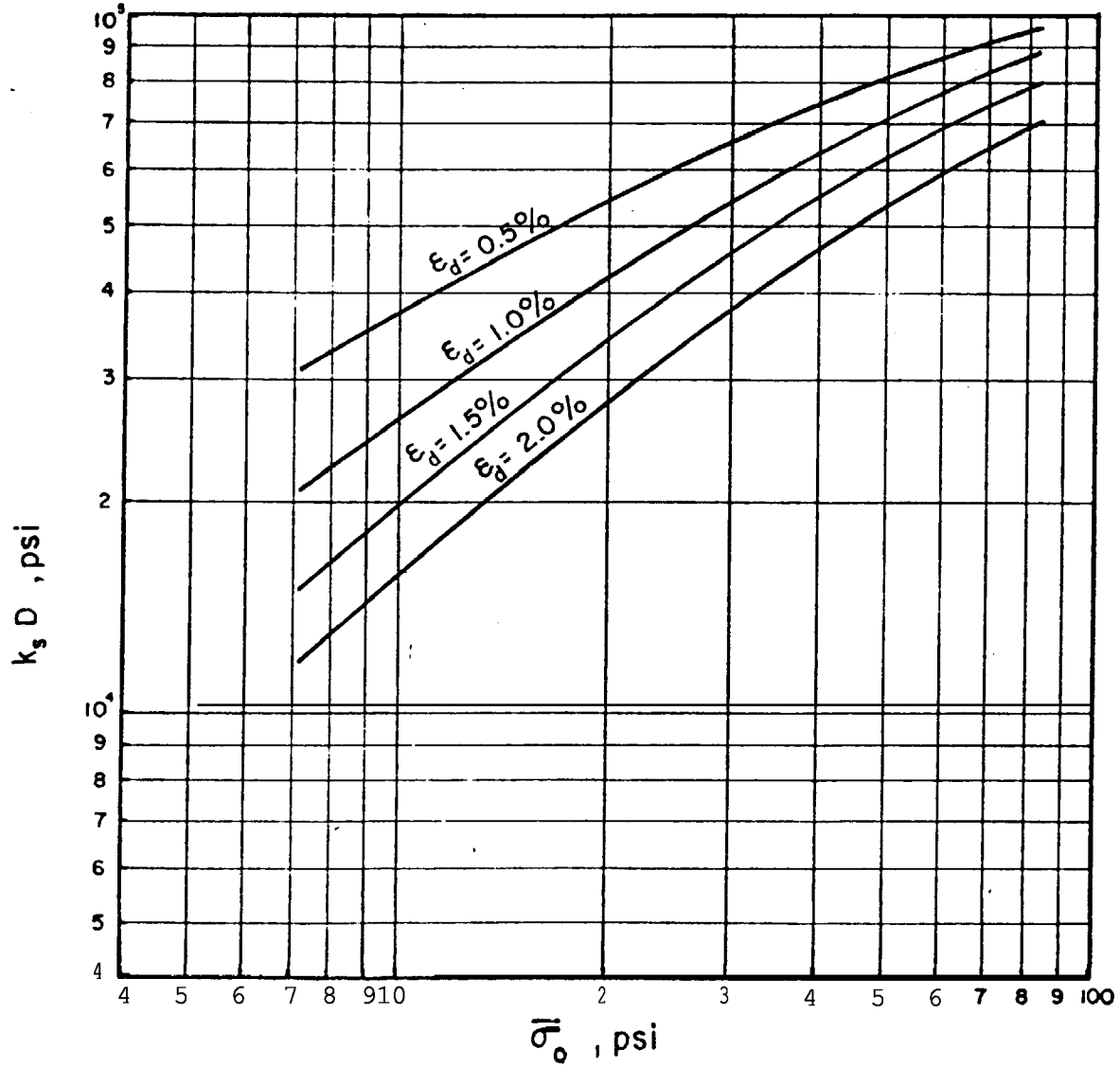

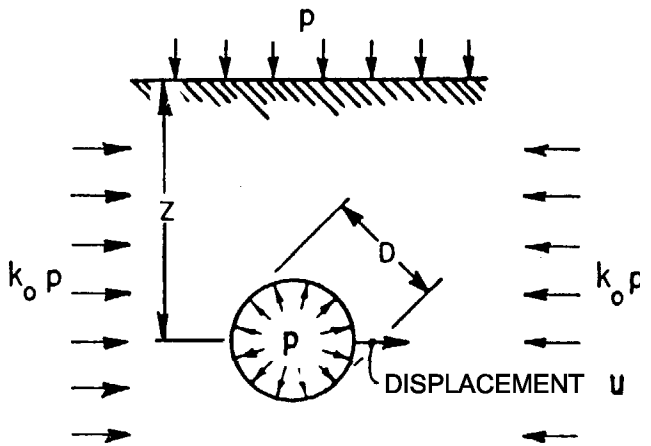

$$k_s = \frac{p}{u}$$

$$\varepsilon_d = \frac{2u}{D}$$

$\bar{\sigma}_o$ = EFFECTIVE VERTICAL STRESS AT DEPTH Z

Public Service Company of New Hampshire	Subgrade Reaction Sand and Sand-Cement Backfill	SURCHARGE PRESSURE ON PIPE IN STRUCTURAL BACKFILL '95% COMPACTION
Geotechnical Engineers Inc. Winchester, Massachusetts	Project 77386	March 13, 1978 Fig. 8

APPENDIX 2P

SEABROOK STATION CONTAINMENT AIRCRAFT IMPACT ANALYSIS

The information contained in this appendix was not revised, but has been extracted from the original FSAR and is provided for historical information.

APPENDIX 2P

SEABROOK STATION CONTAINMENT

AIRCRAFT IMPACT ANALYSIS

Prepared by

UNITED ENGINEERS
& CONSTRUCTORS INC.

OCTOBER 1975

PUBLIC SERVICE COMPANY OF NEW HAMPSHIRE
SEABROOK, NEWHAMPSHIRE

CONTENTS

ABSTRACT

Results are presented which verify the adequacy of the **Seabrook** containment to resist the impact of an FB-111 type aircraft. Included is a description of the dynamic forcing function, the elastic-dynamic analysis, the elastic-plastic analysis, an estimate of reinforcement and liner strain and a verification of the punching shear capability of the containment.

It is shown that there exists **no credible** mechanism by which spilled fuel from the impacting aircraft can access the **annulus.** The ensuing fire is, therefore, postulated to start in the **immediate** vicinity external to **the** enclosure and it is demonstrated that these external fires do not, in any way, inhibit or handicap the safe shutdown capability of the plant following the postulated crash.

It is concluded, that under the aircraft impact, the containment structure is able to withstand postulated impact and that the consequences of the aforementioned fire hazard is mitigated by the inherent design features of **Seabrook** Station.

1.0 STRUCTURAL ANALYSIS OF SEABROOK STATION CONTAINMENT FOR AIRCRAFT IMPACT

1.1 Introduction

The Seabrook Station containment has been analyzed for the effects of a-postulated impact by an FB-111 type aircraft with a speed at impact of 200 mph. Based on the analyses performed;-the adequacy of the containment to withstand the postulated impact is verified. The Seabrook Station containment and enclosure building is described in Section 3.8.1 of the Seabrook PSAR. The FB-111 aircraft, the missile in the postulated impact,is 73.5 feet long, has a wingspan (spread oosition) of 70.0 feet and weighs 81.800 Dounds (See Reference 1).

In order to perform the analyses, a force-time relationship is developed from the mechanical properties of the impacting aircraft. An elastic dynamic analysis indicates that an elastic-plastic dynamic analysis is required to predict the flexural response of the structure. From this analysis of the structure, an estimate is made of the strains experienced by the reinforcing bars and liner. Subsequently, an analysis is performed to verify the adequacy of the containment against punching shear and penetration.

1.2 FORCING FUNCTION FOR IMPACTING AIRCRAFT

The time variation of the load on a rigid surface due to an impacting aircraft may be developed using the momentum principle. The governing equations which are used to determine the time variation of the force experienced by the target are (Reference 2):

$$- P_c(\zeta_n(t)) = \frac{d^2\zeta_n}{dt^2} \int_{\zeta_n(t)}^{L} \omega(x,t)\, dx$$

$$R(t) = P_c(\zeta_n(t)) + \left(\frac{d\zeta_n}{dt}\right)^2 \omega(\zeta_n,t)$$

where

R(t) is the force acting on the target (positive for compression),

$\xi_n(t)$ is the extent of crushing at any time t as measured from the leading edge of nose of the missile,

$P_c(\xi_n)$ is the load required to crush the cross section of the missile at any distance ξ_n from the nose, (positive for compression)

$\omega(\xi_n)$ is the mass density per unit length of the missile as a function of the distance from the nose.

These equations are used to determine the two unknowns, the crushing length, $\xi_n(t)$, and the reaction, R(t), as functions of time. The information required to determine these variables consists of the initial impact velocity, weight or mass distribution and crushing load distribution of the aircraft.

The first equation is integrated numerically to obtain the velocity time history. The reaction force is then determined from the second equation.

Figure 1 shows three views of the FB-111 aircraft. Figure 2a shows the one dimensional idealized model of the same aircraft. Figure 2b describes the weight distribution for an FB-111 with a total weight of 81,800 pounds. The sketch and the weight distribution are obtained from Reference 1. The particular configuration used is essentially the same as that summarized on P. 1.3.3 of Reference 1 with the wing stores and wing useful load removed.

This configuration is consistent with the normal operation (90% of the time) of the FB-111 at Pease AFB. The value of 81,800 pounds is the

weight before the airplane has warmed up and taken off. In normal flights the aircraft would fly a mission and return to Pease AFB with approximately 10,000 pounds of fuel. On this basis, the landing weight would be approximately 59,000 pounds. For those missions when the aircraft is flown with wing tanks the maximum take-off weight is 100,000 pounds. The FB-lllis not allowed to land with fuel in these wing tanks; therefore in all cases the maximum landing weight is 81,800 pounds.

Thus, the 81,800 lbs weight of the FB-111 used in the impact analysis was the fully loaded FB-111 without wing tanks. This weight is conservatively large for any configuration of the aircraft flying out of Pease AFB, but it was used because it represented a maximum upper bound on the weight of the FB-111 in the landing pattern.

The exact crushing load distribution for an PB-111 is not available. The crushing load distribution shown on Figure 2c is arrived at by scaling the known values for a Boeing-720(Ref.2).It is demonstrated in this report that the peak value of the reaction is relatively insensitive to reasonable variations of the crushing load.

Figure 3 shows the reaction-time relationship for the FB-111 striking a rigid wall at an impact velocity of 200 mph. The peak value of the reaction is 8.2 x 10^6 pounds. This peak value occurs when the wing structure is in the process of collapsing. This peak reflects the

concentration of mass in the wing structure and the fuel that is stored in the fuselage in the vicinity of the wing location. It is noted that the cross-sectional area over which the peak occurs will be considerably larger than the area of fuselage cross-section. The secondary peak of 4.2 x 10^6 pounds (at 0.21 sec.) occurs when the airplane is crushing in the vicinity of the engines.

The determination of the sensitivity of the reaction to the magnitude of the crushing load is investigated by determining the reaction for values of one-fifth and five times this crushing load. These results are shown in Figure 4. From Figure 4, the peak values of the reactions are:

$P_c/5$	8.5 x 10^6 pounds
P_c	8.2 x 10^6 pounds
$5xP_c$	7.1 x 10^6 pounds

The peak value of the reaction is relatively insensitive to variations in the magnitude of the crushing load, and the scaled value of P_c is judged to give accurate results.

1.3 Flexural Behavior of Containment

1.3.1 Elastic Dynamic Analysis

For the elastic dynamic analysis, the finite element method was chosen as the analytical method, and a computer program for axisymmetric structures subjected to arbitrary static and dynamic loads was used. (See Reference 3 for the basis of the mechanics of the program.) Damping was not considered. Thus, the predicted structural response is slightly larger than that which does occur.

To accomplish the analysis, several assumptions were made. They are as follows:

i) The containment is fixed at the base of the cylinder.

ii) Impact loads are uniformly distributed over the loading zones.

iii) In the axisymmetric analysis (impact at apex of dome), the loading zone is a circle with a radius of 52.77 inches and an area of 8748.3 square inches.

iv) In the asymmetric analysis (impact at springline), the loading zone is a square, 93.53 inches on a side and 8748.3 square inches in area.

v) The stiffness of the reinforcing steel is neglected; only the gross concrete volume is considered. The modulus of elasticity was taken as 3.0×10^6 lbs/sq. in., Poisson's ratio was taken as 0.15, and the weight density was taken as 150 pcf.

vi) The effect of the enclosure building is neglected. It can be shown that the enclosure absorbs approximately 4% of the energy of the impacting aircraft.

The containment structure is modeled with axisymmetric conical shell elements, a plot of this model is shown in Figure 5.

Two impact positions, the apex of the dome and the springline, are considered. The impact at the dome is uniformly distributed over the first seven (7) elements, and the impact at the springline is uniformly distributed over the six (6) elements nearest to the springline. By means of a half-range cosine series, the load at the springline is confined to a

6.18' arc. Thirty (30) terms were used to represent this Fourier series which is shown, normalized to 1.0, in Figure 6. Experience with loadings similar to the loadings here, has demonstrated that twenty (20) terms of the series were found to be too few and ninety (90) terms were found to yield results very close to those generated by thirty (30) terms.

Selected maximum results for the axisymmetric and asymmetric analyses are given in Tables 1-1 and 1-2, respectively. These moments will cause cracking of the concrete and yielding of the rebar. Therefore, an elastic-plastic dynamic analysis is required.

1.3.2' Elastic-Plastic Dynamic Analysis

The procedure followed for the elastic-plastic analysis of the response of the containment under aircraft impact follows that of Biggs (Reference 4). In this procedure, knowing the load-time relationship, the first natural frequency of that part of the structure participating in the energy absorption, and the allowable ductility ratio (defined as the ratio of the maximum deflection to the deflection at yield), the ratio (F/R_m) of the maximum value of the load-time relationship to the maximum value of the resistance function can be determined. This

can then be compared with the actual estimated maximum values of the load-time relationship and resistance function.

The force-time relationship, given in Figure 3 is approximated by a triangular load-time curve with the same total impulse and peak force. This ideal and the actual force-time relationships are compared in Figure 7 . It is assumed that a circular region of radius "a" will participate in the energy absorption. The natural frequency, associated with this participating region, is estimated on the basis of the first natural frequency of a flat circular plate of radius "a" clamped at the edges. The assumption of clamped edges, in that it gives a smaller period for the first natural frequency than in the actual case, is a conservative simplification. This follows because, in general the value of the maximum allowable forcing function decreases as the first natural period decreases (Ref. 4, p. 78, Figure 2.26). Conversely, ignoring the curvature is non-conservative in that it gives an estimate of the period which is larger than the actual case. For small values of the radius "a", the curvature effect is minimal.

All calculations are based upon the 3'-6" dome section configuration. The first natural frequency of a flat circular plate, clamped at the edge is:

$$P = \sqrt{\frac{D}{M}} \quad \frac{1}{a^2} \quad X.17$$

where D is the flexural rigidity and M is the mass density per unit surface area (See, for example, Ref. 5).

For the 3'-6" thick concrete plate with a Young's modulus of 3×10^6 psi and a unit weight of 150 pounds per cubic foot, the period is:

uncracked section $T = \frac{a^2}{15.94 \times 10^3}$ "a" in feet

cracked section $T = \frac{a^2}{12.86 \times 10^3}$

Using Fig, 2.26 of Reference 4 (p. 78), the ratio F/Rm, as a function of the radius of the participating material of the containment, can be determined for various values of ductility ratio.

For the purpose of this investigation, two (2) ductility ratios, 3 and 10 are used. For plates and shells, the lower value is conservative, the larger value reasonable. The results of the calculations are shown in Table 1-3 and Figure 8. Although the range of Fig. 2.26 of Reference 4 is limited to a td/T of 20, it can be observed that for a ductility ratio greater than two and td/T of 20, F/Rm is greater than unity. Therefore, the allowable peak force, F, can be larger than the maximum value of the resistance, Rm.

1.3.3 Resistance Function

In the vicinity of the impact region, the response of the structure is assumed to have the characteristics shown in Figure 9a.

For values of the force less than Rm, the displacements are limited in magnitude even though the response may be inelastic. As the load reaches the value Rm, the deformations are able

to become arbitrarily large, i.e., the collapse load has been reached. The collapse load for a concentrated load on a curved shell is not readily accessible. As a conservative estimate, the collapse load for a flat plate with reinforcement the same as the dome is used to estimate the collapse load for the shell..

Expecting the yield line formation shown in Figure 9b observation suggests that the clamped boundary condition case should be used. The value of the collapse load, Rm, is then (Reference 6)

$$R_M = 2\pi(M_u^+ + M_u^-)$$

where M_u is the ultimate moment capacity and the notation + and - refers to the outside and inside reinforcement respectively.

The ultimate moment capacities and collapse loads of the containment are:

dome $M^+ = 643$ k-ft./ft.
$M^- = 651$ k-ft./ft.
Rm = 8,131k

springline $M^+ = 1,235$ k-ft./ft
M- = 643 k-ft./ft
Rm = 11,800k

At the dome, the collapse load and peak load are approximately equal. However, from Figure 8 , the dynamic effect allows the structure to withstand loads in excess of the capacity. From Figure 8 the allowable load is 10% larger than the resistance or collapse load. Therefore, the apex will not

collapse. Since the maximum load, 8,200k is less than the capacity of the dome in the springline, 11,800k, collapse will not occur at the springline.

The dome will not collapse, under the applied load.

1.3.4 Estimation of Rebar and Liner Strains

While plastic analysis techniques are useful for finding collapse loads, they cannot be directly used to find the strains and displacements corresponding to collapse loads.

However, a procedure making use of the ductility ratio can be used to approximate the maximum strains in the structure subject to dynamic loading when nonlinear material behavior is encountered. This procedure is described below.

A typical load-displacement curve for reinforced concrete section is shown in Figure 10. This curve is linear up to the load causing cracking (P_{cr}) after which a straight line of somewhat flatter slope is obtained until the load (P_y) is reached which causes yielding of the steel.

Any increase in load beyond (P_y) causes the displacement to increase disproportionately. Further increase in load causes extensive displacements to occur, resulting in eventual collapse. This actual behavior of the structure was idealized as shown in Figure 9a, and was used for the elastic-plastic dynamic analysis previously discussed. This idealized curve represents the resistance function of the structure.

The ductility ratio, μ, referred to in the elastic-plastic dynamic analysis represents the ratio of the maximum displacement of the structure to the deflection established as yield (Y_{el}) for the structure.

While it is recognized that the ductility ratio is not an exact measure of the maximum strain at a particular point of the structure, it can be used as an approximation because the strain at yield in the actual structure is very nearly the strain corresponding to yield for the idealized structure.

The procedure used herein is based on the peak of the actual forcing function resulting from the-aircraft impact, the duration of loading, the idealized resistance function for the structure and the first natural period of the responding part of the structure. By using the above known quantities, the corresponding ductility ratio for the structure may be determined.

For a peak in the forcing function of 8,200k and a maximum force in the resistance function of 8,130 k, the maximum ductility ratio for all ratios of t_d/T is approximately 1.5 (See Fig. 2-26, Ref. 2). Thus, regardless of the natural period of the responding part of the structure, the largest displacement that will occur under the aircraft impact loading is the same as that corresponding to yield for the idealized structure.

The yield strain for the reinforcing steel is

$$\varepsilon_Y = \frac{60}{30 \times 10^3} = 0.002 \text{ in/in}$$

If it is assumed that the strain corresponding to yield (Y_{el}) for the idealized structure is 50% larger than this (actually is much less than this),, then an upper bound for the strain in the reinforcing steel will be:

$$\varepsilon = 1.5 \times 1.5 \times 0.002 \text{ in/in} = 0.0045 \text{ in/in}$$

Since the liner and the tension reinforcing steel are only several inches apart in a 42" thick containment dome, they will be strained to nearly the same values. Hence, there will be no possibility of impairing the leak tight integrity of the liner.

1.4 Response of the Enclosure Building

During the early stages of the impact process, the enclosure building will deform until it comes into contact with the containment. The enclosure building must deflect five feet in order to come into contact with the containment dome. Such a deformation will involve an inelastic response. This inelastic response will involve both flexure and shear.

The 15" thick enclosure building is reinforced with #10's @ 12", both ways and both faces. The collapse load is 635k.

The allowable shear load will depend upon the shear area over which the transverse shear stress acts. This shear area is determined by multiplying the average shear periphery by the effective depth of the shell. The average shear periphery is determined by a contour which is at a distance of one-half the effective depth away from the contour of the contact area (Figure 11). Figures 12 to 21 show the impact area and shear periphery associated with various locations

along the aircraft and for the effective depths of the enclosure building (9") and containment (37").

The reaction as a function of the cross section being crushed is determined from the reaction-time and crushing distance relationship and is shown in Figure 22.

From this information, it is possible to examine the effect of the aircraft impact on the enclosure building as a function of the distance being crushed. Figure 23 shows the average shear stress on the enclosure as a function of distance being crushed. For example, using a shear strength of $4.25\sqrt{f'_c}$, the enclosure building will fail by shear when the aircraft is crushing at 7.25 feet. Also shown on Figure 23 is the reaction as a function of the distance being crushed. For a collapse load of 635k, the enclosure building will collapse when the aircraft is crushing at 9.75 feet. It would appear that, using $4.25\sqrt{f'_c}$ as a shear strength, the enclosure building would fail by shear before collapse, however, the two events would occur at a time difference of 0.0086 sec. Any increase in actual shear strength above $4.25\sqrt{f'_c}$ would increase the possibility of punch through and collapse happening simultaneously. As will be domonstrated in Section 1.5, the actual shear strength can vary considerably above a value of $4.25\sqrt{f'_c}$. No clear conclusion can be drawn as to whether punch through or collapse occurs first. Based on the above discussion, the failure of the enclosure building will involve both extensive shear and flexure damage and it will deform until it comes into contact with the containment.

1.5 Shear Capability of the Containment

The enclosure building will deform until it comes into contact with the containment dome. The dome will then resist the impact force and experience transverse shear stress in the vicinity of the impact area. The maximum average shear stress is determined by defining a shear perimeter and thickness over which the impact force is acting. Figure 24 describes the procedure by which the shear perimeter for the maximum average shear stress acting on the containment dome is determined. The shear perimeter for the containment is at a distance

$$\text{(effective depth of enclosure)} + \left(\frac{\text{effective depth of containment}}{2}\right)$$

away from the perimeter of the impact area.

The values of the shear perimeter for various cross sections of the aircraft are given in Table 1-4. Also shown are the shear area, impact force and average shear stress for the containment building. The values of average shear stress as a function of the cross section being crushed is shown in Figure 25. The shear stress is given in terms of psi and $\sqrt{f'_c}$. The maximum value of the average shear stress occurs when the aircraft is crushing at a distance of 35 feet from the nose. The value of this maximum average shear stress is 229 psi or $4.18\sqrt{f'_c}$.

Various shear strengths have been proposed. A tabulation of these shear strengths, for parameters similar to the aircraft and structure under discussion is shown in Table 1-5. It is seen that the maximum nominal shear stress of $4.18\sqrt{f'_c}$ is less than all the other proposed values except the conservative value of $4\sqrt{f'_c}$ as proposed by the

XI-Committee 326. Hence, it is concluded the the containment will not fail by punch through.

1.6 Requirements to Prevent Perforation

The velocity of the engines as they impact on the enclosure building and containment is 250 fps.

The FB-111 has two Pratt & Whitney JTF10A-270 (Military designation TF30-P-7) jet turbo fan engines with an outside diameter of 50.22 inches. Each engine has a dry weight of 4,121 pounds (Ref. 1). The thickness of the dome required for no performation was determined using procedures reported in Reference 7.

The pertinent nomenclature is :

x	penetration thickness for infinitely thick slab (inches)
e	perforation thickness for reinforced concrete (inches)
dm	diameter of missile (inches)
v	velocity of impact (feet per second)
w	weight of missile
K	$\frac{180}{\sqrt{f'_c}}$
f'_c	ultimate compression strength of concrete (psi)

$$G = K(.72)(.50)\frac{W}{dm^3}\, dm^{0.2}\left(\frac{V}{1000}\right)^{1.8}$$

$$\frac{x}{dm} = 2\sqrt{G}, \quad G < 1.0$$

$$\frac{e}{dm} = 2.57\left(\frac{x}{dm}\right) - 0.454\left(\frac{x}{dm}\right)^2, \quad 0 \leq \frac{e}{dm} \leq 3$$

Since a jet engine is not completely solid (thin shells for torque transmission, blades for fan, compressor and turbine, burner cans for combustion) the engine was assumed to behave similarly to a hollow pipe missile.

For a fan-jet, the outside diameter is slightly larger than the gas generator. Two values of dm (the diameter of the gas generator) were used, SO.23 inches and 40 inches. The results are:

dm (inches)	e(inches)
50.22	21.8
40.00	22.8

These values can be compared with the dome thickness of 42 inches. From these calculations, it can be concluded that there will be no perforation.

1.7 Conclusions

From the above results of the analysis of the Seabrook Station Containment, the following conclusions can be made:

1. The enclosure building will fail and will come into contact with the containment building. The mode of failure will not be by shear or flexure alone, but will involve both types of damage.
2. The containment building will not fail. The flexural strength will prevent collapse. The shear strength will prevent punch through. There will be permanent damage to the structure, but the extent of this damage will not be sufficient to cause loss of the integrity of the building.

3. The liner strains, although inelastic, will be sufficiently small so that tearing of the liner will not occur.
4. The engines will not perforate the containment.

These conclusions can be made even though the above analysis was performed with considerable conservatisms. The conservative aspects of the analysis are:

1. The reaction-time relationship was determined for impact on a rigid target. A realistic, flexible target would reduce the peak value of the reaction.
2. Normal impact was assumed. Any impact angle other than 90^{o} reduces the impact force and increase the area over which the impact force acts.
3. The arcing effect of the doubly-curved dome was ignored. Arching increases the collapse and punching load capacities.
4. The shear stresses can be computed more accurately using the effective force occuring during the time necessary for the structure to respond rather than the peak instantaneous force. The peak instantaneous force will give larger shear stresses than the effective force.
5. The actual concrete compression strength will be larger than the specified strength of 3,000 psi. This would result in a larger value for the shear strength.
6. A conservative estimate of the shear periphery used to calculate shear areas and shear strengths was chosen. The

failure cone was assumed to be through the containment only and not through the combined thicknesses of the containment and enclosure building, The latter would be more accurate.

The integrity of the containment building will not be impaired in the occurrence of the postulated aircraft impact.

1.8 REFERENCES FOR SECTION 1.0

1. "FB-111 Unit Inertia Data, "General Dynamics, Fort Worth Division, Report FZS-12-6010, Revision "A", January, 1968.

2. Riera, J.O., "On the Stress Analysis of Structures Subjected to Aircraft Impact Forces" Nuclear Engineering and Design, North Holland Publishing Company, Amsterdam, Holland, 8 (1968), p. 415-426.

3. Ghosh, S., and Wilson, E., "Dynamic Stress Analysis of Axisymmetric Structures Under Arbitrary Loading", University of California, Berkeley, CA., Revised Sept., 1975.

4. Biggs, J. M., Introduction to Structural Dynamics, McGraw-Hill, Inc., 1964, pps. 69-84.

5. Meiorovitch, Analytical Methods in Vibrations, The Macmillan Company, 1967, p. 183.

6. Save and Massonnet, Plastic Analysis and Design of Plates, Shells and Disks, North Holland, 1972, p. 245.

7. Kennedy, Effects of an Aircraft Crash Into a Concrete Reactor Containment Building. Holmes & Narver, Inc., July, 1966.

TABLE 1-1

MAXIMUM RESPONSE

AXISYMMETRICANALYSIS

(IMPACT AT DOME)

Moments	Meridional	-1006 Ft-K/Ft
	Circumferential	-1005 FT-K/FT
Forces	Meridional	-478 K/Ft
	Circumferential	-478 F/Ft

TABLE 1-2

MAXIMUM RESPONSE

ASYMMETRIC ANALYSIS

(IMPACT AT SPRINGLINE)

ELEMENT 36*	Moments	Meridional	-1139 Ft-K/Ft
		Circumferential	-1309 **Ft-K/Ft**
	Forces	Meridional	383 **K/Ft**
		Circumferential	442 **K/Ft**
ELEMENT 37*	Moments	Meridional	-1148. Ft-K/Ft
		Circumferential	1350 **Ft-K/Ft**
	Forces	Meridional*	378 **K/Ft**
		Circumferential	431 **K/Ft**

* Element 36 is element **immediately** above springline.

Element 37 is element immediately below springline.

TABLE 1-3

ALLOWABLE MAXIMUM FORCE, MAXIM?? RESISTANCE RATIO FOR VARIOUS DUCTILITY RATIOS AND PARTICIPATING TARGET MATERIAL RADII

A* (ft)	T (sec)	td/T	μ	F/Rm
		Uncracked Section		
4	1.00×10^{-3}	170.0		**
a	4.01×10^{-3}	42.4		1
12	9.03×10^{-3}	18.8		
16	1.61×10^{-2}	10.6		
20	2.51×10^{-2}	6.8	3	1.12
			10	1.23
24	3.61×10^{-2}	4.8	3	1.15
			10	1.12
28	4.92×10^{-2}	3.5	3	1.20
			10	1.33
32	6.42×10^{-2}	2.6	3	1.25
			10	1.47
		Cracked Section		
4	1.24×10^{-3}	137.1		
a	4.92×10^{-3}	34.2		1
12	1.12×10^{-2}	15.2		
16	1.99×10^{-2}	a.5	3	1.10
			10	1.20
20	3.11×10^{-2}	5.4	3	1.10
			10	1.30
24	4.48×10^{-2}	3.8	3	1.17
			10	1.36
28	6.09×10^{-2}	2.8	3	1.23
			10	1.47
32	7.96×10^{-2}	2.1	3	1.25
			10	1.70

* Participating Radius; since this is not well defined, a range of values is included.

** By observation, Pigure 2.26, "Introduction to Structural Dynamics" Riggs

TABLE 1-4

AVERAGE SHEAR STRESS - **CONTAINMENT**

Location ft.	Shear Perimeter ft.	Shear Area in^2	Reaction pounds	Average Shear Stress p s i
15	32.6	14,474	**1,284,000**	89
19	37.0	16,428	**1,625,000**	**99**
27	41.8	18,559	**3,298,000**	178
35	50.2	22,288	**5,105,000**	229
41	99.8	44,311	**8,200,000**	**185***
50	45.5	20,202	**2,765,000**	**137**
58	49.2	21,844	**4,200,000**	**191**,+
65	49.2	21,844	686,000	32

SB 1 & 2 FSAR

*If the wings were assumed to have sheared-off at the time that the aircraft were crushing at this location the shear perimeter and reaction would-be reduced to 64.6 ft. and **6,070k** respectively. The average shear stress then becomes 198 psi.

If the horizontal and vertical stabilizers were assumed to have sheared-off at the time that the aircraft were crushing at this location the shear perimeter and reaction would be reduced to 42.1 ft. and **3,900k respectively. The average shear stress then becomes 209 psi.

+The average shear *stress* for the case were the crushing strength is reduced by 5 is 245 psi.

TABLE 1-5

COMPARISON OF ULTIMATE SHEAR STRENGTH CAPACITY*

Ultimate Shear Strength psi	Ultimate Shear Strength $\sqrt{f'c}$	Comment
717	13.1	equation 5-2, ϕ_o = .5
655	11.9	equation 5-1, ϕ_o = .5
607	11.08	equation S-10, ϕ_o = .5
527	9.62	equation 5-5, ϕ_o = .5
525	9.58	equation 5-2, ϕ_o = 1
523	9.55	equation 5-3, ϕ_o = .5
445	8.1	equation 5-1, ϕ_o = 1
391	7.14	equation S-10, ϕ_o = 1
383	6.99	equation 5-5, ϕ_o = 1
363	6.62	equation 5-12**
351	6.41	equation 5-4a
292	5.33	equation 5-6
219	4.00	equation 5-9, Committee 326 shear stress at distance d/2 from periphery ϕ = 1

*"The Shear Strength of Reinforced Concrete Member-Slabs", Joint ASCE-ACI Task Committee 426, Journal of the Structural Division, ASCE, Aug., 1974.

c = 93" $\sqrt{f'c}$ = 3,000 psi p = 0.0099

d = 37" f_y = 60,000 psi

**Adjusted for circular region, evaluated at d/2 away from periphery.

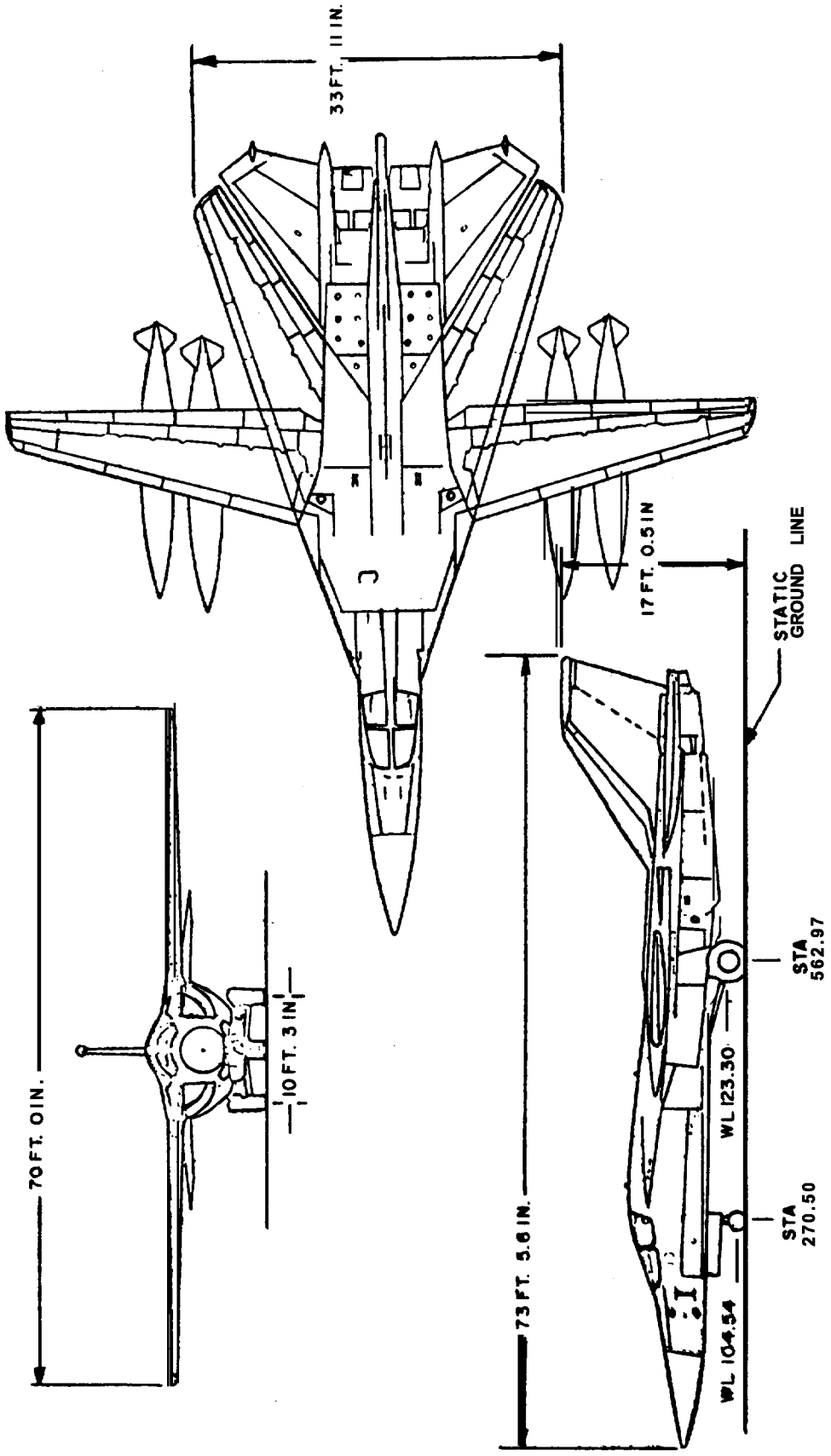

FIGURE 1

FB-111 CONFIGURATION (FROM REFERENCE 2)

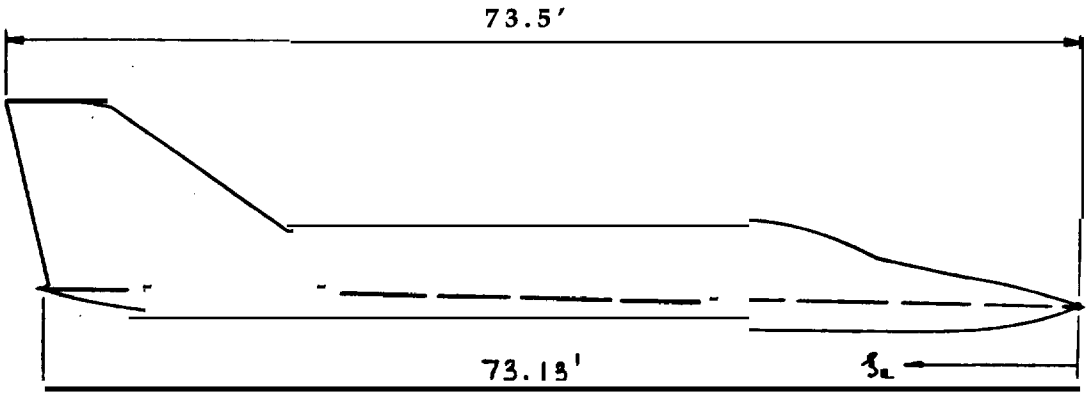

Figure 2A FB III - CONFIGURATION

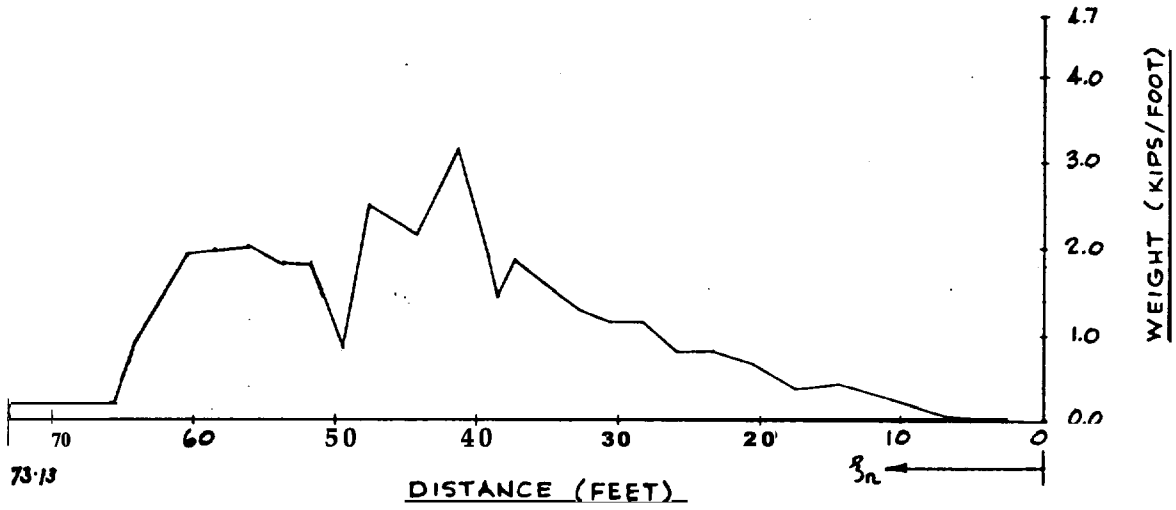

Figure 2B WEIGHT DISTRIBUTION

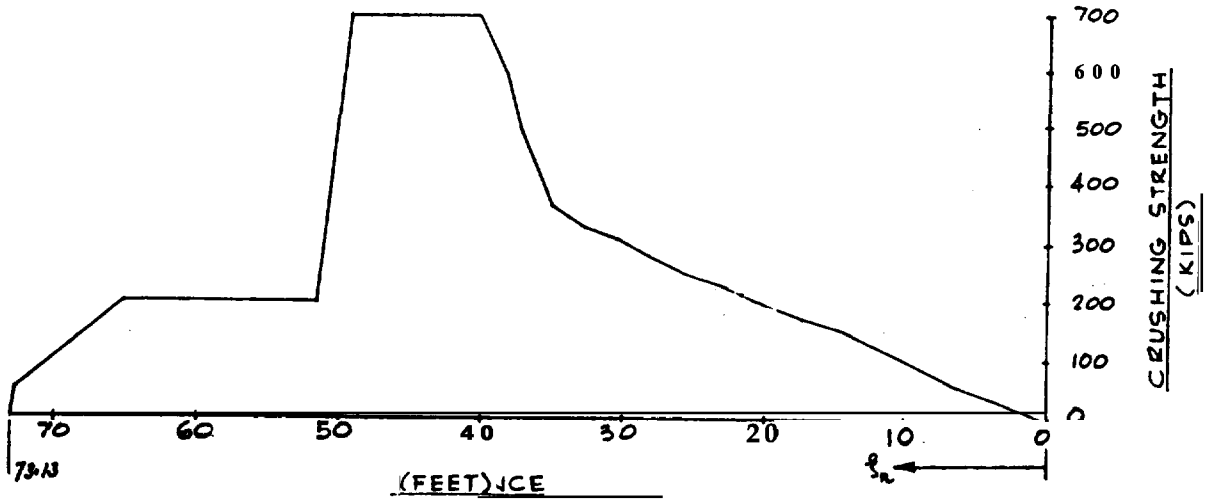

Figure 2C CRUSHING STRENGTH DISTRIBUTION

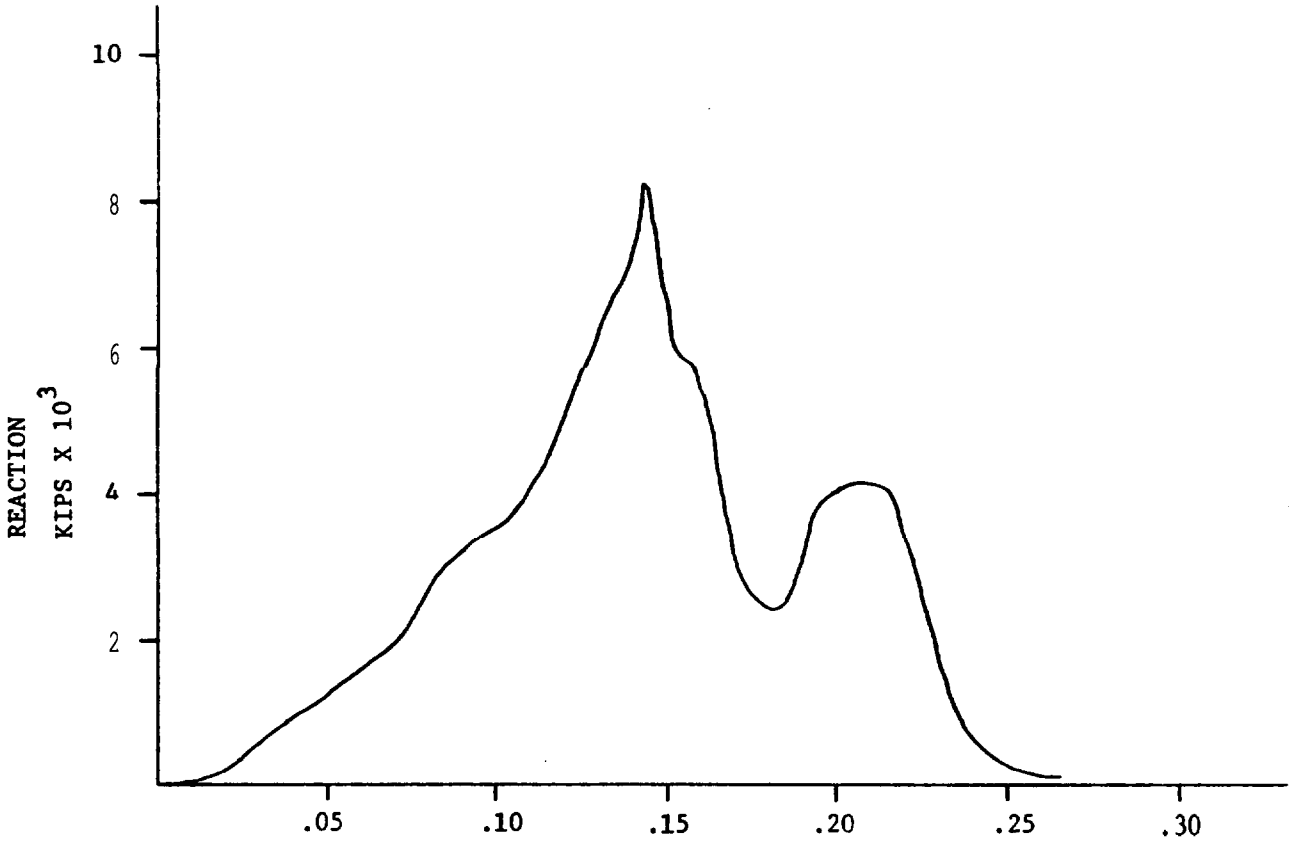

FIGURE 3

REACTION-TIME RELATIONSHIP

$P_c/5$ — — — —

$5P_c$ —·—·—·—·—

P_c denotes the scale crushing load used in the calculation. $P_c/5$ and $P_c \times 5$ denotes that one-fifth and five time the crushing load were used, respectively.

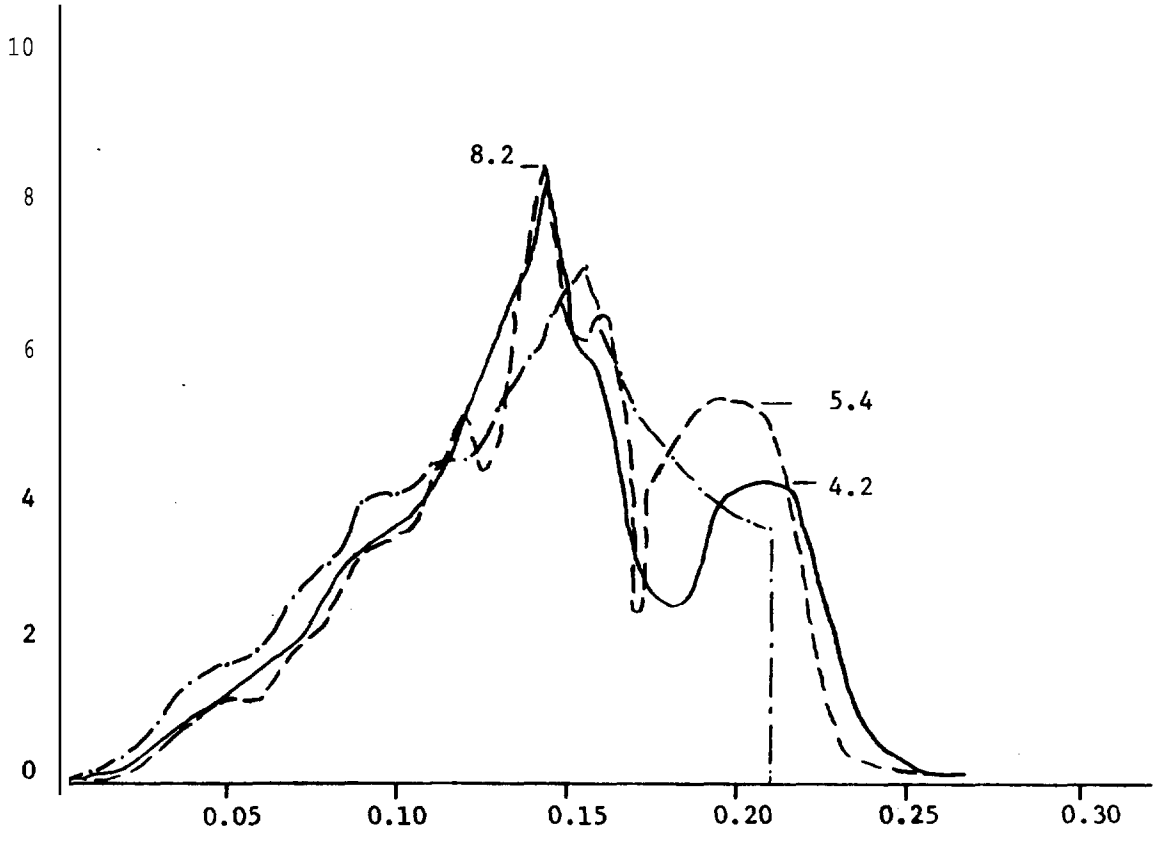

FIGURE 4

Reaction-Time Relationship for FB-111 with impact velocities of 200 mph.

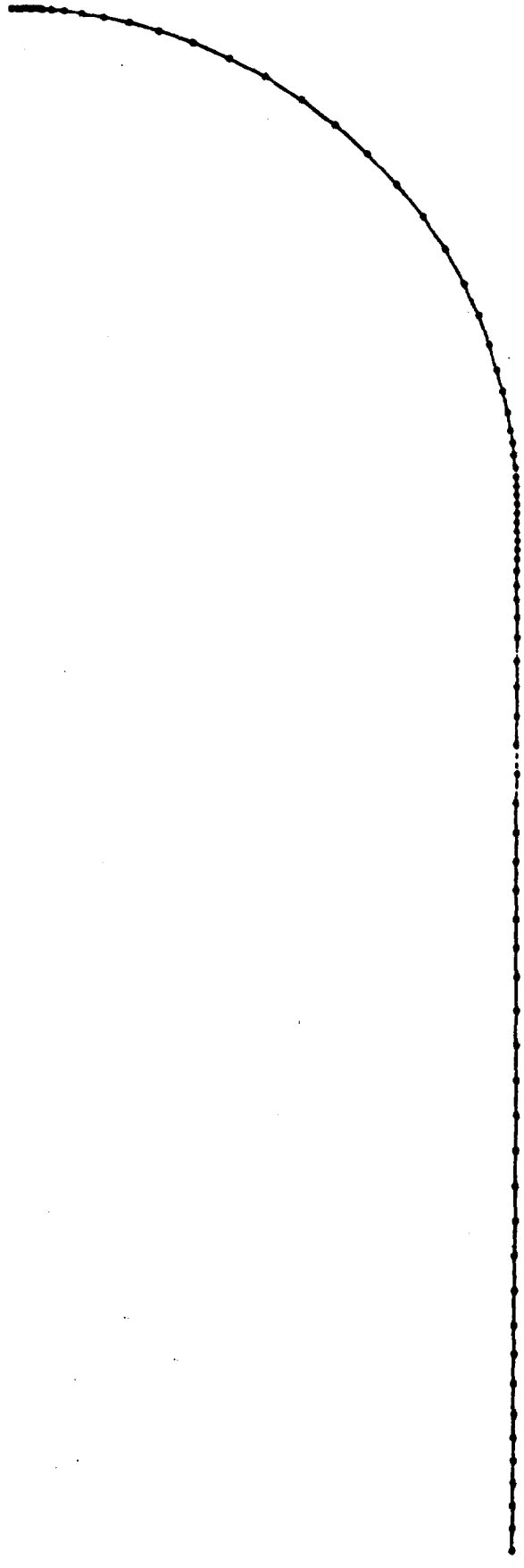

FIGURE 5
FINITE ELEMENT MODEL

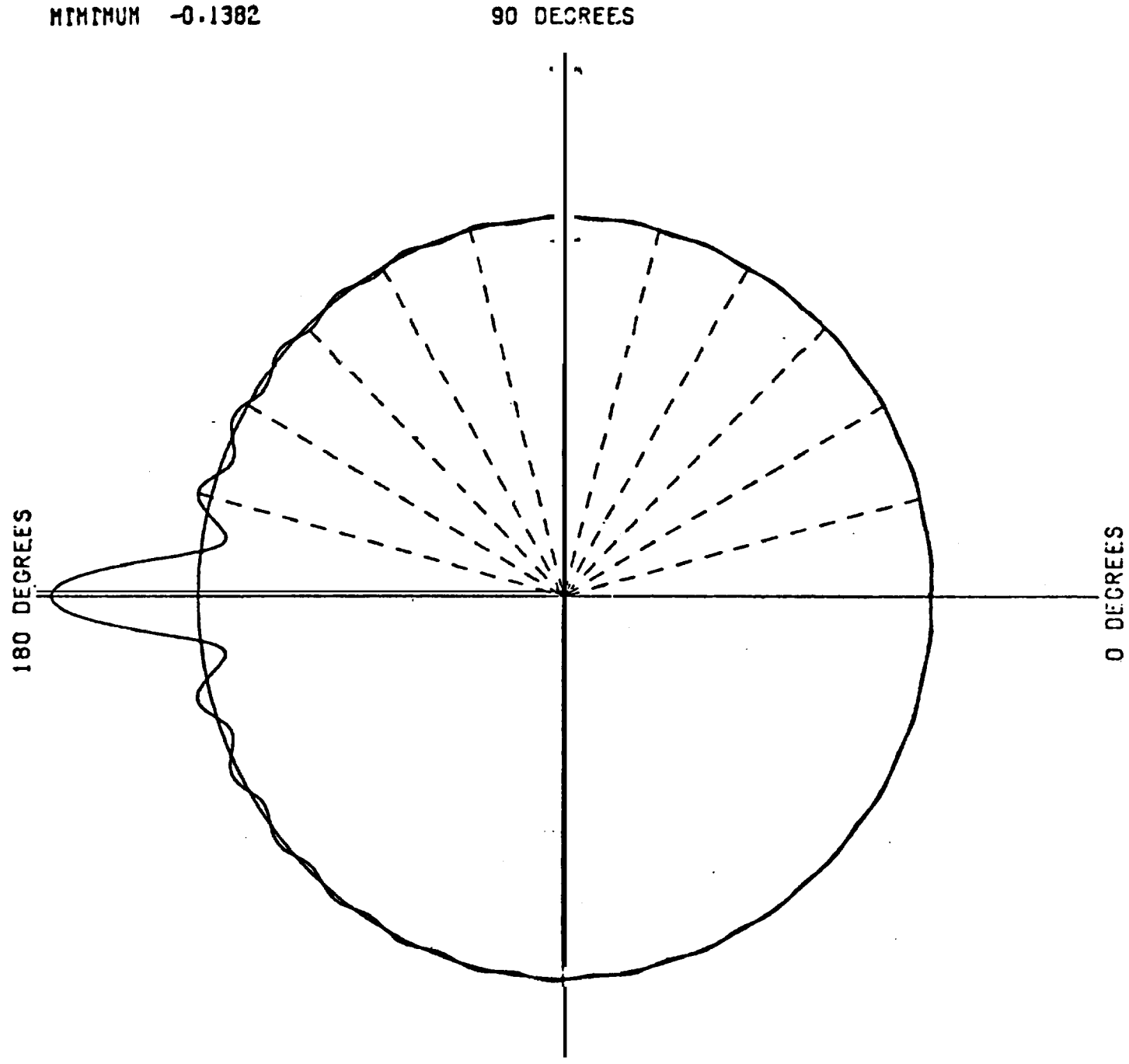

FIGURE.6
FOURIER SERIES REPRESENTATION OF SPRINGLINE LOADING

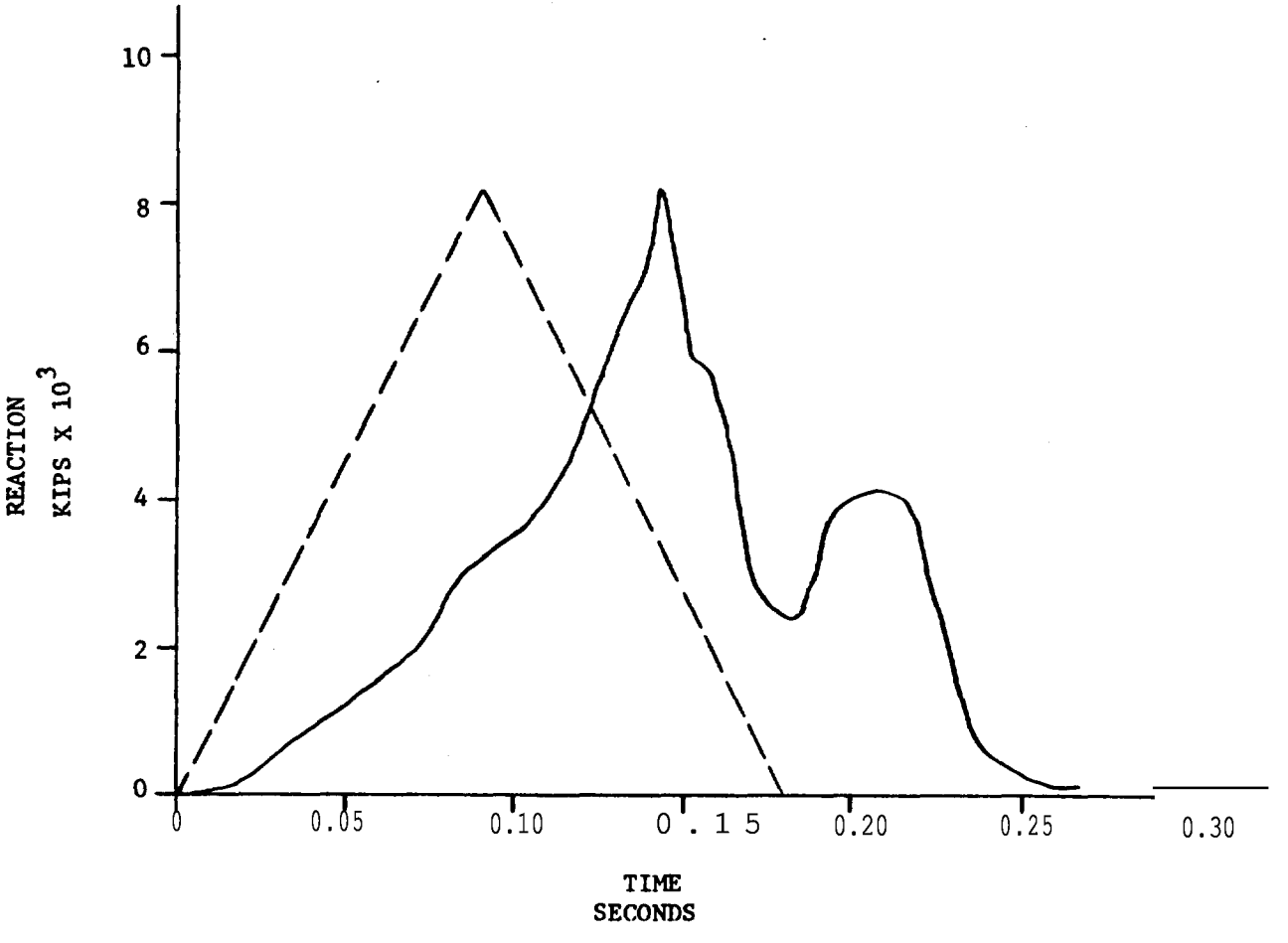

FIGURE 7 ACTUAL AND IDEAL REACTION TIME RELATIONSHIP

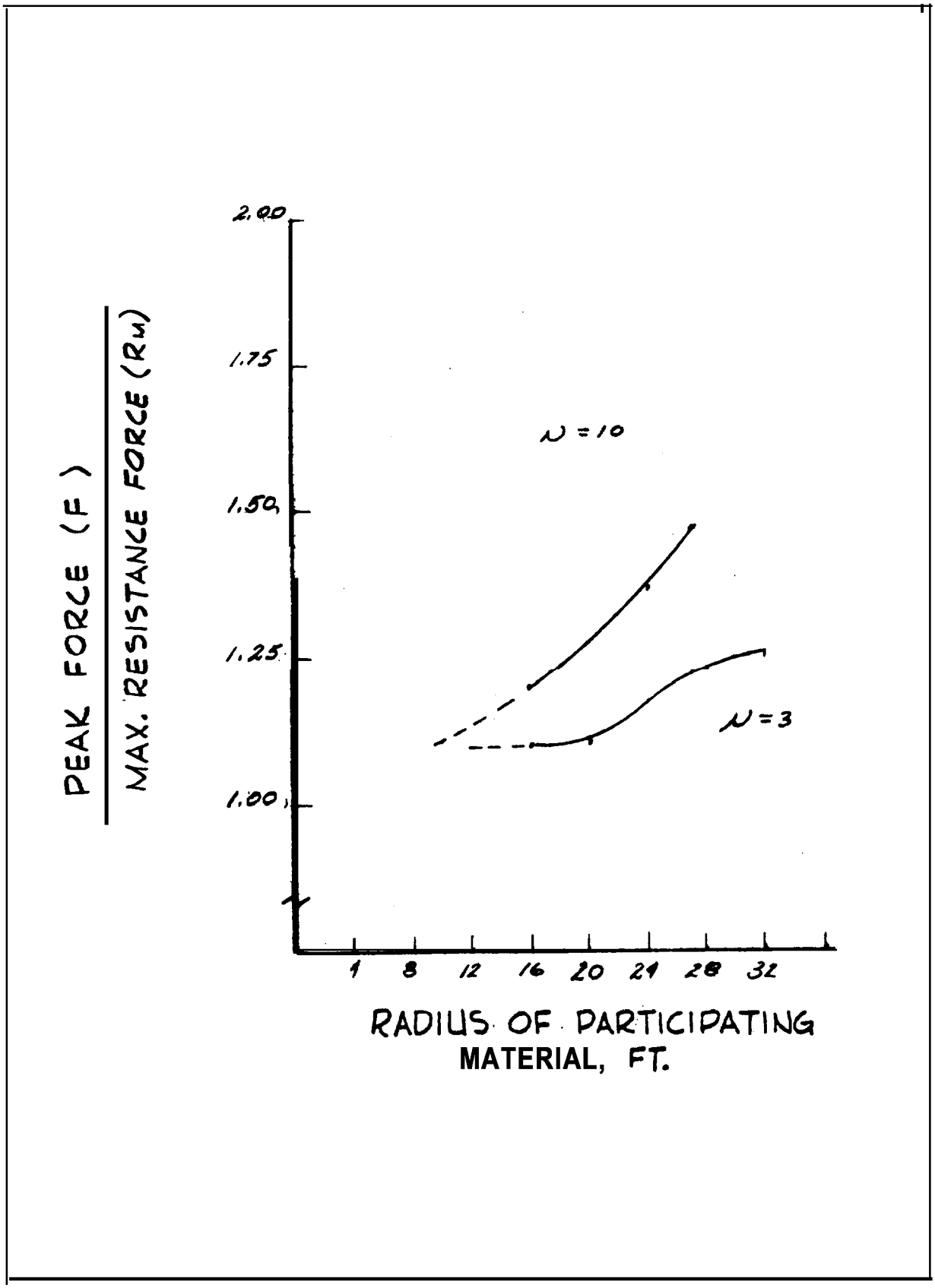

FIGURE 8
ALLOWABLE MAXIMUM FORCE, MAXIMUM RESISTANCE RATIO FOR VARIOUS DUCTILITY RATIOS AND PARTICIPATION TARGET MATERIAL RADII

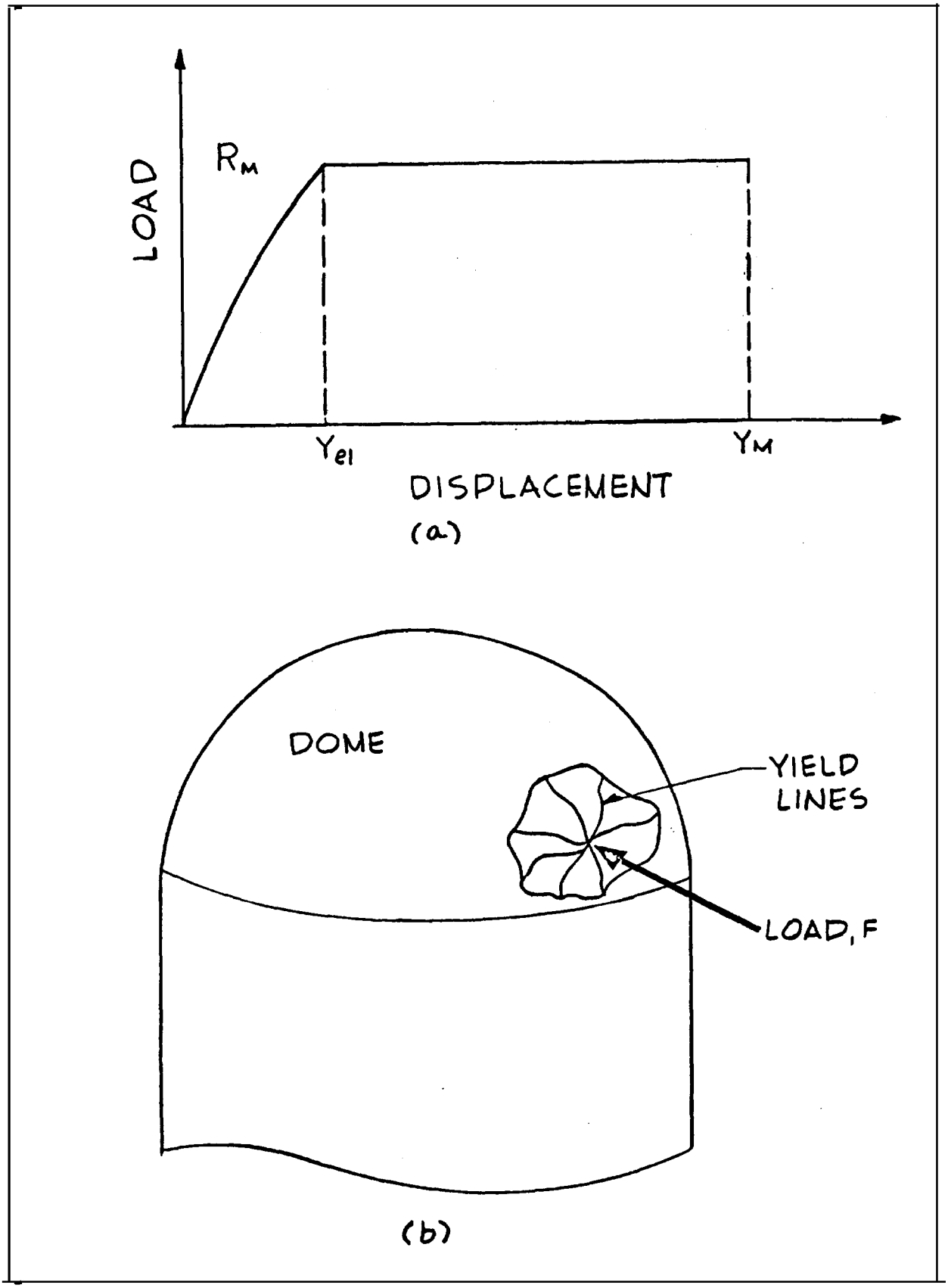

FIGURE 9

LOAD, DISPLACEMENT BEHAVIOR AND **POSTULATED YEILD** LINE CONFIGURATION

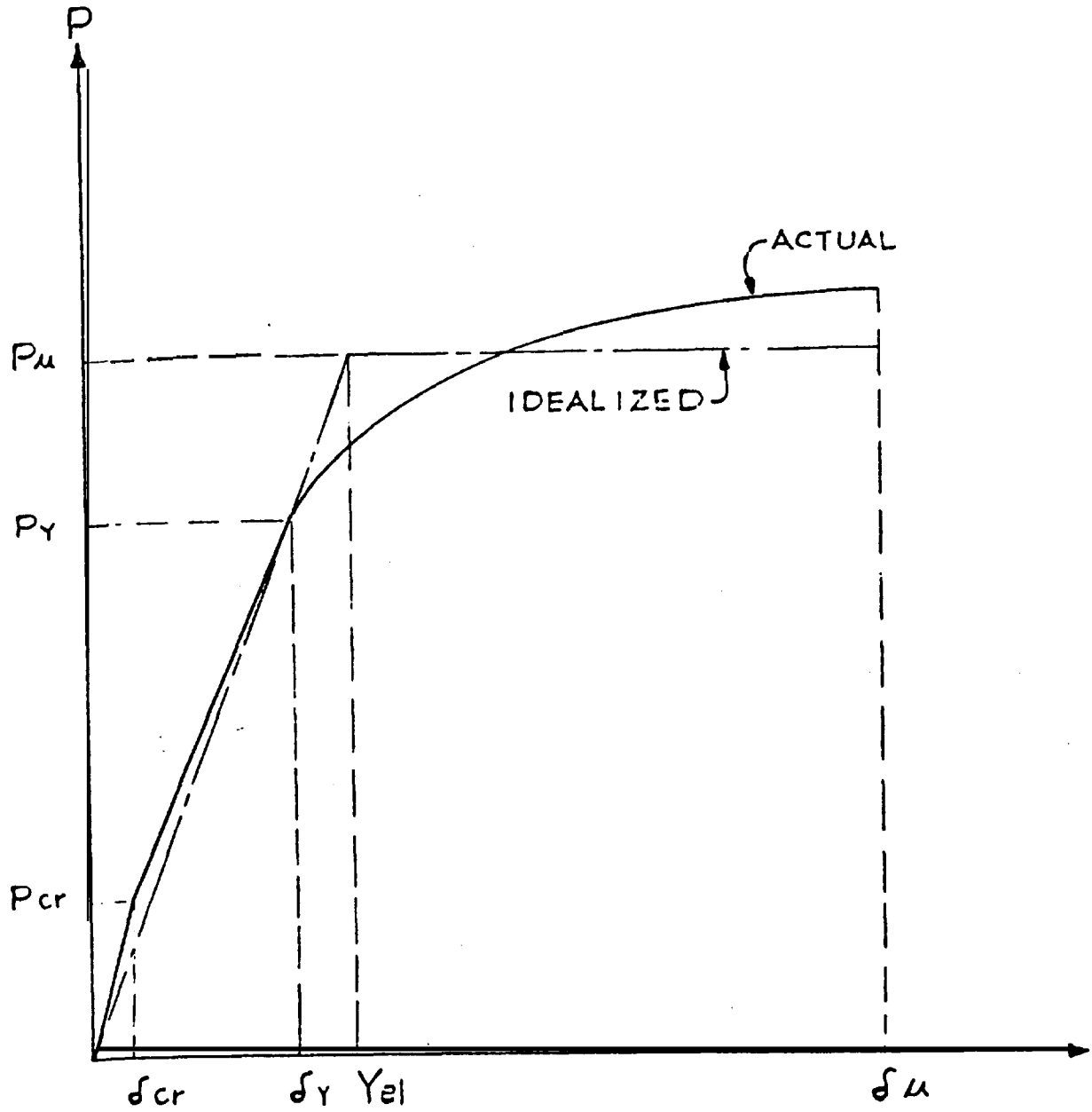

FIGURE 10.
LOAD-DISPLACEMENT CURVE FOR REINFORCED CONCRETE

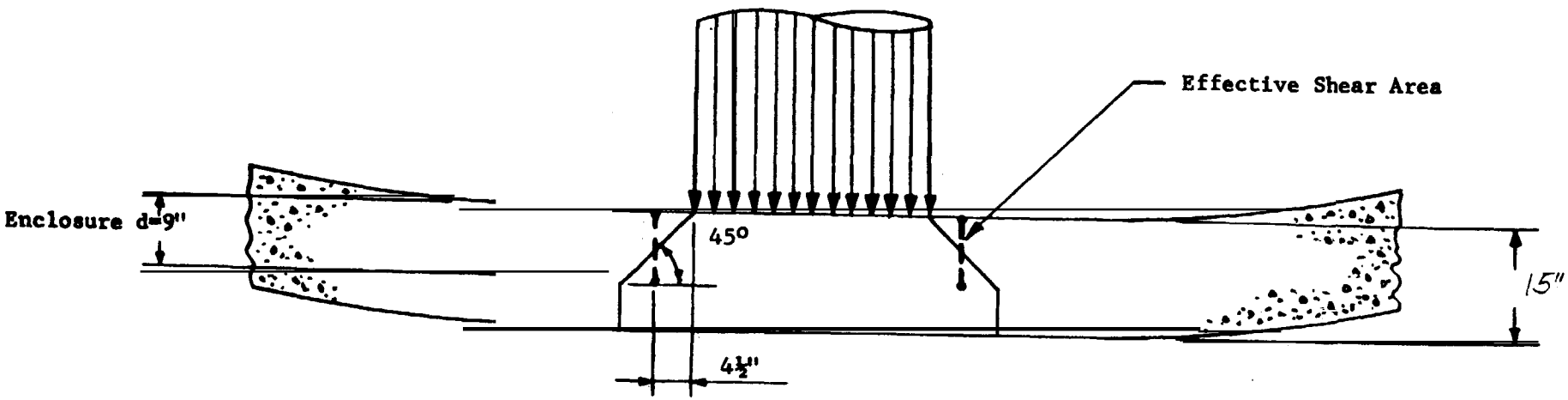

Figure 11, SCHEMATIC FOR EFFECTIVE SHEAR AREA - ENCLOSURE

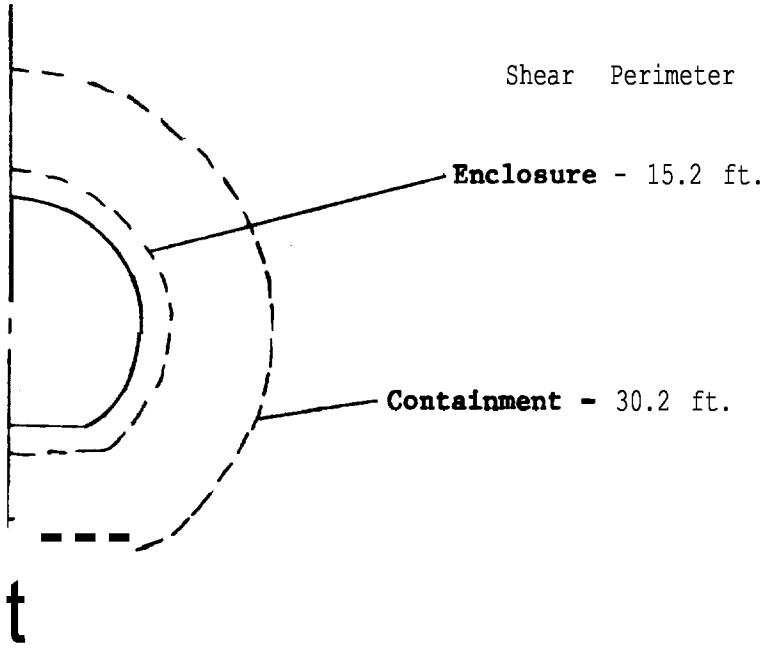

Figure 13, Impact Area and Shear Perimeter at 8.5 Feet From Nose

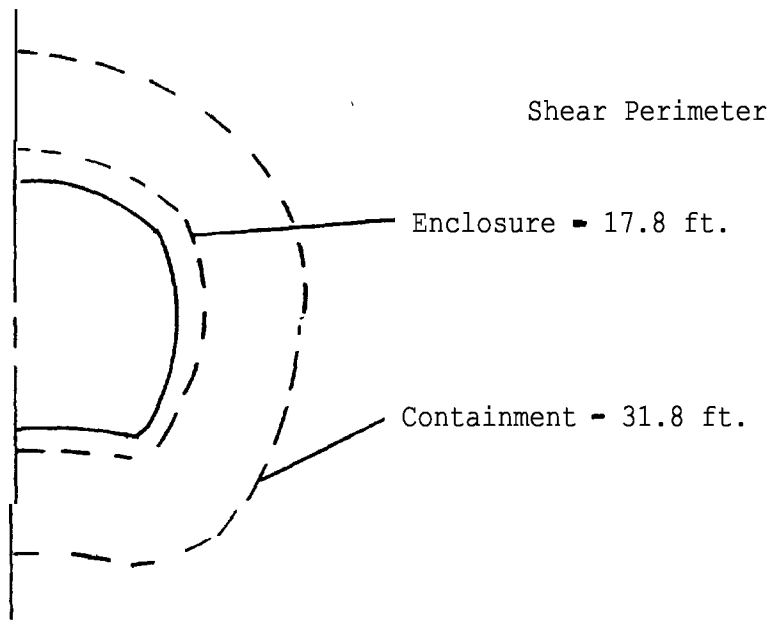

Figure 14, Impact Area and Shear Perimeter at 9.9 feet From Nose

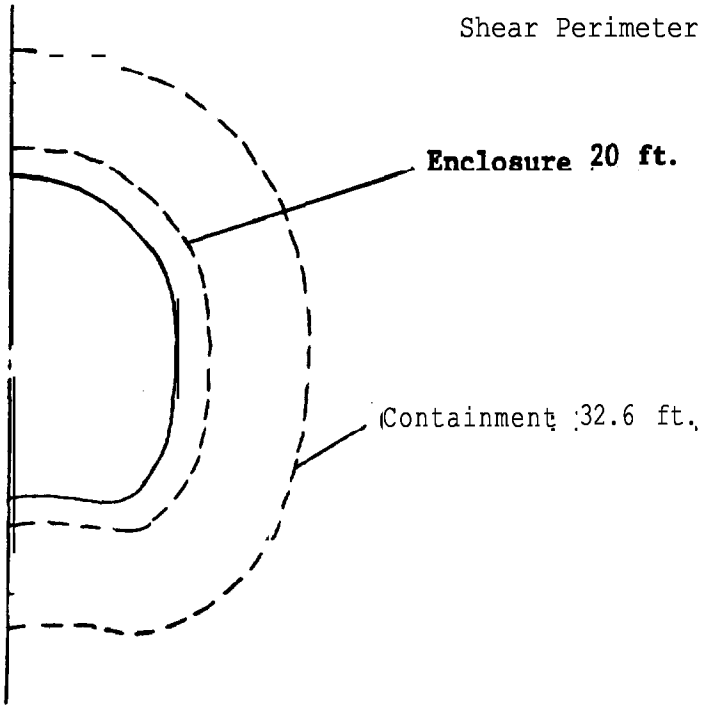

Figure 15 Impact Area and Shear Perimeter at 15 Feet From Nose

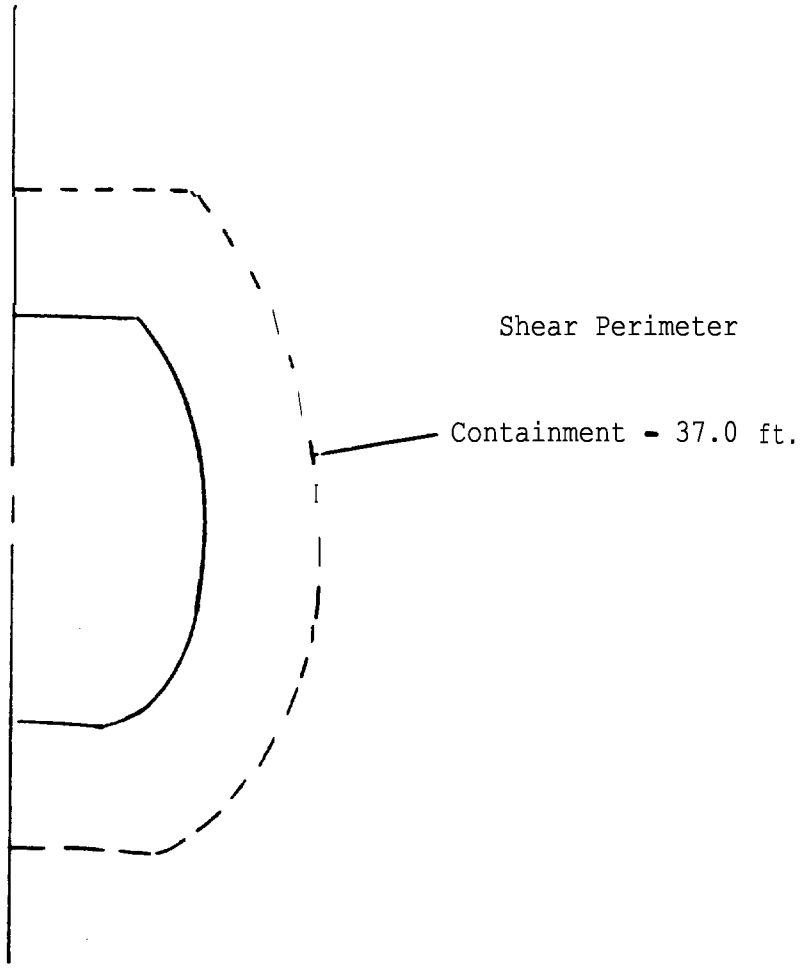

Figure 16, Impact Area and Shear Perimeter at 19.0 Feet From Nose

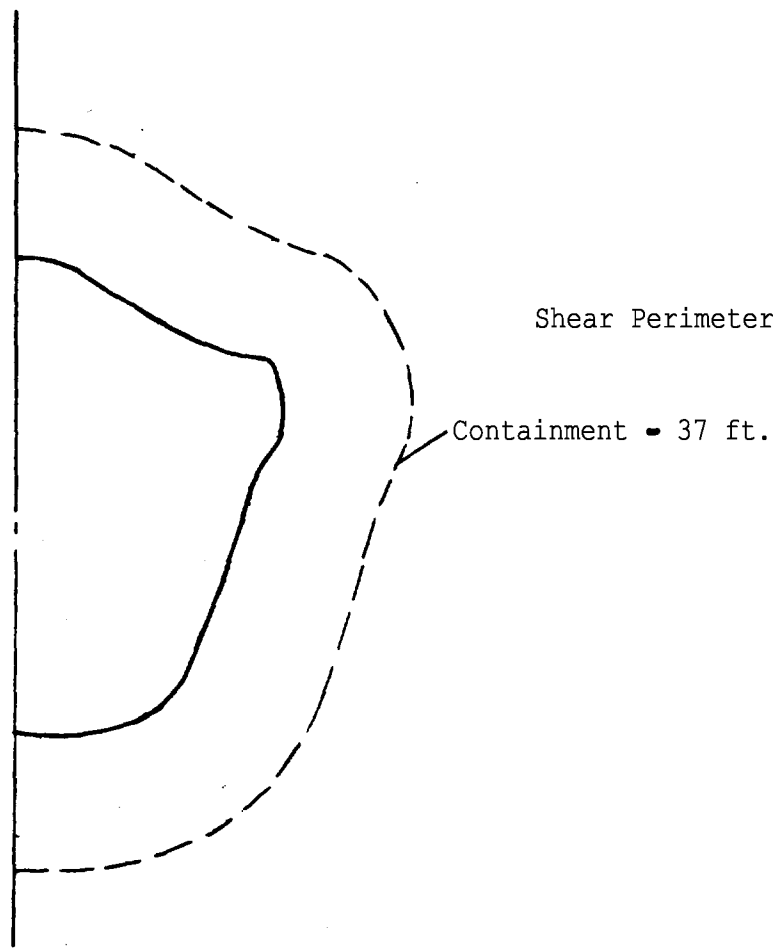

Figure 17, Impact Area and Shear Perimeter at 27 Feet From Nose

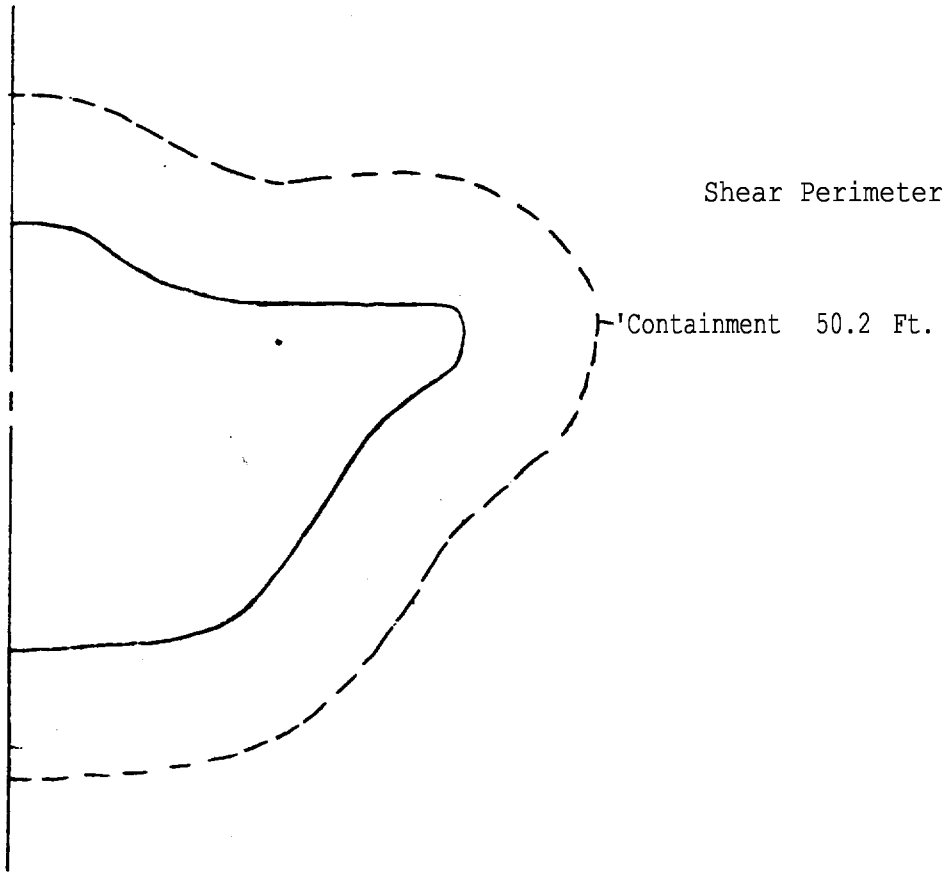

Figure 18 Impact Area and Shear Perimeter at 35 Feet from Nose

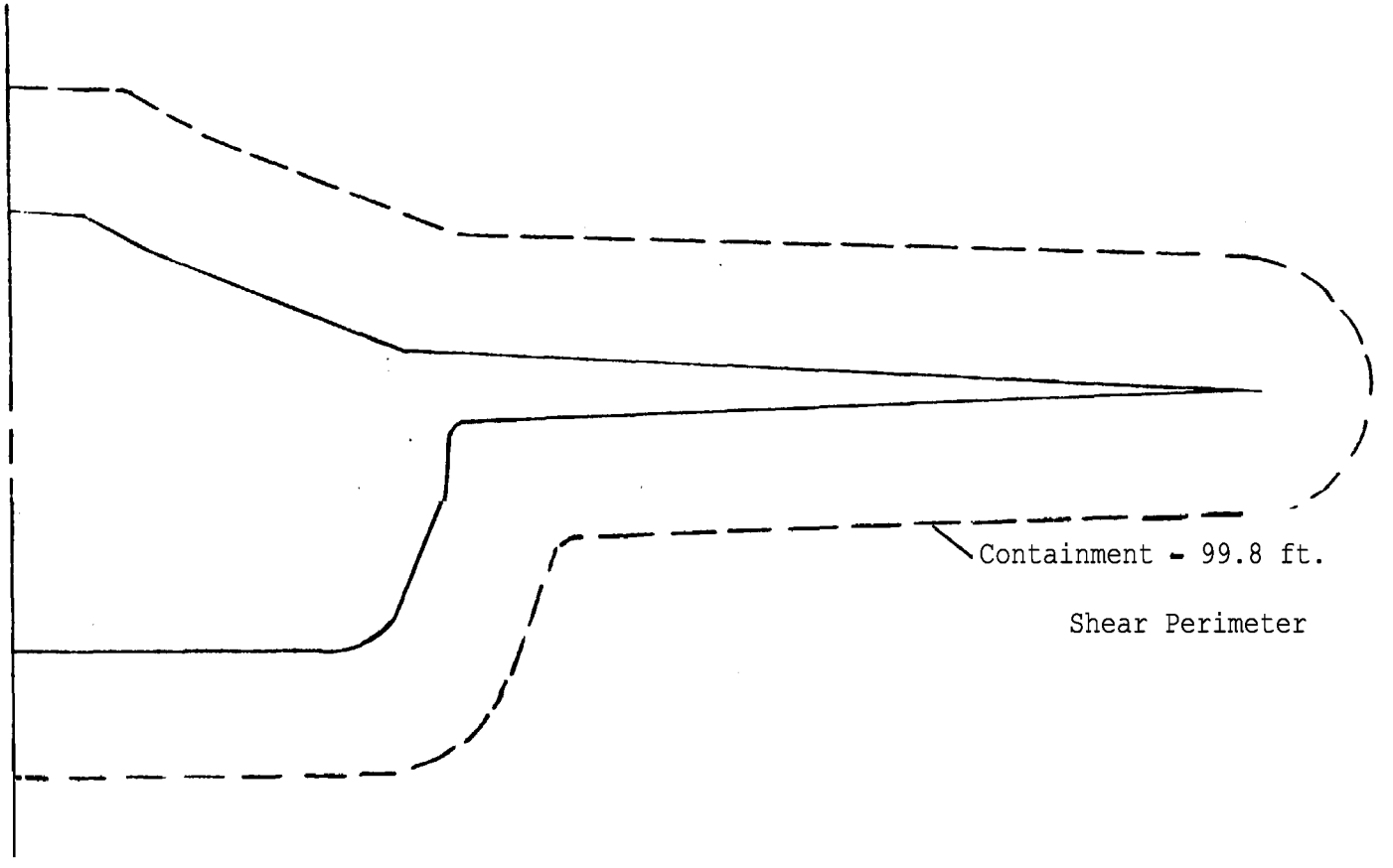

Figure **19,** Impact Area and Shear Perimeter at 41.0 Feet From Nose

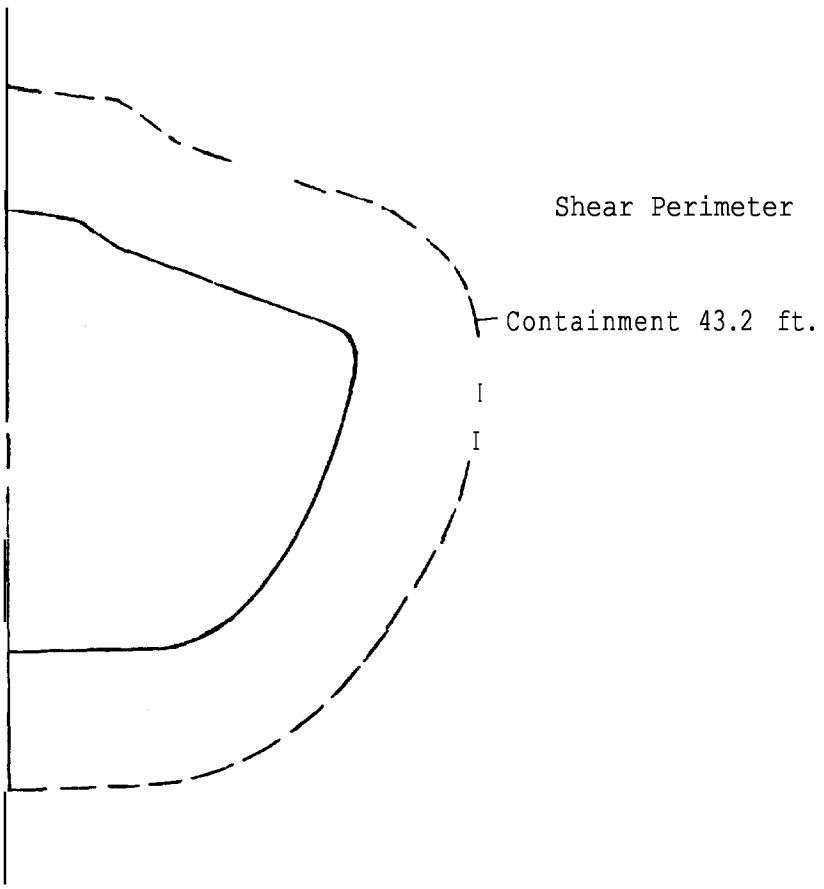

Figure 20, Impact Area and Shear Perimeter at 50.0 Feet From Nose

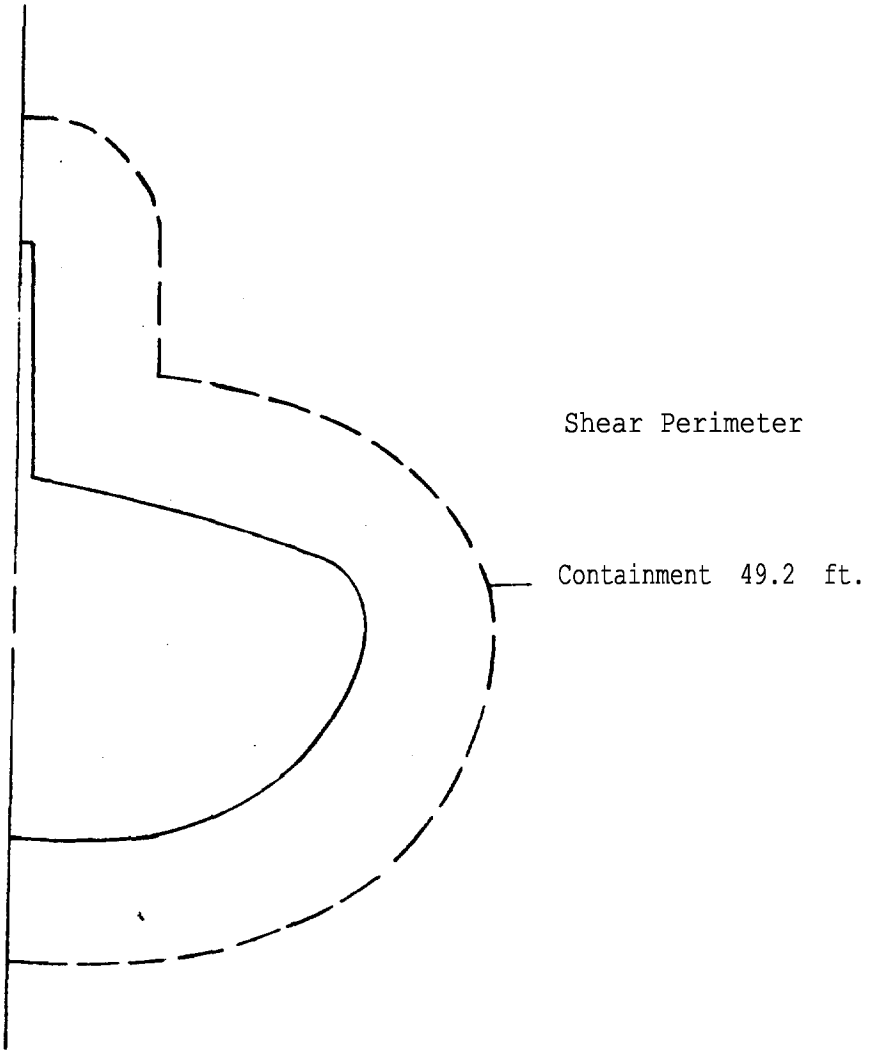

Figure 21 Impact Area and Shear Perimeter at 58.0 Feet From Nose

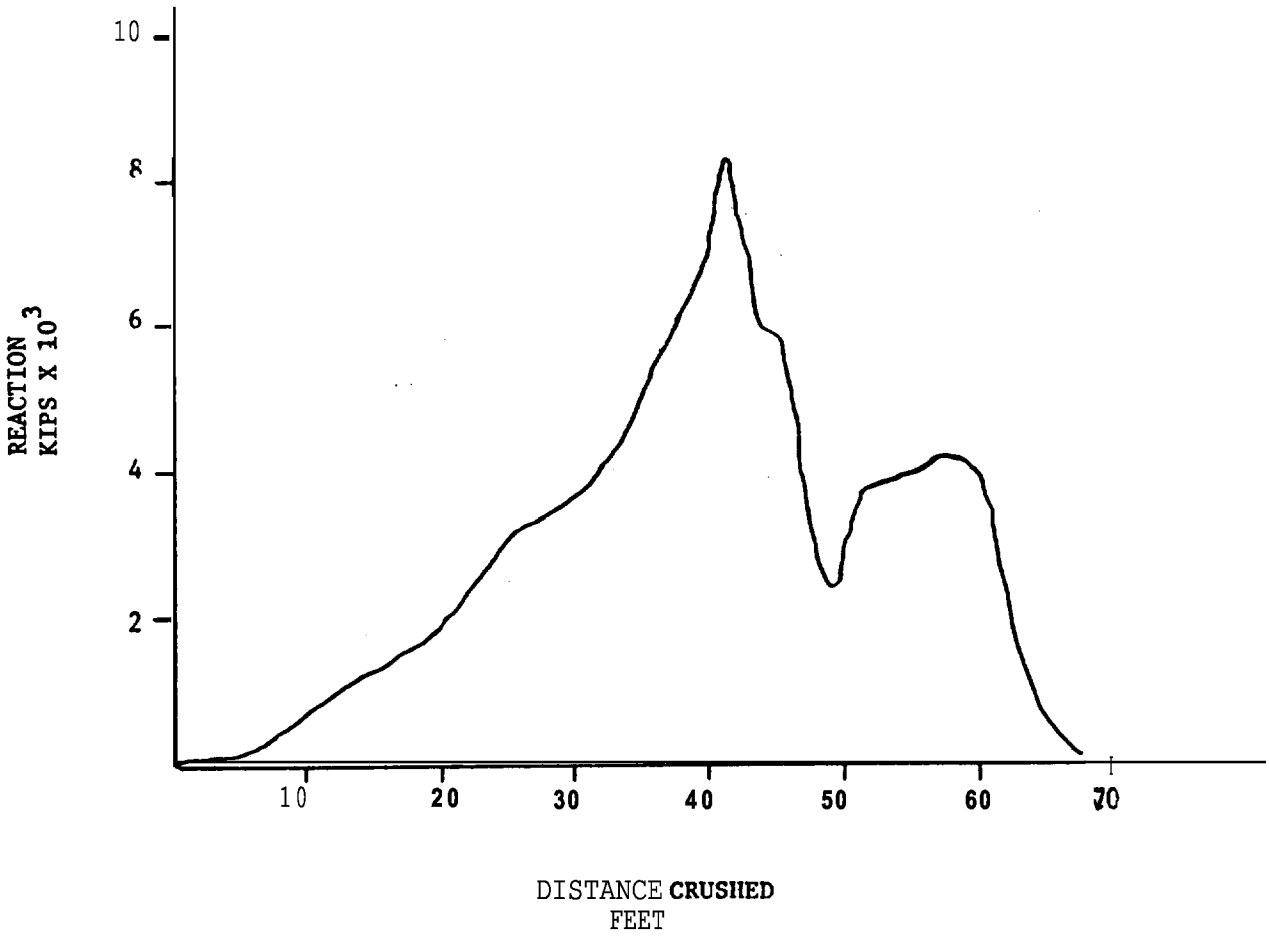

FIGURE 22, REACTION-CRUSHING LOCATION RELATIONSHIP

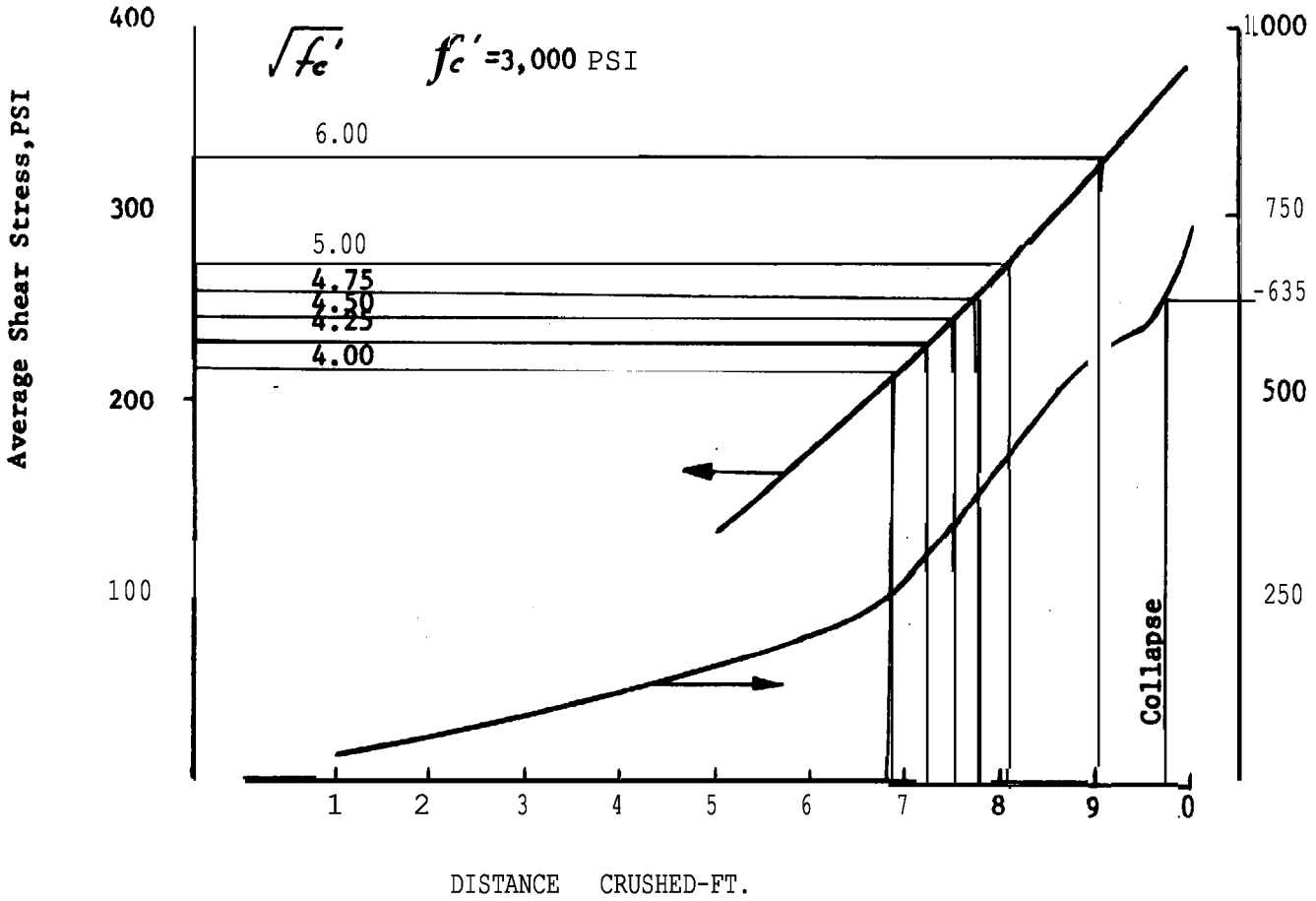

SB 1 & 2
FSAR

Figure 23 Average Shear Stress-Distance Crushed and Reaction Distance Crushed Relationship for the Enclosure Building.

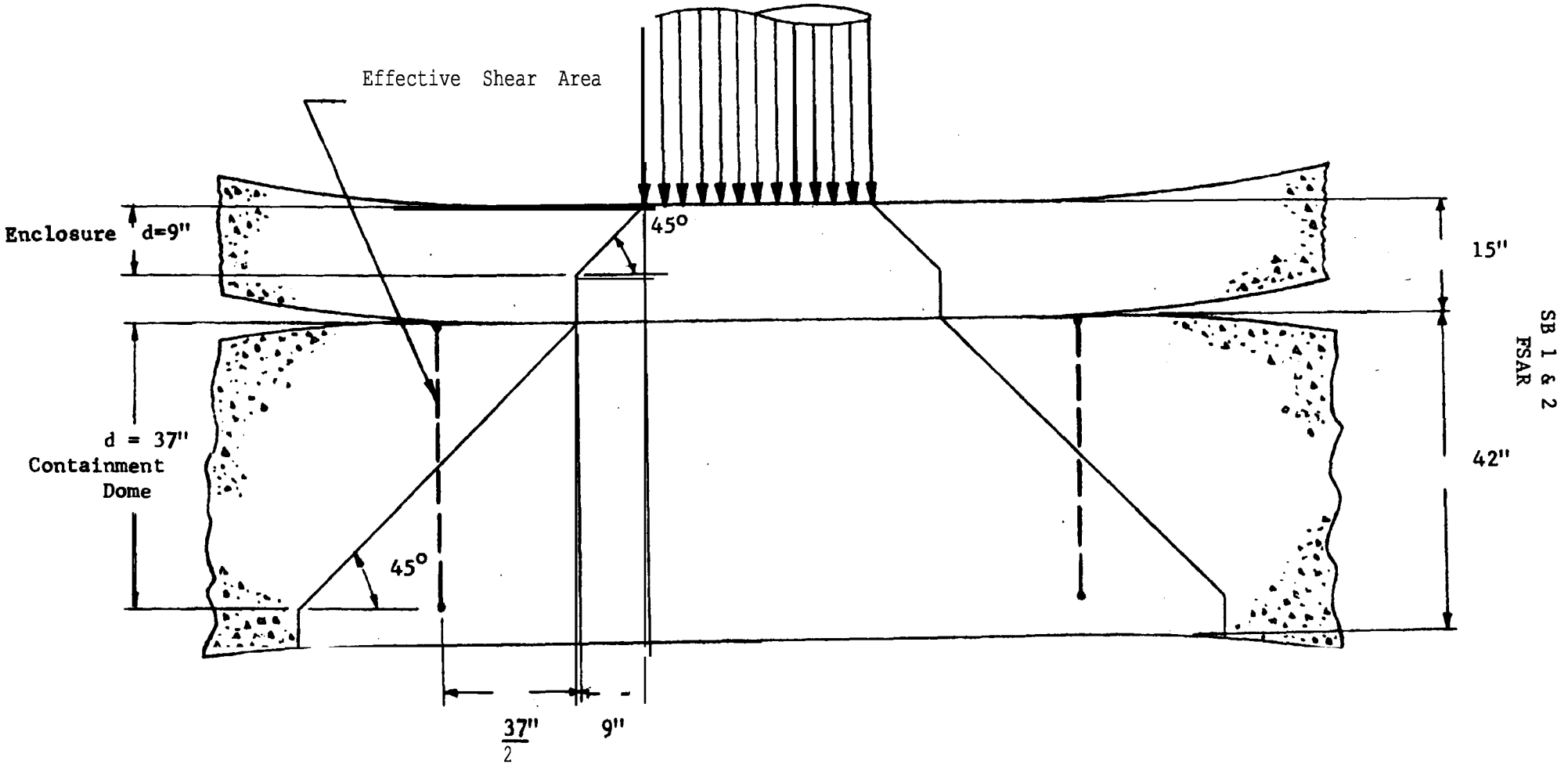

FIGURE 24 SCHEMATIC FOR EFFECTIVE SHEAR AREA - CONTAINMENT

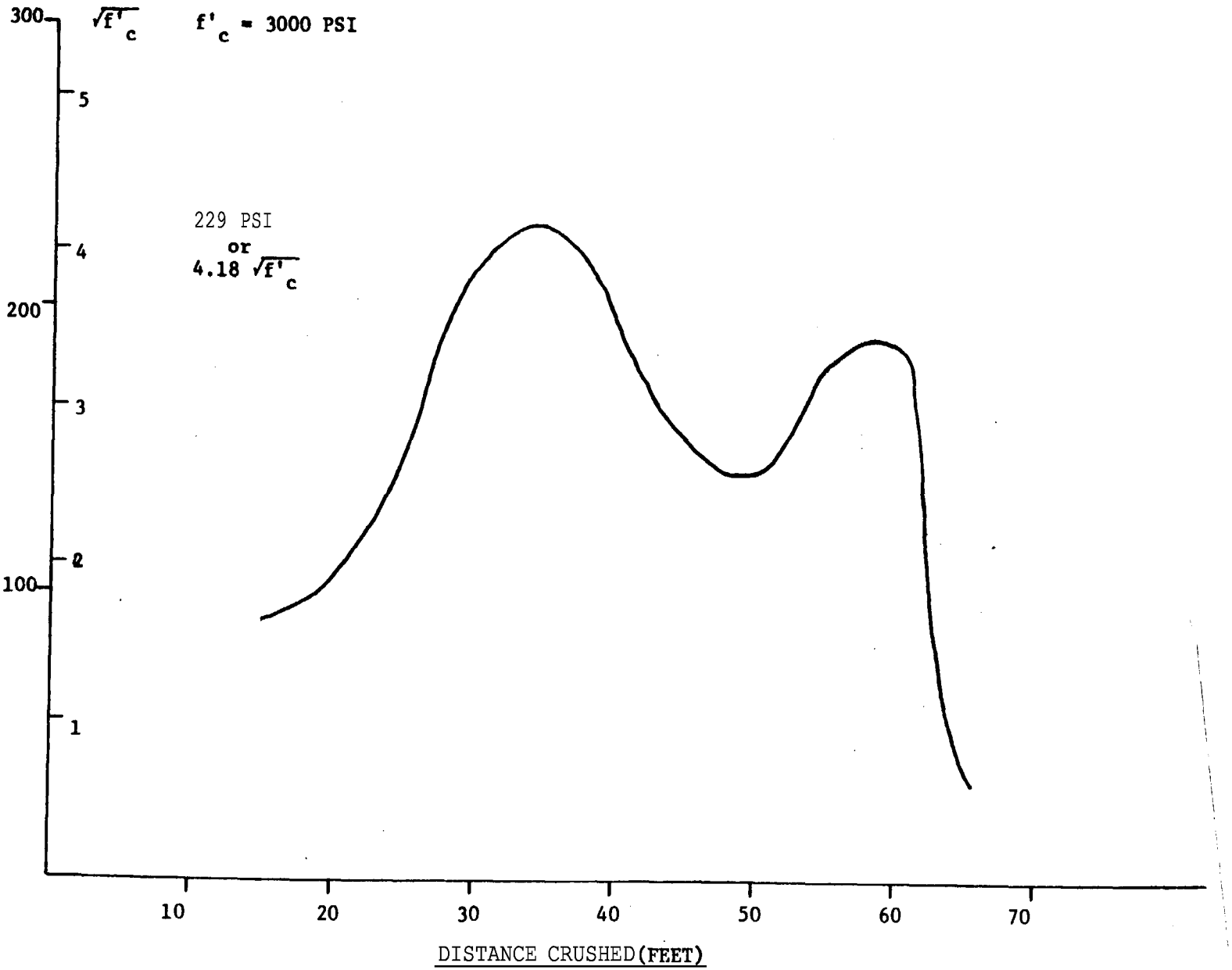

Figure 25 AVERAGE SHEAR STRESS-DISTANCE CRUSHED RELATIONSHIP FOR CONTAINMENT

2.0 FIRE HAZARD ANALYSIS OF SEABROOK STATION CONTAINMENT FOR AIRCRAFT IMPACT

A highly unlikely chain of adverse events is postulated in the following manner:

An FB-111 with a weight of 81,800 lbs and initial speed of 200 mph impacts on one of the two double containment complexes of the Seabrook plant. The enclosure building deforms locally under the initial impact,and the local deformation continues with little to no perforation until the enclosure building comes into contact with the containment building. This fact, plus the fact that if any penetration should occur it would be only the nose of the aircraft, will preclude the spilling of significant amounts of fuel into the annulus space. The annulus space contains no equipment,and all penetrations both mechanical and electrical are isolated from missiles and fuel by reinforced concrete slabs, The enclosure building acts as a barrier and directs the spilled fuel to the exterior area near the enclosure building. The following effects were then studied:

(1) Possible production of combustible vapor, its prompt ignition and the ensuing pressure pulse, and the possibility that the combustible vapor may be sucked into the plant areas and be cause for delayed ignition or toxic atmosphere in habitability systems.

(2) The fuel spilled and its transport to various areas of the plant. An ignition is then postulated, and the effect of the ensuing fire studied in order to evaluate

the safe shutdown capability of the plant.

(3) The effect of smoke and/or toxic gases as may be generated by the fire, with particular reference to control room habitability.

(4) The effects as detailed in (1) and (3) for all smaller aircraft.

2.1 COMBUSTIBLE VAPOR PRODUCTION

The FB-111 carries approximately 32,000 lbs of type JP-4 fuel. As indicated in Reference 1, the process of combustible vapor production is as follows: the crashing aircraft drags along the ground in a relatively slow deceleration (0.4 g) which lasts for a 'long' time (20 **secs**), and the fuel issuing from the wing after some postulated leakage mechanism is atomized to mist by the air as a result of its velocity relative to air. For the direct impact considered here, the decelerations are very high (peak value of 29 g) and of very 'short' duration (0.3 sec.). The atomizing process under these conditions is not significant. It is, therefore, concluded that the combustible vapor production and the associated hazards can be considered to be mitigated.

2.2 FIRE ANALYSIS

Various spill mechanisms are postulated either on the roofs or on the ground adjacent to the containment structure:

(a) The various roof areas adjacent to the containment enclosure with their elevation approximate areas, etc., are detailed in Table 2-1. As stated in PSAR Section 2.4, most of these roofs have parapets, and the roof drainage systems are designed to drain at least 3 inches per hour rain. It is

noted further that 1 inch of fuel takes 10 minutes to burn.[2] Using the minimum area in Table 2-1, and a catastrophic instantaneous mode of fuel release, the maximum expected duration of the fire is 17.9 minutes.

(b) For ground areas adjacent to the containment, there is approximately 1.5 acres of land, the total drainage of which is approximately 6 cfs. The spreading of the fuel over this area and the adequate drainage would result in a film fire with width comparable to the roughness of the pavement, e.g., 1/16 inch. The resulting fire would last only for 1 minute at the most.

(c) The mechanism of fire propagation was examined. No flammable material is normally expected to be present next to the containment which can serve as the propagator of the fire. The range of the fire has very conservatively estimated to be 200 ft. from its point of origin.

(d) Smoke is postulated to be traveling from this centre fire location carried by the wind. Its effect on the habitability systems was then studied.

(e) The possible hazard of fuel getting into the PAB Building through the vent stack is considered remote due to the following reasons:

a) The mechanism is improbable.

b) The entering fuel will be drained off at the base of the vertical stack, just as rainwater would be.

(f) The possible hazard of fuel getting into the main steam line tunnels through the side vent openings is considered not probable since the vent openings are above grade.

2.3 EVALUATION OF VARIOUS SAFETY RELATED AREAS

The various intake points to the safety related areas and their descriptions are detailed in Table 2-2, including the missile shields when applicable, under the accident conditions detailed in Subsection 2.3. All buildings other than the control room and the PAB residual heat removal area are either not needed for safe shutdown or are redundant. However, the conservative analysis below includes the reaction of these areas to the postulated fire.

(a) Control Room

There is no mechanism for the fire to endanger the habitability of the control room, since the split intake vents are at a distance of at least 300 ft. from the containment; therefore, it is beyond the reach of the direct fire. However, in the remote event that the fire finds its way into the intake structure, the temperature and smoke sensors will sense it and the intake opening will be closed. Under these conditions, the other intake will be used for ventilating the control rooms.

(b) Primary Auxiliary Building (PAB)

The air intake is located on the east wall of the primary auxiliary building at an elevation of 56'-0". The area in front of the intake has the containment enclosure roof elevation of 53'-0" and the east wall of the PAB faces the containment and the fuel storage building. There may be a small fire lasting 12.5 minutes at most on the roof of the containment enclosure area, a part of which may be injected into the PAB air intake, as its height is 3 ft. above the

roof of containment enclosure area. The inside of the PAB has roll-type filters after the intake and heating coil panels after the filter. Therefore, the flame and the hot gases would have to penetrate the filter and the coils before reaching the fans.

As indicated in Subsection 2.2, the roof surface of the containment enclosure area will be finished smooth and with proper drainage to drain off the spilled fuel quickly. Smoke and heat sensors will be located at the air inlet so that on a signal from them the operator can stop the fans.

(c) Diesel Generator Building

The diesel generator building intakes are on opposite sides of the building and are located at least 180 ft. from the containment structures. It is considered improbable that the spilled fuel will find its way underneath one of these intakes. Furthermore, the intakes are 28.5' above grade level, and it is unlikely that the fire will rise to that height. In addition, one of the intakes is shielded by the diesel generator building and it is thus not considered credible that the fire could reach that intake. Although it may be postulated that the hot gas from the direct intake point may cause momentary oxygen starvation of one diesel generator, the shielded intake will ensure the integrity of other diesel generator and of one train.

(d) Service Water Building

The intake for the service water building is approximately 280 ft. from the containment'and should be out of reach of the postulated fire. Furthermore, the air intake is located

in the east wall of the building. Consequently, the building serves as a shield for the spilled fuel flow. Additionally, there is a missile shield in front of the structure, which should inhibit any possible fuel flow and subsequent fire. The fire effects are, therefore, considered minimal. However, a minute amount of hot gas may enter the facility, but since the pumps are located at the west end of the building, it will not critically threaten their operation due to rise of temperature.

(e) Vent Stack

The vent stack is not a safety related item and, as indicated in Subsection 2.2, it does not furnish a significant pathway for the fuel to get into the primary auxiliary building. This mechanism of fire propagation is, therefore, considered incredible.

(f) Cable Spreading, Battery Room, Switch Gear Room and Cable Tunnel

The air intake for cable spreading, battery room, switch gear room and cable tunnel areas is through the mechanical equipment room of the diesel generator building, and the various safety aspects discussed for the diesel generator room hold for this case.

2.4 HAZARDS FROM SMALLER AIRCRAFT

The smaller plane crashes were examined for the various areas, as detailed in Subsections 2.2 and 2.3. The fuel in general may be JP-1, kerosene and JP-4. Since the fuel carrying capacity for all these planes is smaller than that of FB-111, and their burning temperatures are of the same order of magnitude, it was concluded that the effect would be enveloped by those in the case of FB-111.

2.5 CONCLUSIONS

In view of the results in Subsections 2.2 and 2.3, it was concluded that the hazard to Seabrook Station from direct fire after the postulated crash of an FB-111 or smaller aircrafts on the containment represents only very minimal potential hazard to the plant. The present design of the plant has inherent safety features so that the consequence of this minimal hazard is mitigated.

2.6 REFERENCES FOR SECTION 2

1. Appraisal of Fire Effects From Aircraft Crash at Zion Power Reactor Facility, I. Irving Pinkel, Consultant, Atomic Energy Commission, July 17, 1972.

2. Flammability Characteristics of Combustible *Gases* and Vapors, Bulletin 627, U. S. Bureau of Mines, 1965, Michael Zabetakis.

TABLE 2-1
ROOF DESCRIPTIONS

BUILDINGS	ROOF AREA (SQ. FT.)	ELEVATION	REMARKS
CONTAINMENT ENCLOSURE **AREA**	4,100	53' - 0"	WITH PARAPET
EMERGENCY FEED WATER PUMP BLDG.	3,000	47' - 0"	WITH PARAPET
FUEL STORAGE BUILDING	9,200	84' - 0"	WITH PARAPET
PRIMARY AUXILIARY BUILDING	8,144	81' - 0"	WITH PARAPET
PAB Filter Room	2,856	108' - 0"	WITH PARAPET

NOTE: GRADE ELEVATION 20' - 0"

TABLE 2-2

VENTILATION SYSTEM DESCRIPTIONS OF THE BUILDING SURROUNDING THE CONTAINMENT

SHEET 1 OF 2

BUILDING	BUILDING SURFACE FACING THE CONT.	LOCATIONS OF THE INTAKES			TYPE OF SHIELDING	REMARKS
		SURFACE	PATHWAY FROM CONT. WALL	ELEVATION		
Diesel Gen.	South wall	South Wall	200 ft.	28.5 ft. above gr.	Other Bldg. at 40' dist.	Ventilation & Combustion air; not necessary for safe shutdown.
		North Wall	240 ft. (thru roof)	28.5 ft. above gr.	Other Bldg. at 40' dist.	
PAB	East wall	East Wall	20 ft.	3 ft. above adjacent roof.	Shielded by the Cont. & F. Stg. Bldg.	Normal ventilation air; only RHR pump area safe shutdown related.
		North Wall	95 ft. (thru roof)	29 ft. above gr.	2' thick conc. missile shield.	Ventilation air to safety related primary component cooling water pump area and Boron injection pump area.
Emergency Feedwater Pump Bldg.	South Wall	North Wall	30 ft. (thru roof)	18 ft. above gr.	2' thick concrete missile shield	Ventilation air to the emergency feedwater pump area.

TABLE 2-2 (CONT.)
SHEET 1 OF 2

BUILDING	BUILDING SURFACE FACING THE CONT.	LOCATION OF THE INTAKES			TYPE OF SHIELDING	REMARKS
		SURFACE	PATHWAY FROM CONT. WALL	ELEVATION		
Service Water Pump House	West Wall	East Wall	290 ft. (t h r u roof)	45 ft. above gr.	2' thick conc. missile shield.	Ventilation air to the service water pump house.
		West Wall	180 ft.	13.5 ft. above gr.	2' thick conc. missile shield.	Air intake to the electrical areas.
Control Room & Computer Room	South 6 East Walls	Remote Intake Ports	300 ft. (at least)	At gr. level	Covered with grating.	Ventilation air to the habitable areas of the control and computer room.

APPENDIX 2Q EAB AND LPZ SHORT TERM ACCIDENT DIFFUSION ESTIMATES FOR AST

2Q.1 OBJECTIVE

Conservative values of atmospheric diffusion at the site boundary (EAB) and the low population zone (LPZ) were calculated for appropriate time periods using meteorological data collected onsite during the time period 1998 through 2002.

2Q.2 METHODOLOGY

The methodology used for this calculation is consistent with Regulatory Guide 1.145 as implemented by the PAVAN computer code (Reference 2). Using joint frequency distributions of wind direction and wind speed by atmospheric stability, the PAVAN computer code provides relative air concentration (CHI/Q) values as functions of direction for various time periods at the site boundary and LPZ. Three procedures for calculation of CHI/Qs are utilized for the site boundary and LPZ; a direction-dependent approach, a direction-independent approach, and an overall site CHI/Q approach. The CHI/Q calculations are based on the theory that material released to the atmosphere will be normally distributed (Gaussian) about the plume centerline. A straight-line trajectory is assumed between the point of release and all distances for which CHI/Q values are calculated.

The theory and implementing equations employed by the PAVAN computer code are documented in Reference 2.

2Q.3 CALCULATIONS/PAVAN COMPUTER CODE INPUT DATA

The boundary distance used in each of the 16 downwind directions from the site was set to 914 m. The LPZ boundary distance was set to 2,011 m.

All of the releases were considered ground level releases because the highest possible release elevation is from the plant stack at 185 ft above plant grade. From Section 1.3.2 to Reference 1, a release is only considered a stack release if the release point is at a level higher than two and one-half times the height of adjacent solid structures. For the Seabrook plant, the elevation of the top of the containment is 199.25 ft. Therefore, the highest possible release point is not 2.5 times higher than the adjacent containment buildings, and thus all releases were considered ground level releases. As such, the release height was set equal to 10.0 meters as required by Table 3.1 of Reference 2. The building area used for the building wake term was 2,416 m^2.

The tower height at which the wind speeds were measured is 10.05 m above plant grade. The windspeed units are given in miles per hour, therefore the PAVAN variable UCOR was set equal to 101 to convert the windspeeds to meters per second as described in Table 3.1 of Reference 2. The maximum windspeed in each windspeed category was chosen to match the raw joint frequency distribution data, which conforms to the windspeed bins in Table 1 of Reference 3.

2Q.4 RESULTS

PAVAN computer runs for the EAB and LPZ boundary distances were performed using the data discussed previously. Per Section 4 of Reference 1, the maximum CHI/Q for each distance was determined and compared to the 5% overall site value for the boundary under consideration. For dose calculations, the most limiting 2 hour CHI/Qs were combined with the worst 2 hour EAB doses to maximize calculated EAB doses (conservative approach).

The maximum EAB and LPZ CHI/Qs that resulted from this comparison are provided in the table below:

Offsite Boundary χ/Q Factors for Analysis Events		
Time Period	EAB χ/Q (sec/m^3)	LPZ χ/Q (sec/m^3)
0-2 hours	3.17E-04	1.54E-04
0-8 hours	2.08E-04	8.63E-05
8-24 hours	1.68E-04	6.46E-05
1-4 days	1.06E-04	3.45E-05
4-30 days	5.51E-05	1.40E-05

2Q.5 REFERENCES

1. USNRC Regulatory Guide 1.145, "Atmospheric Dispersion Models for Potential Accident Consequence Assessments at Nuclear Power Plants," Revision 1, November 1982, (Reissued February 1983 to correct page 1.145-7).

2. NUREG/CR-2858, "PAVAN: An Atmospheric Dispersion Program for Evaluating Design Basis Accidental Releases of Radioactive Materials from Nuclear Power Stations," November 1982.

3. Safety Guide 23, "Onside Meteorological Programs," February 17, 1972.

APPENDIX 2R SHORT-TERM (ACCIDENT) DIFFUSION FOR THE CONTROL ROOM

2R.1 OBJECTIVE

Conservative values of atmospheric diffusion to the Control Room were calculated for appropriate time periods using meteorological data collected onsite during the time period 1998 through 2002.

2R.2 METHODOLOGY

The ARCON96 computer code is used by the USNRC staff to review licensee submittals relating to control room habitability (Reference 1). Therefore, the ARCON96 computer code was used to determine the relative concentrations (CHI/Qs) for the control room air intakes and inleakage locations.

The ARCON96 computer code uses hourly meteorological data for estimating dispersion in the vicinity of buildings to calculate relative concentrations at control room air intakes that would be exceeded no more than five percent of the time. These concentrations are calculated for averaging periods ranging from one hour to 30 days in duration.

The theory and implementing equations employed by the ARCON96 computer code are documented in Reference 1.

2R.3 CALCULATIONS/ARCON COMPUTER CODE INPUT DATA

Five years of meteorological data (1998-2002) were used for the ARCON96 computer code runs. The percentage of valid data over this time period was 98.8% which exceeds the minimum value of 90% data recovery specified in Reference 2.

A number of various release-receptor combinations were considered for the control room CHI/Qs. These different cases were considered to determine the limiting release-receptor combinations for the various events. The case matrix for these combinations is provided in Table 2R-2.

The distance and direction inputs for the ARCON96 runs may be found in Table 2R-1. The distances were converted from feet to meters with a factor of 0.3048 m/ft. The distances in meters were then rounded down to the nearest tenth for conservatism. The elevation difference term was set equal to zero for each case since all elevation points are taken with respect to the same datum.

The lower and upper measurement heights for the meteorological data were entered as 10.05 m and 60.66 m, respectively, for each case. The mph option was selected for the windspeed units.

A ground level release was chosen for each scenario since none of the release points are 2.5 times taller than the closest solid structure as called out in Section 3.2.2 of Reference 3 for stack releases. The top of the containment structure is at an elevation of 199.25 ft. The highest release point is from the top of the plant stack at an elevation of 185 ft., which is not 2.5 times higher than the nearby containment structure. The vertical velocity, stack flow, and stack radius terms were all set equal to zero since each case is a ground level release. The vent release option was not selected for any of the scenarios.

The actual release height was used in the cases. No credit was taken for effective release height due to plume rise; therefore, for the releases from the stacks, the release elevations were set equal to the stack top elevation. The release heights were taken as the release elevations less the plant grade elevation of 19 ft.

The only cases in this analysis that take credit for the building wake effect are the scenarios where the release is from the containment building, the tank farm, or the waste processing building. Some of the other scenarios have buildings between the release and receptor points, but for these cases the building wake was not credited for the sake of conservatism. Not crediting wakes was accomplished by setting the building area term equal to 0.01 m^2 as stated in Table A-2 of Reference 3. The first building area used is a conservatively determined containment cross sectional area. The area is calculated as the sum of the cross sectional areas created by the cylindrical portion of the containment structure above the highest nearby roof and the hemispherical area of the dome. The width used is equal to the diameter of the containment structure. The height of the cylindrical portion is taken as the distance between the top of the cylinder portion of the containment structure (represented by the spring line elevation) and the primary auxiliary building roof elevation. The radius of the hemispherical dome is taken as one half of the calculated diameter. The containment area was determined to be 1,506 m^2. The second building area is calculated as the product of the minimum roof height of the waste processing building and tank farm and one half the width of the waste processing building and tank farm. The minimum roof height and one half of the width are used for conservatism. This building area was determined to be 337 m^2.

All of the default values in the ARCON96 code were unchanged from the code default values with the following exceptions. Table A-2 of Reference 3 suggests use of a value of 0.2 for the Surface Roughness Length, and use of a value of 4.3 for the Averaging Sector Width Constant. These two changes were made for each case. The minimum wind speed was left at 0.5 m/s per the guidance instruction in Table A-2 of Reference 3.

2R.4 RESULTS

ARCON96 computer runs for the various release points and control room intake locations were performed using the data discussed previously. Per Reference 3, the 95th percentile CHI/Q values were determined. The resulting CHI/Qs are listed in Table 2R-2.

2R.5 REFERENCES

1. NUREG/CR-6331 PNL-10521, "Atmospheric Relative Concentrations in Building Wakes," May 1995, with Errata dated July 1997.

2. Safety Guide 23, "Onside Meteorological Programs," February 17, 1972.

3. USNRC Regulatory Guide 1.194, "Atmospheric Relative Concentrations for Control Room Radiological Habitability Assessments at Nuclear Power Plants," June 2003.